Crustal structure and active deformation in the westernmost Betic Cordillera and its foreland

Lourdes González Castillo

Ph.D. Thesis 2015
Universidad de Granada
Departamento de Geodinámica

PhD Program
in Earth Sciences

Editorial: Universidad de Granada. Tesis Doctorales
Autora: Lourdes González Castillo
ISBN: 978-84-9125-121-7
URI: http://hdl.handle.net/10481/40237

Universidad de Granada

Departamento de Geodinámica

IACT Instituto Andaluz de Ciencias de la Tierra

CSIC Consejo Superior de Investigaciones Científicas

Jesús Galindo Zaldívar, Catedrático de Geodinámica Interna de la Universidad de Granada,

HACE CONSTAR:

Que la presente tesis titulada "**Crustal structure and active deformation in the westernmost Betic Cordillera and its foreland**" ha sido realizada bajo mi dirección y cumple las condiciones suficientes para que su autora, **Lourdes González Castillo**, opte al grado de Doctor en Ciencias Geológicas por la Universidad de Granada.

Granada, Marzo de 2015

Vº Bº del Director

Fdo. Jesús Galindo Zaldívar **Fdo. Lourdes González Castillo**

La doctoranda **Lourdes González Castillo** y el director de la tesis **D. Jesús Galindo Zaldívar** garantizamos, al firmar esta tesis doctoral, que el trabajo ha sido realizado por el doctorando bajo la dirección del director de la tesis y hasta donde nuestro conocimiento alcanza, en la realización del trabajo, se han respetado los derechos de otros autores a ser citados, cuando se han utilizado sus resultados o publicaciones.

Granada, Marzo de 2015

Director/es de la Tesis

Fdo.: Jesús Galindo Zaldívar

Doctoranda

Fdo.: Lourdes González Castillo

A mi madre, Paco,

Cecilio, Lourdillas y Mª Isabel

“Nunca digas no lo intenté”

(Lourdes Castillo Alférez)

Así empieza todo en mi vida

AGRADECIMIENTOS

Es muy difícil expresar en pocas líneas la gratitud que siento hacía las personas que, de una forma u otra, me han ayudado a realizar este trabajo. Lo que viene a continuación es sólo un intento.

A Jesús Galindo Zaldívar, como director, agradecerle su confianza, orientación y disposición constantes. Las grandes oportunidades que me ha brindado a lo largo de estos años y que he intentado aprovechar con la mayor ilusión y esfuerzo posibles. La emoción y optimismo que pone y transmite en cada nuevo reto que nos planteamos. Como amigo, su cariño, respeto, generosidad y discreción. El agradecimiento se transforma en admiración y orgullo al pronunciar su nombre.

A Andreas Junge, *Professor* del Instituto de Geociencias de la Universidad de Frankfurt (Alemania), le agradezco la amabilidad con que me ha recibido en cada una de las estancias y colaboraciones con su grupo de investigación, el considerarme y hacerme sentir un miembro más de su equipo. La paciencia con la que me ha enseñado todo lo que sé de MT. Pero sobre todo, a él y a Heike, gracias por abrirme las puertas de su casa y ofrecerme momentos, conversaciones y lecciones de vida inolvidables.

A Francisco José Martínez Moreno, Fran... todo. Éramos amigos antes que compañeros y al final se ha convertido en uno más de la familia. Es uno de los pilares de este trabajo, así lo siento. Siempre disponible y dispuesto a ayudar sin reproches. Pendiente de todo sin hacer ruido. Hemos disfrutado mucho, incluso en los peores momentos. Somos un equipo para lo bueno y lo malo, y que así sea durante muchos años. Gracias Fran por ser como eres, cruzarte en mi camino y quedarte a mi lado.

Al Departamento de Geodinámica de la Universidad de Granada, por haberme facilitado con todos sus medios disponibles la conciliación de mi vida laboral y familiar. Me gustaría agradecer especialmente a Antonio Azor el esfuerzo e interés que ha mostrado en la última etapa de mi trabajo.

A todos los investigadores con los que he tenido la suerte de trabajar, aprender y compartir momentos inolvidables. Los trabajos que se presentan en esta Tesis son fruto de la estrecha colaboración con Carlos Sanz de Galdeano, Ángel Carlos López Garrido, Ana Ruiz, Antonio Pedrera y Patricia Ruano. Equipo insuperable en las tediosas campañas de MT. A Antonio Gil por la buena disposición y colaboración eficiente en el desarrollo de las investigaciones geodésicas.

Me gustaría también dar las gracias a Curro Roldán por los sabios consejos que me ha dado a lo largo de estos años, por las lecciones de geología y su trato siempre cariñoso y divertido. A Ahmed Chalouan y Mohamed Benmakhlouf compañeros indispensables en las campañas de Marruecos.

A Fernando Bohoyo por confiar en mí para formar parte de un gran proyecto en el que espero no defraudarle.

Al Instituto Nacional Antártico Ecuatoriano y la Universidad Técnica Particular de Loja (Ecuador) por darme la oportunidad de ampliar mi experiencia investigadora en una zona apasionante distinta de mi área de Tesis, La Antártida. A los compañeros del Centro Austral de Investigaciones Científicas de Ushuaia (Argentina), especialmente a Pablo, por su calurosa acogida y colaboración en todas las investigaciones desarrolladas en Tierra de Fuego.

A los dueños y trabajadores de las fincas de Cádiz, Málaga y Sevilla en las que he instalado los equipos de MT, así como al Parque Natural de los Alcornocales, por su buena disposición e interés.

A Jean Sanders, por su ayuda en la revisión y mejora del manuscrito en inglés y por su amable disponibilidad durante sus vacaciones.

A mis compañeros de Frankfurt, especialmente a Alex y Annika Löwer, grandes amigos, y a Marcel Cembrowski, porque su paciencia a la hora de contestar mis largas listas de preguntas ha sido infinita.

A mis amigos de la becaría, Irene (mi "chiquitilla *presiosa*"), Manuel, Ángel, Lara, Pedro, Carlos, Rafa, Idaira y Yasmina, siempre receptivos a mis

achuchones matutinos y dispuestos a reírse de todo. A pesar de mi escasa disponibilidad para los momentos lúdico-festivos me han hecho sentir como una becaria más.

A mis "niños grandes" Inma y Juampe por haberme dado lo mejor que se puede esperar de los verdaderos amigos, saber que están. Y por seguir llamándome "mini-mami" a pesar de que ya me cuidan más que yo a ellos.

A "Mis dos Mosqueteras" por estar dispuestas a echarme una mano con los niños y mucho más. Especialmente a Ana, servicial y discreta no ha faltado en ninguna de mis numerosas ausencias.

A mi padre y mis hermanos, por animarme desde el principio a conseguir este nuevo reto. A los Moreno-Vida por su ayuda en algunos malos momentos. A Ignacio de Orbe, gracias por sus consejos y palabras de ánimo constantes.

A mi madre, porque de su ejemplo he heredado la fuerza y el espíritu de lucha. Por compartir mis sueños y ayudarme siempre a conseguirlos. Con ella comparto esta Tesis, por muchos motivos es de las dos.

A Paco, por quererme y estar incondicionalmente a mi lado para todo y desde siempre, sin un solo reproche. Alcanzar la última meta de este trabajo se lo debo especialmente a él.

Finalmente pido perdón a mis hijos por robarles más tiempo del que me hubiera gustado. Espero que algún día lleguen a entenderlo y les pueda servir de ejemplo. Gracias hijos míos por hacerme sentir orgullosa de ser madre.

Este trabajo ha sido posible gracias a una beca de Formación de Profesorado Universitario concedida por el Ministerio de Educación y Ciencia, a los medios materiales del Grupo de investigación, RNM-148 y del Departamento de Geodinámica de la Universidad de Granada, y a los proyectos CSD2006-00041, CGL-2008-03474-E/BTE, CGL2009-07721, CGL2010-21048, P09-RNM-5388, RNM148.

Abstract

The westernmost Betic Cordillera is located along the northwestern Gibraltar Arc, which constitutes a curved orogen formed by the interaction of the Eurasian and African plates and the Alborán continental domain in between. This is a key region for understanding the alpine evolution of the western Mediterranean. This Ph.D. Thesis examines the crustal structure in the westernmost Betics and its foreland, also determining the present-day activity of the mountain front in this area. In addition, this research provides new data that contribute to discussion of the main models of the evolution of the Gibraltar Arc proposed to date. Integration of geological, geophysical and geodetic data in the region proved crucial for these purposes, given the complex regional structure and the lack of quality outcrops.

The analysis of magnetic anomalies along several profiles crossing the main magnetic dipole in the southwesternmost Iberian Peninsula helps constrain the geometry of the Monchique Alkaline Complex. This body crops out in southwestern Portugal and extends in depth eastward to the Betic Cordillera. A sharp step in the anomalous body coincides precisely with the southern channel of the Guadiana River, revealing the presence of a deep N-S crustal fault unknown to date, the Guadiana Fault. Gravity and geological observations support these results.

Long period magnetotelluric data are useful to elucidate the conductivity of deep crust and upper mantle, whereby it is possible to infer the lithospheric and asthenosphere structure. Sea water constitutes the main conductive body at shallow crustal levels and its influence can mask 3D geological structures. 3D forward modelling studies have been developed to constrain the bathymetry and irregular coastline effect on phase tensor and tipper vectors in the Gibraltar area and appraise the influence of the narrow Gibraltar Strait.

Long period magnetovariational observations in the westernmost Betic Cordillera, considering the sea influence in the area, highlight the presence of a major conductive body (0.05 Ω·m) within the basement of the southern Guadalquivir foreland basin: the Villafranca body. Magnetic anomaly data also evidence this major structure and help constrain its intermediate or basic igneous nature, with high sulphide mineralization. Its origin is discussed in the framework of the regional geological setting.

Although previous research efforts held the western Betic Cordillera frontal area to be inactive, new GPS data suggest a very consistent westward motion with respect to the foreland, reaching maximum displacement values in the Gibraltar Strait area. The rectilinear character of the northwestern mountain front, together with the southeastward increasing thickness of the Guadalquivir basin infill, support the activity of the westernmost Betics. Deformation is mainly accommodated by active folds showing a roughly WNW-ESE to W-E shortening, at least since the Pliocene. The displacement pattern is in agreement with the present-day clockwise rotation of the tectonic units in the westernmost Betic Cordillera. All these data support active lithospheric subduction and slab-rollback as the main model of tectonic evolution of the Gibraltar Arc.

Resumen

El extremo occidental de la Cordillera Bética está situado al noroeste del Arco de Gibraltar, un orógeno arqueado formado por la interacción de las placas Euroasiática y Africana y el Dominio de Alborán entre ambas. Constituye una región fundamental para el conocimiento de la evolución alpina del Mediterráneo occidental. Este trabajo de investigación comprende el análisis de la estructura cortical del extremo occidental de la Cordillera Bética y su antepaís así como la actividad actual del frente montañoso en esta región. Además, aporta nuevos datos para la discusión de los modelos de evolución del Arco de Gibraltar propuestos hasta el momento. La integración de datos geológicos, geofísicos y geodésicos ha sido fundamental para conseguir este objetivo, dada la complejidad de la estructura de la zona y la escasez de afloramientos de calidad.

El análisis de anomalías magnéticas a lo largo de varios perfiles que cortan el principal dipolo magnético de la parte suroccidental de la Península Ibérica ha permitido definir la geometría del Complejo Alcalino de Monchique. Este cuerpo aflora al Suroeste de Portugal y se extiende en profundidad hacia la Cordillera Bética. En la parte meridional del cauce del rio Guadiana, se produce un salto brusco del cuerpo anómalo lo que revela la existencia de una falla cortical de orientación N-S, la falla del Guadiana. Datos gravimétricos y geológicos apoyan estos resultados.

Los estudios magnetotelúricos de largo periodo son útiles para determinar la conductividad de la corteza profunda y el manto a través de la cual es posible inferir la estructura de la litosfera y astenosfera. El agua del mar representa el principal conductor en la corteza superficial y su influencia puede enmascarar las estructuras geológicas tridimensionales. En la zona de Gibraltar se ha realizado un estudio a través de modelización *forward* 3D para definir el efecto en el *phase tensor* y los *tipper vectors* de la batimetría y líneas de costa irregulares así como del Estrecho de Gibraltar.

Los datos magnetovariacionales de largo periodo adquiridos en el extremo occidental de la Cordillera Bética, que consideran la influencia del mar en el área, destacan la presencia de un gran cuerpo conductor (0.05 Ω·m), Villafranca, en la parte Sur del basamento de la cuenca del Guadalquivir. Las anomalías magnéticas también reflejan la presencia de esta estructura y nos ayudan a definir su naturaleza ígnea, intermedia o básica, con alto contenido de mineralización de sulfuros. El origen de este cuerpo se discute según el contexto geológico regional.

A pesar de que tradicionalmente se ha considerado inactivo el frente occidental de la Cordillera Bética, nuevos datos de GPS reflejan firmemente el movimiento hacia el Oeste con respecto al antepaís. Los valores de desplazamiento máximos se alcanzan en el área del Estrecho de Gibraltar. El carácter rectilíneo del frente montañoso noroccidental junto con el engrosamiento del relleno de la cuenca del Guadalquivir hacia el Sureste confirman la actividad tectónica del extremo occidental de la Cordillera. La deformación en la zona se acomoda principalmente por pliegues que evidencian un acortamiento general de orientación ONO-ESE a O-E al menos desde el Plioceno. Los patrones de desplazamiento concuerdan con la rotación horaria actual de las unidades tectónicas en el extremo occidental de la Cordillera Bética. Todos estos datos soportan la subducción activa junto con *slab rollback* como principal modelo de evolución tectónica del Arco de Gibraltar.

Table of contents

PART I

PART II

Part I

1. Introduction

2. Aims and Ph.D. Thesis structure

3. Regional setting and background

4. Methodology

Chapter 1

Introduction

The Betic and Rif Cordilleras constitute an arched Alpine belt connected through the Gibraltar Arc developed since the Cretaceous. The latest stages of relief uplift occurred from the Neogene onward, due to the NW-SE Eurasian and Africa plate convergence and the westward motion of the Alborán continental Domain in between (Dewey *et al.*, 1989; Rosenbaum *et al.*, 2002). The Iberian Massif constitutes the stable foreland of the Betic Cordillera and belongs to the central Europe Variscan belt formed as consequence of the late Paleozoic collision of Gondwana and Laurasia. At present, east of the North Atlantic spreading axis, the Eurasian-Africa plate boundary constitutes a dextral strike-slip fault, the Gloria fault, changing to a broad band of transpressional deformation eastward the Gorringe Bank in the westernmost Mediterranean (Roest and Srivastava, 1991) (Fig. 1.1).

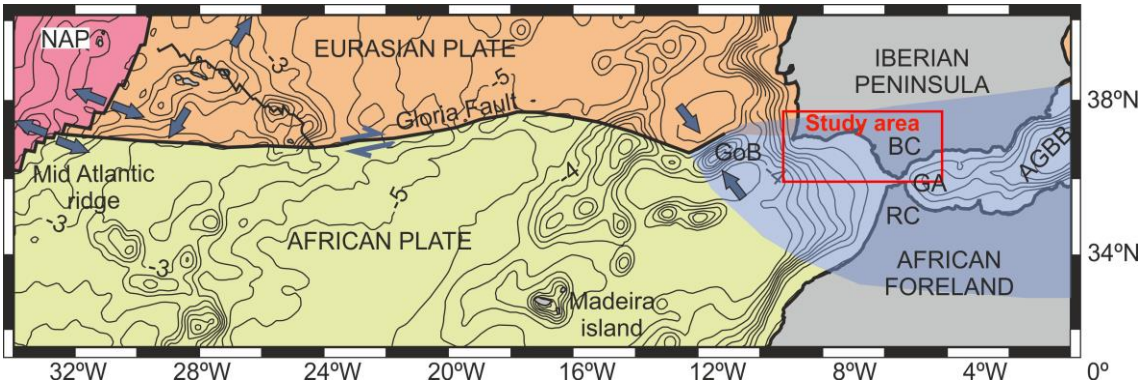

Figure 1.1: Eurasian and African plate boundary sketch; NAP: North American plate; GoB: Gorringe Bank; GA: Gibraltar Arc; BC: Betic Cordillera; RC: Rif Cordillera; AGBB: Algero-Balear Basin. Modified from Ruiz-Constán, (2009).

The Betic-Rif Cordilleras has undergone a complex evolution including compressional and extensional deformations that sometimes occurred simultaneously in different settings. Up to date, geological and geophysical research has focused on the description of recent and active structures in order to elucidate the mechanism responsible for the orogen's tectonic evolution; these studies mainly deal with the central and east parts of the Cordillera. Diverse and controversial models have been proposed for the development of the Gibraltar Arc based on subduction with associated slab roll-back and detachment of the subducted slab (Araña and Vegas, 1974; Torres-Roldán *et al.*, 1986; Wortel and Spakman, 1992; Pedrera *et al.*, 2011; Ruiz-Constán *et al.*, 2011) or on lithospheric delamination beneath the Alborán Sea (Houseman *et al.*, 1981; Seber *et al.*, 1996; Calvert *et al.*, 2000; de Lis Mancilla, 2013).

The westernmost Betic Cordillera, the Guadalquivir foreland Basin and southwestern Iberian Massif constitute a key region because of their setting by the western-northwestern boundary of the Gibraltar Arc. This region has not been studied in detail to date due to its complexity. The lack of good quality outcrops in this region conditions the development of recent tectonic studies related to surface geological observations. Studies of active structures in the westernmost front as well as the westernmost part of the Betic Cordillera have been highly constrained by this fact. Moreover, previous geophysical research have focused on broadly describing the lithospheric structure given the scarcity of further detailed data in the area.

This Ph.D. Thesis integrates new geological, geophysical and geodetical data on the westernmost Betic Cordillera and its foreland so as to shed light on deep structure and tectonic activity of the area. New magnetic and gravity data acquired along several transects of the South Portuguese Zone, the Algarve Basin and the westernmost Betic Cordillera together with a magnetovariational 3D study in the western Betics, provide additional constraints for the lithospheric structure of the

Iberian Massif and its prolongation below the Betic Cordillera. Methodological research regarding the influence of sea water, irregular continental borders and bathymetry on magnetotelluric data was performed in order to appropriately interpret regional magnetovariational data in the region. In addition, the study addresses recent and active folds and brittle structures in the mountain front, the westernmost Cordillera and the Guadalquivir foreland Basin. This analysis is supported by new GPS data in the region. The integration of these results provides new insights that will be useful when discussing the recent evolution of the Gibraltar Arc.

Chapter 2

Aims and Ph.D. Thesis structure

This Ph.D. Thesis focuses on the westernmost part of the Betic Cordillera and its foreland. Its location in the western-northwestern boundary of the Gibraltar Arc makes this area a key region for our understanding of the Alpine evolution of the western Mediterranean related to the Eurasian-African plate interaction. The lack of high quality outcrops in this region conditions the development of detailed tectonic studies related to surface geological observations. Furthermore, geophysical researches to date are more concerned with broadly describe the lithospheric structure due to the scarcity of detailed data about the area.

The main aim of this research is to shed light on the knowledge of the westernmost Betic Cordillera and its foreland, and more specifically the crustal structure and recent evolution of this Alpine orogen, with an emphasis on determining the westernmost front activity. In addition, this work provides new data that will enrich discussion of the main hypotheses proposed for the evolution of the Gibraltar Arc. To this end, this study develops the following aspects:

- Providing new geophysical data —gravity, magnetic, long period magnetovariational and audiomagnetotelluric data—, and integrating them with the previous geophysical data, including seismic reflection profiles. These data enhance our knowledge of the crustal structure in the studied area.
- Determining the influence of the sea on magnetotelluric data in the region, considering a detailed bathymetry of Atlantic Ocean,

Mediterranean Sea and Gibraltar Strait, in order to accurately constrain the structures by means of magnetovariational studies.

- Analysing folds and brittle deformation in the westernmost front of the Betic Cordillera and its foreland. The observations related to the front are concentrated on the recentmost deformation to describe its activity.
- Characterizing the recent paleostress pattern in the Betic Cordillera northwestern mountain front through microtectonic measurements in the area.
- Contributing new geomorphologic observations to support the presence of blind faults in the Betic Cordillera foreland, and evidence recent and present-day deformation in the westernmost front in order to assess its activity.
- Studying the sedimentary thickness infill of the Guadalquivir foreland Basin based on new geophysical data and its integration with sedimentary studies, so as to explain its geometry in relation with the mountain front activity.
- Analysing new and previous GPS data to provide relevant structural constraints that elucidates the active tectonic structures of the western Betic Cordillera.
- Finally, proposing a Tectonic model for the westernmost Betic Cordillera by integrating all the analysed data.

Ph.D. Thesis Structure

In what follow now, a brief description of the structure of this Ph.D. Thesis is given to facilitate comprehension of the text and how the aims were approached and achieved. Note that the Ph.D. Thesis is presented in the ensemble of publications format in accordance with the rules of the University of Granada. The

volume is divided in three main parts: Part I is a summary of relevant introductory data as well as previous geological, geophysical and GPS researches findings in the studied region. In addition, models of the recent tectonic evolution of the Gibraltar Arc presently under discussion are succinctly exposed. Part II comprises five articles, published or submitted for publication, that provide new geological and geophysical data regarding the westernmost Betic Cordillera and its foreland. They draw new insights about the crustal structure of the region and contribute to the discussion of its recent evolution. Finally, Part III is divided into two chapters that expound and discuss the results presented here and summarize the main conclusions in the frame of the Gibraltar Arc evolution.

In Part II, the main body of the Ph.D. Thesis, each article is presented as it would appear in the corresponding journal. This implies an element of repetition, given that all the studies are developed in the same region. Having said that, Part II of the Ph.D. Thesis is made up of the following chapters:

Chapter 5: "Magnetic evidence of a crustal fault affecting a linear laccolith: the Guadiana Fault and the Monchique Alkaline Complex (SW Iberian Peninsula)". The aim of this study was to improve our knowledge of the main crustal structure of the western Betic Cordillera foreland. Constraining the eastward extension of the Monchique alkaline laccolith helps elucidate the continuity of the deep structures of the South Portuguese Zone toward the Betic Cordillera. This regional research may enhance understanding of the major covered faults (i.e. Guadiana fault) through the integration of magnetic, gravity and geological data.

Chapter 6: "Influence of a narrow strait connecting a large ocean and a small sea on magnetotelluric data: Gibraltar Strait". On account of the location of the studied region, near the Gibraltar strait and surrounded by irregular bathymetry, it is indispensable to accurately constrain the sea influence on magnetotelluric research.

Chapter 7: "Long period magnetovariational evidence of a large deep conductive body within the basement of the Guadalquivir foreland basin and tectonic implications (Betic Cordillera, S Spain)". This study looks into the crustal structure by means of magnetovariational data acquired through a grid of sites covering the westernmost Betic Cordillera and its foreland. It provides insights about a new major conductive body located in the Iberian Massif below the Guadalquivir foreland basin. These results therefor shed light on the basement structure.

Chapter 8: "Shallow frontal deformation related to active continental subduction: structure and recent stresses in the westernmost Betic Cordillera". A combination of geological and geophysical observations supported by (available) previous GPS data leads to new findings that enrich discussion of the present-day tectonic activity in this key area. This study elucidates the activity of the area, mainly related to folds.

Chapter 9: "Active rollback in the Gibraltar Arc: evidences from CGPS data in the Western Betic Cordillera". After demonstrating the activity of the mountain front, this study provides new GPS data as well as geological observations that support the variability of deformation along the Western Betic Cordillera. These results contribute to the discussion of the tectonic models for the Betic Cordillera's development.

Chapter 3

Regional setting and background

The study area covered in this Ph.D. Thesis is located in the South and southwestern Iberian Peninsula including Spain and Portugal regions (Fig. 3.1). For the purpose of characterize the structure of the southwestern Betic Cordillera foreland, several transects were performed along the Algarve and Bajo Alentejo regions in South Portugal. One of this transects crosses the Guadiana River which constitute the Spain and Portugal border in the area. Nevertheless, the main body of the research focuses in the westernmost Betic Cordillera and the Guadalquivir foreland Basin, covering the Andalucía (Spain) provinces of Huelva, Cádiz, Sevilla and the West of Málaga.

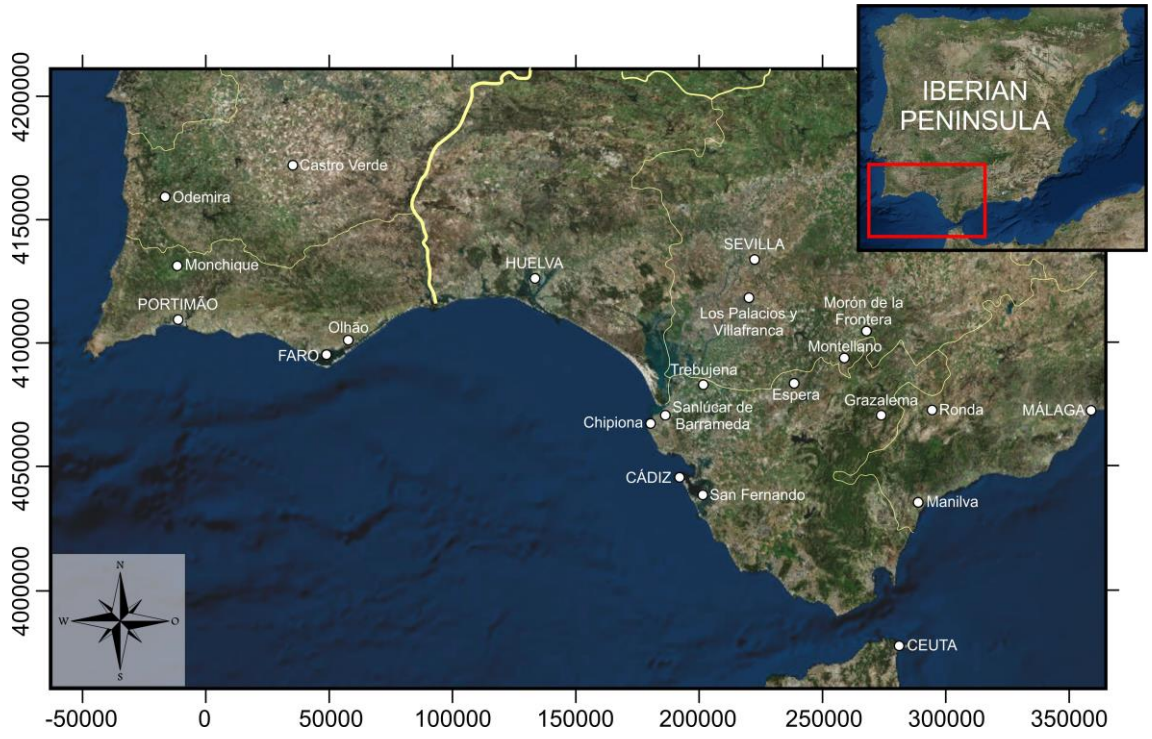

Figure 3.1: Geographical setting of the study area.

3.1 Geological setting

The Betic-Rif Cordilleras constitutes an arcuate Alpine orogenic belt, connected through the Gibraltar Arc. The Alborán Sea Neogene basin is located at the inner part of this orogen. These cordilleras are formed by the interaction of the Eurasian-African NW-SE plate convergence and the westward motion of the Alborán Domain in the West Mediterranean, consequence of the Algero-Balearic Basin oceanic spreading during the Oligocene and early Miocene (Dewey *et al.*, 1989; Rosembaum *et al.*, 2002; Rosembaum and Lister, 2004) (Fig. 1.1). The Betic Cordillera corresponds to the northern branch of the Gibraltar Arc. It overthrusts the Variscan Iberian Massif which is partially subducted beneath the western part of the Betics (Morales *et al.*, 1999; Serrano *et al.*, 2002; Ruiz-Constán *et al.*, 2010).

3.1.1 Iberian Massif

The Iberian Massif is part of the Variscan belt that extends along central Europe, formed due to the late Paleozoic collision of Gondwana and Laurasia. It comprises several zones characterized by its tectonometamorphic evolution (Ribeiro *et al.*, 1990). The southern Iberian Peninsula, from SW to NE, holds the South Portuguese (SPZ), the Ossa Morena (OMZ) and the Central Iberian Zones. In addition, the Algarve basin, located in the southernmost Portugal, together with the SPZ corresponds to the External Zones of the variscan orogen (Fig. 3.2). This region constitutes the relatively stable Betic Cordillera foreland, which extends below the Guadalquivir foreland basin and beneath the External Zones of the cordillera. The main regions of the Variscan orogen enclosed in this research are the South Portuguese Zone and the Algarve Basin briefly described next.

The SPZ (Fig. 3.2) is mainly formed by Devonian and Carboniferous rocks in some cases affected by low to very low grade metamorphism (Pinheiro *et al.*,

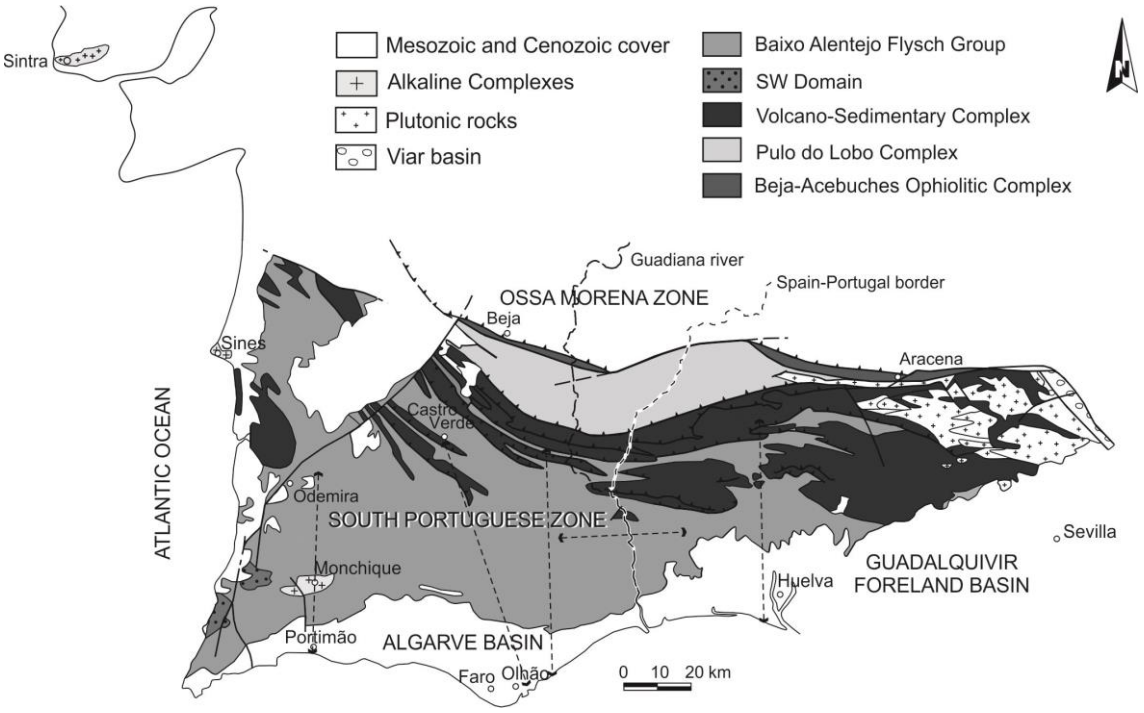

Figure 3.2: Geological setting of the South Portuguese Zone and the Algarve Basin.

1996; Abad *et al.*, 2001, 2002; Simancas, 2004). During variscan thin-skinned tectonics, three fold episodes and later thrusts involved structures of SW vergence, followed by a late brittle deformation phase (Silva *et al.*, 1990; Mantero *et al.*, 2011). Therefore, deep seismic refraction and reflection profiles (Díaz and Gallart, 2009) indicate that crustal detachments are delineated within the variscan cover. The OMZ/SPZ contact is marked by a band of amphibolites with oceanic affinity, the so-called Beja-Acebuches Amphibolite unit. These rocks have been traditionally considered as the Devonian suture of the Rheic Ocean (Bard, 1977). However, U-Pb zircon ages of the protholits point out an Early Carboniferous oceanic-like crust that opened during the volcanic massive sulfide (VMS) occurrence (Azor *et al.*, 2008). Considering stratigraphic and structural criteria, Oliveira (1990) and Silva *et al.* (1990) propose a division of the SPZ on the following major subdomains from North to South (Fig. 3.2): (a) The Northem Domain, also called the Pulo do Lobo unit, formed by detritic metasediments including mafic rocks that have been interpreted as an accretionary prism associated with a north-dipping (Eden and Andrews, 1990)

or south-dipping (Azor *et al.*, 2008) subduction zone. (b) The Central Domain, also known the Iberian Pyrite Belt, constitutes a volcano-sedimentary complex of Devonian to Early Carboniferous age including VMS deposits interlayered with metapelites or directly linked to acidic volcanic rocks (Tornos *et al.*, 1998). (c) The Baixo Alentejo Flysch Group, or Culm Group, is mainly formed by metapelitic rocks. (d) The Southern Domain, outcrops only in the South of Portugal with low extension. It is chiefly composed by metapelitic rocks similar to the Culm group but younger. Many authors consider these last subdomains as part of the Iberian Pyrite belt (Onézime *et al.*, 2003). The variscan research of this Ph.D. Thesis mainly focuses in the last two subdomains.

Since early Cretaceous, probably associated with the motion of the Iberian plate above a mantle plume (Merle *et al.*, 2009), large magmatic intrusions occurred along the West margin of the Iberian Peninsula. Onshore, the main subvolcanic complexes include the massifs of Sintra, Sines and Monchique, NNW-SSE aligned, of late Cretaceous age. Although there is no surface evidence, a large NNW-SSE crustal structure (the Sintra-Sines-Monchique fault) has been proposed as a weakness that facilitates magma ascent (Ribeiro *et al.*, 1979). The Monchique Alkaline Complex is the largest and youngest complex, located in the Southern Domain of the South Portuguese Zone, northward the Algarve Basin. The age of the alkaline rocks is around 72 Ma (Miranda *et al.*, 2009). Rock (1978) describes this massif as a subvolcanic laccolith emplaced into late Carboniferous marine sediments. It has an E-W elliptical shape, probably controlled by ESE-WNW variscan fractures, with a concentric structure formed mainly by two nepheline sienite bodies (Valadares and González-Clavijo, 2004). These fractures were reactivated as normal faults during the formation of the Algarve Basin (Ribeiro *et al.*, 1990).

The Mesozoic Algarve Basin (Fig. 3.2) is located at the southern tip of Portugal and overlays the South Portuguese Zone, separated by an angular unconformity. It is characterized by carbonate sediments with a few levels of

sandstone, marls and clays (Heimhofer *et al.*, 2008). These Mesozoic deposits are formed by the collapse and dismantling of the variscan orogen. They accumulated in a passive margin developed owing extensional regime during the opening of the Atlantic and Tethys oceans. The Mesozoic section is characterized by a sharp thickening toward the South across ENE-WSW flexures trending subparallel to the coastline (Ribeiro *et al.*, 1984). These flexures are most likely connected with basement normal faults that formed during the extensional tectonics related to margin rifting (Ribeiro *et al.*, 1990). A clear tectonic inversion occurred during the alpine orogeny and several compressive episodes have been identified (Manuppella *et al.*, 1988; Terrinha, 1998; Terrinha *et al.*, 2002). As a consequence, the Cenozoic evolution of the Algarve basin is characterized by the compressional reactivation of variscan extensional basement faults and the deformation of the Mesozoic deposits. At present, the main alignments identified by photo interpretation have NNE-SSW, N-S and ENE-WSW orientations, probably corresponding to the most important brittle structures in the region (Moniz *et al.*, 2003).

3.1.2 Betic Cordillera

The Betic Cordillera is traditionally divided in two main tectonic crustal domains (García-Dueñas and Balanyá, 1986): the Alborán Domain corresponding to the Internal Zones, and the South Iberian Domain, that are equivalent to the External Zones, separated by the Flysch Units (Fig. 3.3).

Internal Zones

The Internal Zones are made up of several superposed complexes including Paleozoic rocks, and affected by Alpine metamorphism. From bottom to top: the main complexes are the Nevado-Filábride (Egeler, 1964), the Alpujárride (Van Bemmelen, 1927) and the Maláguide (Blumenthal, 1927) (Fig. 3.3). These complexes are separated by low-angle normal faults (Aldaya *et al.*, 1984; García-Dueñas and Balanyá, 1986; Galindo-Zaldívar *et al.*, 1989). In addition, the

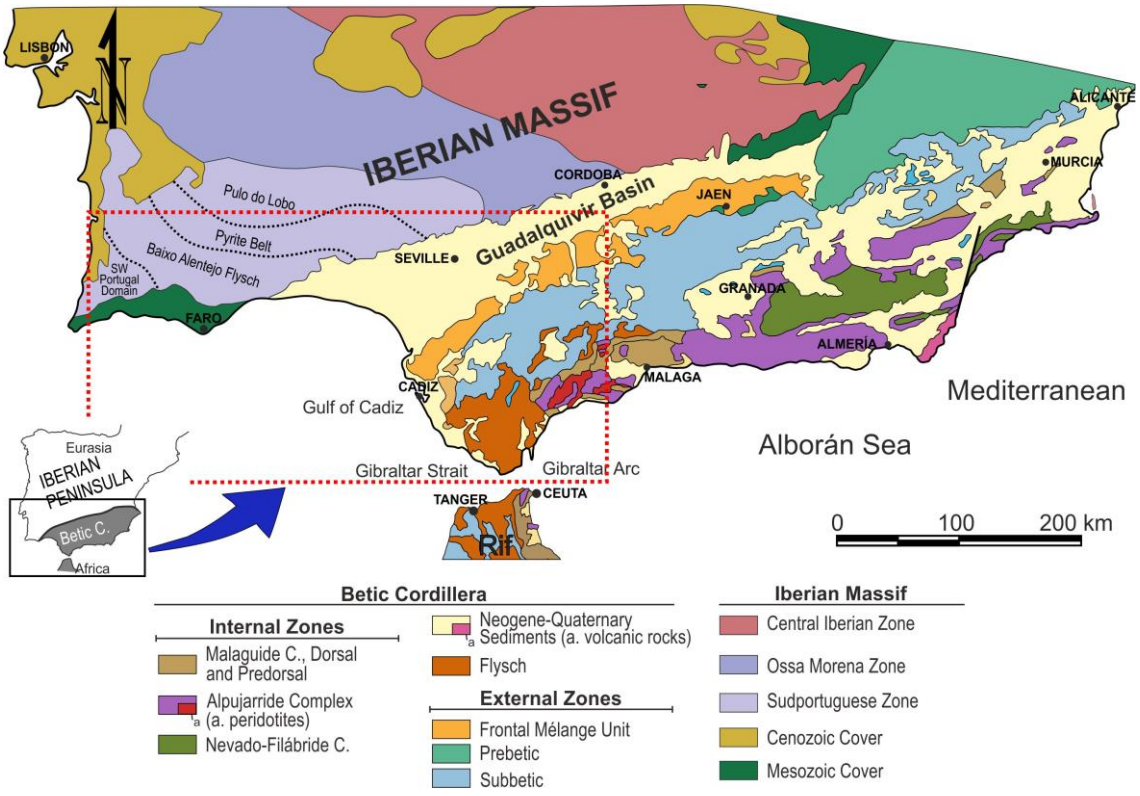

Figure 3.3: Geological map of the Betic Cordillera and the southwestern Iberian Massif. Dashed red box marks the study area.

Dorsal and Predorsal complexes, formed by Triassic to Early Neogene sedimentary rocks, constitute the frontal imbricated units chiefly outcropping in the western and central Betic Cordillera. The Nevado-Filábride and Alpujárride complexes include a succession of thrust sheets with Paleozoic to Mesozoic lithostratigraphic sequences, drawing an extensive Alpine ductile evolving to brittle deformation and high pressure (HP) metamorphism progressing to high temperature-low pressure (HT-LP) gradients. The Alpujárride upper unit includes large peridotite bodies at its base that widely outcrop at the Ronda Massif. A crustal-scale extension during the Early and Middle Miocene produced the exhumation of the Alpujárride and later the Nevado-Filábride complexes (Galindo-Zaldívar *et al.*, 1989; Monié *et al.*, 1991; García-Dueñas *et al.*, 1992; Watts *et al.*, 1993). The former is supported by a sharp decompression in the metamorphic P–T path of these complexes (Vissers, 1981; Gómez-Pugnaire and Fernández-Soler, 1987; Bakker *et al.*, 1989; García-Casco and Torres-Roldán,

1996). The Maláguide complex is formed by Paleozoic to Middle Miocene rocks that were deformed but not affected by Alpine metamorphism (Martín-Algarra *et al.*, 2009; Chalouan and Michard, 1990). All these complexes are located in the southeastern part of the Betic Cordillera and continue towards the basement of the Alborán Sea. The Paleozoic basement of the Internal Zones was partially affected by the Variscan orogen (Martín-Algarra *et al.*, 2009; Gómez-Pugnaire *et al.*, 2004; 2012). However, the most penetrative deformation and metamorphism occur from the Eocene to Early Miocene (Monié *et al.*, 1991). A late extensional stage between Early and Middle Miocene developed low-angle normal faults and detachments (Galindo-Zaldívar *et al.*, 1989; Jabaloy *et al.*, 1992). They are followed by the neotectonic deformations that are related to the present-day relief development (Sanz de Galdeano, 1990).

Flysch

The Flysch units (Fig. 3.3) correspond to the former oceanic or thin continental swell located among the two main domains filled by siciliclastic deposits from Oligocene to Miocene (Durand-Delga *et al.*, 2000; Luján *et al.*, 2006) and not affected by Alpine metamorphism. In the last stages of the Alpine orogeny these units have been imbricated forming an accretionary prism with an N–S structural trend and W to NW vergence in the Betic Cordillera that is also denominated Campo de Gibraltar Units (Luján *et al.*, 2006). At present, they extend along the Internal/ External Zones boundary, in an ENE–WSW direction. The main tectonic unit of the Flysch Complex is the Aljibe thrust (Didon *et al.*, 1973). The Paleogene sequence of this unit comprises claystones and intercalations of calcareous limestones, while the Neogene sequence is made up of a characteristic quartzite formation with minor marly levels.

External Zones

The External Zones represents the deformed Mesozoic to Cenozoic continental deposits of the South Iberian paleomargin (García-Dueñas and Balanyá, 1986). They have been differentiated in the Prebetic (formely located nearby the continent, now outcropping toward the Northeast of the Betic Cordillera) and Subbetic (in a more distal position, located in more southern and West area of the Cordillera) (Fig. 3.3), based on their tectonic, stratigraphic and paleogeographic features (Blumenthal, 1927; Fallot, 1948). These Zones consist mainly of carbonate-marly series with local volcanic intercalations. The Late Triassic is represented by claystones with gypsum and fine-grained sandstones (Keuper facies) which during late Alpine deformations constitute a regional detachment surface from the Variscan basement. Above, different carbonate series developed depending on the position in respect to the continental margin. The South Iberian Domain was deformed, but not metamorphosed, during the continental collision in the Alpine orogen as a NW to W vergent fold-and-thrust belt (Sanz de Galdeano and Vera, 1992; Lonergan and White, 1997). In a frontal position, in contact with the foreland basin, a mélange unit is widely developed especially in the Subbetic Zone (Sanz de Galdeano *et al.*, 2008; Roldán *et al.*, 2012). This unit constitutes a chaotic mix of huge mass of rocks, known as Olisthostromes, placed by tectonic deformation and gravity gliding and involving Mesozoic and Tertiary sediments, mainly silts and gypsum. It is related to mass wasting and breaking processes due to contractional events responsible of the cordillera prism accretion and extensional processes linked to the orogen exhumation. In the External Zones, alpine deformation started during Cretaceous, remaining active up to Pliocene (Cano-Medina, 1981). Present-day relief features in the Betic Cordillera are related to large folds and faults active since the Upper Miocene (Sanz de Galdeano, 1990; Braga *et al.*, 2003; Sanz de Galdeano and Alfaro, 2004).

3.2.3 Neogene - Quaternary basins

During the westward emplacement of the Internal Zones on the South Iberian Margin in Early-Middle Miocene, sedimentation in an incipient Guadalquivir foreland Basin took place. The sedimentary infill is composed by detrital Neogene and Quaternary deposits featuring interlayered calcarenites and limestones (Roldán, 1995). The most recent evolution of the cordillera includes the development of minor sedimentary basins over the External and the Internal Zones and along its boundary, from the Late Miocene onward. They are filled by detritic sequences with intercalated calcarenites and locally with lacustrine and reef limestones. These intramontane basins (e.g. Granada and Ronda) developed simultaneous to relief uplift, and therefore are highly conditioned by the recent tectonic structures. In addition, the Alborán Sea is the main Neogene – Quaternary basin remaining below sea level and located between the Betic and Rif Cordilleras. Its metamorphic basement is in continuity with the Internal Zones. Among them, the Guadalquivir Basin is the only outcropping in the study area and will be described next.

The Guadalquivir foreland Basin

The Guadalquivir Basin is an elongated Neogene-Quaternary basin limited by Iberian Massif to the North and the Betic Cordillera to the South which respectively form its passive and active margins (Salvany *et al.*, 2001) (Fig. 3.3). It has an asymmetric geometry narrowing to the East and gradually increases its depth toward the SSE, so the basement is found up to 5000 m below the Betic thrust front (Fernández *et al.*, 1998; García-Castellanos *et al.*, 2002; Salvany *et al.*, 2011). During the Early and Middle Miocene, it was a large marine basin constituting the northern connection between the Atlantic Ocean and the Mediterranean (the North Betic Strait; Sanz de Galdeano and Vera, 1992). The Guadalquivir Basin developed during Neogene and Quaternary as result of the subsidence due to the flexure of the Iberian Massif related to the load of the allochthonous units of the Betic Cordillera. The sedimentary infill, Langhian-

Pliocene in age, is mainly marine and of clastic nature, chiefly formed by autochthonous sediments in its northern part while the southern border is made up of chaotic allocthonous sediments from the Subbetic.

Most of the researches developed in the Guadalquivir Basin regarding to this study are mainly focused in the Lower Guadalquivir Basin. Since Early Pliocene, the basin has principally been filled by alluvial sediments as well as by aeolian and shallow marine sediments. Each sequence is characterised by: first, an initial period of erosion that produced a regional unconformity; second, a fast alluvial progradation supplied by the craton margin of the basin along the thrust front; and third, a slow alluvial retrogradation cratonward. In the third sequence, retrogradation occurred together with a shallow marine transgression that flooded the southern part of the basin (Salvany *et al.*, 2011). The late evolution of the lower Guadalquivir basin, at least since Late Pliocene, was mainly controlled by tectonic uplift and sediment supply from the northern variscan foreland.

3.2 Previous geophysical data

For the purpose to constrain as far as possible the deep structure in the western Betic Cordillera, many geophysical methods including active and passive seismic, gravity, magnetic and magnetotelluric researches, have been longer applied in the region (Fig. 3.4). Their results contribute to elucidate what is missing from geological surface observations. The main features evidenced up to date by the available geophysical data are: the crustal thickness variation between the different geological regions, the eastward to southeastwards subducting slab below the Gibraltar Arc (Serrano *et al.*, 1998; Morales *et al.*, 1999; Calvert *et al.*, 2000; Ruiz-Constán *et al.*, 2011) and the anomalous mantle in the Alborán Sea (Bonini *et al.*, 1973; Torné *et al.*, 2000).

The aim of this section is to summarize the main geophysical researches carried out in the Betic Cordillera and its foreland, especially focused in their western part, which constituted the starting point for the acquisition of the new geophysical data in the frame of this Ph.D. Thesis. Both previous and new data together with the geological observations have been essential in the development of this research.

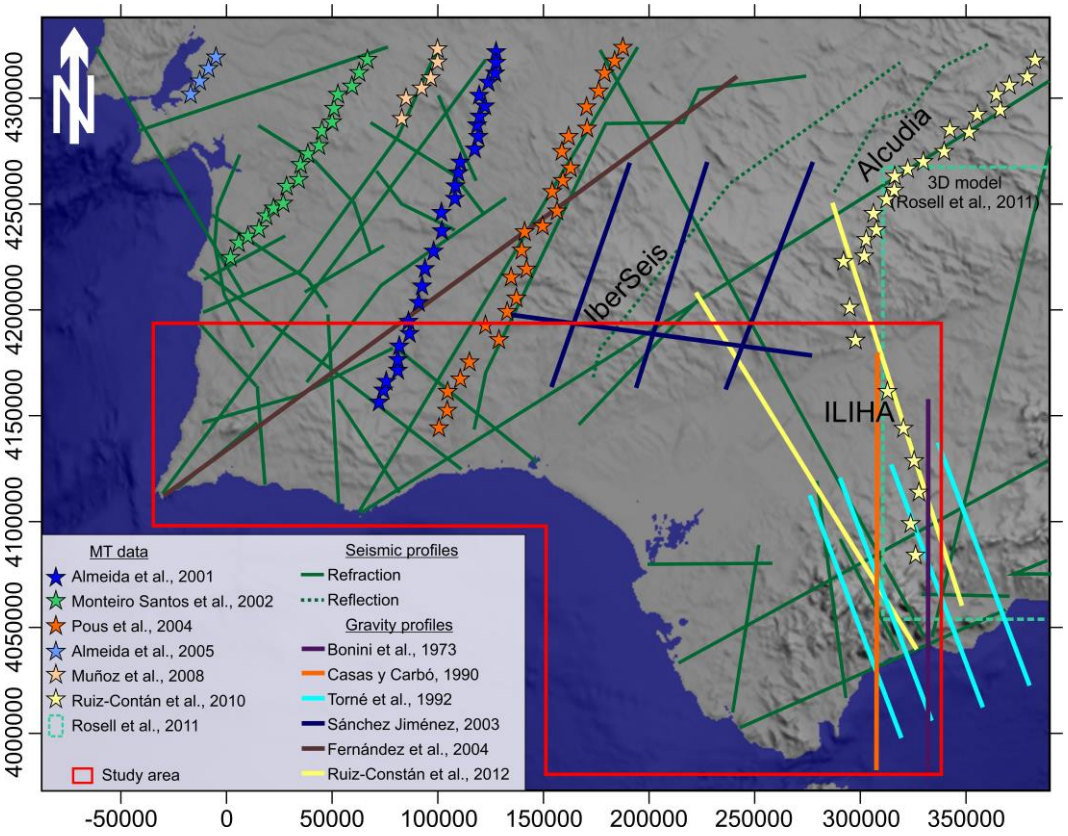

Figure 3.4: Location of the main gravity, magnetotelluric and seismic researches performed in the western Betic Cordillera and the southwestern Iberian Massif. Red box marks the study area of this Ph.D. Thesis.

3.2.1 Gravity data

The 1:1.000.000 free air and Bouguer anomaly maps of Spain (I.G.N., 1976) were performed from gravity measurements on the surface. The Bouguer anomaly map holds a good correlation between the regional geological features and the gravity anomalies. It shows negative values within the Iberian Peninsula

related to the thick continental crust that mostly become 0 mGal close to the coast. In fact, the minima (up to -160 mGal) are located in the Betic Cordillera between the Internal and External Zones boundary drawing the presence of a thickened crust below and the low density of the Guadalquivir, Ronda, Granada and Guadix-Baza basins sedimentary infill. Toward the Alborán Sea, the anomaly values increase reaching positive ones in its central zone (Casas and Carbó, 1990). Gravimetric models for the Betic Cordillera and the Alborán Sea are helpful to establish the crustal thickness in the region (Suriñach and Udías, 1978; Casas and Carbó, 1990; Galindo-Zaldívar *et al.*, 1998; Torné *et al.*, 2000 Ruiz Constán *et al.*, 2012) (Fig. 3.4). This increase of the Bouguer anomaly from the Internal Zones of the Betic Cordillera toward the Alborán Sea has been modelled drawing a continental crustal thickness from 38 km bellow the Internal Zones up to less than 15 km beneath the central Alborán Sea (Torné and Banda, 1992). Regional gravity studies focused on the southwestern Iberian Massif propose a moderate crustal thickening and a lithospheric mantle thinning bellow the OMZ and SPZ (Fernández *et al.*, 2004). Crustal studies suggest different crustal nature of both Zones separated by a slice of lithospheric mantle (Sánchez-Jiménez *et al.*, 1996).

Summarizing, gravity data support the presence of a standard continental crust in the Iberian Massif (Sánchez-Jiménez *et al.*, 1996; Fernández *et al.*, 2004) that is southeastward bounded by the relatively thick crust of the Betic Cordillera and followed by the very thin continental crust of the Alborán Sea above an anomalous mantle (Hatzfeld, 1976; Torné *et al.*, 2000).

3.2.2 Magnetic data

The aeromagnetic map of the Iberian Peninsula (Socias and Mezcua, 2002) is the only magnetic research that helps to elucidate the Iberian Massif and the Betic Cordillera regional structure on depth in the southwestern part of Iberia. Its resolution is not high enough to feature bodies smaller than 10 Km. Thus,

field magnetic data are necessary to constrain the crustal structure in detail. The magnetic anomalies in Southern Iberian Massif are mainly characterized by a WNW-ESE band related to the basic igneous rocks of the OMZ. Their analysis reveals the Variscan basement extension below the Guadalquivir foreland basin, at least as far as the External Zones of the Betic Cordillera in its central sector (Bohoyo *et al.*, 2000; Serrano *et al.*, 2002). González-Castillo *et al.* (2014) evidence the presence of a large E-W elongated dipole, extending more than 200 km in the southernmost Iberian Massif foreland, related to the Monchique Alkaline Complex and identify by first time the N-S oriented crustal Guadiana Fault. The former research corresponds to the first chapter of Part II of this Ph.D. Thesis. Eastward, the most intense aeromagnetic maximum of the westernmost Betic Cordillera is located by the Guadalquivir foreland basin that it is also analysed in Part II.

3.2.3 Seismic Data

Seismic refraction data (Fig. 3.4) (Banda and Ansorge, 1980; Medialdea *et al.*, 1986; Díaz and Gallart, 2009) support the presence of a crustal thickness of 30 km in the Iberian Massif that reach up to 37 km in the Betic Cordillera, extending along the Gibraltar Arc and decreasing down to 22 km in Alborán Sea (Suriñach and Vegas, 1993). The deep seismic reflection profiles (Fig. 3.4) have provided new data on the structure of the variscan crust of the Iberian Massif (Simancas *et al.*, 2003; Martínez-Poyatos *et al.*, 2012) revealing differences on the upper crust dominated by magmatic structures in the Central Iberian Zone, high deformation by folds and thrust in the Ossa Morena Zone and fold and thrust belt in the South Portuguese Zone. In the Betic Cordillera and the Guadalquivir foreland basin there is a widespread set of shallow seismic reflection profiles, mainly covering the Neogene-Quaternary sedimentary basins as the Guadalquivir foreland basin (Roldán, 1995), the Gulf of Cadiz (Gutscher *et al.*, 2002) and the Alborán Sea (Comas *et al.*, 1992) that reveal the structure of the sedimentary infill. However the only available deep profiles (ESCIBéticas,

García-Dueñas *et al.*, 1994; Galindo-Zaldívar *et al.*, 1997) are located in the eastern transect of the Betic Cordillera showing a flat Moho below a lower crust that is probably in continuity with the Iberian Massif and an upper detached crust.

Shallow seismicity in the westernmost Betic Cordillera and Rif is widespread along a broad 400 km band (Buforn *et al.*, 1995, 2004; Bokelman *et al.*, 2011) in addition to an intermediate seismicity reaching up to 120 km depth (Morales *et al.*, 1997; Buforn *et al.*, 2004, Ruiz-Constán *et al.*, 2011). Moreover scarce deep earthquakes occur in the central Betic Cordillera (Buforn *et al.*, 1991). Tomographic images at crustal depths (Dañobeitia *et al.*, 1998; Carbonell *et al.*, 1998) and reaching the upper mantle (Blanco and Spakman, 1993; Morales *et al.*, 1999; Gurria *et al.*, 2000; Calvert *et al.*, 2000; Spakman and Wortel, 2004; Serrano *et al.*, 2005; Díaz *et al.*, 2010) and more recently receiver functions (de Lis Mancilla *et al.*, 2013) and anisotropy (Alpert *et al.*, 2013) reveal the deep structure of the Cordillera mainly characterized by the presence of high heterogeneous and anisotropy zones including subduction slab and an anomalous mantle in the Alborán Sea. Seismic and gravity data have been integrated in lithospheric models (Fullea *et al.*, 2007; 2010).

3.2.4 Magnetotelluric data

Magnetotelluric researches underline the anisotropy of the eastern (Martí *et al.*, 2004) and the western Betics (Ruiz-Constán et al 2010) suggesting a roughly arched anisotropy variable in depth. 2D MT researches have focused to investigate the elongated shallow crustal structures in the southern part of the Iberian Massif (Almeida *et al.*, 2001, 2005; Pous *et al.*, 2004; Muñoz *et al.*, 2005, 2008; Pous *et al.*, 2011), and the central-western Betic Cordillera (Ruiz-Constán *et al.*, 2012). Monteiro Santos *et al.* (1999, 2002) suggest the presence in the Ossa Morena zone of a high conductivity middle crustal band probably related to the presence of graphite (Almeida *et al.*, 2005). 3D MT models have been developed in the easternmost Betic Cordillera (Martí *et al.*, 2009) and have been

extended up to the central sector (Rosell *et al.*, 2011). Although they support the presence of several major anomalies in the crust and upper mantle, their accuracy is low for deep structures. In the westernmost Iberian Massif, Vieira da Silva *et al.* (2007) analyzed the SPZ and OMZ. However, in the westernmost Betic Cordillera there is a complex 3D structure surrounded by an irregular sea that has avoided the development of MT studies up to date (Fig. 3.4).

3.3 Previous GPS data

Betic Cordillera is the most active tectonic region of southwestern Europe owing to the proximity to the Eurasian and African plate boundary and constitutes a suitable area to develop geodetical researches on active tectonic deformations. Plate reconstructions indicate that the whole region underwent a NW-SE shortening of 4 to 5 mm/yr heterogeneously distributed (Argus *et al.*, 1989; DeMets *et al.*, 1990; Nocquet, 2012). The detailed correlation between the tectonic activity and displacement is drawn by the accurate results of GPS geodetical networks that have been installed through the Cordillera. The regional networks are observed from continuously recording GPS stations and local structures are analyzed by survey-mode GPS sites.

The regional continuous GPS networks show a roughly westward motion of the Betic Cordillera with respect to the Iberian Massif, with southwestward component in the eastern regions and NW to WNW displacement in the western part (Serpelloni *et al.*, 2007; Vernant *et al.*, 2010; Koulali *et al.*, 2011). These data demonstrate that the deformation related to the westward migration of the Internal zone (Alborán Domain) in respect to Eurasian and African plate boundary continues active at present. Even so, studies generally aim to trace sharp rectilinear Eurasian-African plate boundaries and crustal blocks that not accurately integrate the active tectonic structures. The quality of the settings has been largely enhanced in the last years on account of the equipment improvement and the longer recording. Since the first results based on very

scarce data from Fadil *et al.* (2006) and Serpelloni *et al.* (2007) deriving a relative westward motion of the Betic-Rif Cordilleras, the observations have been largely accurate. Tahayt *et al.* (2008) evidences the westward motion in the Gibraltar Strait area with respect to Eurasia. Pérez-Peña *et al.* (2010) points the heterogeneous deformation during the NW displacement of the Betic Cordillera and northern Rif related to the main faults and seismicity. Pérouse *et al.* (2010) focus their researches in the Rif and propose the presence of a local detached slab. Vernant *et al.* (2010) and de Lis Mancilla *et al.* (2013) also evidence the westward motion of the Betics with scarce data. Koulali *et al.* (2011) include data acquired in the period 1999-2009, suggesting an arcuate pattern of displacement ranging from WSW in the eastern Betic and WNW displacements in the western area (Fig. 3.5). Since 2008, in relation with the Topo Iberia project, new stations have been installed for the purpose to provide more accurate results and fulfill the gaps of the available continuous GPS network (Fig. 3.6).

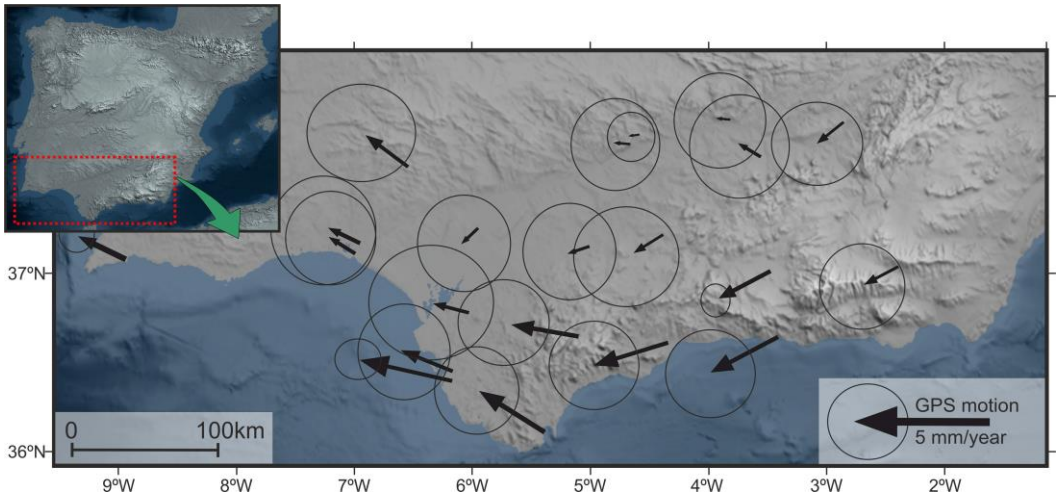

Figure 3.5: GPS motion in the South Iberian Peninsula with respect to stable Eurasian plate from Koulali *et al.* (2011). Error ellipses denote 95% confidence intervals.

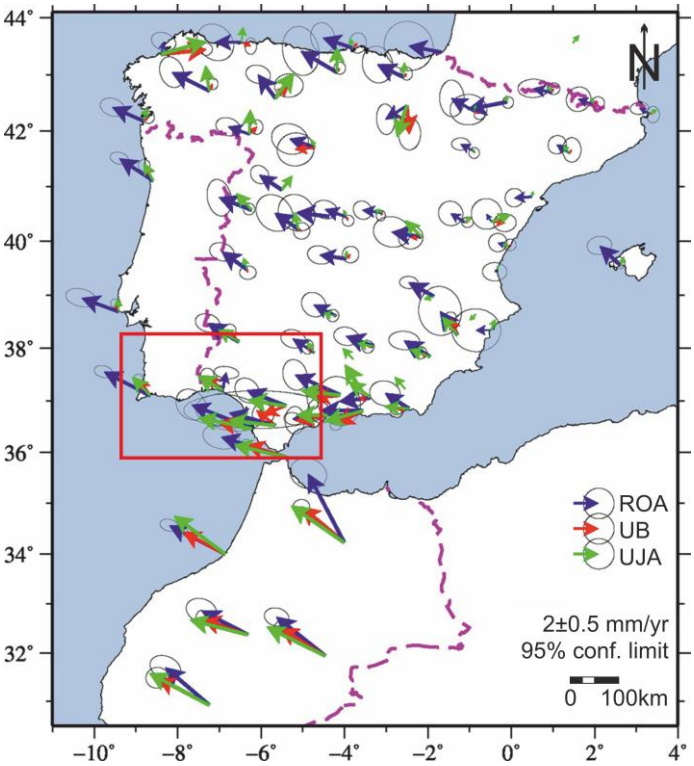

Figure 3.6: GPS velocities in the Iberian Peninsula and northern Morocco. Error ellipses denote 95% confidence intervals. Modified from Garate *et al.* (2015).

These data have been processed by different software (Garate *et al.*, 2015) by Real Observatorio de la Armada, University of Barcelona and University of Jaén. While in the central and eastern Betics there are more discrepancies in the results, the western region has a very consistent well constrained W to WSW displacement of the Betic Cordillera with respect to the Iberian Massif and its foreland.

3.4 Models of recent tectonic evolution of the Gibraltar Arc

The recent tectonic evolution of the Gibraltar Arc is still under debate since the 1970s supported by the progressive adding of new geological and geophysical data that contribute to shed light on the geodynamic models. The starting point of the geodynamic analysis may consider the following features of the Betic and Rif Cordilleras: (a) The arcuate and narrow shape of the Betic-Rif Cordilleras; (b) Distribution of the deformation along a wide-spread plate boundary; (c) Early to Middle Miocene thrusting in the External Zones coeval to

the development of low-angle normal faults in the Internal Zones; (d) Thin continental crust in the central sector of the Alborán Sea; (e) Distribution and nature of volcanism since the Middle Miocene; (f) Intermediate and deep seismicity with a complex earthquake pattern and the location of seismic anomalous bodies on depth.

Many hypotheses have been discussed for the development of the Gibraltar Arc (Fig. 3.7). First proposals (Fig. 3.7a) suggest that the westward motion of a rigid Alborán microplate between the Eurasian and African plates determines its arched character and the folds and thrust belt structure of the External Zones (Andrieux *et al.*, 1971; Andrieux and Mattauer, 1973). Meanwhile, the Alborán Domain displacement to the West was interpreted in the frame of a tectonic scape as result of plate's boundaries irregularities (Tapponier, 1977). This argument led to explain the development of roughly E-W dextral strike-slip faults in the Betic Cordillera and sinistral strike-slip faults in the Rif (Bourgois, 1978; Sanz de Galdeano, 1983; Leblanc and Olivier, 1984; Bouillin *et al.*, 1986, Martín-Algarra, 1987; Durand-Delga and Olivier, 1988; Dewey *et al.*, 1989). The thinned lithosphere in the inner part of the orogen was explained as consequence of mantle diapir rising, radial emplacement of gravitational nappes, and subsequent cooling below the Alborán Sea (Cloetingh and Nieuwland, 1984; Weijermars *et al.*, 1985) (Fig. 3.7b). The emplacement of the Ronda peridotites was also explained as result of a diapiric intrusion (Bonini *et al.*, 1973; Loomis, 1975). The contact between the metamorphic complexes of the Internal Zones, traditionally considered as thrust (Egeler and Simon, 1969), were reinterpreted on the 80s as low-angle normal faults (Aldaya *et al.*, 1984; Galindo-Zaldívar, 1986; García-Dueñas and Balanyá, 1986; Galindo-Zaldívar *et al.*, 1989; Platt and Vissers, 1989). This fact implied an extensional tectonic in the back sector of the Alborán Domain during its emplacement to the west (Balanyá and García-Dueñas, 1987; Jabaloy *et al.*, 1992).

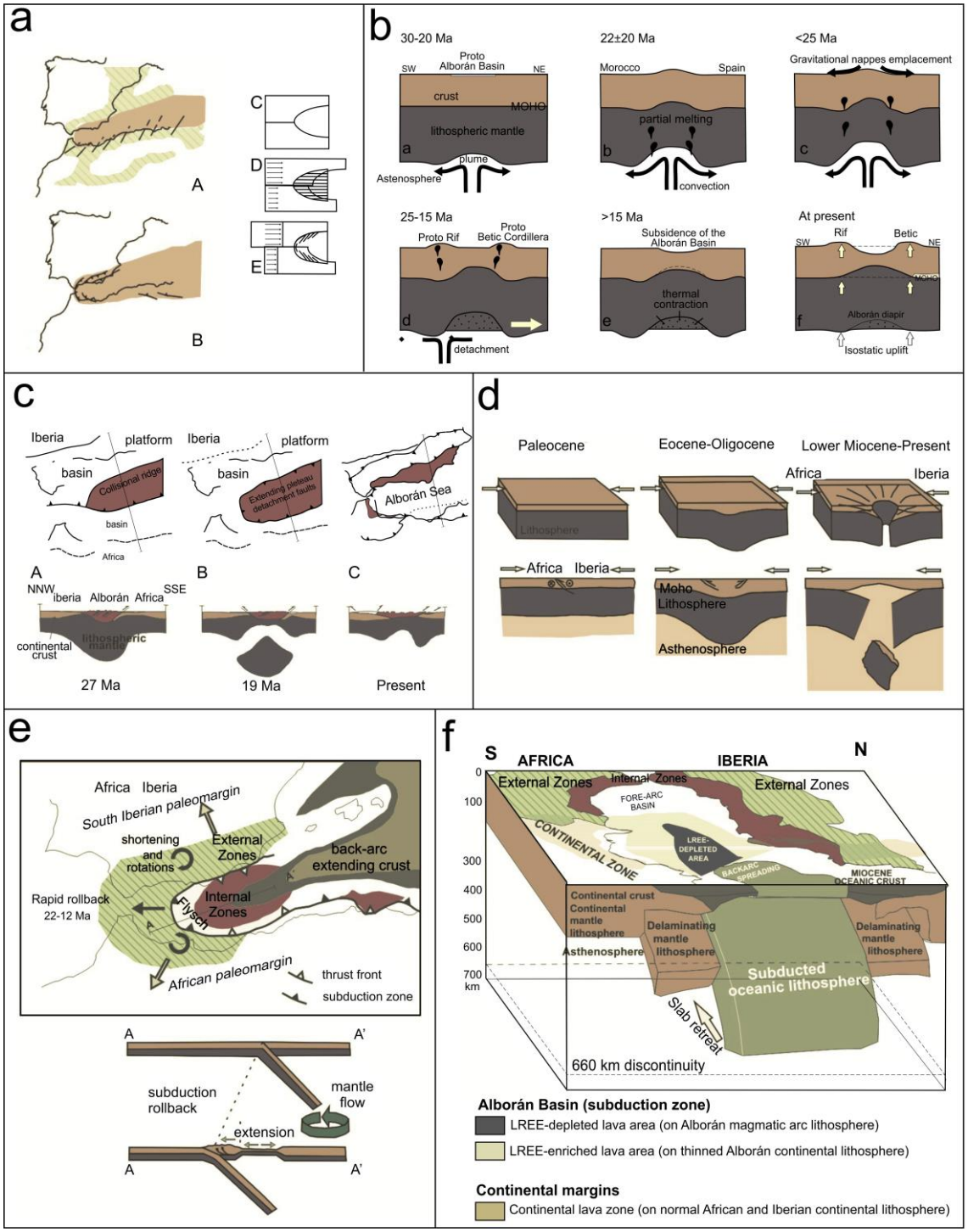

Figure 3.7: Outline of the main geodynamic models proposed for the Gibraltar Arc. Modified from Ruiz-Constán (2009). (a) Andrieux *et al.* (1971); (b) Weijermars *et al.* (1985); (c) Platt and Vissers (1989); (d) Seber *et al.* (1996); (e) Lonergan and White (1997); (f) Duggen *et al.* (2008).

During the Miocene, fast extension in the Internal Zones coeval to shortening in the External Zones, together to the exhumation of metamorphic rocks occurred. The latest tectonic models attempt to explain the mechanical factor that may cause this process. Despite all them agree that there is a tectonic element (Alborán Domain) among the two major plates, different hypotheses nowadays under discussion can be clustered in three groups:

- Detachment and/or delamination of subcontinental lithosphere beneath the Alborán Sea

According to these models, the thick and cold lithospheric root of the orogeny as result of the convergence between Africa and Eurasia was removed and assimilated during Late Oligocene-Early Miocene by convection (beneath a fixed depocentre) (Fig. 3.7c) (Houseman *et al.*, 1981; Platt and Vissers, 1989) or lithospheric delamination (West migratonial depocentre) processes (García-Dueñas *et al.*, 1992; Seber *et al.*, 1996; Calvert *et al.*, 2000; de Lis Mancilla *et al.*, 2013) (Fig. 3.7d). This fact provoked the collapse and radial extension of the crust which led the exhumation of metamorphic rocks. In the late Miocene the convergence between Eurasia and Africa became the main deformational process again increasing the shortening within the External Zones. Two high velocity bodies dipping to the SE beneath the Alborán Basin at intermediate (60-400 km) and very deep levels (570-650 km) have been observed from seismic tomography data (Calvert *et al.*, 2000) and related to the existence of a delaminated lithosphere.

- Subduction with or without associated slab roll-back and/or detachment of the subducted slab

Several subduction models have been confronted depending on their geometry and polarity. Some authors propose a northward dipping subduction zone (Araña and Vegas, 1974; De Jong, 1991 and 1993; Wortel and Spakman, 1992; Zeck *et al.*, 1992). Torres-Roldán *et al.* (1986) suggest the existence of a

double oceanic crust subduction zone active up to the Late Miocene also interpreted from metamorphic ages by Chalouan *et al.* (2001) and Chalouan and Michard (2004). Seismic tomography studies reveal an eastward to southeastward dipping subduction with subsequent slab rollback (Fig. 3.7e) (Blanco and Spakman, 1993; Morley, 1993; Royden, 1993; Lonergan and White, 1997; Hoernle *et al.*, 1999; Wortel and Spakman, 2000; Gutscher *et al.*, 2002; Gill *et al.* 2004; Spakman and Wortel, 2004; Thiebot and Gutscher, 2006; Brun and Faccena, 2008; Pedrera *et al.*, 2011; Ruiz-Constán *et al.*, 2011, 2012a). Models supporting the rollback have been proposed based on GPS data in the Rif (Fadil *et al.*, 2006; Pérouse *et al.*, 2010). In addition, it has been also described the break-off of the slab and its sinking into the asthenosphere (Buforn *et al.*, 1991; Blanco and Spakman, 1993; Zeck, 1996; Spakman and Wortel, 2004; García-Castellanos and Villaseñor, 2011; van Hinsbergen *et al.*, 2014). Finally, intermediate seismicity distribution, stress state and seismic tomography of the crust and the upper mantle of southern Iberia elucidate a southward dipping continental subduction of the Iberian Massif in western Alborán Sea, South of the Málaga region (Serrano *et al.*, 1998; Morales *et al.* 1999). The Alborán Basin may be interpreted as a backarc basin although related to different proposed subduction slabs (Doglioni *et al.*, 1997; Gueguen *et al.*, 1997; Galindo-Zaldívar *et al.*, 1998; Gueguen *et al.*, 1998; Doglioni *et al.*, 1999; Pedrera *et al.*, 2011; Carminati *et al.*, 2012; van Hinsbergen *et al.*, 2014). Although most of the former models focus on the Miocene evolution, Gutscher *et al.* (2002), Thiebot and Gutscher (2006), Pedrera *et al.* (2011) and Ruiz-Constán *et al.* (2012) suggest that the subduction is still active at present.

- Subduction of oceanic lithosphere below the Alborán basin and delamination of subcontinental lithosphere

This hypothesis attempts to explain the geochemical evolution of the Neogene magmatism in the region (Duggen *et al.*, 2003, 2008) (Fig. 3.7f). The roll-back of an E-dipping Miocene oceanic slab subduction beneath the Alborán

Basin could produce the Late Miocene delamination of subcontinental lithosphere beneath the continental Iberia and Africa margins (Martínez-Martínez *et al.*, 2006). The upwelling of plume-contaminated sublithospheric mantle beneath these margins replaced the delaminating subcontinental lithospheric mantle.

In this framework, the acquisition of new geological and geophysical observations is essential to shed light on the discussion and choice of the most suitable model of the geodynamic evolution of the Gibraltar Arc. Most of the present day studies are based on scarce dataset which are considered for very controversial interpretations.

Chapter 4

Methodology

Geological, geophysical and geodetic methods have been combined to constrain as far as possible the crustal structure and the active deformation in the westernmost part of the Betic Cordillera and its foreland. The surface geological observations provide insights of tectonic structures and reveal their geometry and kinematic. However, due to the scarcity of outcrops in the region where this Ph.D. Thesis is focused, and the poor constrain of the deep structures as consequence of its complexity, geophysical methods are essential to determine the shallow and depth structure of the studied area. In addition, geodetic networks supply present-day deformation patterns that show the activity of geological structures and eventually reveal the general deformation tectonic models.

4.1 Geological methods

The field work related to this Ph.D. Thesis comprises a wide range of geological methods that are carefully described in the chapters of part II. Even so, the main techniques are briefly exposed in this section.

The review of the geological maps from the Instituto Geológico y Minero de España (mainly MAGNA, 1:50.000) constitutes the starting point of the geological database. It allows identify the main geological structures and point to the better areas to develop more detailed studies. These maps provide a good tool to derive a mean value of shortening in a suitable transect of the mountain

front that may be taken into account for the whole frontal area (Chapter 9.6). Available paleomagnetic data contribute to precise the clockwise rotation of blocks considered in the proposed recent evolution tectonics models.

I would like to emphasize the field work disadvantages especially in areas as the Guadalquivir Basin on account of outcrops lack, the flat topography and the regional agriculture. The field observations mainly involve the most recent rocks, including the Neogene and Quaternary infill of the Guadalquivir Basin. Nevertheless, some researches were carried out through the Variscan Units of the south Portuguese Zone.

The researches have been focused in the recentmost deformations, including folds and brittle structures. Their main geometrical elements have been analysed. The kinematic of fault has been determined by surface features such as striae, steps, mineral growth or the fault gouge structures (S-C, trails). However, the low amount of well exposed faults focuses the researches to the joint analysis (Fig. 4.1).

In order to characterize the recent paleostress pattern in the region, microtectonic measurements have been made in a wide zone along the mountain front. The structural analysis was developed from the geometry of the fracture system according to Hancock (1985). The recentmost sediments are generally affected by one set of fractures interpreted as tensional joints, supported by calcite growth, pointing the orientation of minimum stress (Fig. 4.1a). It has also been observed two oblique joint sets that correspond to hybrid or shear joints (Fig. 4.1b). These data allow determining the orientation of the maximum and minimum horizontal stresses, although they do not provide information on the axial ratio of the stress ellipsoid.

Geomorphic observations and analysis in the whole region are helpful to determine the tectonic activity of this Betic Cordillera boundary and support the

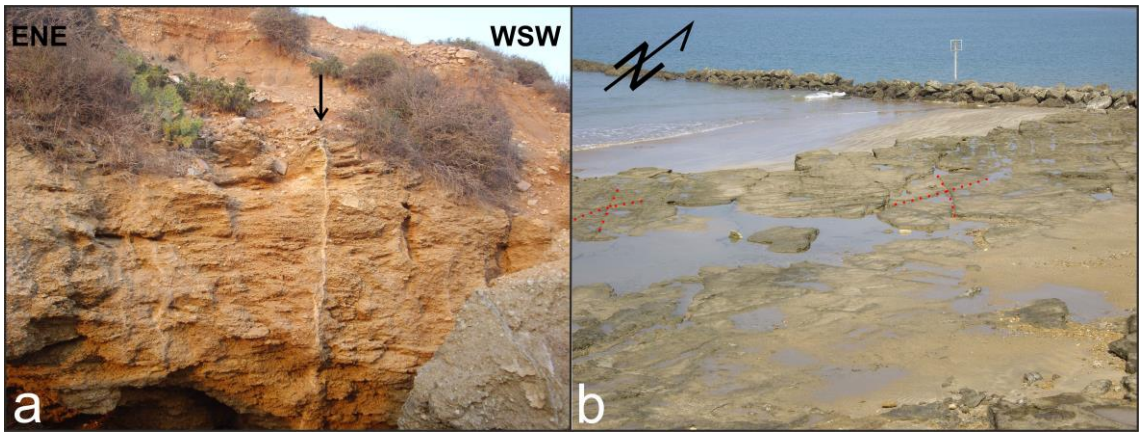

Figure 4.1: Field examples of joints. (a) Tensional joint. (b) Hybrid and shear joints.

presence of blind structures. Among other, it has been performed the sinuosity index of the westernmost mountain front (Bull and McFaden, 1977; SMF= length of the mountain front/ length of straight line of the mountain front) (Chapter 8.3). The rectilinear character of the Guadiana River near its mouth draws the presence of a brittle structure (Chapter 5.6).

4.2 Geophysical methods

4.2.1 Gravity

In a homogeneous, sphere and non-rotational Earth, gravitational acceleration (g) values along its surface would be constant. However, these values change owing to the rotation, shape and lateral density heterogeneities of the Earth. It is defined as 'Anomaly' the difference between the observed and the theoretical g values at one point of the Earth surface. The anomalies study allows determining a probable geological structure on depth in a region depending on the geometry and density of the bodies.

As consequence of the space and time dependency of the gravity field, it will be necessary to apply several corrections to the measured g values with the purpose to fix the density contrast effect of the geological structures. Time variations as result of the sun and moon attraction are removed by the tidal

correction. Moreover, data acquisition was carried out in closed cycles with the purpose to correct the tide variation and the instrumental drift. Due to the Earth's elliptical shape and rotation, it is necessary apply some additional correction to the observed gravity (g_{obs}) to obtain the gravity anomaly value:

The theoretical value of the gravity at sea level (g_l) dependant on the latitude is subtracted from the gobs. This value is obtained by the Geodetic Reference System formulae (GRS, 1967),

$$g_l = 978031.849\ (1+0.005278895 \sin^2 \phi + 0.000023462 \sin^4 \phi)\ (\text{mGal})$$

(ϕ is the latitude in degrees)

Free air correction (0.3086 mGal/m) considers the elevation differences at the gravity stations with respect to the datum itself. It provides the Free Air anomaly (g_{fa}).

$$g_{fa} = gobs - g_l + 0.3086\ h\ (\text{mGal})$$

(h is the elevation above sea level)

The Bouguer correction accounts for the excess or deficit of mass underlying observation points placed at higher or lower locations than the elevation datum. The Bouguer gravity anomaly (BG) is calculated by:

$$BG = go_{bs} - g_l + (0.3086\ h) - (0.04193\ \rho\ h)\ (\text{mGal})$$

(ρ is the average density of the rocks underlying the survey area in g/cm^3)

Topographic or Terrain correction (TC) considers for variations in the observed gravitational acceleration caused by topography near each station.

Finally, the Bouguer anomaly (g_{bt}) including the terrain correction is given by:

$$g_{bt} = gobs - g_l + (0.3086\ h) - (0.04193\ \rho\ h) + TC\ (\text{mGal})$$

This anomaly is just related to density changes of the materials and allows constraining the geological bodies' distribution in depth only depending on this property.

Equipment

A Scintrex CG-5 AutoGrav gravimeter with accuracy up to 0.001 mGal and standard deviation less than 0.005 mGal was used to acquire the gravity data (Fig. 4.2a). It has an internal memory to storage the measurements and built-in GPS for approximate positioning and precision in time and date. It also incorporates an electronic level for a correct positioning of the equipment prior to measurements. Tidal corrections are performed by the equipment in the final data.

The relative positioning of the gravity stations was performed using a global positioning system (GPS) receiver, and the altitude of the stations was determined with a barometric altimeter with an accuracy of 0.5 m (Fig. 4.2b). A barograph was located near the base station during the measurement cycles to accurately correct diurnal variations in elevation due to the atmosphere pressure evolution. The precise elevation of the sites was determined through the measurements at different geodetic reference points of the Instituto Geográfico Nacional (IGN) during the field data acquisition.

Figure 4.2: Equipment used to acquire gravity data. (a) Scintrex CG-5 Autograv gravimeter on a tripod. (b) Barometric altimeter and Garmin e-trex GPS. (c) Gravity measurement over a field station.

Processing and modelling

The Bouguer anomaly was obtained by CICLOS and ANOMALIA developed Fortran programs from J. Galindo-Zaldívar. The instrumental drift and residual tides were linearly corrected through the CICLOS program to obtain the Observed Gravity (go_{bs}) at each field station. The Free Air and the Bouguer corrections were calculated using the ANOMALIA program. The Terrain correction was determined with the GRAVMASTER program, by applying the Hammer circle (Hammer, 1939 and 1982). Topographic correction was calculated using a digital terrain elevation model with a grid of 90 meters of cell size for the first 22 km (B-M Zones).

Once the Bouguer anomaly is already calculated for each data station, it is necessary to line up all the sites along a rectilinear profile in order to get the data in the suitable format for the modelling software. The PERFIL Fortran program from J. Galindo-Zaldívar makes it possible.

The wavelength of the anomaly is indicative of the depth of the anomalous bodies in profiles orthogonal to the anomaly elongation. Deep and far geological structures show large wavelengths and low gradients (regional anomaly) whereas local shallow bodies give rise to small anomalies with high horizontal gradients (noise). Bodies located at an intermediate range of depths, which are the most interesting from a geological standpoint, produce the residual anomaly. The Bouguer anomaly will be the addition of the three components so it would be necessary to isolate the residual anomaly before modelling the geological structures. With this purpose, the regional gravity anomaly may be estimated by smoothing the Bouguer Anomaly. A second alternative could be to consider the regional anomaly map of the IGN (1:500.000) that provides a suitable support to estimate the regional anomalies. Even so, in regional studies as presented in this Ph.D. Thesis only the noise is removed.

Finally, the observed anomalies were modeled using the GRAVMAG v.1.7 software of the British Geological Survey (Pedley *et al.*, 1993), which makes it possible to perform 2D and 2.5D models.

4.2.2 Magnetic

Earth's magnetic field, also known geomagnetic field, mostly behaves as the field of a magnetic dipole slightly tilted with respect to the Earth's rotation axis. It chiefly originates to the friction due to the inner core movement in relation to the liquid outer core and the convection cells coming from the last one. The three per cent of the geomagnetic field dues to external causes associates to the sun and moon influence in addition to magnetic storms and the auroras borealis. The overall intensity of geomagnetic field is approximately 30,000 nT at the equator and 60,000 nT at the poles. Magnetic prospection is based on the analysis of the magnetic anomalies coming from the local distortion of the geomagnetic field due to the presence of contrast in magnetic properties of the rocks. The Koenigsberger ratio relates the remnant and induced magnetization, both properties determine the presence of the magnetic anomalies. Magnetic method is restricted in depth depending on the Curie point which limits the permanence of the magnetic properties of the rocks.

Magnetic anomaly maps

Aeromagnetic maps allow distinguishing regional anomalies related to large bodies even if they do not outcrop. The aeromagnetic anomaly map for the Iberian Peninsula mainland (Socías and Mezcua, 2002) is the result of compiling the aeromagnetic anomaly maps of Portugal (Miranda *et al.*, 1989) and Spain (Ardizone *et al.*, 1989). The flight lines considered were oriented N-S and spaced 10 km, while E-W control lines were separated 40 km. Flight barometric elevation was 3000 m above sea level with accuracy of 30 m. However, field surveys are necessary to study regional anomalies in detail in order to better

constrain the geometry, properties and location of the bodies responsible of the anomalies.

Equipment

Total magnetic field data has been measured in several transect of the study region using a GSM-8 proton precession magnetometer (Fig. 4.3) with an accuracy of 1 nT at a mean height of 2 m above the topography. Susceptibility measurements of outcrops rocks were acquired with an Exploranium KT-9 kappameter.

Figure 4.3: Magnetic equipment. (a) Standard GSM 8 proton precession magnetometer. (b) Exploranium kappameter KT-9 Susceptometer. (c) Magnetic data acquisition over a field station.

Acquisition, Processing and Modelling

The magnetic profiles included in this Ph.D. Thesis have been measured in a roughly N-S direction crossing orthogonally the anomaly dipoles. Because anthropic noise, such as electric power lines or ferromagnetic material, distorts the natural magnetic field, magnetic measurements were not performed near settlements.

Total field magnetic anomalies were calculated through a standard procedure including reduction to the IGRF 2010 (IAGA, 2010). Diurnal variations were corrected considering the total field intensity data of the nearest permanent magnetic station in San Fernando (Cádiz, Spain), which belongs to the Royal Army Observatory (www.intermagnet.org). The residue of diurnal

variations is removed by comparing the values obtained from periodic returns to a measured base. The estimation of the anomaly has been calculated using CICLOS and ANOMALIA Fortran programs from J. Galindo Zaldívar, including PERFIL program which line up the measurement points along rectilinear profiles .

In turn, 2D magnetic models were calculated using GRAVMAG V.1.7 software of the British Geological Survey (Pedley *et al.*, 1993). This software makes it possible to remove the regional trend and model the residual magnetic anomaly.

Simultaneous modelling of aeromagnetic and field magnetic anomalies may help to determine the magnetic body depth: the difference between the magnetic anomaly intensity determined with the two methods decreases when the body depth increases.

4.2.3 Magnetotelluric Method

The Magnetotelluric (MT) Method is based on simultaneous measurement of the natural variations of the earth's electric and magnetic fields in orthogonal directions at the surface throughout a wide range of frequencies (Kato and Kikuci, 1950; Tikhonov, 1950; Cagniard, 1953; Vozoff, 1972, 1991). The Electromagnetic Induction defines the dependent relationship between the electric and magnetic fields at the Earth's surface (Fig. 4.4). The electromagnetic fields behave roughly like plane waves at the Earth's surface. A

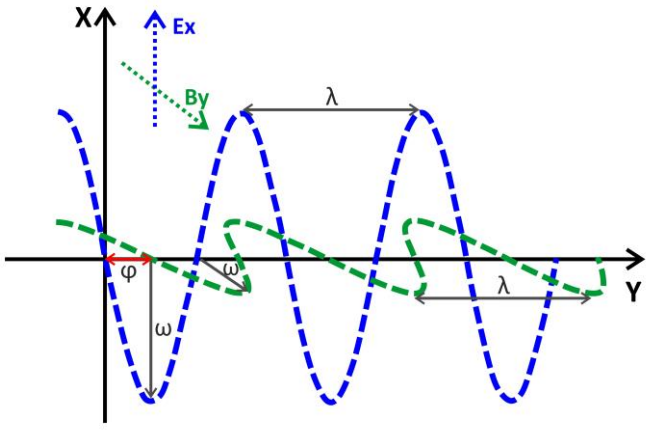

Figure 4.4: Sketch of Electric (E) and Magnetic (B) field behaviour as plane waves in a homogeneous half space. $\omega = 2\pi f$= Amplitude, λ = wavelength and φ = Phase (delay of B with respect to E).

small part of their energy propagates downward into the Earth and the amplitude, phase and orthogonal direction between both electric (E) and magnetic (B) fields depend on the distribution of the electrical conductivity in depth (Vozoff, 1991).

Natural sources of MT fields below 1Hz are related to the time-variations of the Earth's magnetic field caused by the interaction of the solar wind with the Earth's magnetosphere (Vozoff, 1991). Charge currents in the Ionosphere originate the oscillation of the magnetic field which induces an electric current at the Earth's surface that generates an electric field. At frequencies above 1Hz thunderstorms worldwide represent the main signal source.

Then, the MT method is an useful geophysical method that allow delineate the electrical conductivity structure within the Earth from shallow depths to the upper mantle. The electrical conductivity is usually expressed in terms of its reciprocal that is called *electrical resistivity,* because of numerical convenience. The electrical resistivity of most of the Earth's rocks is comprised in a wide range of values from 1 Ω·m to several thousands of Ω·m (Telford *et al.*, 1990), in spite of values lower than 1 Ω·m can be measured as in sulphide or graphite concentrations. This feature of the rocks depends on several factors such as temperature, pressure, porosity, physical and chemical state and especially the presence of water and salinity of fluids in the material. The depth of investigation is function of the resistivity of the materials and the measuring frequency that means as lower the frequency is, deeper induced currents will flow. Thus, we can draw the resistivity variation in depth beneath a point by measuring the magnetic and electric fields at different frequencies.

Equipment

The magnetotelluric equipment used to carry out the Long Period Magnetovariational measurements presented on this Ph.D. Thesis consists in a series of elements to record the electrical and magnetic field oscillations

(Fig. 4.5). A flux-gate magnetometer which is designed for 4Hz frequency registers the three components of the magnetic field (Bx, By, Bz). Two pairs of non-polarizable electrodes placed in orthogonal directions, generally N-S and E-W, allow determining the two horizontal components of the electric field (Ex, Ey) by measuring a potential difference. The electrodes have to be sufficiently spaced (50-100 meters) in order to keep the noise level low. Moreover, they must be in contact with the soil and buried 30-70 cm deep in order to avoid temperature and humidity changes. Moreover, it is common to put wet kaolin and copper sulphate at the base of the electrode to preserve humidity and provide a good contact with the soil. The electric and magnetic sensors are connected by cables and a connection box to the data logger (LEMI-417) that includes an analog-digital-converter and stores the data. Finally, exact time and location of each measurement is necessary. Therefore, the system is connected to a GPS antenna.

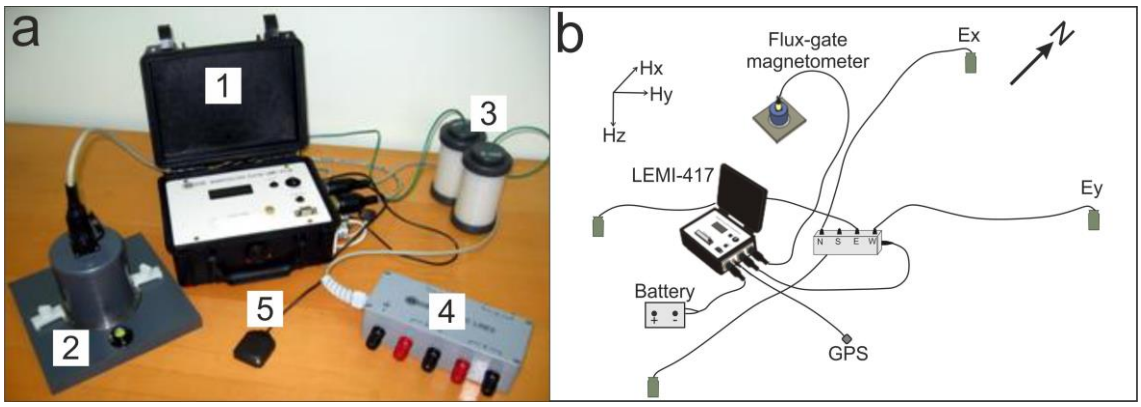

Figure 4.5: Long period magnetotelluric equipment. (a) long period LEMI-417 equipment; 1, LEMI-417 data logger; 2, flux-gate magnetometer; 3, pair of non-polarizable electrodes; 4, connection box; 5, GPS antenna. (b) Field installation sketch of the different components of long period LEMI-417 equipment.

All the equipment is installed underground except the GPS receiver. With the purpose to avoid as much as possible anthropogenic noise, regions close to wide settlements have not been observed.

Processing and Modelling

The processing procedure is focused on extracting noise signals from the recorded data trying to get be most accurately Earth's response in frequency domain (Vozoff, 1991). The MT data acquired during the development of this Ph.D. Thesis has been processed according to the linear bivariate approach by standard robust processing (Ritter *et al.*, 1998) using the Processing Software "Frankfurt MT-Tools" (Löwer, 2014).

The MT variables most commonly used are frequency dependent transfer functions between the natural time variations of the magnetic and electric field (Chave and Jones, 2012). The field components observed at different locations on the Earth's surface are the magnetic induction $\underline{B} = (B_x, B_y, B_z)^T$ and the telluric field $\underline{E} = (E_x, E_y)^T$. Both are treated as vectors which are function of time t (s). Note that the magnetic induction $\underline{B}$ is related to the magnetic field by $\underline{B} = \mu_o * \underline{H}$, where μ_o is the magnetic permeability of the vacuum. The data is observed in the time domain. The signals are transformed to the frequency domain using the Fourier transformation. Then B and E are complex values and functions of space and frequency. They are connected by the impedance tensor *Z,* also called transfer function, and by the tipper vector $\underline{T}$ through the linear and frequency dependent relationships

$$\begin{pmatrix} E_x \\ E_y \end{pmatrix} = \begin{pmatrix} Z_{xx} & Z_{xy} \\ Z_{yx} & Z_{yy} \end{pmatrix} \begin{pmatrix} B_x \\ B_y \end{pmatrix}$$

$$B_z = T_x B_x + T_y B_y$$

$$\text{With } Z = \begin{pmatrix} Z_{xx} & Z_{xy} \\ Z_{yx} & Z_{yy} \end{pmatrix} \text{ and } \underline{T} = \begin{pmatrix} T_x \\ T_y \end{pmatrix}$$

The Impedance tensor has eight components corresponding to real [Re(Z)] and imaginary [Im(Z)] parts. Its analysis allows estimate two main MT parameters, the apparent resistivity (ρ_a) (Ω·m) and phase (φ) (degrees) for each frequency:

$$\rho_a(T) = \mu_0 \frac{T}{2\pi}|Z|^2 \qquad \varphi = \arctan\left(\frac{\mathrm{Im}(Z)}{\mathrm{Re}(Z)}\right)$$

(T) Represents the period T=$2\pi/\omega$, ω as the wave amplitude.

Note that when Phase value is 45º the medium is homogeneous, values above 45º indicate a resistive to conductive contrast and values below 45º a conductive to resistive boundary.

The Tipper vector T is a complex (i.e., containing real and imaginary parts) geomagnetic transfer function that represents the ratios of vertical magnetic field component (Bz) to the horizontal magnetic fields components (Bx,By) (Schmucker, 1970). Since vertical magnetic fields are generated by lateral conductivity gradients, tipper vectors can be used to infer the presence or absence of lateral variations in resistivity of the Earth on depth. The horizontal projection of the tipper is called *Induction Arrow* that is displayed on diagrams as real and imaginary arrows which orientation and length depend on the location of a conductivity contrast and its intensity. In this work, it is assumed the Wiese (1962) convention: the real part of the arrows point away from the conductivity anomalies. Broadly speaking, the direction of the imaginary arrows for short periods is reversed to the real arrows and rotates toward the parallelism at long periods (Lilley and Arora, 1982; Agarwal and Dosso, 1990). Magnetovariational studies are only focused in the response of tipper vector such a lot of information can be derived from it.

Often the impedance tensor Z is influenced by frequency independent distortions owing to near surface conductivity inhomogeneities (Chave and Jones, 2012). A measure independent from such galvanic distortions is the phase tensor Φ after Caldwell *et al.* (2004). The phase tensor is reducing the impedance tensor to its phase relations:

$$\Phi = Z_r^{-1} Z_i$$

With $\Phi = \begin{pmatrix} \Phi_{xx} & \Phi_{xy} \\ \Phi_{yx} & \Phi_{yy} \end{pmatrix}$ and Z_r and Z_i as the real and imaginary parts of Z

According to Caldwell *et al.* (2004) phase tensor can be displayed as an ellipse (Fig. 4.6a).

$$\Phi(\Upsilon) = \begin{pmatrix} \Phi_{xx} & \Phi_{xy} \\ \Phi_{yx} & \Phi_{yy} \end{pmatrix} \begin{pmatrix} cos\Upsilon \\ sin\Upsilon \end{pmatrix}$$

Due to the rotational invariant character of ϕ_{max} and ϕ_{min} we can assume the phase tensor in a 3D environment as (Fig. 4.6b)

$$\underline{\Phi}_{3D} = \underline{\underline{R}}^{T}(\alpha - \beta) \begin{pmatrix} \Phi_{max} & 0 \\ 0 & \Phi_{min} \end{pmatrix} \underline{R}\ (\alpha + \beta)$$

Where R (α + β) is the rotation matrix and R^T is the transposed or inverse rotation matrix.

We can perform a dimensionality analysis of the geoelectrical structures from the phase tensor rotational invariant components. We consider 1D dimensionality the structures which the resistivity only depends on depth, thus $\phi_{max} = \phi_{min}$ and $\beta = 0$. If the resistivity also depends on one of the horizontal directions the structure is considered 2D, then $\phi_{max} \neq \phi_{min}$ and $\beta = 0$. Finally, 3D structures present a resistivity change in the three directions (x,y,z) with $\phi_{max} \neq \phi_{min}$ and $\beta \neq 0$.

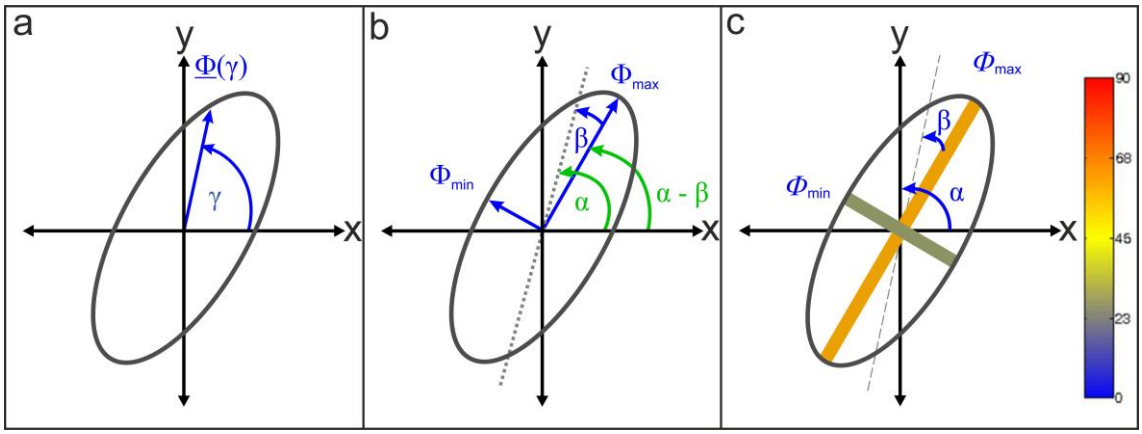

Figure 4.6: Phase tensor ellipse and bars (PT bars). (a) Phase tensor ellipse. (b) Phase tensor in a 3D environment. (c) Phase tensor bars in a 3D environment. Colour phase scale in degrees.

Among different presentations of ϕ (Booker, 2014), in this Ph.D. Thesis, the phase tensor is displayed by $\Phi_{min,max} = arctang\Phi_{min,max}$ (Häuserer *et al.*, 2011) (Fig. 4.6c).

Another variable that is important to consider is the *Skin Depth* (δ) which is the depth at an electromagnetic field is diffusely attenuated through a medium. It depends on the resistivity (ρ) of the medium and the measured frequency (inverse of the period, T) and is expressed as

$$\delta = 0.5\sqrt{\rho T}$$

The electric and magnetic field variations are modeled for 3D conductivity structures using "MT3D" modelling software for Comsol Multiphysics 5 (Löwer, 2014). An internal Comsol FE-routine generates a grid which density is controlled by a scheme of half ellipsoids. Grid resolution depends on the frequency. Conductivity distribution is interpolated to the grid elements from an arbitrary distribution of supporting points (Fig. 4.7). More detailed basics of MT modelling with Comsol Multiphysics are described by Kütter (2009).

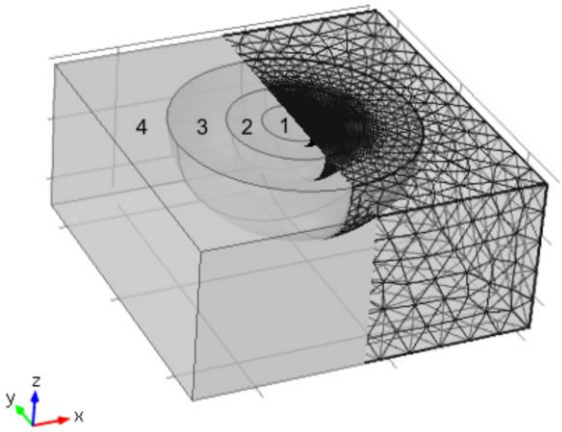

Figure 4.7: Block diagram of the Comsol Multiphysic grid from Löwer (2014).

Bathymetry

Sea water constitutes the main widespread electrical conductor at shallow levels of the Earth crust. Its low resistivity values, around 0.25 Ω·m, contrast

sharply with most geological structures of solid earth. Consequently, the presence of irregular continental borders and varying bathymetries significantly influences LMT data parameter, such as phase tensor and tipper vectors. In areas where large and small oceans are connected by narrow gateways, this fact constitutes an additional current channelling effect. The bathymetry is included in the 3D forward models developed in the MT studies related to this Ph.D. Thesis using the General Bathymetric Chart of the Oceans (GEBCO, www.gebco.net). It provides a digital terrain model of 30 arc-second grid sizes that is precise enough to consider most of the main seafloor features for MT modelling. In addition, it delivers accurate coastline geometry.

Audiomagnetotelluric (AMT) data

The AMT method allows investigating of the electrical resistivity structure downward the earth surface from measurements of natural variations of the surface electromagnetic fields over high frequency range (Vozoff, 1991). A detailed audiomagnetotelluric profile orthogonal to the mountain front of the Betic Cordillera was recorded with Strata Gem EH4 equipment, in a frequency range from 70 kHz to 10 Hz, reaching depths of tens to hundreds of meters. A transmitter antenna was used to enhance the natural electromagnetic field from 1 kHz to 5 kHz, where the natural signal decreases. Geoelectric dimensionality was analysed by means of Bahr decomposition (Bahr, 1988, 1991). The curves show a general 1D behaviour up to 10^{-1} s and 2D structure from 10^{-1} and 10 s with a N70-90ºE strike. We checked the internal consistency of the rho and phase estimated at each site (Parker and Booker, 1996) and corrected static shift problems in some of the curves. A joint 2D inversion of resistivities and phases was carried out integrating all the data (Rodi and Mackie, 2001). An error floor of 3% for the apparent resistivity and the phases was selected.

4.3 Geodetic studies

Geodetic networks provide deformation patterns that show the activity of geological structures and eventually reveal the general deformation tectonic models. The continuous GPS observations used in this work were recorded from March 2008 up to December 2013 allows determine the GPS velocity field in the western Betic Cordillera based on a sub-network of 10 sites (Fig. 4.8) ALJI, LOJA, CAST, LIJA pertain to the Topo-Iberia research project (http://www.igme.es/TopoIberia/default.html); COBA, HUEL, MALA, CEU1, LAGO are stations of the Euref Permanent Network (http://www.epncb.oma.be); and SFER (ROA). The Topo-Iberia sites are located in open field on the concrete pillars founded above bedrock, implying great stability and a high quality of observations in contrast with other available stations that undergone the effects of building deformation.

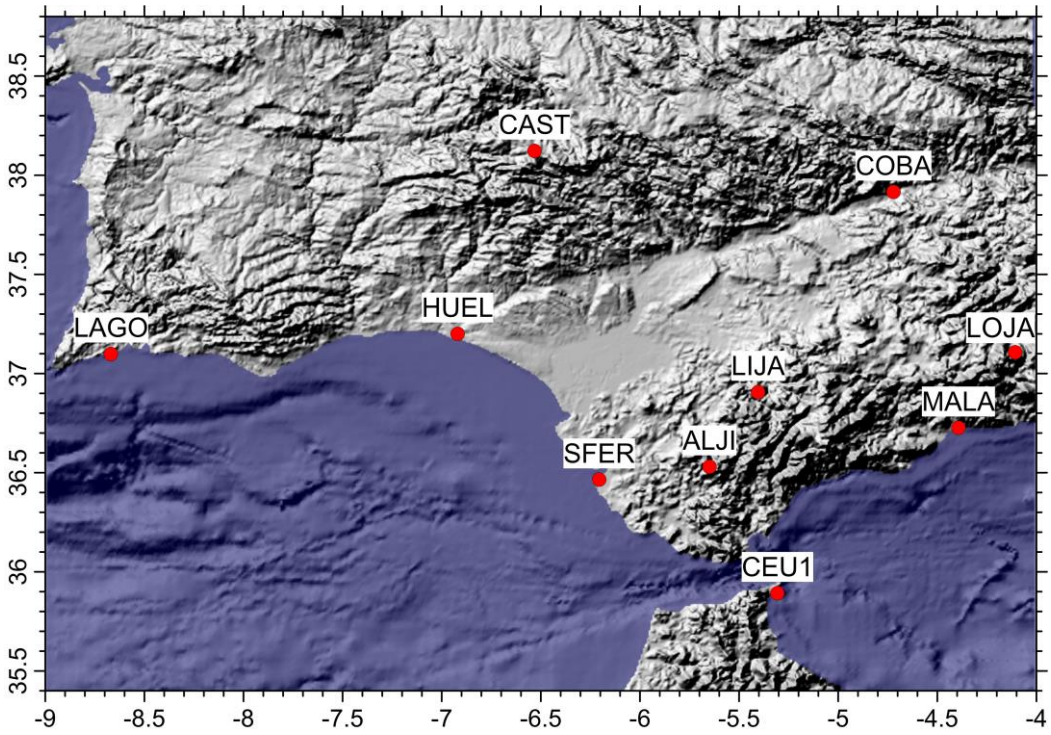

Figure 4.8: Location of the Continuous GPS stations in the westernmost Betic Cordillera.

The data analysis was performed using the Bernese Processing Engine (BPE) of Bernese 5.0 software, after checking the quality of data by means of TEQC software developed by UNAVCO (Estey and Meertens, 1999). At the end of this step, one daily solution in a loosely constrained reference frame was estimated. The output file is composed of the coordinates of the stations along with their covariance matrix in SINEX format. Loosely constrained solutions can be combined regardless of the datum definition of each contributing solution. The solution reference frame is defined stochastically by the input data; although it is basically unknown, there is no need to estimate or apply relative rigid transformations (rotation-translation-scale) for reference frames, which naturally leads to a combined solution not distorted by any constraint or transformation. Daily loosely constrained cluster solutions were then merged into global daily loosely constrained solutions of the whole network, applying a classical least squares approach where the mathematical model is defined by the time propagation operator (Bianco *et al.*, 2003). After that, the daily combined network solutions can be minimally constrained and transformed into the IGb_08 frame, estimating translations and scale parameters. In this particular case, the realization EPN_A_IGb08 was used and 13 core stations contributed to the rigid transformation: AJAC, BOR1, BUCU, CAGL, EBRE, GRAS, GRAZ, LAMP, MATE, NOT1, SFER, SJDV and ZIMM. Then, the velocity field was estimated from the IGb_08 time series of daily coordinates with the complete covariance matrix using ad hoc software (NEVE) that manages the stochastic model (Devoti *et al.*, 2008, 2011). Velocities were estimated simultaneously, together with annual signals and sporadic offsets at epochs of instrumental changes. Velocity errors were derived through direct propagation of the daily covariance matrix. Finally, the IGb_08 solutions were transformed into the Eurasian Reference Frame in view of the Euler pole of the Eurasian plate. These data provide the most accurate available base to constrain the activity of the tectonic structures.

Part II

Chapter 5

Magnetic evidence of a crustal fault affecting a linear laccolith: the Guadiana Fault and the Monchique Alkaline Complex (SW Iberian Peninsula)

Lourdes González-Castillo [a], Jesús Galindo-Zaldívar [a,b], Ana Ruiz-Constán [c], Antonio Pedrera [b].

Published on:

Journal of Geodynamics, 2014

Volume 77, Pages 149-157

DOI: 10.1016/j.jog.2013.10.007

(Received 22 March 2013; Accepted 28 October 2013)

[a] Departamento de Geodinámica, Universidad de Granada, Spain.

[b] Instituto Andaluz de Ciencias de la Tierra. CSIC-UGR. Spain.

[c] Instituto Geológico y Minero de España, Spain.

ABSTRACT

Magnetic anomalies can help reveal the structure of the upper crust in regions with intermediate or basic igneous rocks, and their continuity is essential to determine the position of crustal faults. The southwestern Iberian Peninsula constitutes the foreland of the Betic Cordillera and is characterized by an elongated E-W dipole extending 200 km toward its external zones. The anomaly is related to the outcropping Monchique Alkaline Complex, characterized by rocks of moderate magnetic susceptibility (0.029 SI) intruding into the metapelitic host rock of the South Portuguese Zone. Analysis of aeromagnetic and field magnetic anomalies serves to constrain the geometry of this laccolith. Toward the east, the magnetic dipole has a 60 km long N-S sharp boundary that coincides with the southern part of the Guadiana River. Field magnetic and gravity anomalies confirm the presence of this structure. It is produced by a sharp step in the elongated anomalous body, with an E downthrown block, interpreted as the offset produced by a deep N-S crustal fault—the Guadiana Fault. Therefore, the Guadiana River has three long linear segments near its mouth, locally coinciding with a N-S trending joint set, that support the presence of this major fault. To date, no evidence of this tectonic discontinuity, coinciding with the Spanish-Portuguese border, has been reported. Magnetic research is essential for understanding the structure of wide regions intruded by intermediate and/or basic igneous rocks.

Keywords: Magnetic anomalies; Magnetic susceptibility; 2D magnetic models; South Portuguese Zone; Intermediate igneous rocks; Crustal fault.

Highlights

- A large magnetic dipole characterizes the southwestern part of the Iberian Peninsula.
- Monchique Alkaline Complex, that extends eastward hundreds km, is the responsible of the anomaly.
- The dipole has a N-S sharp discontinuity across the Guadiana River.
- A depth crustal fault, The Guadiana Fault, conditions the sharp step of the body.

5.1 Introduction

Geophysical methods are essential for determining crustal structures in covered regions and in areas of complex geological features. Magnetic studies over continental areas conventionally focus on mineral exploration and on establishing regional geologic and tectonic frameworks. The trends of magnetic anomalies are directly linked to the geometry of the magnetic rocks and, therefore, to the deformation undergone (Blakely and Simpson, 1986). Magnetic methods are useful to study the upper crust in regions with intermediate and basic igneous rocks because of related major magnetic anomalies. They are very relevant in the analysis of large linear batholiths, such as the Cretaceous gabbro intrusion along the Antarctic Peninsula, related to the Pacific Margin Anomaly or West Coast Magnetic Anomaly, and more than 1500 km long (Garrett, 1990). In recent times, some magnetic studies have been applied in the analysis of specific faults that produce the sharp juxtaposition of rocks with different magnetic properties (Pilkington, 2007). Aeromagnetic data reveal a large strike-slip fault in the northern Willamette Valley, Oregon (Blakely *et al.,* 2000) and the location and structure of the Seattle fault zone, in Washington (U.S.) (Blakely *et al.*, 2002); as well as a left-lateral strike-slip fault in the Libyan Sirte Basin (Saheel *et al.*, 2011), and several buried tectonic lineaments in the Kutahya-Denizli region (western Anatolia) (Bilim, 2007).

In the specific case of a fault downwardly displacing a thin anomalous magnetic layer, a sharp fall-off of magnetic effects would coincide with the fault trace (Reid, 2003). High resolution magnetic surveys make it possible to detect and model geometries of faults affecting thin magnetic bodies such as magnetic sedimentary strata or laccolith formed by magnetic rocks. For example, the faults that offset the Albuquerque basin fill, in New Mexico (U.S.) feature a layer with magnetic properties and have a clear aeromagnetic expression (Grauch *et al.*, 2001 and Hudson *et al.*, 2001).

The southwesternmost part of the Iberian Peninsula corresponds to the external zones of the Variscan orogen, and comprises the South Portuguese Zone and the Algarve Basin (Fig. 5.1). This region constitutes the Betic Cordillera foreland, which extends below the Guadalquivir foreland basin and beneath the external zones of the cordillera. It is characterized by large linear magnetic anomalies (Socias and Mezcua, 2002) (Fig. 5.2) that can also be observed offshore, in the nearby Gulf of Cádiz. These magnetic anomalies have been related to large basic bodies (Dañobeitia *et al.*, 1999) associated with the alkaline intrusions that affected the region during the Cretaceous (Bernard-Griffiths *et al.*, 1997, Féraud *et al.*, 1982 and Rock, 1982). The Monchique Alkaline Complex is the most voluminous one, and the only one exclusively intruding Paleozoic rocks (Miranda *et al.*, 2009). Surface geological data do not reveal the presence of large N-S Variscan or Alpine faults, although a set of fractures with this orientation is recognized in the Gulf of Cádiz (Lopes *et al.*, 2006).

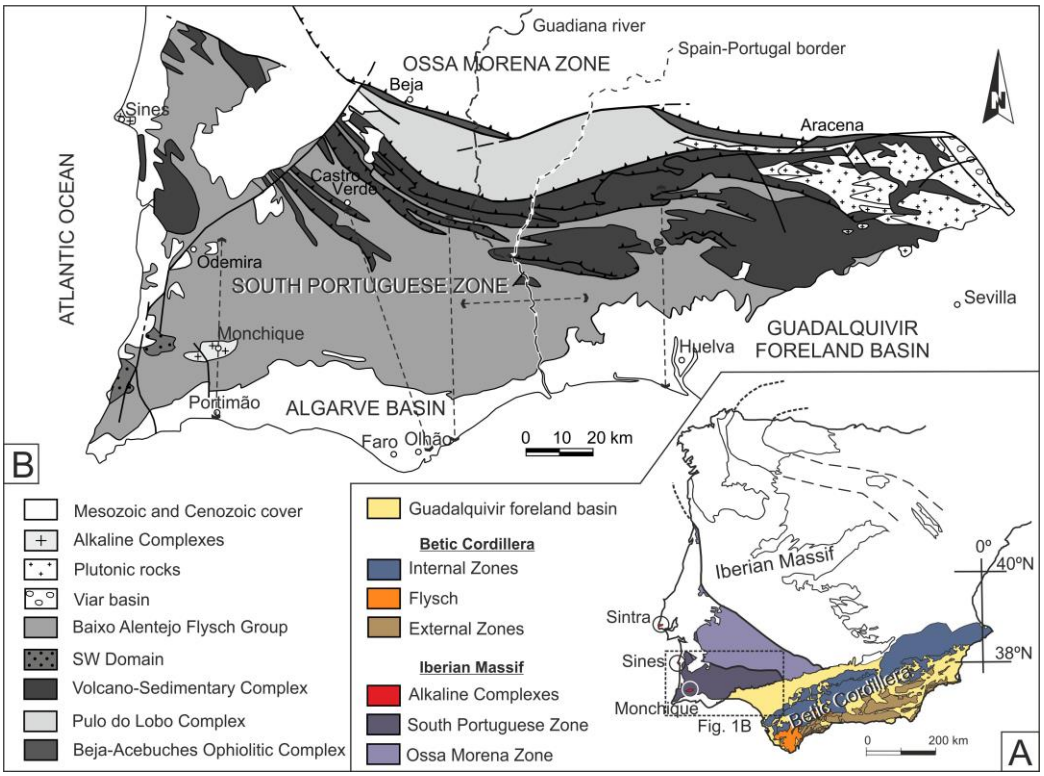

Figure 5.1: Geological setting of the studied area. (A) Regional geological setting including the Sintra, Sines and Monchique Massifs. (B) Geological setting of the South Portuguese Zone and the Algarve Basin.

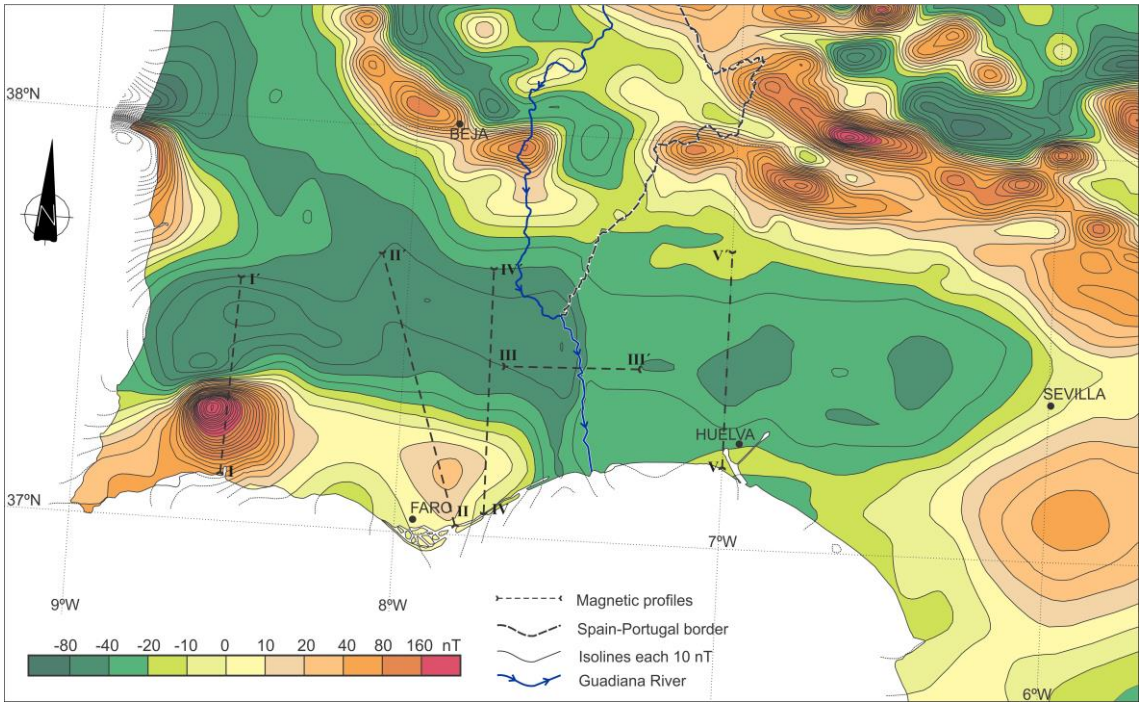

Figure 5.2: Aeromagnetic map including location of field profiles. Modified of Socias and Mezcua, 2002.

The aim of this research is to combine geophysical and surface geological data in order to determine the extension of the Monchique alkaline laccolith along the Southwestern Iberian Peninsula and discuss the nature of its boundaries. Its outcrop is related to a wide magnetic dipole that extends eastward several hundreds of kilometers in a region where only metapelitic rocks crop out. A sharp magnetic discontinuity across the Guadiana River reveals, for the first time, the presence of a probable crustal fault, the Guadiana Fault. This regional research may improve our understanding of major covered faults through the integration of magnetic, gravity and geological methods.

5.2 Geological setting

The studied area is located in the southwesternmost part of the Iberian Massif, corresponding to the South Portuguese Zone and the Algarve Basin (Fig. 5.1). This area constitutes the western foreland of the Betic Cordillera.

The South Portuguese Zone represents the external zones of the Variscan orogen and was formed by an accretionary prism over oceanic crust during the

Pangaea formation. It comprises Devonian and Carboniferous rocks, some of them affected by very low grade metamorphism (Pinheiro *et al.*, 1996). Its northern boundary is determined by an ophiolite. During Variscan thin-skinned tectonics, three fold episodes and later thrusts involved structures of SW vergence, followed by a late fracture phase (Mantero *et al.*, 2011 and Silva *et al.*, 1990). Therefore, deep seismic refraction and reflexion (Díaz and Gallart, 2009) profiles indicate that crustal detachments are delineated within the Variscan cover. The South Portuguese Zone is divided into the following structural and stratigraphic subdomains from north to south: the Beja-Acebuches Ophiolitic Complex, the Pulo do Lobo Domain, the Volcano-Sedimentary Complex and the Southern Domain (Oliveira, 1990 and Silva *et al.*, 1990). The studied area is located in Southern Domain, and is mainly formed by metapelitic rocks.

Since early Cretaceous, large magmatic episodes occurred along the west margin of the Iberian Peninsula, probably associated with the motion of the Iberian plate above a mantle plume (Merle *et al.*, 2009). Onshore, the main subvolcanic complexes of late Cretaceous age are NNW-SSE aligned and include the massifs of Sintra, Sines and Monchique (Fig. 5.1A). Although there is no surface evidence, a large NNW-SSE crustal structure (the Sintra-Sines-Monchique fault) has been proposed as a weakness that facilitates magma ascent (Ribeiro *et al.*, 1979). The Monchique Alkaline Complex is the largest and youngest complex, and it is located in the Southern Domain of the South Portuguese Zone, north of the Algarve Basin. Rock (1978) describes this massif as a subvolcanic laccolith emplaced into late Carboniferous marine sediments. The age of the alkaline rock is around 72 Ma (Miranda *et al.*, 2009). It has an E-W elliptical shape, probably controlled by ESE-WNW Variscan fractures, with a concentric structure formed mainly by two nepheline sienite bodies (Valadares and González Clavijo, 2004). These fractures were reactivated as normal faults during the formation of the Algarve Basin (Ribeiro *et al.*, 1990).

The Algarve Mesozoic Basin is located at the southern tip of Portugal and is characterized by carbonate sediments with a few levels of sandstone, marls and clays (Heimhofer *et al.*, 2008). It overlays the South Portuguese Zone, separated by an angular unconformity. These Mesozoic deposits are formed by the collapse and dismantling of the Variscan orogen. They accumulated in a passive margin developed in an extensional regime during the opening of the Atlantic and Tethys oceans. The Mesozoic section is characterized by a sharp thickening toward the south across ENE-WSW flexures trending subparallel to the coastline (Ribeiro *et al.*, 1984). These flexures are most likely connected with basement normal faults that formed during the extensional tectonics related to margin rifting (Ribeiro *et al.*, 1990). At any rate, some compressive episodes have been identified, and a clear tectonic inversion occurred during the Alpine orogeny (Manuppella *et al.*, 1988, Terrinha, 1998 and Terrinha *et al.*, 2002). As a consequence, the Cenozoic evolution of the Algarve basin is characterized by the compressional reactivation of Variscan basement faults and the deformation of the Mesozoic deposits. At present, the main alignments identified by photo interpretation have NNE-SSW, N-S and ENE-WSW orientations, probably corresponding to the most important brittle structures in the region (Moniz *et al.*, 2003).

5.3 Methodology

This research explores the crustal structure of the westernmost Betic Cordillera foreland using magnetic (aeromagnetic and new field data) and gravity methods combined with field observations.

The aeromagnetic anomaly map for the Iberian Peninsula mainland (Socias and Mezcua, 2002) is the result of compiling the aeromagnetic anomaly maps of Portugal (Miranda *et al.*, 1989) and Spain (Ardizone *et al.*, 1989). The flight lines considered were oriented N-S and spaced 10 km, while E-W control lines were separated 40 km. Flight barometric elevation was 3000 m above sea level with an

accuracy of 30 m. Data acquired in this survey enabled us to determine the major crustal structures.

Field surveys are necessary to study regional anomalies in detail. Total magnetic field data were measured using a GSM 8 proton precession magnetometer with an accuracy of 1 nT at a mean height of 2 m above the topography. Susceptibility measurements were done with an Exploranium KT-9 kappameter. Magnetic measurements were taken in May 2010 and January 2011, with a mean spacing of 500 m, along two NNW-SSE profiles (Portimão-Odemira and Olhão-Castro Verde) in the Algarve Basin, and an E-W profile across the Guadiana River (Fig. 5.2). Because anthropic noise, such as electric power lines or ferromagnetic material, distorts the natural magnetic field, magnetic measurements were not acquired near settlements. Total field magnetic anomalies were calculated through a standard procedure including reduction to the IGRF 2010 (IAGA, 2010). Diurnal variations were corrected considering the total field intensity data of the nearest permanent magnetic station in San Fernando (Cádiz, Spain), which belongs to the Royal Army Observatory (www.intermagnet.org). In turn, 2D magnetic models were calculated using GRAVMAG V.1.7 software of the British Geological Survey (Pedley *et al.*, 1993). This software makes it possible to remove the regional trend and model the residual magnetic anomaly.

Simultaneous modelling of aeromagnetic and field magnetic anomalies may help determine the magnetic body depth: the difference between the magnetic anomaly intensity determined with the two methods decreases when the body depth increases.

Along the E-W Guadiana River profile, gravity measurements were performed simultaneously with the magnetic data acquisition in order to confirm and characterize the sharp gradient. These data were gathered using a Scintrex Autograv CG-5 gravity meter whose maximum accuracy is 0.001 mGal. Measurement cycles were a complete working day, since this gravity meter features tidal correction. Measurements were referenced to the Granada base

station of the Instituto Geográfico Nacional (IGN) (Spain) gravimetric network to calculate the absolute gravity value. Complete Bouguer anomaly was determined with a reference density of 2.67 g/cm^3. It includes a terrain correction determined by Hammer circles (Hammer, 1939 and Hammer, 1982) for a total distance of 22 km from the stations (B-M zones) using the SRTM3 NASA digital terrain elevation model (http://www2.jpl.nasa.gov/srtn/) with 90 m of cell size.

Location of field magnetic and gravity sites was determined using a Garmin Dakota model global positioning system (GPS) receiver, with an accuracy higher than 5 m, which includes a barometric altimeter with an accuracy of 1 m. In addition, during the measurement cycles, a barograph located near the base station was used to correct apparent diurnal variations in elevation due to the atmospheric pressure evolution.

5.4 Magnetic anomaly dipole in SW Iberia

Aeromagnetic data reveal that the onshore southwestern Iberian Peninsula is characterized by an intense E-W elongated dipole about 200 km in length (Fig. 5.2). The mean width of the magnetic dipole is 80 km. Although the maximum in the westernmost side is well constrained, reaching 280 nT, eastward it is located offshore and is not covered by the aeromagnetic data. Toward the north, the minimum is as low as -74 nT; it is disrupted along the Guadiana River by a N-S sharp gradient (roughly 20 nT) decreasing westward, right at the Spain-Portugal border.

Field magnetic anomaly data were acquired to confirm the main features of the aeromagnetic anomalies and to compare both sets of anomaly data. Two N-S profiles are located along transects of the main dipole, in the area of the most intense anomalies (Portimão-Odemira) (Fig. 5.3A) and eastward, in the best accessed cross section (Olhão-Castro Verde) (Fig. 5.3B).

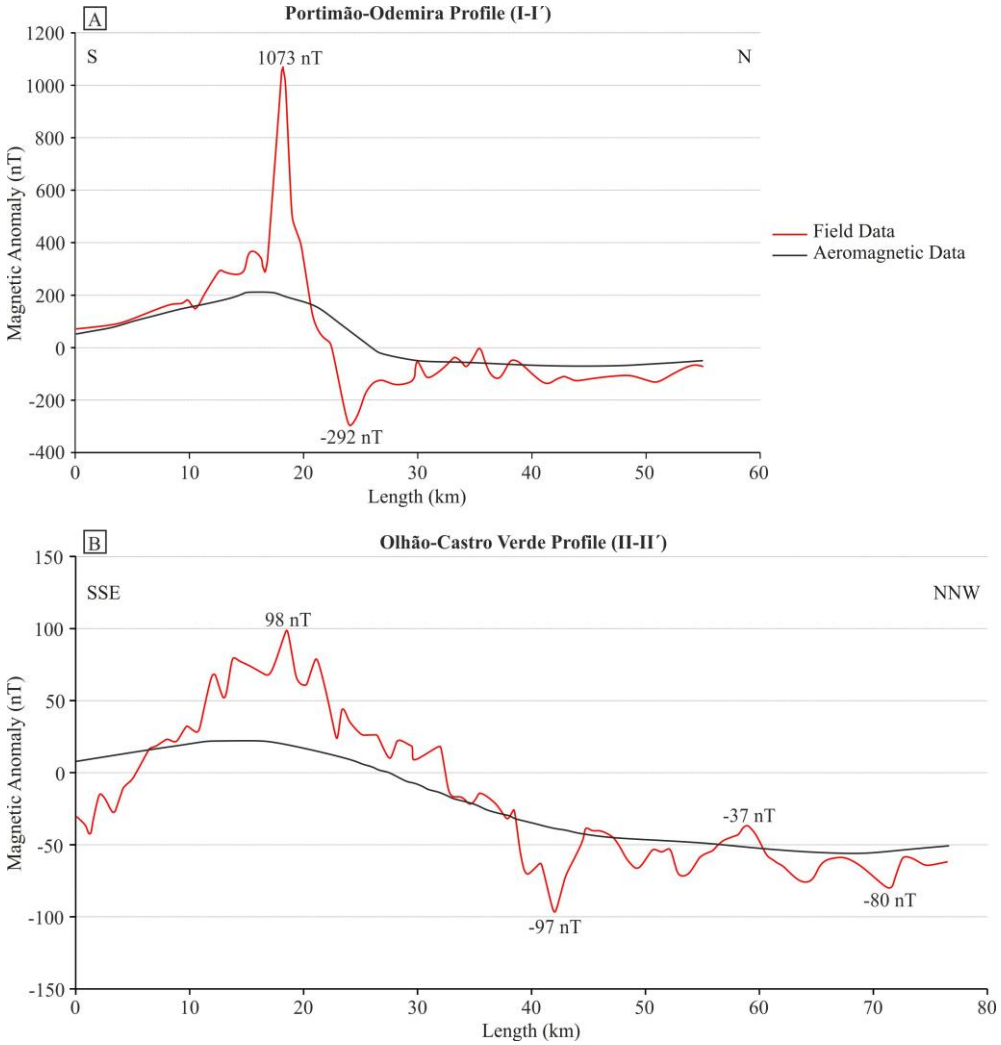

Figure 5.3: Magnetic anomalies along the Portimão-Odemira (A) and the Olhão-Castro Verde (B) profiles. Vertical scale is different in both profiles because of the different magnitude range of the anomalies.

The Portimão-Odemira field profile reaches 1073 nT in the southern maximum and down to -292 nT in the northern minimum, and extends northward with a wide region of negative anomalies around -70 nT. Aeromagnetic data show the same anomaly trends, although anomaly values are smoother than field data, with a difference of over 750 nT in the maximum.

The Olhão-Castro Verde profile shows the same dipole, yet most of the profile is characterized by negative anomaly values. The aeromagnetic maximum is 22 nT and the minimum is -56 nT, while the field data have a maximum of 98 nT

and a minimum of -97 nT extending along a region of negative anomalies comprised between -37 nT and -80 nT. Metapelites are the only exposed rocks along the profile, and they show a magnetic susceptibility of 0.00018 (SI).

In addition, an E-W profile along the minima crosses the Guadiana River (Fig. 5.2). It was acquired along a Portuguese road providing good access, and then extends to Spain along a field path where it was difficult to take regular measurements. The profile confirms the sharp gradient reflected by aeromagnetic data, although the field anomalies are more irregular and intense (Fig. 5.4A).

5.5 Magnetic anomaly models

Along both N-S profiles, 2D aeromagnetic and field magnetic anomaly models (Fig. 5.5) were developed to discern the shape and depth of the anomalous magnetic body. The combination of these data is essential for characterizing the depth of the body.

The sienite of Monchique Alkaline Complex are the only outcropping rocks that may cause magnetic anomalies in the whole region. They are exposed in the Portimão-Odemira profile, which also crosses the most intense anomalies (Fig. 5.1, Fig. 5.2 and Fig. 5.3A). Hence, this profile is the best one for constraining the main features of the anomalous magnetic body.

Field measurements of magnetic susceptibility in Monchique sienites have a mean value of 0.029 SI, which is also in the range proposed for these rocks (Telford *et al.*, 1990). Magnetic modelling accounts only for the contrast in magnetic susceptibility. In the Portimão-Odemira profile, the best fit is obtained considering 0.034 SI susceptibility (Fig. 5.5A), slightly higher than field measurements. Although remnant magnetization may occur, it would have the same orientation as the induced magnetization, because the dipole shows a normal attitude. It may cause slightly higher susceptibility values in the model than those obtained by field measurements. Still, the Olhão-Castro Verde profile is modelled

with a susceptibility of 0.025 SI (Fig. 5.5B), which is also in the range of these types of rocks.

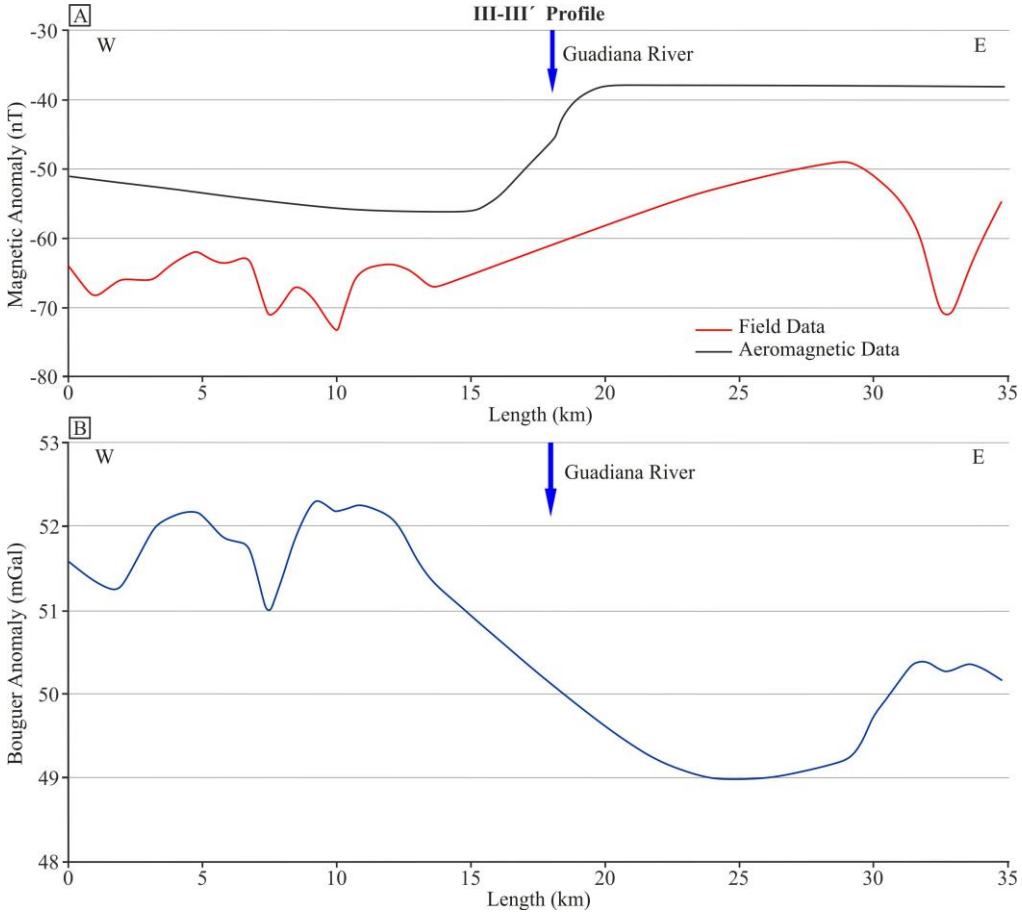

Figure 5.4: Magnetic and Gravity profiles across the Guadiana River. (A) Magnetic anomalies. (B) Bouguer anomaly.

In the southern side of the Portimão-Odemira profile (Fig. 5.5A), the body crops out along a 5.5 km stretch. The best model of both field and aeromagnetic anomalies is obtained when a moderately northward decreasing regional magnetic anomaly is considered. In this section it has an asymmetric lenticular shape that is 35 km long and thins northward. The maximum thickness is more than 3 km.

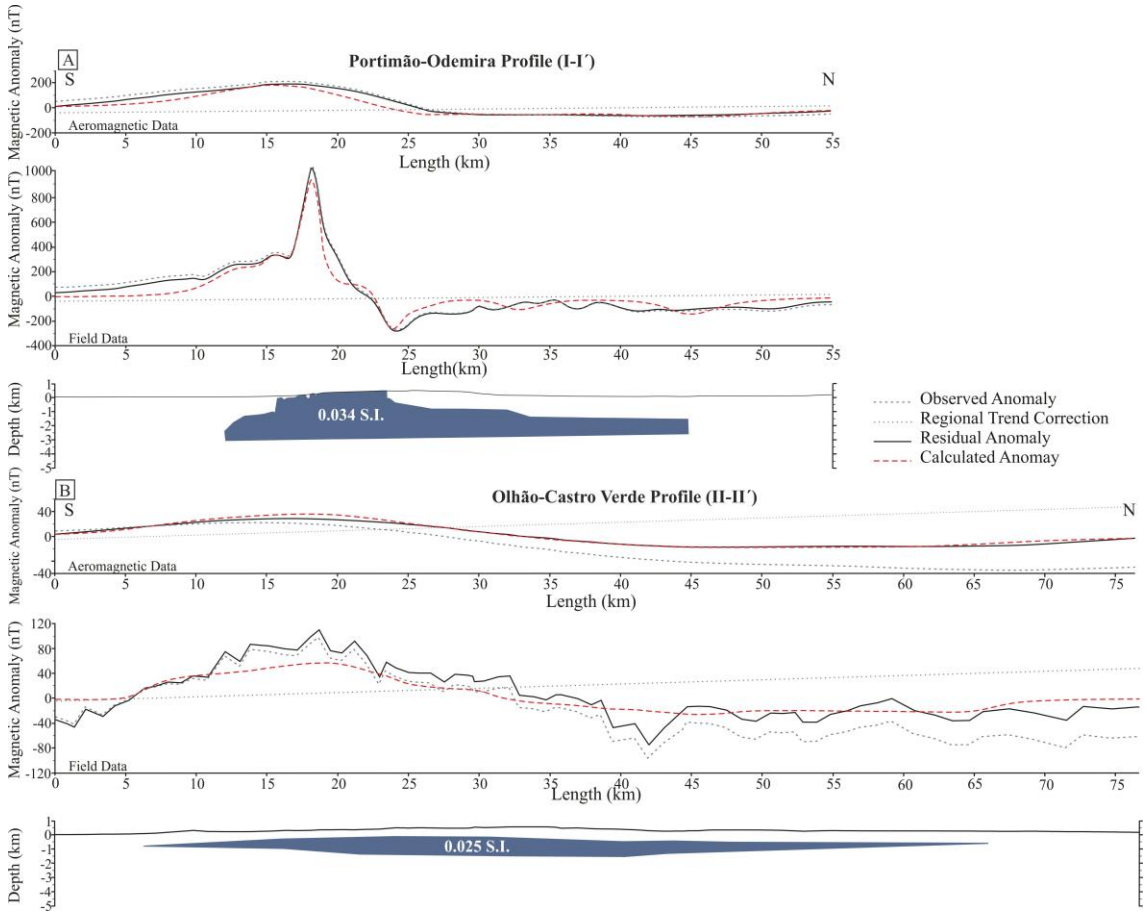

Figure 5.5: Total field intensity magnetic anomalies and magnetic models of Portimão-Odemira (A) and Olhão-Castro Verde (B) profiles.

The eastward extension of the magnetic dipole in the Olhão-Castro Verde profile (Fig. 5.2) suggests that the magnetic anomalies are related to the same body, which does not outcrop. However, the wide and intense minima in contrast with the low maxima make modelling difficult. Induced magnetism in this region always produces more intense maxima than minima, unlike the observed field and aeromagnetic anomalies (Fig. 5.2 and Fig. 5.3). Moreover, if reverse remnant magnetism occurred, the dipole should be opposite the observed one, with maxima located northward and minima southward. Thus, the only way to fit a model is by taking into account an external negative regional anomaly (Fig. 5.5B). In this case, the combined aeromagnetic and magnetic anomalies point to the presence of a relatively shallow body, 50 km wide and with a lenticular cross section.

5.6 Gravity, geomorphological and fracture evidences of the Guadiana River structure

One of the most interesting features of the aeromagnetic anomaly is the sharp N-S gradient observed along the Guadiana River (Fig. 5.2), confirmed by field magnetic measurements (Fig. 5.4A). To date, available geological maps do not identify any structure that might correspond to this feature. Based on new field gravity data, as well as geomorphic and structural observations, we analysed its origin.

Gravity observations along the E-W profile (Fig. 5.4B) confirm that the structure is different on the two sides of the Guadiana River. Despite Bouguer Anomaly irregularities, a sharp eastward decrease of more than 2 mGal is observed. The absence of other geophysical data to help constrain the crustal bodies impedes development of an accurate gravity model. In sum, both gravity and magnetic data confirm the presence of this clear N-S structure along the Guadiana River.

The Guadiana River channel has several N-S to NNW-SSE rectilinear segments that coincide with the structure revealed by geophysical data. They extend 34 km from Sanlúcar del Guadiana to the mouth of the river (Fig. 5.6). Three main segments may be differentiated from N to S. The first, approximately 5 km length and the most irregular, has a smooth curvature and ends southward in two sharp meanders. The second segment runs along 14 km, as far as a broad curve in the channel. The third one is the most rectilinear and extends 8 km, up to the mouth. Seven kilometers correspond to the two short curved connections. The three segments are aligned and suggest the presence of a rectilinear structure.

Metapelite outcrops are similar on either side of the rectilinear channel. The foliation has a N110ºE dominant trend and dips northeastward. The fractures are frequent but concentrated in narrow bands, mainly corresponding to joints and reverse faults. Only one set of N-S to NNW-SSE joints evidences the presence of

a tectonic structure coinciding with the orientation of the Guadiana river rectilinear channels (Fig. 5.6).

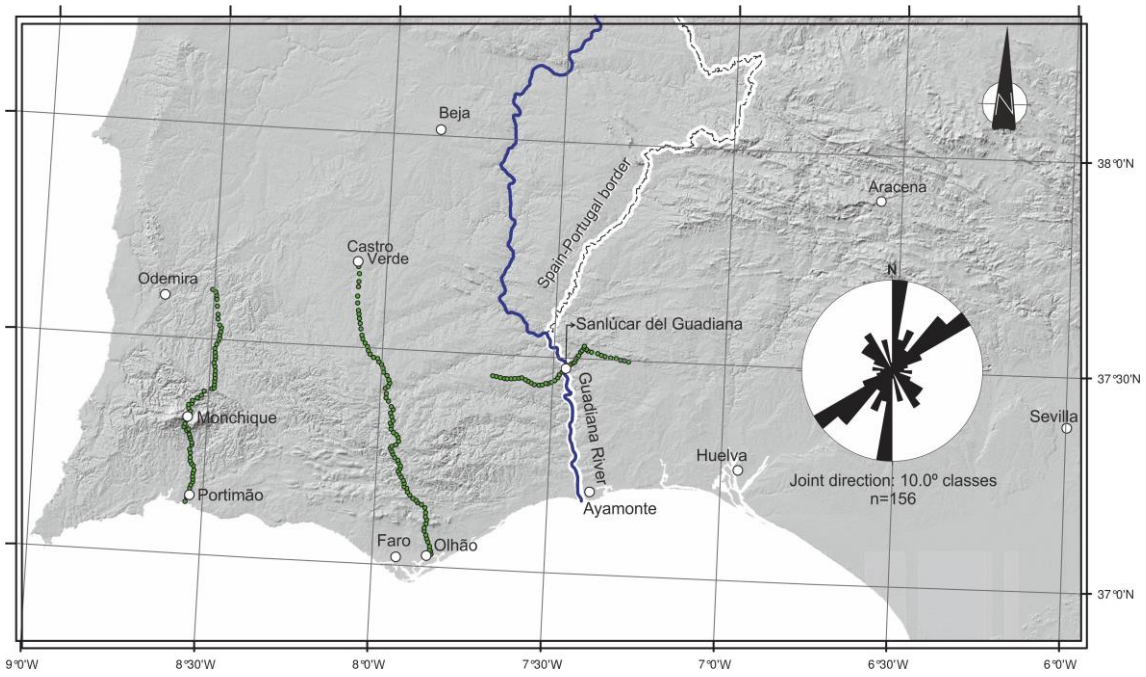

Figure 5.6: MDT showing profile locations, Guadiana river sinuosity and joints rose diagram.

5.7 Discussion

Magnetic anomalies enable us to discern deep structures in regions intruded by intermediate or basic igneous rocks. They provide new insights regarding the geological evolution of the Antarctica, covered by a thick ice sheet (Galindo-Zaldívar *et al.*, 2013). Such anomalies reveal the presence of bodies located in the upper crust, to a depth with temperatures cooler than the Curie Point. This temperature limit is between 550 ºC and 600 ºC for most ferromagnetic minerals (Telford *et al.*, 1990) and is reached in a normal geothermal gradient at about 30 km (Maus *et al.*, 1997).

Although magnetic data generally must be supported by other geophysical data to constrain body features, the combination of aeromagnetic and field measurements is a sound tool for characterizing a body and determining its depth. Gravity data support the presence of crustal structures. The South Portuguese

Zone and the Algarve Basin constitute a region suitable for integration of such data, particularly due to the absence of other detailed geophysical research and the homogeneous outcropping lithology.

The origin of the largest dipole of the South Portuguese Zone is clearly related to the Monchique Alkaline Complex, as the most intense anomalies are caused by the sienite outcrops of this complex. Northward the study area, another magnetic anomaly dipole can be observed (Fig. 5.2). The most intense anomalies related to this dipole are located at the northern edge of the Volcano-Sedimentary Complex outcrops and could also be produced by Ossa Morena Zone basic rocks. Anyway, the influence of this dipole is negligible in the studied Monchique Alkaline Complex dipole. In the absence of other sources of magnetic anomalies in the South Portuguese Zone and the Algarve Basin, the E-W elongated dipole of up to 200 km in length suggests that this body extends laterally at shallow crustal levels, below the outcropping metapelites. Comparison of aeromagnetic and field magnetic anomalies indicates that the depth of the body increases progressively eastward, with a sharp step along the Guadiana River.

The models of the magnetic anomalies constrain the geometry of the sienite laccolith along the Portimão-Odemira profile accurately, pointing to a roughly lenticular and asymmetrical section extending in depth toward the north. This geometry is typical of large laccolith plutons emplaced in the upper crust. The best models obtained in the Olhão-Castro Verde profile suggest a similar section of this body eastward. However, because the regional negative magnetic anomalies were more intense than the positive ones, it was necessary to remove a negative anomaly in order to model the anomaly along this profile.

This wide region of negative magnetic anomalies affecting the whole dipole may have an external origin, as suggested in the modelling section. The regional values for both aeromagnetic and magnetic anomalies were similar, although calculated with different geomagnetic reference fields (Portugal, IGRF 1980; Spain, IGRF 1985 for aeromagnetic and IGRF 2010 (IAGA, 2010) for field

magnetic measurements). Hence, it is not a consequence of mis-estimation of the IGRF fields. The region is affected by the minima related to a major dipole, probably associated with the oceanic crust that floors the Gulf of Cádiz to the south (e.g. Roest *et al.*, 1996).

Magnetic and gravity data (Fig. 5.4) support the presence of a N-S crustal discontinuity along the Guadiana River, just at the Spain-Portugal border. Field geophysical data confirm the accuracy of aeromagnetic data and the presence of this structure, previously undetected by field geological observations. The most intense anomalies are reached by shallow bodies, and they decrease as they become deeper, for the same magnetization intensity. The minima values in the western side of the Guadiana River are 20 nT less than on the eastern side, most likely due to a sharp step in the lateral extension of the anomalous body. Two N-S profiles on the E and W sides of the river were modelled, removing a regional negative anomaly, to show the sharp increase in depth of the anomalous body eastward (Fig. 5.7). In addition, the dipole maximum corresponding to the eastward profile lies offshore, so that the aeromagnetic map shows only the minimum values, and the body extends to the south beyond the modelled section. Therefore, we lack sufficient data to constrain the geometry of the body and accurately estimate the step in depth. Yet these profiles show that only a depth difference of the body would explain the sharp gradient in the anomaly values.

Crustal faults generally have a geomorphic expression because they affect the present-day relief or constitute previous heterogeneities that are underlined during erosion. Faults generally determine the rectilinear character of river channels (Keller and Pinter, 1996). In covered areas or in regions with homogeneous lithology, analysis of the fluvial network is essential for this purpose. Whereas several N-S faults have been described offshore (Lopes *et al.*, 2006) no fault has been observed along the Guadiana River, characterized by homogeneous metapelite outcrops.

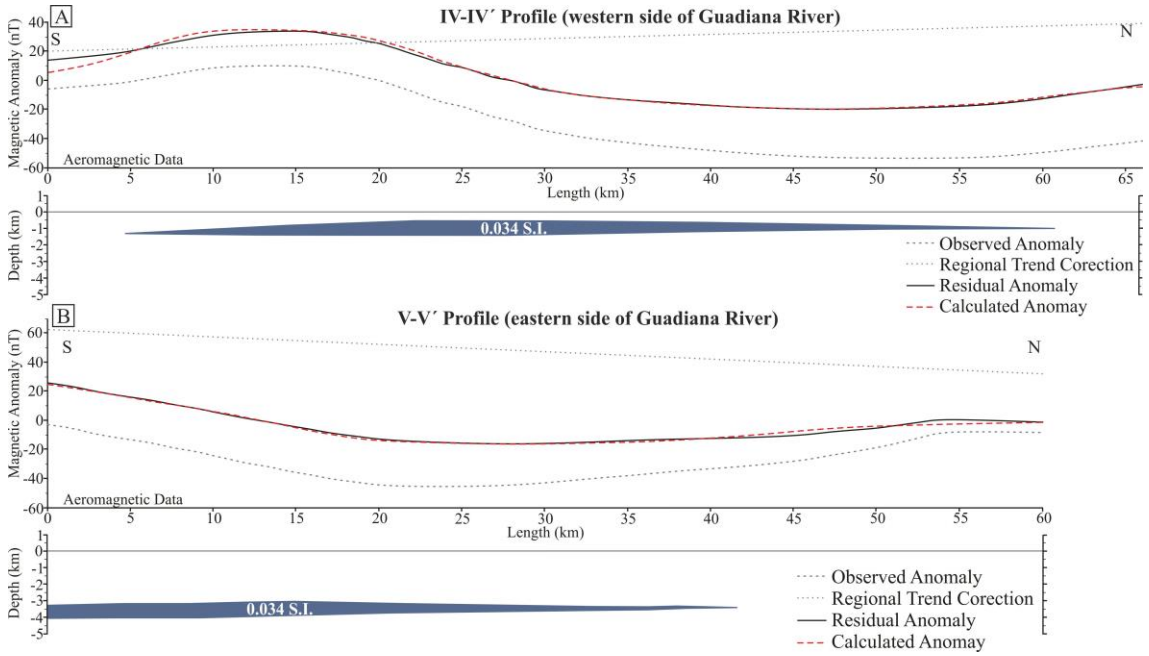

Figure 5.7: Anomalous body depth and influence in the values of the minimum aeromagnetic anomaly. N-S aeromagnetic models in both E and W sides of the Guadiana River.

Just one set of joints (Fig. 5.6) follows the trend of this structure. The rectilinear trace of the Guadiana River channel evokes the surface effects of this heterogeneity.

These apparently contradictory geophysical and geological data throw new light on the late Variscan to Alpine evolution model of the region studied. The sharp structure is probably a N-S subvertical Variscan fault affecting at least the upper crust and representing a crustal discontinuity. Metapelite units that crop out at surface are probably displaced by the late Variscan thrusts with respect to the basement, previously affected by the N-S crustal fault. The Monchique Alkaline Complex, Cretaceous in age, would have been emplaced in this heterogeneous crust and led the fault surface to have a sharp steep geometry. Finally, during Alpine orogeny, this previous discontinuity contributed to the development of a N-S to NNW-SSE fracture set and broadly determined the linear segments of the Guadiana River channel. In this context, the Guadiana Fault may be considered one of the main crustal faults of the South Portuguese Zone and the

Algarve Basin basement, right along the Spain-Portugal border, but having only a gentle expression at present.

5.8 Conclusions

The southwestern part of the Iberian Peninsula constitutes the foreland of the Betic Cordillera and is characterized by a large N-S dipole elongated in an E-W direction, measuring 200 km in length and more than 50 km in width. This anomaly is related to the Monchique Alkaline Complex, featuring the highest mean magnetic susceptibility values of the whole region (0.029 SI). Overprinted on the dipole, the area is affected by negative magnetic anomaly values, probably related to the nearby oceanic crust of the Gulf of Cádiz, southward.

Simultaneous 2D modeling of aeromagnetic and field magnetic data along several profiles allowed us to constrain the depth of the bodies responsible for the anomalies between 0 and 3.5 km (Fig. 5.8). The Portimão-Odemira profile crosses the sienites of the Monchique Alkaline Complex, indicating a roughly lenticular shape 50 km wide. The best value for magnetic susceptibility in models is 0.034 SI, slightly higher than field values, suggesting low remnant magnetization. The E-W elongated anomaly dipole supports a body elongation of about 200 km.

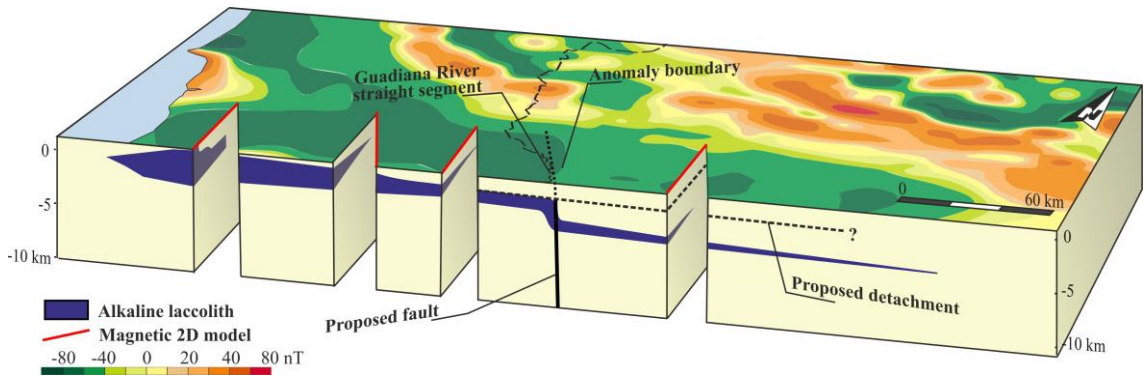

Figure 5.8: 3D Diagram of the Monchique laccolith and Guadiana River Fault.

A large N-S linear discontinuity was identified along the Guadiana River and near its mouth, on the basis of magnetic and gravity data. Rectilinear channel segments and joints support the presence of this structure, interpreted as a major blind crustal fault, the Guadiana Fault (Fig. 5.8), probably of late Variscan age. This anisotropy entails a sharp step, rising westward, of the Cretaceous laccolith across the Guadiana River.

Integration of aeromagnetic, field magnetic and gravity data is a suitable methodology to characterize the upper crustal structure of the Betic Cordillera Variscan basement and foreland. In addition, it may prove useful to identify the presence of large faults affecting rocks with magnetic properties that are not revealed by field geological observations.

Acknowledgements

We are very grateful to F. Alonso-Chaves and an anonymous reviewer for the positive comments that have contributed to improve this paper. The first author has a FPU grant of the Spanish Ministry of Education. The results presented in this paper rely on the data collected at San Fernando Intermagnet observatory (www.intermagnet.org). This research was supported by the Consolider-Ingenio 2010 Program (Topo-Iberia project CSD2006-0041), CGL2010-21048, P09-RNM-5388, and RNM-148 projects.

Chapter 6

Influence of a narrow strait connecting a large ocean and a small sea on magnetotelluric data: Gibraltar Strait

Lourdes González-Castillo [1], Andreas Junge [2], Jesús Galindo-Zaldívar [1, 3], Alexander Löwer [2].

Submitted to:

Journal of Applied Geophysics, 2015

(Received 18 February 2015)

[1] Departamento de Geodinámica, Universidad de Granada, Spain.

[2] Institut für Geowissenschaften, Goethe Universität Frankfurt/Main, Germany.

[3] Instituto Andaluz de Ciencias de la Tierra. CSIC-UGR. Spain.

ABSTRACT

Long period magnetotelluric (LMT) data are generally used as the prime tool to shed light on the conductivity of the deep crust and upper mantle structure. LMT allows for deep study of the lithospheric tectonic plates and the asthenosphere dynamics. Because it investigates the variability of the upper mantle conductivity at different depths, LMT complements seismic data. Naturally, LMT data are sensitive to the influence of highly conductive bodies even at far distances. Sea water constitutes the main widespread electrical conductor at shallow levels of the Earth crust. Its low resistivity values, around 0.25 Ω·m, contrast sharply with most geological structures of solid earth. Consequently, the presence of irregular continental borders and varying bathymetries significantly influences LMT parameter, such as phase tensor and tipper vectors. This effect is especially important in areas where large and small oceans are connected by narrow gateways. The Gibraltar Strait (southern Spain) connects the vast Atlantic Ocean with the irregular and relatively small Mediterranean Sea. Several 3D models have been developed in the region nearby the Strait, some featuring a roughly simplified geological structure, to show the influence of seawater on tipper and phase tensor. Here, detailed bathymetry (General Bathymetric Chart of the Oceans, GEBCO) including the coastline is considered in a model that enables us to analyse the influence of the Strait of Gibraltar on LMT data. We stress the significance of the Sea for LMT data interpretation and the development of 3D conductivity models, especially in regions involving complex coastline geometries and bathymetry near narrow straits. Forward modelling studies are essential to accurately appraise the sea influence, which may mask 3D geological structures.

Keywords: Long Period Magnetotellurics (LMT); 3D models; Phase tensor; Tipper vector; Bathymetry; coast effect.

Highlights

- Detailed bathymetry is essential in magnetotelluric 3D modelling nearby the sea.
- Narrow straits represent connection channels that increase sea effects.
- An irregular coastline influences tipper behaviour.
- 3D forward modelling precisely determines geological features and sea effect.

6.1 Introduction

Long period magnetotelluric research (LMT) is the main geophysical prospecting method used to reveal the resistivity structure of the Lithosphere (Vozoff, 1980; Jones, 1992; García-Castellanos *et al.*, 2009). LMT data complement the results obtained by seismic reflection (Jones, 1987) and seismic tomography studies (Vauchez and Tommasi, 2003) that reveal the main features of the deep crust and upper mantle. However, the ocean, constituting the main conductive body (around 0.25 Ω·m) above the solid earth, has an influence recognized even in early studies that tried to constrain coastal effects (Mackie *et al.*, 1988; Dosso and Meng, 1992). Most research performed near the coast or on islands takes the sea effect into account (Heise *et al.*, 2007; Monteiro Santos *et al.*, 2001; Pous *et al.,* 2002; Yang *et al.*, 2010, Key and Constable, 2011; Piña-Varas *et al.*, 2014). A recent study by Malleswari and Veeraswamy (2014) presented numerical 2D models to study the TE and TM phase tensor modes and test the suitability of long period magnetotelluric data to explore deep earth structures; they conclude that the coast effect depends on land distance, land resistivity and depth to the top of the conducting asthenosphere. The deeper the structure to be investigated, the further from the coast line the measurements should be taken. For regular coastlines, and 2D models orthogonal to the continental margins, the Sea influence may be accurately constrained. Yet in areas with irregular coastal geometries, variable bathymetries and narrow straits, 2D models do not provide accurate solutions, distinguishing the geological structures from the sea effect.

A unique setting to try to reveal the sea's influence on LMT models is the Gibraltar Strait (Fig. 6.1) in the westernmost part of the Mediterranean Sea. It is the narrowest gap located between two continents and constitutes a highly conductive channel between a large ocean (Atlantic Ocean) and a small sea (Mediterranean Sea). The Gibraltar Strait was formed by interaction between the Eurasian and African plates and the westward motion of the Alborán domain during the Alpine orogeny that developed the Gibraltar Arc. This arcuate

mountain belt connects the Betic Cordillera in the Iberian Peninsula and the Rif Cordillera in North Africa. Although the deformation started in Late Cretaceous, most of the present-day relief formed in the last 10 Ma, since Late Miocene (Braga *et al.*, 2003). At this time, the Atlantic Ocean and Mediterranean Sea were connected. During the Messinian salinity crisis (5.96 Ma) the narrow continental connection between Africa and Eurasia isolated the Mediterranean Sea. This connection was dramatically broken 5.33 Ma ago, and initially controlled by the tectonic subsidence of the Gibraltar sill. High rates of erosion caused the abrupt flooding of the Mediterranean Sea in a short period of time (between a few months and two years) (García-Castellanos *et al.*, 2009).

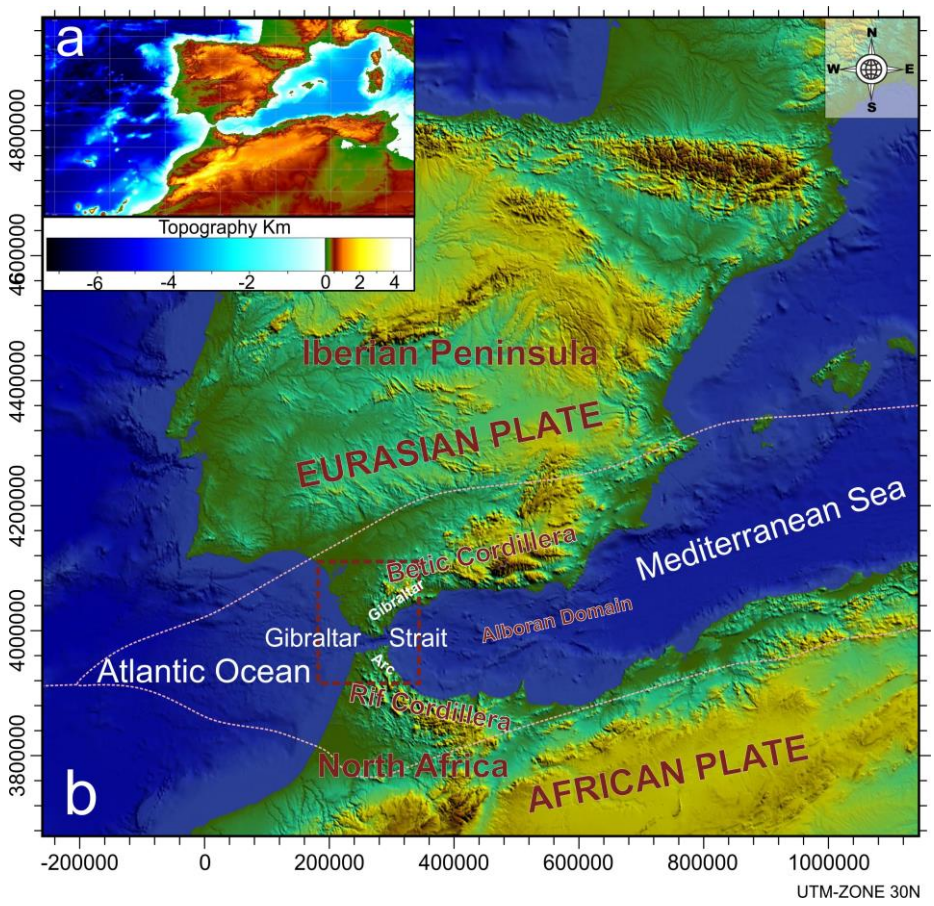

Figure 6.1: Bathymetry of the Gibraltar Strait area according to GEBCO v.2.13 (British Oceanographic Data Centre, www.gebco.net). (a) Whole area considered for modelling. (b) Enlarged sector including Gibraltar Strait. The red square indicates the area illustrated in Fig. 6.2.

This study describes the effect of a narrow strait on magnetotelluric transfer functions such as phase tensor and tipper vectors. To analyse these effects, we selected the Gibraltar Strait as the optimal natural example. In addition to folding 3D forward models suitable for highly resolved bathymetry, we evaluate the influence of the sea and a narrow strait to contribute to future research involving hypothetical major geological structures in nearby regions.

6.2 Methodology

The MT variables most commonly used are frequency dependent transfer functions between the natural time variations of the magnetic and electric field (Chave and Jones, 2012). The field components observed at different locations on the Earth's surface are the magnetic induction $\underline{B} = (B_x, B_y, B_z)^T$ and the telluric field $\underline{E} = (E_x, E_y)^T$. Usually the observed time series are transformed into the frequency domain such that B and E are complex values and functions of space and frequency. They are connected by the impedance tensor $\boldsymbol{Z}$ and by the tipper vector $\underline{T}$ through the linear and frequency dependent relationships

$$\begin{pmatrix} E_x \\ E_y \end{pmatrix} = \begin{pmatrix} Z_{xx} & Z_{xy} \\ Z_{yx} & Z_{yy} \end{pmatrix} \begin{pmatrix} B_x \\ B_y \end{pmatrix}$$

$$B_z = T_x B_x + T_y B_y$$

with $\boldsymbol{Z} = \begin{pmatrix} Z_{xx} & Z_{xy} \\ Z_{yx} & Z_{yy} \end{pmatrix}$ and $\underline{T} = \begin{pmatrix} T_x \\ T_y \end{pmatrix}$.

Often the impedance tensor $\boldsymbol{Z}$ is influenced by frequency independent distortions due to near surface conductivity inhomogeneities. It can be shown that the phase tensor Φ is independent from such distortion (Caldwell *et al.*, 2004). It is related to the impedance tensor $\boldsymbol{Z}$ by

$$\boldsymbol{\Phi} = \boldsymbol{Z}_r^{-1} \boldsymbol{Z}_i$$

with $\mathbf{\Phi} = \begin{pmatrix} \Phi_{xx} & \Phi_{xy} \\ \Phi_{yx} & \Phi_{yy} \end{pmatrix}$ and Z_r and Z_i as the real and imaginary parts of Z. Among different presentations of ϕ (cf Booker, 2013), in this study the phase tensor is displayed by $\boldsymbol{\phi} = \tan^{-1} \mathbf{\Phi}$ (Häuserer and Junge, 2011).

The spatial and frequency dependency of $\boldsymbol{\phi}$ and T is modeled for 3D conductivity structures using Comsol Multiphysics (Häuserer and Junge, 2011). Basics of MT modelling with Comsol Multiphysics are described by Kütter (2009). The bathymetry is included in the model using the General Bathymetric Chart of the Oceans (GEBCO, www.gebco.net). It provides a digital terrain model of 30 arc-second grid sizes that is precise enough to consider most of the main seafloor features for MT modelling. In addition, it delivers accurate coastline geometry.

6.3 The influence of the Gibraltar Strait on phase tensors and induction arrows

The influence of the Gibraltar Strait on phase tensors and induction arrows is investigated by comparing two 3D models (Fig. 6.2) —with and without a connection by sea water between the Mediterranean Sea and the Atlantic Ocean through the Strait of Gibraltar. The models take into account the Earth´s main structural layers and its roughly average resistivities: crust (0-30 km, 300 Ω·m), lithospheric mantle (30-100 km, 1000 Ω·m) and asthenosphere (>100 km, 25 Ω·m). The bathymetry was considered with a constant sea water resistivity of 0.25 Ω·m. For each model LMT transfer functions were calculated at 27 hypothetical sites equally distributed throughout Southern Spain and Northern Africa for periods between 10 – 10,000 s (Fig. 6.2).

For the shortest period of 10s, only the tipper vectors at the sites close to the coastline are affected by the sea water, whereas the phase tensor take on values of about 45°. Under increasing period, the influence of the sea water is seen at all sites. However, a comparison of the two models reveals significant differences only for the real part of the induction vectors; the imaginary part and the phase tensor

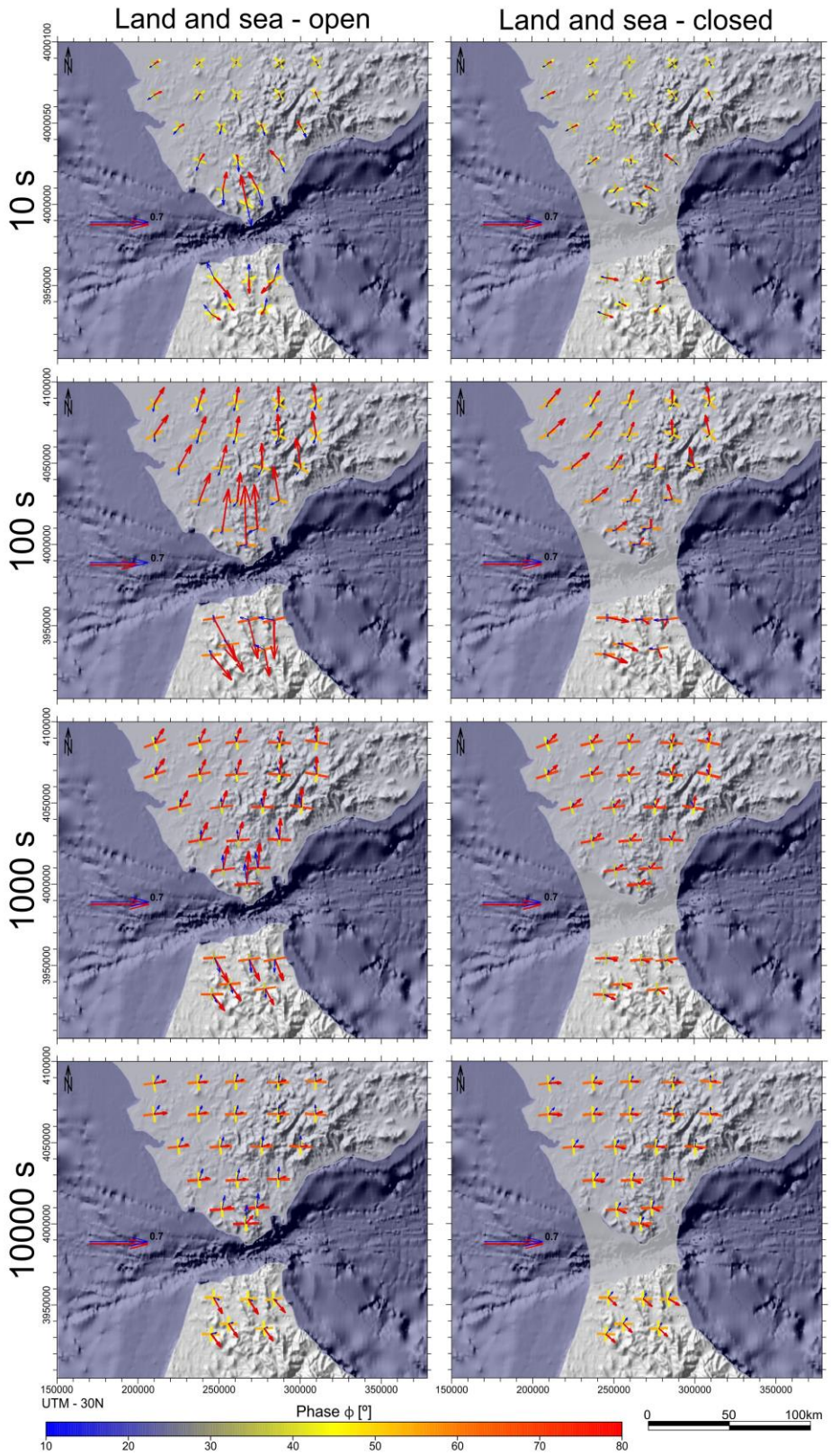

Figure 6.2: Comparison of transfer functions on a grid of hypothetical sites in Southern Spain and Northern Africa for open (left) and closed (right) Strait of Gibraltar. Real (red) and imaginary (blue) tipper vectors (Wiese convention) and phase tensor bars (colour coded) for periods of 10, 100, 1000 and 10,000 seconds. For further explanation see text.

remain similar even in close proximity to the Strait of Gibraltar. There, the real parts of the induction vector are conspicuously large for the open Strait model, and they are oriented perpendicular to the Strait. For the period of 1000s, the influence of the strait extends to all sites with smaller but comparable size. In turn, for 10,000s the influence of the Atlantic Ocean is dominant for all transfer functions except the imaginary part of the induction vector, which rotates at all sites from north via west to the south. The phase tensors show a consistent pattern for periods longer than 100s, with phases above 45° for the east-west bar and below 45° for the north-south bar, obviously caused by the extended sea water bodies to the east and west. Note that the sea water within the strait of Gibraltar does not affect the phase tensors, only the real induction vectors.

As the influence of the Sea reaches far inland for periods above 100 s, its influence is tested on representative hypothetical geological bodies (Fig. 6.3) related to existing structures in the area. The structures are an extended resistive and conductive fault zone (0-15 km depth, 7 km wide and 110 km long, 1000 and 10 Ω·m) (Figs. 6.3 and 6.4); a sedimentary basin (0-3 km, 60 km wide, 10 Ω·m) representing upper crustal bodies; and a zone of partial melt within the upper mantle (40-80 km, 70 km wide, 10 Ω·m) (Figs. 6.3 and 6.5). In general, for periods longer than 100 s the Ocean response dominates the transfer functions and hides the geological signals (Figs. 6.4 and 6.5).

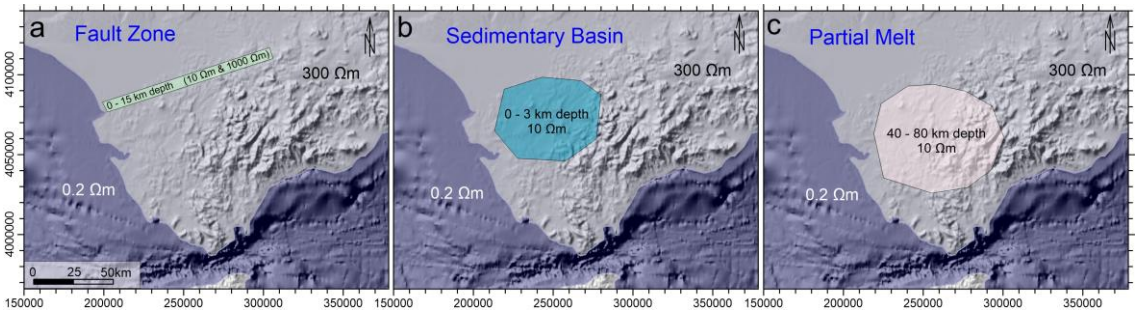

Figure 6.3: Location of hypothetical geological structures. A resistive (1000 Ω·m) and a conductive (10 Ω·m) fault zone were considered.

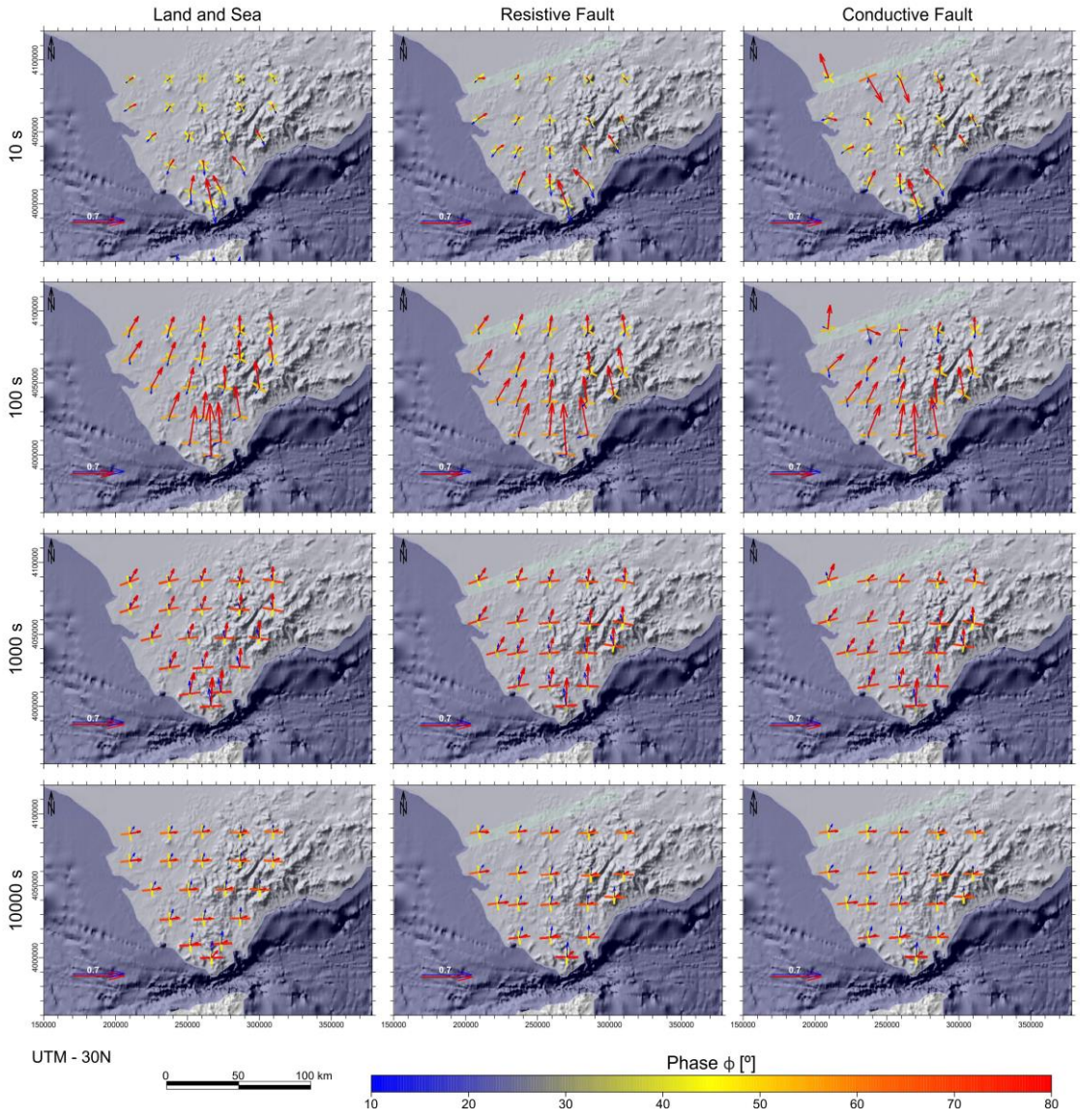

Figure 6.4: Comparison of transfer functions for different hypothetical geological structures: resistive and conductive fault zones (cf. open strait model in Fig. 6.2). Real (red) and imaginary (blue) tipper vectors (Wiese convention) and phase tensor bars (colour coded) for periods of 10, 100, 1000 and 10,000 seconds. For further explanation see text.

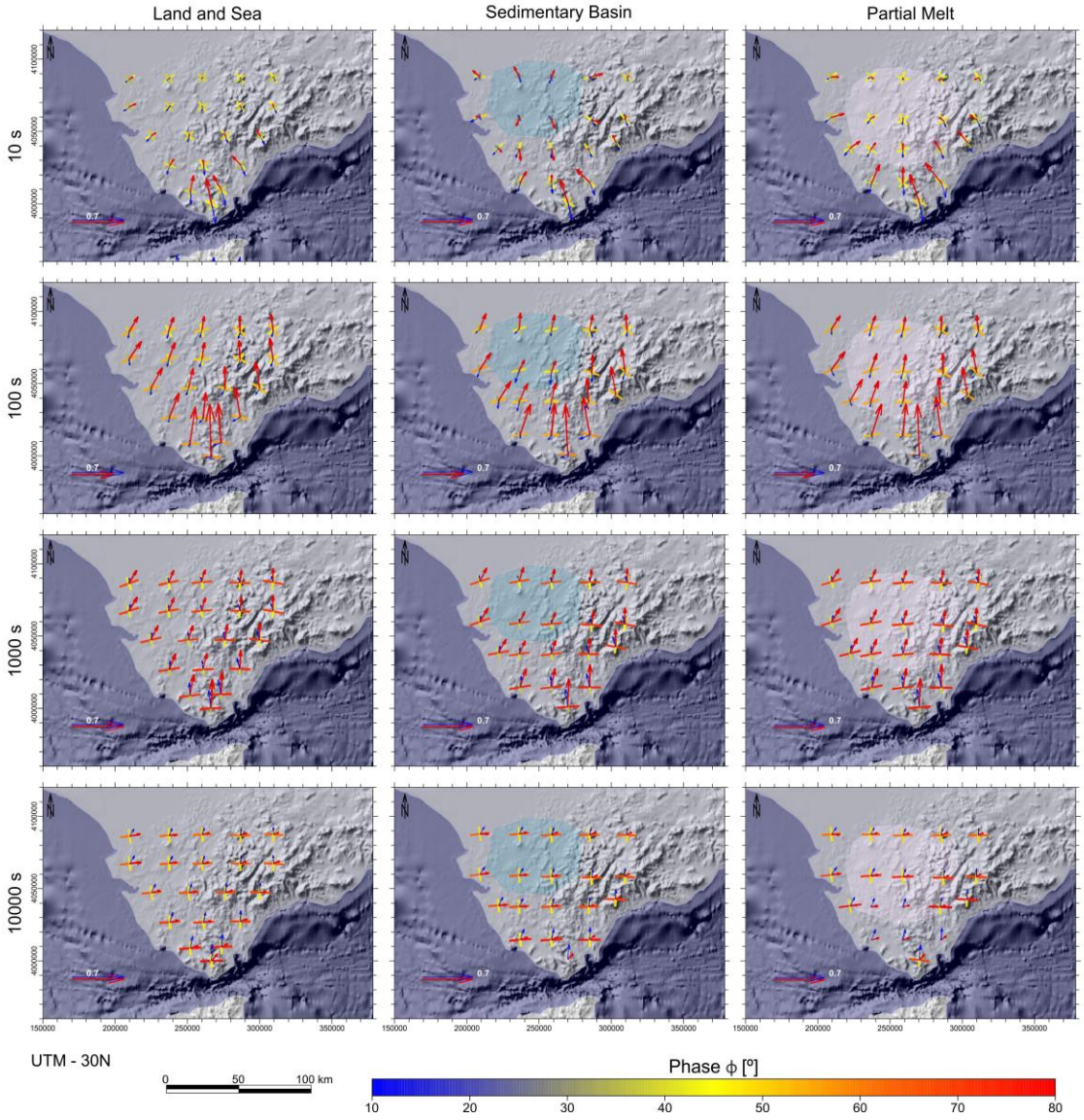

Figure 6.5: Comparison of transfer functions for different hypothetical geological structures: sedimentary basin and partial melt. (cf. open strait model in Fig. 6.2). Real (red) and imaginary (blue) tipper vectors (Wiese convention) and phase tensor bars (colour coded) for periods of 10, 100, 1000 and 10,000 seconds. For further explanation see text.

6.4 Discussion

The bathymetry broadly determines the LMT response in areas surrounding straits and near irregular coastlines. The behaviour of the real tipper vectors and of the phase tensors for the longest period (Fig. 6.2) reflects the 2D situation of a roughly north-south striking boundary with a conductor to the west, and the sites on the resistive quarter space to the east. It is obvious that for this period the extension of the Atlantic Ocean outweighs the influence of the Mediterranean Sea. As it is a large scale effect, the appearance of the phase tensors of all sites is quite homogeneous, with E-W respective to N-S orientation of the major axis and phases above and below 45º. The former resemble TE mode currents oriented north-south, the latter TM mode currents flowing E-W. Obviously, the influence of the sea water within the Strait of Gibraltar does not suffice to compensate this large scale effect, not even for short periods down to 100s or at sites very close to the Strait. Yet the effect of the Atlantic Ocean smoothly affects the tipper orientation at those sites.

It is surprising that toward the shorter period end only the real tipper vectors respond to the influence of the Strait of Gibraltar (Fig. 6.2). We attribute this behaviour to the current channelling through the strait, which does not significantly change the electrical field nearby, but strongly affects the vertical component of the magnetic field. Depending on period, this effect reaches far inland —up to a distance of over 100 km— and must be considered in any interpretation of tipper vectors in that area.

The ocean influence strongly affects the interpretation of geological structures based on MT within areas of southernmost Spain (Figs. 6.4 and 6.5). It is obvious that the detection of such bodies is restricted to MT transfer functions with periods less than 100s due to the influence of the Sea. Phase tensors at sites above the conductive structures indicate their existence by values above 45º, while induction vectors are significant at sites above their lateral boundaries. Special caution is needed when interpreting the real tipper vectors due to the far inland-

reaching influence of the Strait of Gibraltar. Naturally, the conductive fault (Fig. 6.4) produces a more intense effect than the resistive one. The resistive fault only affects the nearby sites for periods of 10s; whereas the effect of the conductive fault is more widespread and covers periods up to 1000s. However, at the long period end (10,000 s) both shallow crustal structures are masked. The conductive sedimentary basin (Fig. 6.5) has an effect on the transfer functions similar to that of the conductive fault, but affecting a wider area for periods up to 100 s. The hypothetical mantle plume (Fig. 6.5) has a very minor effect, and it is only detected for short periods around 10s. The maximum detectable depth of these bodies depends on the skin depth of the electromagnetic waves within the mentioned period range: for average crustal resistivities above 300 Ω·m, which seems to be the lower limit for the crust in southern Spain, there would appear to be evidence of a conductive mantle plume (Fig. 6.5).

6.5 Conclusions

The bathymetry crucially influences the behaviour of MT response functions at sites onshore, depending on their distance to the sea and the period. With respect to the situation north and south of the Strait of Gibraltar, the Atlantic Ocean predominates over the impact of the Mediterranean Sea for periods larger than 100 s.

Within the Strait of Gibraltar, the electric currents induced in both Seas are concentrated; this provokes large real tipper vectors at sites close to the Strait but has a negligible influence on the phase tensors.

Fault zones can be detected preferably by tipper vectors only if they are deep and conductive with respect to the surrounding environment. This is a common setting due to higher permeability, fluid circulation and metallic mineralization within such structures. Thick sedimentary basins can be investigated by phase tensors for high frequencies. At longer periods, the basin response will be masked

by the sea water response. It proves challenging to detect mantle anomalies below 40 km and/or for smaller conductivity contrasts found in areas near the sea and a narrow strait.

We claim that it is essential to take into account the detailed bathymetry and coastline geometry in the context of any onshore modelling or inversion study when the induction volume includes non-negligible parts of sea water. Tipper vectors and phase tensors may complement each other, depending on the geological situation.

Acknowledgements

We thank Professor Steven Constable for his comments in the 22nd EM Induction Workshop (Weimar (Germany), 2014) that have contributed to improve this study. The assistance of the Ph.D Student Marcel Cembrowski while 3D forward modelling and the Ph.D Francisco J. Martínez Moreno is greatly appreciated. The first author is supported by a FPU grant of the Spanish Ministry of Education. The Spanish Government founding through projects CGL2010-21048, P09-RNM-5388 and CSD2006-0041 (European Regional Development Fund-ERDF) and the RNM-148 research group of the Junta de Andalucía.

Chapter 7

Long period magnetovariational evidence of a large deep conductive body within the basement of the Guadalquivir foreland basin and tectonic implications (Betic Cordillera, S Spain)

González-Castillo, L.[1], Galindo-Zaldívar, J.[1, 2], Junge, A.[3], Martínez-Moreno, F.J.[1], Löwer, A.[3], Sanz de Galdeano, C.[2], Pedrera, A.[4], López-Garrido, A.C.[2], Ruiz-Constán, A.[4], Ruano, P.[1, 2], Martínez-Martos, M.[2]

Submitted to:

Tectonophysics, 2015

(Received 16 January 2015)

[1] Departamento de Geodinámica, Universidad de Granada, Spain.

[2] Instituto Andaluz de Ciencias de la Tierra. CSIC-UGR. Spain.

[3] Institut für Geowissenschaften, Goethe Universität Frankfurt/Main, Germany.

[4] Instituto Geológico y Minero de España, Spain.

ABSTRACT

The Betic Cordillera is an Alpine belt formed by the interaction of the Eurasian and African plates and the westward motion of the Alborán Domain. Long Period Magnetovariational observations at 26 sites in its westernmost part provide induction arrows that have been compared with 3D forward models including bathymetry and major geological bodies. The results highlight the presence of a major conductive body (0.05 Ω·m) unknown to date and located within the basement of the Guadalquivir foreland basin. Aeromagnetic and field magnetic measurements further support the occurrence of magnetic anomalies related to the top of this anomalous body. This major structure is interpreted as an intermediate or basic igneous rock, with a high proportion of metallic mineralization. Its origin is discussed in the framework of the regional geological setting, possibly produced in the southern Iberian Variscan Massif by a huge concentration of volcanogenic massive sulphide (VMS) in the prolongation of the Iberian Pyrite Belt during Devonian-early Carboniferous times. Another possibility is that the conductive anomaly is due to magmatic intrusions associated with the Mesozoic fragmentation of Southern Iberia and the opening of the Tethys.

Keywords: Gibraltar Arc; Long Period Magnetovariational observations; magnetic anomalies; deep basic rock intrusion; Pyrite Belt; Tethys.

Highlights

- Long Period Magnetovariational data were acquired in the west Gibraltar Arc.
- The most remarkable conductive body is located in Guadalquivir Basin basement.
- The intense magnetic positive anomaly suggests metallic mineralized rocks.
- The anomaly could be related to a concentration of volcanogenic massive sulphide.
- The Tethys opening could also explain the Mesozoic emplacement of the body

7.1 Introduction

Magnetotelluric investigations provide insights into the spatial distribution of deep lithosphere resistivity. While broad band studies mainly delineate crustal structures, Long Period Magnetotelluric (LMT) data make it possible to characterize the structure of the upper mantle as well (Chave and Jones, 2012).

Most LMT studies focus on continental areas and cratons (Schultz *et al.*, 1993; Jones *et al.*, 2001; Korja *et al.*, 2007; Epov *et al.*, 2012) and describe the deep resistivity pattern (e.g. in Europe; Olsen, 1998). This technique also contributes to constraining the geometry of subduction zones (Jones, 1993), as in the Carpathians (Stanica and Stanica, 1993) and the subducting Juan de Fuca plate (Kurtz *et al.*, 1986; Wannamaker *et al.*, 1989) as well as the fluid cycle in these areas (Worzewski *et al.*, 2010). Magnetotelluric is especially sensitive to interconnected metallic mineralization and sulphides that appear as conductive sectors (Ducea and Park, 2000). Hence, LMT has proven useful in detecting and delineating mineralized areas linked to faults and shear zones (Unsworth *et al.*, 1997; Bedrosian *et al.*, 2002) and to intrusive bodies (Häuserer and Junge, 2011). Given its suitability for deep studies, LMT was one of the main geophysical techniques used to constrain the structure and recent tectonic evolution of Iberia and Northern Africa in the framework of the Topo Iberia project (Pedrera *et al.*, 2010; Ruiz-Constán *et al.*, 2010; Anahnah *et al.*, 2011a; 2011b; Pous *et al.*, 2011). It also helped to elucidate the crustal structure in the southern and southwestern part of the Iberian Massif (Monteiro-Santos *et al.*, 1999, 2002; Almeida *et al.*, 2001, 2005; Pous *et al.*, 2004; Muñoz *et al.*, 2005; Vieira da Silva *et al.*, 2007).

The Mediterranean Sea, located between the Eurasian and African plates, comprises a complex array of oceans and continental margins (Fig. 7.1). The present-day setting, resulting from the evolution of the Tethys Sea from the Mesozoic up to date, was mainly controlled by a transtensive sinistral motion between Laurasia and Gondwana, with local dextral events in the lower late Cretaceous and from 20 Ma to date (Schettino and Turco, 2010). Since the

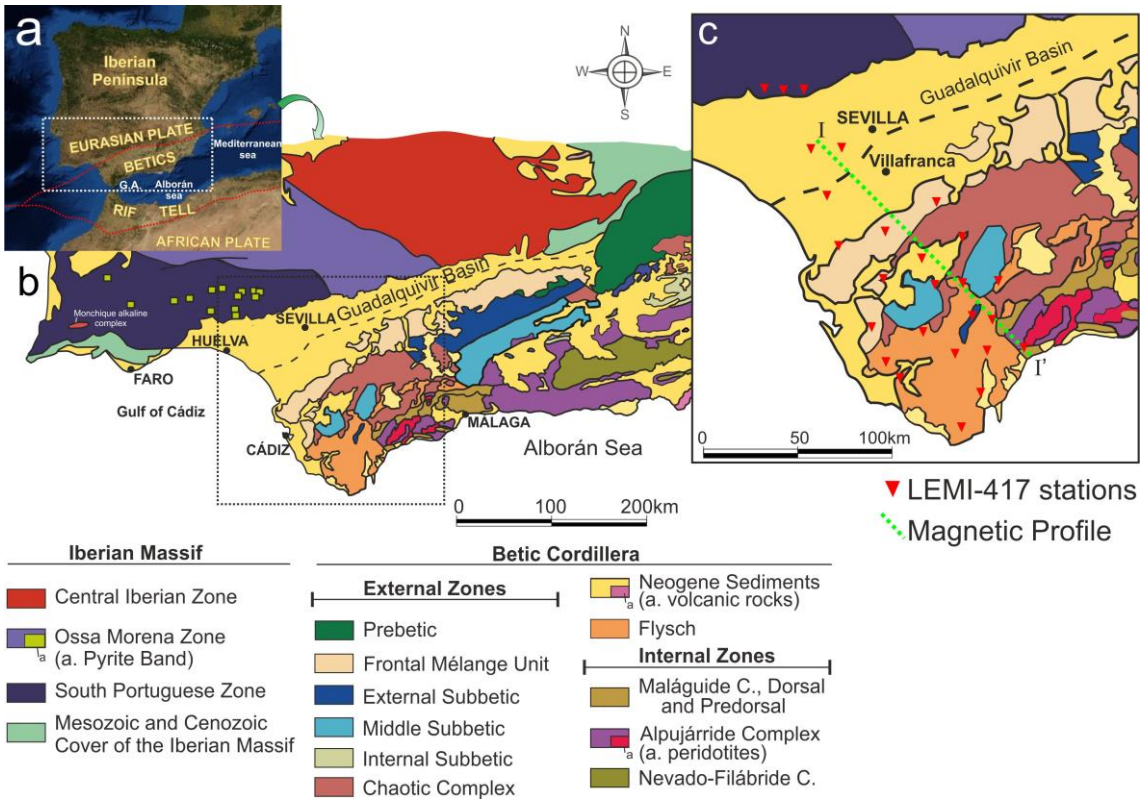

Figure 7.1: Geological setting of the Betic Cordillera. (a) Gibraltar Arc location in the western Mediterranean. (b) Main geological units of the Betic Cordillera and its foreland. (c) Detailed setting of the studied area, including the observed station location and the field magnetic profile (dashed green line).

Oligocene, the development of the Western Mediterranean has determined the uplift of several Alpine orogens (Gueguen *et al.*, 1998), such as the Betic and Rif Cordilleras, connected by the Gibraltar Arc.

Until now, the deep structure of the westernmost part of the Betic Cordillera has not been studied in detail due to its complexity, yet it is a key region to understand the evolution of the South Iberian margin and the Gibraltar Arc. Moreover, its location between the Atlantic Ocean and the Mediterranean Sea and the irregular continental borders involved have a great influence on magnetotelluric studies, something to be carefully taken into account.

Previous analysis of magnetic anomalies has shed light on the distribution and geometry of the main intermediate and basic intrusive bodies located in the

upper crust of the southwestern Iberian Massif (Socias *et al.*, 1991; González-Castillo *et al.*, 2014). However, some intense magnetic anomalies in the westernmost Betic Cordillera and its foreland have not yet been analysed in detail.

The aim of this research is to identify and interpret the main deep electrical and magnetic anomalies located in the westernmost part of the Betic Cordillera and its foreland, mainly on the basis of Long Period Magnetovariational observations combined with magnetic research carried out in the framework of the TopoIberia project. To this end, we performed a 3D forward resistivity model of the lithosphere. In addition, its interpretation has been hold on magnetic data. The magnetovariational study focuses on time variations of the magnetic field, as they are less dependent of galvanic distortions than the telluric field (Chave and Jones, 2012).

7.2 Geological Setting

The Betic Cordillera is an Alpine arcuate orogenic belt that corresponds to the northern branch of the Gibraltar Arc (Fig. 7.1). Together with the Guadalquivir Foreland Basin, it is located above the Variscan Iberian Massif which is partially subducted beneath its western part (Serrano *et al.*, 2002; Ruiz-Constán *et al.*, 2010). This Cordillera is traditionally divided in two main domains (García-Dueñas and Balanyá, 1988): the Alborán Domain (Internal Zones) and the South Iberian Domain (External Zones), the two generally separated by Flysch Units. The Internal Zones are made up of several superposed metamorphic complexes including Paleozoic rocks (from bottom to top: the Nevado-Filábride, the Alpujárride and the Maláguide) in addition to the Dorsal and Predorsal complexes. The Alpujárride upper unit includes large peridotite bodies at its base. All these complexes are located within the southeastern part of the Betic Cordillera, and continue toward the basement of the Alborán Sea. The Flysch Units correspond to the former oceanic or thin continental swell located between

the two main domains, filled by siliciclastic deposits from the Oligocene to Miocene (Luján *et al.*, 2006). The South Iberian Domain represents the Mesozoic to Cenozoic continental margin deposits of the South Iberian Peninsula (García-Dueñas and Balanyá, 1988). It consists mainly of a carbonate-marly series with local volcanic intercalations. They were deformed during the Alpine orogeny as a NW-to-W-vergent fold-and-thrust belt. In a frontal position, in contact with the foreland basin, a Mélange Unit is widely developed (Sanz de Galdeano *et al.*, 2008; Roldán *et al.*, 2012). The Guadalquivir foreland basin and the intramontane basins are filled by detrital Neogene and Quaternary sedimentary deposits featuring interlayered calcarenites and limestones (Roldán, 1995). The Alborán Sea is the main basin remaining below sea level and located between the Betic and Rif Cordilleras. Its metamorphic basement lies in continuity with the Internal Zones.

The Variscan Iberian massif comprises several zones with a characteristic tectonometamorphic evolution (Ribeiro *et al.*, 1990). The southern Iberian Peninsula, from SW to NE, holds the South Portuguese (SPZ), the Ossa-Morena (OMZ) and the Central Iberian zones (Fig. 7.1). The SPZ, mainly formed by low grade metapelites, represents the External Zone fold-and-thrust belt of Variscan orogen. Toward the base of the metapelitic sequence, volcanogenic massive sulphide (VMS) deposits crop out, placed within a Volcano-Sedimentary Complex of Devonian to Early Carboniferous age known as the Iberian Pyrite Belt. The VMS deposits are interlayered with metapelites or directly linked to acidic volcanic rocks (Tornos *et al.*, 1998). The OMZ/SPZ contact, in turn, is marked by a band of amphibolites with oceanic affinity (Bard, 1977). U-Pb zircon ages of the protoliths point to a lower Carboniferous oceanic-like crust that opened during the VMS occurrence (Azor *et al.*, 2008), constituting the core of Variscan orogen.

7.3 Previous geophysical studies

The deep structure of the Betic Cordillera and its foreland has been constrained by means of many geophysical methods, including active and passive seismic, gravity, magnetic and magnetotelluric research. Bouguer gravity anomalies (I.G.N., 1976) support the presence of a standard continental crust in the Iberian Massif (Sánchez-Jiménez, 1996; Fernández *et al.*, 2004) bounded to the southeast by the relatively thick crust of the Betic Cordillera; it is followed by the very thin continental crust of the Alborán Sea, which lies above an anomalous mantle (Hatzfeld, 1976; Torné *et al.*, 2000). Seismic refraction data (Banda and Ansorge, 1980; Medialdea *et al.*, 1986; Suriñach and Vegas, 1993; Díaz and Gallart, 2009) determine the average crustal thickness and support this structure. There is a widespread set of shallow seismic reflection profiles in the Betic Cordillera and the Guadalquivir foreland basin —mainly covering the Neogene-Quaternary sedimentary basins (Roldán, 1995), the Gulf of Cadiz (Gutscher *et al.*, 2002) and the Alborán Sea (Comas *et al.*, 1992)— revealing the structure of the sedimentary infill. However, the only available deep profiles (ESCIBéticas, García-Dueñas *et al.*, 1994; Galindo-Zaldívar *et al.*, 1997) are located in the eastern transect of the Betic Cordillera, and show a flat Moho below a lower crust that is probably in continuity with the Iberian Massif, and an upper detached crust. The deep seismic reflection profiles defining the structure of the Variscan crust of the Iberian Massif (Simancas *et al.*, 2003; Martínez-Poyatos *et al.*, 2012) reveal differences in the upper crust: it is dominated by magmatic structures in the Central Iberian Zone, metamorphic rocks highly deformed by folds and thrust in the Ossa Morena Zone, and fold-and-thrust belt in the South Portuguese Zone. The intermediate seismicity, reaching up to 120 km depth (Morales *et al.*, 1997; Ruiz-Constán *et al.*, 2011), reveals the presence of a subduction slab in the western Alborán Sea.

Aeromagnetic anomalies (Socias *et al.*, 1991; Socias and Mezcua, 2002) provide new data regarding the deep structure of the Iberian Massif and the basement

structures of the Betic Cordillera. The Variscan basement extends below the Guadalquivir foreland basin, at least as far as the External Zones of the Betic Cordillera (Serrano *et al.*, 2002). González-Castillo *et al.* (2014) evidence the presence of a large E-W elongated dipole, extending more than 200 km in the southernmost Iberian Massif foreland, related to the Monchique Alkaline Complex. Eastward, the most intense aeromagnetic maximum of the westernmost Betic Cordillera is located by the Guadalquivir foreland basin and the Betic Cordillera front (Figs. 7.1 and 7.2).

Magnetotelluric (MT) researches underline the anisotropy of the eastern (Martí *et al.*, 2004) and the western Betics (Ruiz-Constán *et al.*, 2010), suggesting a roughly arched anisotropy that varies at depth. 2D MT researches have looked into the elongated shallow crustal structures in the southern part of the Iberian Massif (Pous *et al.*, 2004, 2011; Muñoz *et al.*, 2005, 2008), and the central-western Betic Cordillera (Ruiz-Constán *et al.*, 2012). Monteiro-Santos *et al.* (1999) suggest the presence, in the Ossa Morena Zone, of a high conductivity middle crustal band probably related to the presence of graphite. 3D MT models have been developed in the easternmost Betic cordillera (Martí *et al.*, 2009) and

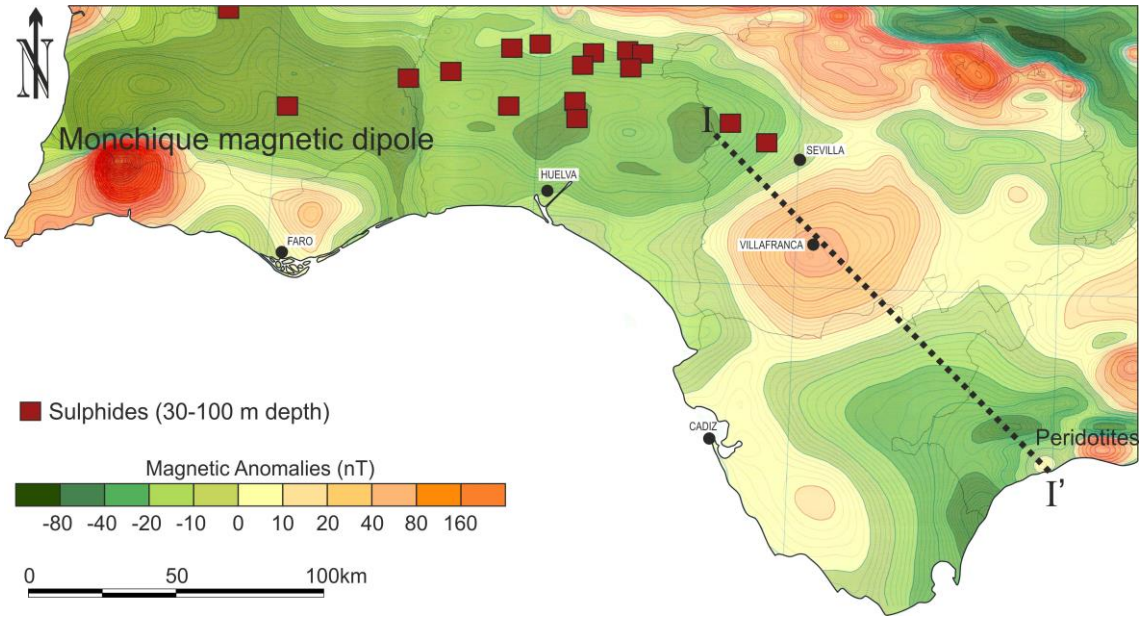

Figure 7.2: Aeromagnetic map of the Western Betic Cordillera and its foreland, including field observed magnetic profile and location of main Iberian Pyrite Belt ores.

extended up to the central part (Rosell *et al.*, 2011). Although they support the presence of several major anomalies in the crust and upper mantle, their accuracy is low for deep structures. In the westernmost Iberian Massif, Vieira da Silva *et al.* (2007) analyzed the South Portuguese and Ossa-Morena zones. However, in the westernmost Betic Cordillera there is a complex 3D structure surrounded by an irregular sea impeding the development of MT studies to date.

7.4 Methodology, data acquisition and processing

In order to obtain accurate insights regarding the deep 3D structure of the westernmost part of the Betic Cordillera, Long Period Magnetovariational observations were combined with magnetic interpretations in this study.

7.4.1 Long Period Magnetovariational observations

Time variations of the natural Earth magnetic field components (Bx, By, Bz) were observed at 26 sites with an average spacing of 10-20 Km, during three surveys from 2011 to 2013 (Fig. 7.1c). The area near the city of Sevilla was not observed because of its high anthropogenic noise level. The three components of the magnetic field were recorded by fluxgate magnetometers (LEMI-417) with a sampling rate of 0.25 seconds for at least 15 days at each site.

Transfer functions Tzx and Tzy between the magnetic field components were estimated in the frequency domain according to the linear bivariate approach

$$Bz = TzxBx+TzyBy$$

by standard robust processing (Ritter *et al.*, 1998). Tzx and Tzy are complex functions of frequency, respective period depending on conductivity variations in the subsurface. The real and imaginary values of Tzx and Tzy are presented separately by induction arrows within an x-y coordinate system, the positive x and y axes respectively referring to the North and East directions. The Wiese convention is used to present the induction arrows —e.g. the real arrows point in

the direction of laterally increasing resistivity (Wiese, 1962). As the induction volume increases toward the long period end, the conductive sea water will obviously influence the induction arrows accordingly.

7.4.2 Magnetic observations

Aeromagnetic anomalies from the Iberian Peninsula (Ardizone, 1989; Socias and Mezcua, 2002) were derived from a grid of flight lines at a barometric elevation of 3000 m above sea level. The flight tracks comprise N-S lines spaced 10 km, with E-W control lines separated 40 km, and evidence the features of the large crustal anomalous bodies.

Furthermore, total magnetic field survey measurements were obtained along a NW-SE transect of the main dipole (Figs. 7.1 and 7.2) using a GSM 8 proton precession magnetometer with an accuracy of 1 nT measured at 2 m above the topography. Measurement spacing was 500 m on average, the position of the stations being determined by a Garmin GPS. Because of anthropogenic noise, measurements were not acquired near settlements. Magnetic data processing was carried out through a standard procedure including reduction to the IGRF 2010 (IAGA, 2010). Diurnal variations were corrected considering the total field intensity of the nearest permanent magnetic station in San Fernando (Cádiz, Spain), which belongs to the Royal Army Observatory (www.intermagnet.org). In turn, the 2D magnetic model was calculated using GRAVMAG v.1.7 software from the British Geological Survey (Pedley *et al.*, 1993), which allows for removal of the regional trend to model the residual magnetic anomaly.

7.5 Induction arrows from Long Period Magnetovariational observations

Figure 7.3 displays the pattern of the real and imaginary induction arrows for the periods 1000s and 6250s at all field sites underlain by the major geological units. For both periods the real arrows have an eastward component, which reflects the predominating influence of the Atlantic Ocean compared to that of

the Mediterranean Sea. The pattern of the northern sites contrasts with that of the sites south of the Guadalquivir basin: the northern arrows are much larger and point almost to the north, whereas the southern arrows turn to the east. Note that for the shorter period, the arrows at the southern boundary of the Guadalquivir basin turn to the south, while the pattern is more homogeneous for the longer period. In general, the differences between the real arrows of the two periods are not as large as for the imaginary arrows, which show a striking change in direction and size for the two periods: they generally point to the same direction as the real arrows for the long period, but to the opposite or perpendicular direction for the shorter period at almost all the sites. Again there is a conspicuous change in its pattern between the northern sites and the sites to the south of the Guadalquivir basin.

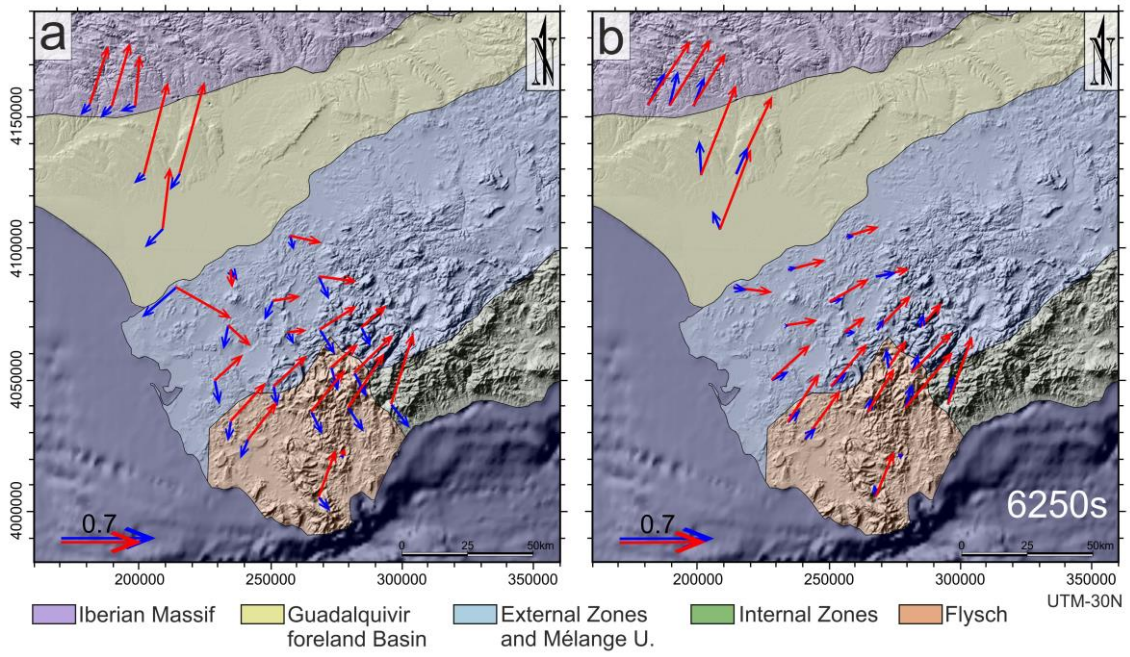

Figure 7.3: Observed real (red) and imaginary (blue) part of induction arrows for periods 1000 s (top) and 6250 s (bottom) at all field sites. Major geological units are underlain (cf Fig. 7.1).

7.6 Conductivity models

3D models were constructed using Comsol 4.3 software (Häuserer and Junge, 2011) to provide a preliminary pattern of hypothetical induction arrows at

the field sites for different periods. The models take into account the known conductivity distribution, such as the bathymetry and coast lines and the major geological units in the area (Fig. 7.4). A comparison of the modelled and observed data can thus indicate the existence of further unknown bodies hidden in the subsurface.

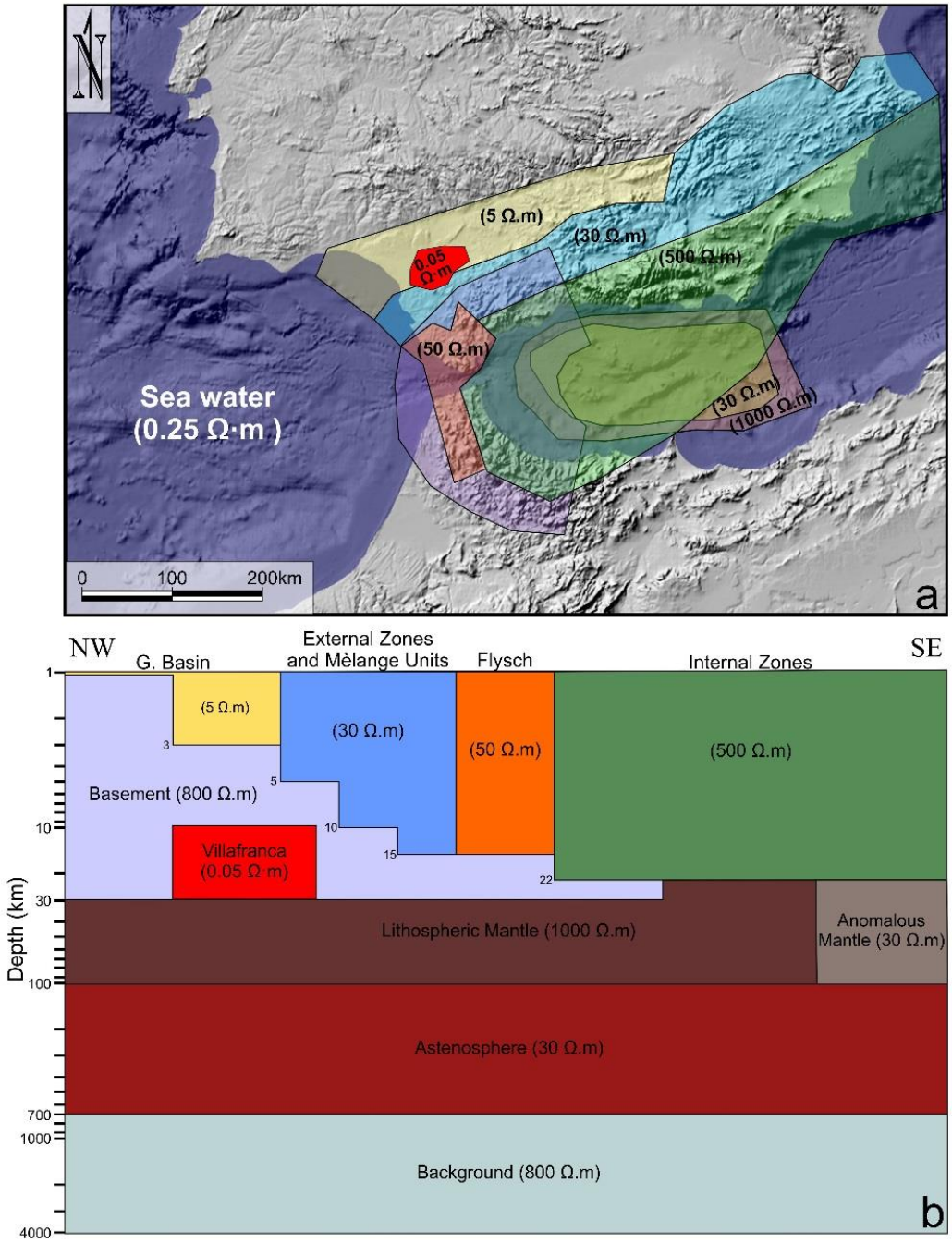

Figure 7.4: Sketch of the main known geological bodies considered for Long Period Magnetovariational models and the new anomalous Villafranca body (solid red). (a) Map view. (b) Idealized cross section.

The main influence in the area —resulting from the bathymetry and the irregular coast line— is demonstrated by the model based on the bathymetry obtained using GEBCO v.2.13 from the British Oceanographic Data Centre (www.gebco.net) with an average sea water resistivity of 0.25 Ω·m (Figs. 7.4 and 7.5a). It includes further an approximate depth dependence of the resistivity considering: crust (0-30 km, 800 Ω·m), lithospheric mantle (30-100 km, 1000 Ω·m) and asthenosphere (>100km, 30 Ω·m). This model reveals the influence of the sea on the induction arrows in the study area. For the short period the real arrows point northward, increasing to the south, and rotating slightly eastward at the northern sites. This rotation is visible at all sites for the longer period, whereas the imaginary arrows basically maintain their direction with a slight rotation to the west for the longer period. This behaviour demonstrates the complicated 3D situation generated by the trace of the coast line and possible current channelling through the strait of Gibraltar. It makes it clear that it is essential to take into account the 3D conductivity structure reflecting the large conductivity contrast between land and sea.

The main known geological bodies in the region (Fig. 7.4) were added in model b (Fig. 7.5b). Resistivities were determined considering the dominant lithologies and previous MT studies in the neighbouring area (Martí *et al.*, 2009; Anahnah *et al.*, 2011a, 2011b; Rosell *et al.*, 2011; Ruiz-Constán *et al.*, 2012). The following geological units were taken into account (Fig. 7.4): Guadalquivir foreland sedimentary basin (5 Ω·m) increasing in thickness towards the Betic Cordillera boundary down to 3 km; the External Zones and Mélange units (30 Ω·m), thickness from 5 km to 15 km; the Flysch Units (50 Ω·m), mainly located in the westernmost Betic Cordillera reaching a depth of 15 km; and the Internal Zones (500 Ω·m), 22 km thick and extending from the Cordillera toward the Alborán Sea. All these bodies are implemented within a crustal background (800 Ω·m) that represents the Variscan basement. Additionally, an anomalous conductive upper mantle (30 Ω·m) was included towards the Alborán Sea, as well

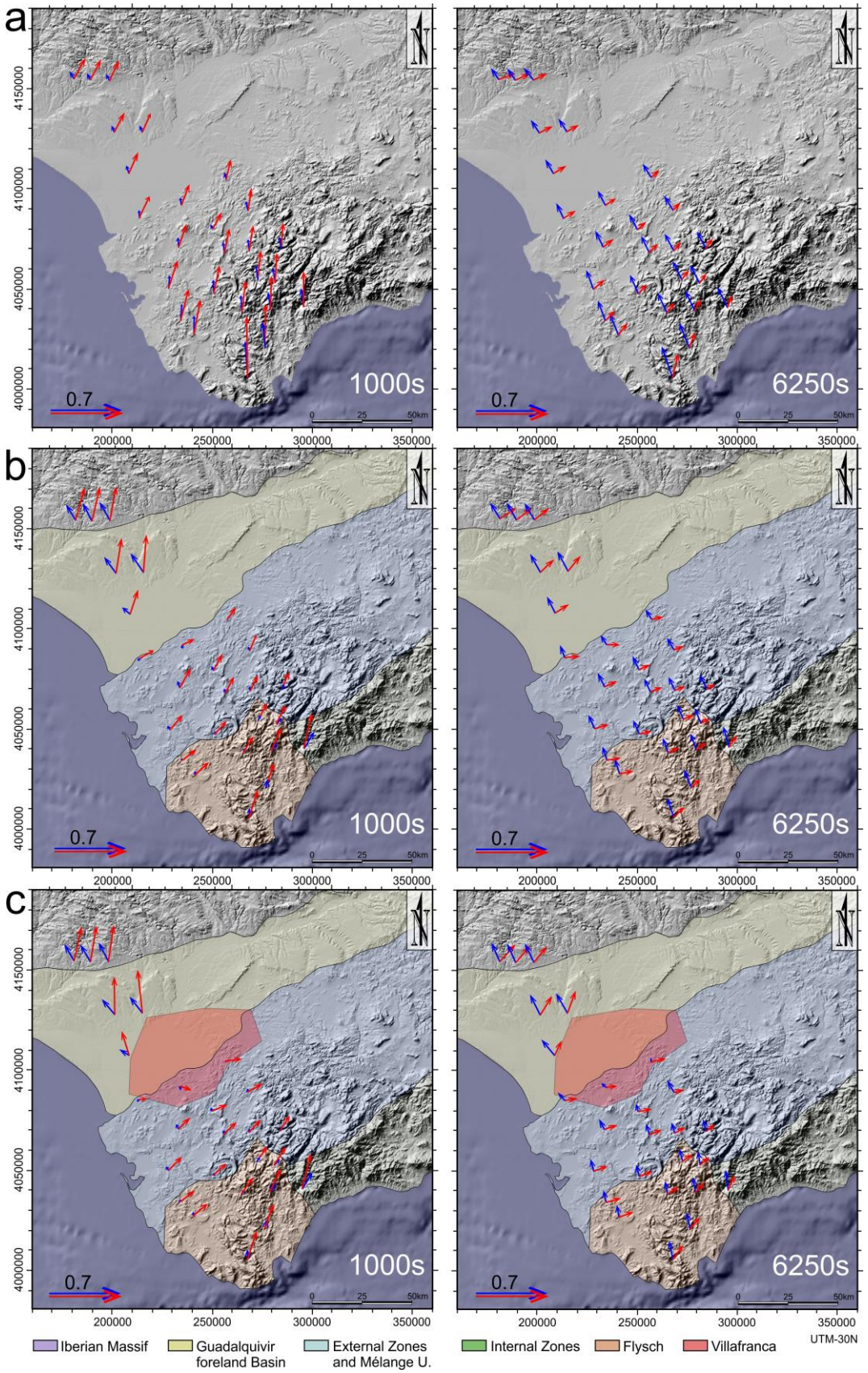

Figure 7.5: Modelled real (red) and imaginary (blue) part of induction arrows for periods 1000s (top) and 6250s (bottom) at all field sites. (a) Bathymetry model. (b) Model a with known geological bodies included. (c) Model b with new conductive anomalous Villafranca body.

as a continental slab (1000 Ω·m) reaching down to 120 km depth. Whereas there are moderate changes in the arrows' direction as compared to the land-sea model (Fig. 7.5a) for the long period, the period of 1000s exhibits significant differences in size (northern sites) and direction of the arrows. This shows the influence of the conducting sediments of the Guadalquivir basin, the External Zones and the Flysch. Note that this pattern already features the major components of the observed data as discussed above.

Still, differences remain and so an attempt was made to include a further geological body located in the crustal basement of the westernmost part of the Betic Cordillera foreland basin, model c, with enhanced conductivity and spatial extent derived from the aeromagnetic anomaly (Fig. 7.2). The result is shown in Fig. 7.5c. Significant changes occur only for the short period at sites close to the boundary of the anomalous body: to the north the magnitude of the real arrows increases, and to the southeast they rotate clockwise, more closely resembling the observed field data.

7.7 Magnetic anomalies

Aeromagnetic anomalies suggest the presence of a large anomalous body in the basement of the western part of the Guadalquivir foreland basin related to the most intense (+46 nT) and widest magnetic anomaly maximum in Villafranca village. This anomaly is located east of the Monchique magnetic dipole (Fig. 7.2) with low intensity minimum. To the southeast, other aeromagnetic anomalies are related to the peridotite outcrops in the Internal Zones of the Betic Cordillera.

The magnetic anomaly profile measured in the field (Figs. 7.1, 7.2 and 7.6) confirms the presence of the aeromagnetic anomaly. Its smooth and low intensity suggests that it corresponds to a wide, deep body. This anomaly contrasts with the southeastward high intensity anomalies that are related to the shallow peridotite bodies.

A total field magnetic anomaly 2D model (Fig. 7.6) was developed to test this hypothesis. A good fit was obtained when considering only the magnetic susceptibility contrast (0.06 SI) of a body whose top would be located at about 10 km depth.

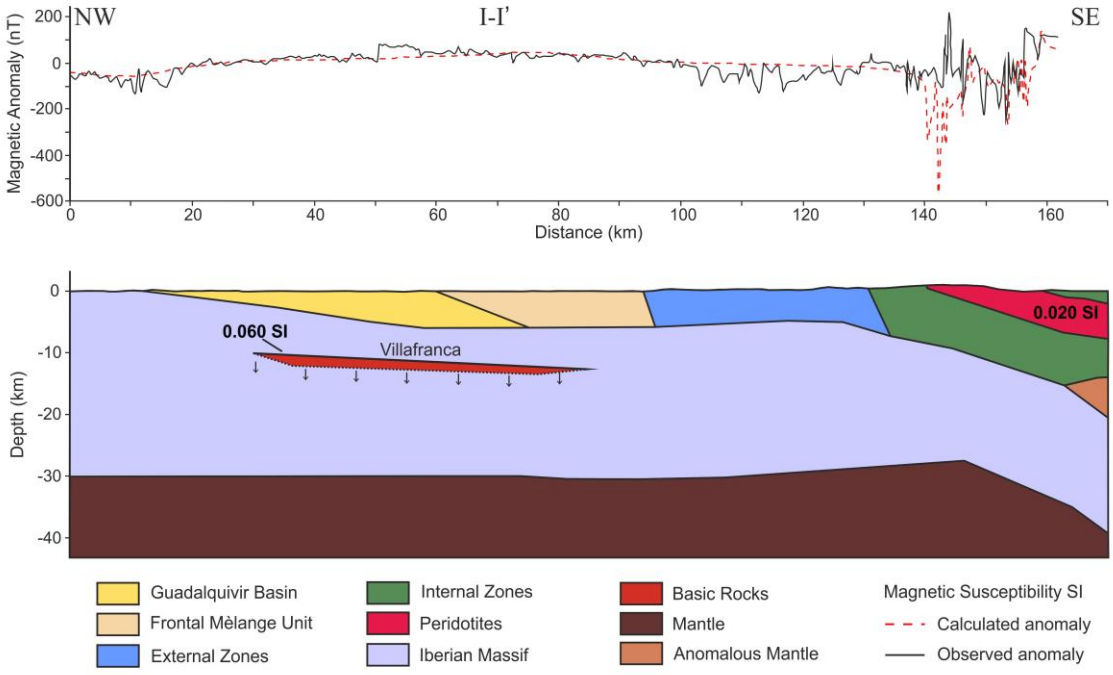

Figure 7.6: Field magnetic anomalies and magnetic model included in a simplified sketch of the main geological units of the Betic Cordillera along the cross section. The top of Villafranca is fixed and could extend in depth as black arrows indicate.

7.8 Discussion

The analysis of deep structures in highly deformed regions requires the integration of geophysical data based on different rock properties. Although seismic research generally provides exceptional results regarding the crust and the upper mantle, gravity and magnetotelluric methods can complete the image. In addition, magnetic research can better locate bodies which contrast magnetic properties in the upper crust. The Long Period Magnetovariational observations acquired for the first time in the westernmost part of the Gibraltar Arc (Fig. 7.3) demonstrate the 3D character of the regional structures and the high influence of the sea water, according to the bathymetry. The irregular geometry of the coast

line, the differential influence of the deep Atlantic Ocean and the shallow Alborán Sea, and the presence of the Gibraltar Strait all come to determine an induction arrow pattern (Fig. 7.5a) that should be considered before arriving at any geological interpretations.

After considering induction arrow patterns for 3D forward models for periods 1000 s to 6250 s —including all the known major structures (Fig. 7.5b)— the well-constrained difference between the observed data (Fig. 7.3) and the model results can be explained by the presence of a major conductive anomalous body (Fig. 7.5c). This structure, which we call the Villafranca body, would be located in the basement below the western part of the Guadalquivir basin, at a depth of 10 to 30 km. The extremely high conductivity (0.05 Ω·m) suggests graphite or a structure with a high metallic content, typical of igneous bodies. The presence of this body escaped previous seismic research, perhaps because of a lack of detailed data in this region.

The nature of this major anomalous body should be discussed in light of its high conductivity and magnetic anomalies. The fact that the same region shows the most intense magnetic anomaly maximum, with similar anomaly values for aeromagnetic and field magnetic data, would signal a body whose top lies at a depth of roughly 10 km, and has very different magnetic properties with respect to the host rocks (Fig. 7.6). Although the presence of graphite-bearing layers is suggestive of the main origin for highly conductive crustal bodies (Monteiro-Santos *et al.*, 2002), they usually correspond to wide horizontal layers, whereas the observed anomalous body extends mainly in depth. Besides, the presence of magnetic anomalies is typical of metallic mineralized bodies, never related to graphite. While it is not possible to determine its magnetic remanence, because the body does not crop out, the maximum suggests a high contrast in magnetic susceptibility possibly due to the occurrence of intermediate rocks, such as the Monchique Alkaline complex (González-Castillo *et al.*, 2014) or basic rocks (Dañobeitia *et al.*, 1999). Moreover, the magnetic anomaly displays rectilinear

ENE-WSW and NNW-SSE oriented borders. In this setting, the most probable lithological interpretation is the occurrence of a crustal intermediate or basic body highly intruded by hydrothermal mineralization; given its low resistivity (0.05 Ω·m) it may be sulphide, with very substantial vertical extension.

One of the world's foremost sulphur ore belts is located along the Devonian-lower Carboniferous Iberian Pyrite Belt, close to the Villafranca body. Although the two might be related, there are some aspects that do not fit with this hypothesis: its southern location in respect to the belt continuity below the Guadalquivir basin, the shallow character and small size of the sulphur ore, and the absence of significant magnetic anomalies in VMS outcrops (Fig. 7.7). Also incompatible is the northward origin of the volcanic deposits, later thrusted toward the south (Onézime, 2003).

Two alternative tectonic settings for the emplacement of the Villafranca body would account for the Mesozoic Tethys evolution along the south Iberian margin (Schettino and Turco, 2010). The area was affected by a regional sinistral transtensional deformation during the Jurassic and lower Cretaceous. In this framework, NW-SE-oriented relay faults could develop local pull-apart or crustal thinning areas accommodating the emplacement of igneous bodies with high sulphide mineralization. Schettino and Turco (2010) also suggest that from the latest lower Cretaceous and during the upper Cretaceous a well-defined ENE-WSW dextral transcurrent fault line crossed this region, and may have caused the development of local pull-apart structures and crustal thinning areas. At any rate, there are no other highly metallic mineralized bodies of this age cropping out in the Betic Cordillera; and although the proposed setting is feasible, there are not enough data to unequivocally determine its emplacement.

7.9 Conclusions

Long Period Magnetovariational observations along 26 sites were carried out in the westernmost part of the Betic Cordillera in order to highlight the presence of deep conductive bodies. The induction arrow pattern of 1000 s to 6250 s from

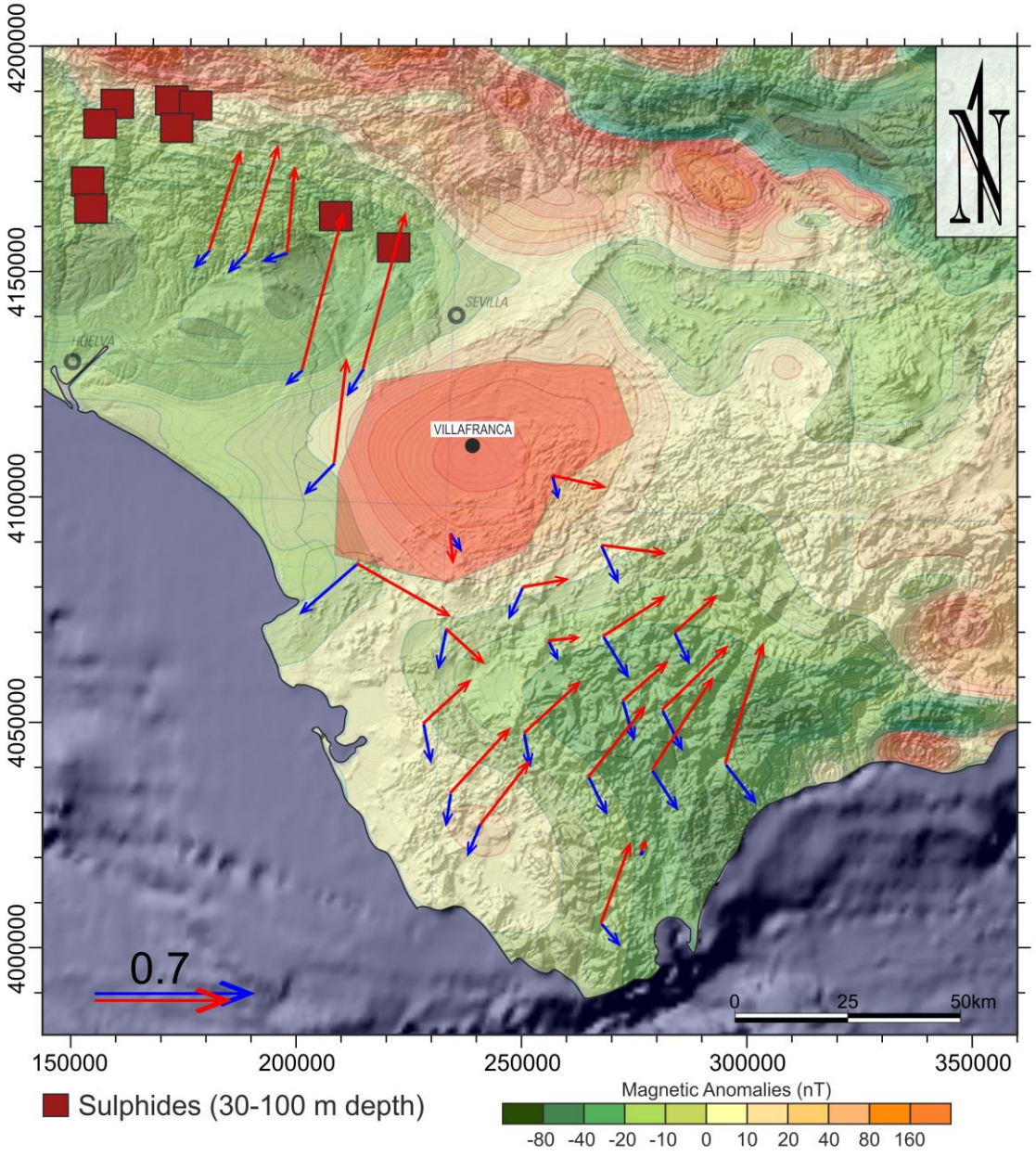

Figure 7.7: Integration of Long Period Magnetovariational field observation, geological setting and aeromagnetic anomalies suggesting the location of the new Villafranca body.

3D forward modelling with respect to bathymetry and the known geology of the region, supports the presence of a highly conductive (0.05 Ω·m) body at a depth of 10 to 30 km, which we call Villafranca. Magnetic anomalies in the region constrain the location of its top in depth. The integration of results from the two geophysical methods points to the sulphuric nature of the anomalous body, probably in an igneous host rock.

This major anomaly located in the Variscan basement of the Guadalquivir foreland basin may represent a structure related to the Iberian Pyrite Belt, or else a body emplaced along the South Iberian Margin during the Mesozoic Tethys evolution.

Acknowledgements

This research was funded by the Spanish Government through projects CGL2010-21048, P09-RNM-5388 and CSD2006-0041 (European Regional Development Fund-ERDF) and the RNM148 research group of the Junta de Andalucía.

Chapter 8

Shallow frontal deformation related to active continental subduction: structure and recent stresses in the westernmost Betic Cordillera

Lourdes González-Castillo [a], Jesús Galindo-Zaldívar [a,b], Antonio Pedrera [b], Francisco José Martínez-Moreno [a], Patricia Ruano [a,b]

Published on:

TERRA NOVA, 2015

DOI: 10.1111/ter.12138

(Received 27 May 2014; Accepted 14 January 2015)

[a] Departamento de Geodinámica, Universidad de Granada, Spain.

[b] Instituto Andaluz de Ciencias de la Tierra. CSIC-UGR. Spain.

ABSTRACT

The westernmost Betic Cordillera front is located along the arcuate Alpine belt formed by the interaction of the Eurasian-African plate boundary and the Alborán continental domain in between. Although classical geological data suggest that the western Cordillera front is inactive, recent GPS data show a westward–north-westward motion of up to 3.4 mm/yr with respect to the foreland. In addition, the increasing thickness of Guadalquivir sedimentary infill toward the Cordillera, and the rectilinear character of the front formed by soft sediments, suggest that the Cordillera is still active. Large ENE–WSW-oriented open folds detected in the field, seismic reflection profiles and new audiomagnetotelluric data are consistent with active deformation. Fracture analysis in Quaternary deposits evidences recent NW–SE horizontal compression. The GPS motion and maximum stress orientation may be due to north-westward tectonic collision of the westernmost Betic Cordillera, accommodated at depth by active continental subduction of the Iberian lithosphere.

Key words: Recent and active tectonics, shallow geophysics, brittle fractures, active folds, tectonic collision.

8.1 Introduction

The transition from oceanic subduction to continental collision contributes to the development of orogenic belts in two main end-member geodynamic settings. (i) When continental lithosphere keeps subducting, aided by the pull down of the nearby oceanic lithosphere (Chemenda *et al.*, 2001), its detachment produces uplift and a contractional deformation front (Gerya *et al.*, 2004). (ii) If decoupling or delamination of the mantle lithosphere occurs, uplift, high heat flow, uncompensated high elevation and significant magmatic activity can be expected (Wortel and Spakman, 2000). The Eurasian-African plate boundary is associated with a broad band of continental deformation and seismicity in the westernmost Mediterranean (Buforn *et al.*, 2004; Stich *et al.*, 2010; Billi *et al.*, 2011; Palano *et al.*, 2013). In this region, the interaction of the roughly westward motion of the Alborán continental domain with this major plate boundary, since the late Oligocene, has created the Betic and Rif cordilleras. They surround the continental Alborán Neogene basin (Fig. 8.1).

Some authors propose delamination and mantle lithosphere detachment below the Alborán Domain (Docherty and Banda, 1995; Seber *et al.*, 1996; De Lis Mancilla *et al.*, 2013). However, other researchers support subduction models (Doglioni *et al.*, 1999a,b) – based on seismic tomography studies that imaged an oceanic subducted slab with SW–NE to N–S orientation (Blanco and Spakman, 1993; Gutscher *et al.*, 2002, 2012; Piromallo and Morelli, 2003; Spakman and Wortel, 2004; Bezada *et al.*, 2013; Palomeras *et al.*, 2014) and E to SE-dip – including slab roll-back (Lonergan and White, 1997; Pedrera *et al.*, 2011) with partial or total slab break off and/or tearing (Blanco and Spakman, 1993; Spakman and Wortel, 2004; García-Castellanos and Villaseñor, 2011; van Hinsbergen *et al.*, 2014). Eastward (Gutscher *et al.*, 2002, 2012) and south-eastward (Ruiz-Constán *et al.*, 2009, 2011, 2012a) dipping slabs have been considered. The Alborán Basin may be interpreted as a backarc basin, although related to different proposed subduction slabs (Doglioni *et al.*, 1997; Gueguen *et al.*, 1997; Galindo-Zaldívar *et*

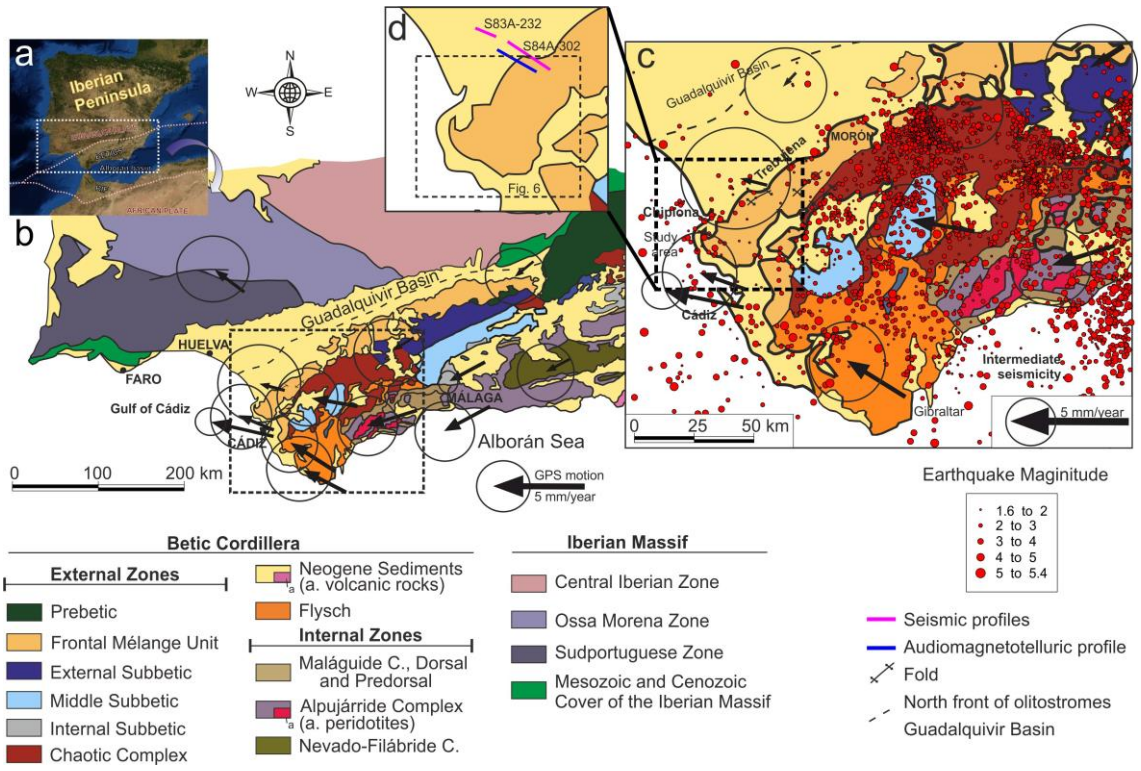

Figure 8.1: Geological Setting. (a) Betic-Rif Cordillera in the Western Mediterranean Sea. The boundaries of this Alpine belt are indicated by the white dashed lines. (b) Main tectonic units of the Betic Cordillera and its foreland, including GPS motion and 95% confidence ellipses (Koulali et al., 2011). (c) Detail of the Western Betic Cordillera including seismicity, GPS motions and 95% confidence ellipses (Koulali et al., 2011). (d)Detailed location of seismic and audiomagnetotelluric lines. Dashed lines indicates the area covered in Fig. 8.6.

al., 1998; Gueguen *et al.*, 1998; Doglioni *et al.*, 1999a,b; Pedrera *et al.*, 2011; Carminati *et al.*, 2012; van Hinsbergen *et al.*, 2014).

The major lithosphere-scale fault along the boundary between the External and Internal Zones was active during the westward motion of the Alborán domain before the contact was covered by Tortonian marine sediments (Martín-Algarra, 1987). Yet GPS data in the central and western Betics indicate a relative westward displacement of the Internal Zones with respect to Eurasia of up to 3.4 mm/yr (Fig. 8.1; Koulali *et al.*, 2011). At present, the eastern part of the cordillera mountain front seems to be scarcely active (Ruano *et al.*, 2004). However, late Miocene faults located within the Iberian basement have been reactivated under the present-day NW–SE convergence, often leading to shallow seismicity (Pedrera

et al., 2013). To the west, however, there is widespread shallow seismicity in the Iberian basement beneath the Morón de la Frontera area (Fig. 8.1; Ruiz-Constán *et al.*, 2009, 2012b). Farther west, seismic reflection profiles and bathymetry in the Gulf of Cadiz (Gutscher *et al.*, 2002, 2012) suggest thrust activity on the front offshore. To date, there are no studies of the activity and structures related to the westernmost part of the onshore Betic cordillera front.

The aim of this study was to characterize the westernmost Betic cordillera front to determine the recent and present-day tectonic activity. A combination of geological and geophysical observations supported by available GPS data provides new results that enrich discussion of the present-day setting of this key area.

8.2 Geological setting

The westernmost part of the Betic Cordillera and the Guadalquivir Neogene foreland basin are located above the Iberian Massif (Fig. 8.1). The Betic Cordillera is traditionally divided into three main zones. The Alborán Domain (Internal Zones) and the South Iberian Domain (External Zones) are separated by a Flysch Complex. The South Iberian Domain represents the Mesozoic to Paleogene cover of the former South Iberian margin, deformed as a thin-skinned fold-and-thrust belt between the latest Oligocene and late Miocene, and consists of carbonates with intercalated marls, along with siliciclastic and, locally, volcanic rocks. A synorogenic Mélange unit (Bourgois, 1973; Pedrera *et al.*, 2012; Roldán *et al.*, 2012) occurs in the frontal area of the Cordillera, formed during the early Miocene to early Serravallian. The Guadalquivir foreland basin has an ENE–WSW elongated triangular shape, opening toward the Gulf of Cadiz. It developed as a consequence of flexure of the Variscan lithosphere by the load of the Alborán Domain during its emplacement (García-Castellanos *et al.*, 2002). Stratigraphic studies (Martínez del Olmo *et al.*, 1984; Sierro *et al.*, 1990; Roldán, 1995; Riaza and Martínez del Olmo, 1996; Salvany *et al.*, 2011; Rodríguez-Ramírez *et al.*, 2014) as well as several boreholes and seismic reflection profiles (Fernández *et al.*,

1998) have determined the pattern of the sedimentary infill, whose thickness at some points is greater than 5 km.

Plate relative angular velocities reveal a NW–SE convergence between the African and European plates in the western Mediterranean (Argus *et al.*, 1989; DeMets *et al.*, 1994). Stresses characterized by brittle deformation and earthquake focal mechanisms show a regional NW–SE compression, subparallel to the relative major plate motion, as well as variable to NE–SW tension in the Internal Zones of the Betic Cordillera (Galindo-Zaldívar *et al.*, 1993; De Vicente *et al.*, 2008; Pedrera *et al.*, 2011; Palano *et al.*, 2013). In the western Betics, large E–W and ENE–WSW folds have been observed, deforming late Tortonian to Pliocene rocks (Balanyá *et al.*, 2007; Ruiz-Constán *et al.*, 2009, 2012b).

In the western part of the Betic Cordillera, the depth of earthquakes progressively increases toward the south–south-east – from shallow seismicity at the Morón mountain front segment (Ruiz-Constán *et al.*, 2009) to events at approximately 120 km depth beneath the western Alborán Sea, where an arc is traced south of the Málaga coast (Buforn *et al.*, 1995; Morales *et al.*, 1999; Pedrera *et al.*, 2011; Ruiz-Constán *et al.*, 2011). In contrast, seismicity is very scarce in the westernmost part of the mountain front, the sector studied here.

GPS research (McClusky *et al.*, 2000; Vernant *et al.*, 2010; Koulali *et al.*, 2011) shows regional westward movement of the Betic Cordillera with respect to the Iberian Massif. In the central Betics the displacement is roughly to the WSW, but further west the largest velocities are reached in a WNW direction, even affecting the External Zones (Fig. 8.1). The movement progressively decreases toward the mountain front and is practically absent in the Guadalquivir Basin.

8.3 Morphology of the westernmost Betic Cordillera mountain front

The Betic Cordillera relief developed in stages, as evidenced by continental deposits since the Aquitanian (Martín-Algarra, 1987). The north-western limit of

the Betic Cordillera front was traditionally considered to be an inactive thrust. Onshore, the westernmost mountain front in south-west Spain draws a linear step along the Gulf of Cadiz coastline between the towns of Chipiona and Sanlúcar de Barrameda (Figs. 8.1 and 8.2). To the east, the lower Guadalquivir Basin is characterized by a large flat marsh area in sharp contact with the mountain area. The rectilinear front continues along the southern boundary of the Guadalquivir Basin, at least as far as Cabezas de San Juan, with discontinuous segments corresponding to elongated hills with steep NW rectilinear boundaries (Fig. 8.2). The sinuosity mountain front index (Bull and McFadden, 1977; SMF = length of the mountain front/length of straight line of the mountain front) of 1.13 indicates its active character.

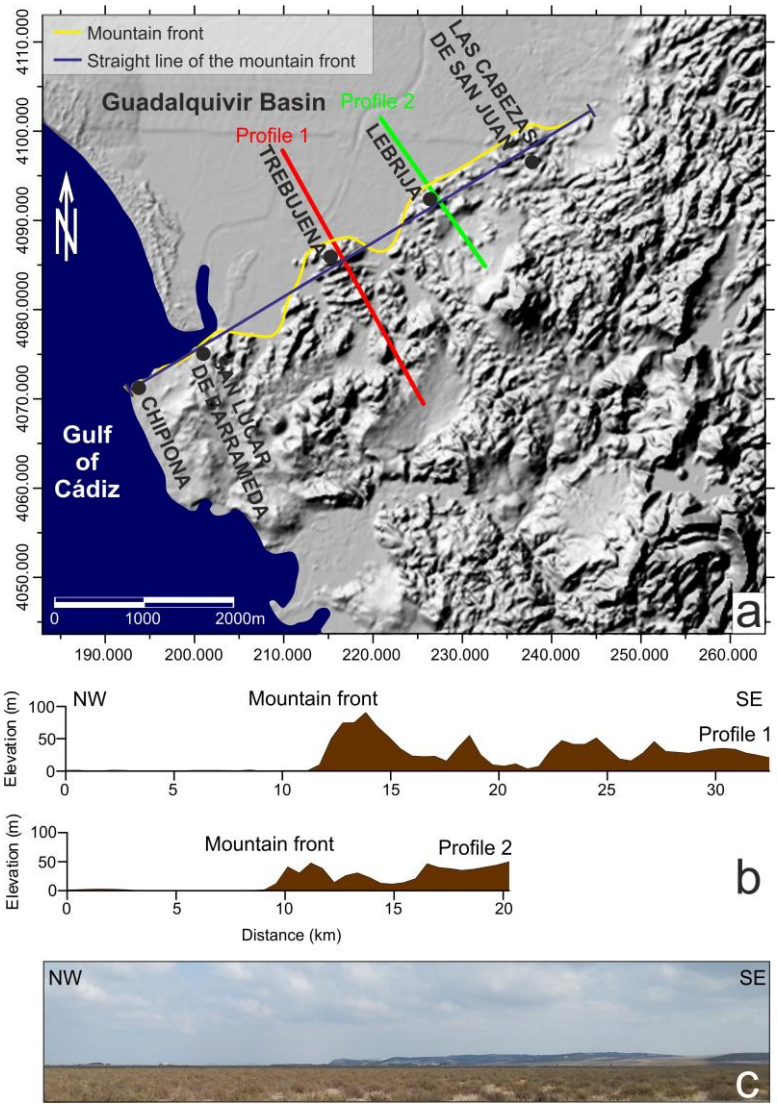

Figure 8.2: The relief of the western mountain front. (a) Shadow relief image of the western mountain front. (b) Topographic profiles. (c) Field panoramic. SMF index= 1.13.

8.4 Structure of the mountain front

The mountain front is formed mainly by folds with ENE–WSW axes (Fig. 8.1). Antiform culminations consist of Tortonian moronite formations. There is no surface field evidence of recent sediment deformation. In contrast, borehole data (Salvany *et al.*, 2011) indicate progressive thickening toward the south-east up to Holocene of the Guadalquivir deposits.

8.4.1 Seismic reflection profiles

Multichannel seismic reflection profiles (Fig. 8.3) were processed by means of a standard sequence including migration.

The S83A-232 profile has a NW–SE orientation and crosses the mountain front orthogonally, near Trebujena (Fig. 8.1). A roughly continuous subhorizontal deep reflector is recognized at about 3.6 s TWT and may represent the top of the Variscan basement. Horizontal reflectors belonging to the sedimentary infill of the Guadalquivir basin contrast with the folds in the Betic Cordillera Front, where antiforms determine the main hills of the area and the varying reflector curvature along synforms supports a synsedimentary character. No surface faults are recognized, suggesting that the mountain front formed mainly as a consequence of fold activity above a detachment level.

The S84A-302 profile, in the Guadalquivir basin, shows a SE-ward dipping reflector corresponding to the top of the Variscan basement below the cross-bedding, thus indicating SE progradation of the sedimentary infill. Subhorizontal layers correspond to the top of the sedimentary sequence.

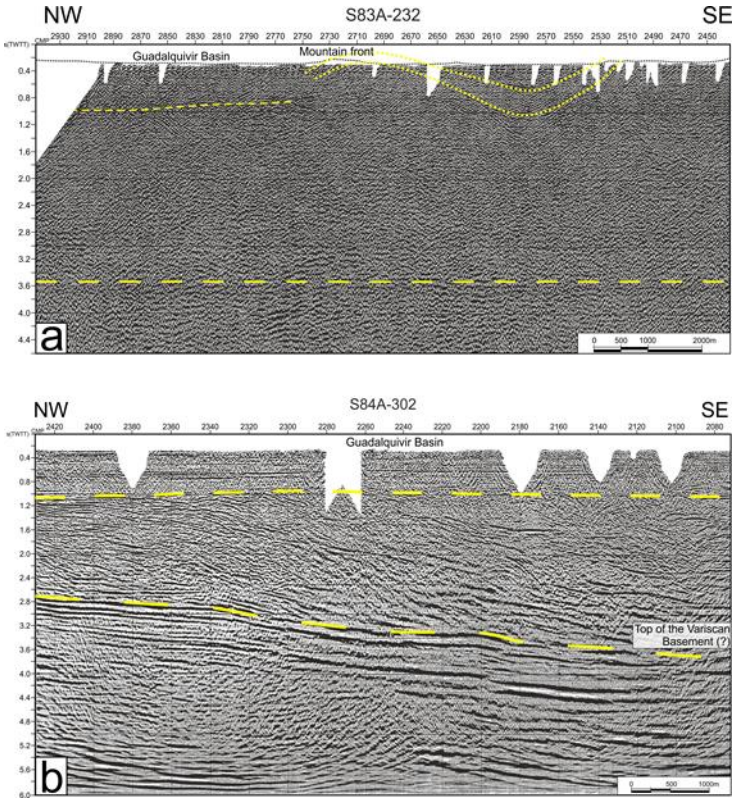

Figure 8.3: Multichannel seismic profiles. SIGECO database (http://cuarzo.igme.es/sigeco). Location in Fig. 8.1c.

8.4.2 Audiomagnetotelluric data

A detailed audiomagnetotelluric profile orthogonal to the mountain front was recorded with Strata Gem EH4 equipment, in a frequency range from 70 kHz to 10 Hz, reaching depths of tens to hundreds of meters. A transmitter antenna was used to enhance the natural electromagnetic field from 1 kHz to 5 kHz, where the natural signal decreases. Geoelectric dimensionality was analysed by means of Bahr decomposition (Bahr, 1988, 1991). The curves show a general 1D behaviour up to 10−1 s and a 2D structure from 10−1 to 10 s with a N70-90° E strike. We checked the internal consistency of the rho and phase estimated at each site (Parker and Booker, 1996) and corrected static shift problems in some of the curves. A joint 2D inversion of resistivities and phases was carried out integrating all the data (Rodi and Mackie, 2001). An error floor of 3% for the apparent resistivities and the phases was selected.

The north-western part of the profile (Fig. 8.4) is characterized by a low-resistivity sector, extending from the surface down to 300 m (~1 ohm·m), corresponding to the sedimentary Guadalquivir basin infill, made up of saturated clays and silts. To the south-east, uplift of the resistive layer is related to an antiformal structure that reaches the surface along an elongated hill, determining a sharp mountain front extending down the basin sediments.

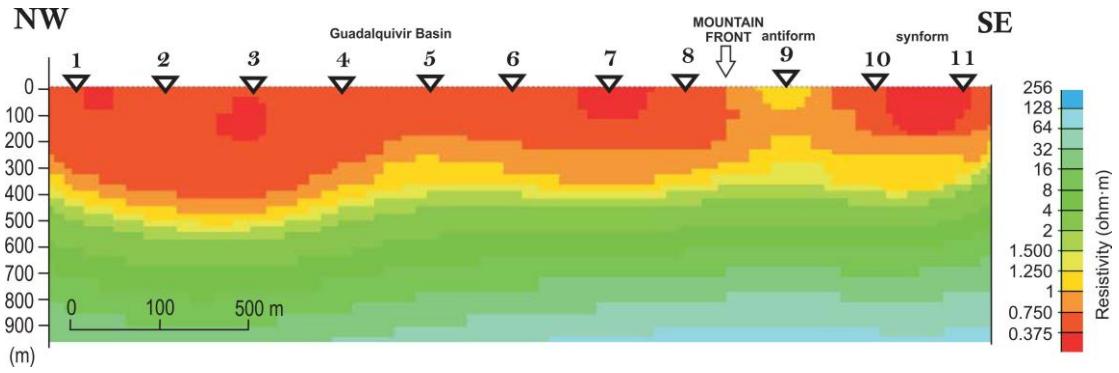

Figure 8.4: Audiomagnetotelluric profile across the mountain front. Location in Fig. 8.1d. Root mean-square-misfit between the data and the synthetic response was 4.1.

8.5 Brittle deformation and stresses

In order to characterize the recent palaeostress pattern in this region, microtectonic measurements were made in a wide zone along the mountain front. According to Hancock (1985), the main joint system (Figs. 8.5 and 8.6) consists of a NW–SE tensional set or two hybrid sets forming an acute angle, suggesting that the mountain front underwent NW–SE compression and orthogonal NE–SW tension. This stress field is recognized all along the mountain front and is well constrained in the Chipiona sector, where the coastal area is formed from Quaternary consolidated beach deposits. Faults are scarce, with normal regime and restricted to antiformal areas (Fig. 8.5).

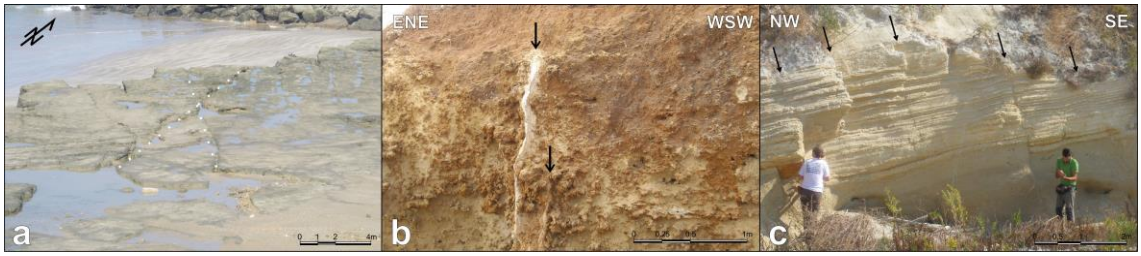

Figure 8.5: Field examples of fractures. (a) Conjugate fractures in Quaternary beach deposits ('Corrales de Peces', Chipiona). (b) Vertical tension joints. (c) Normal faults in antiformal areas.

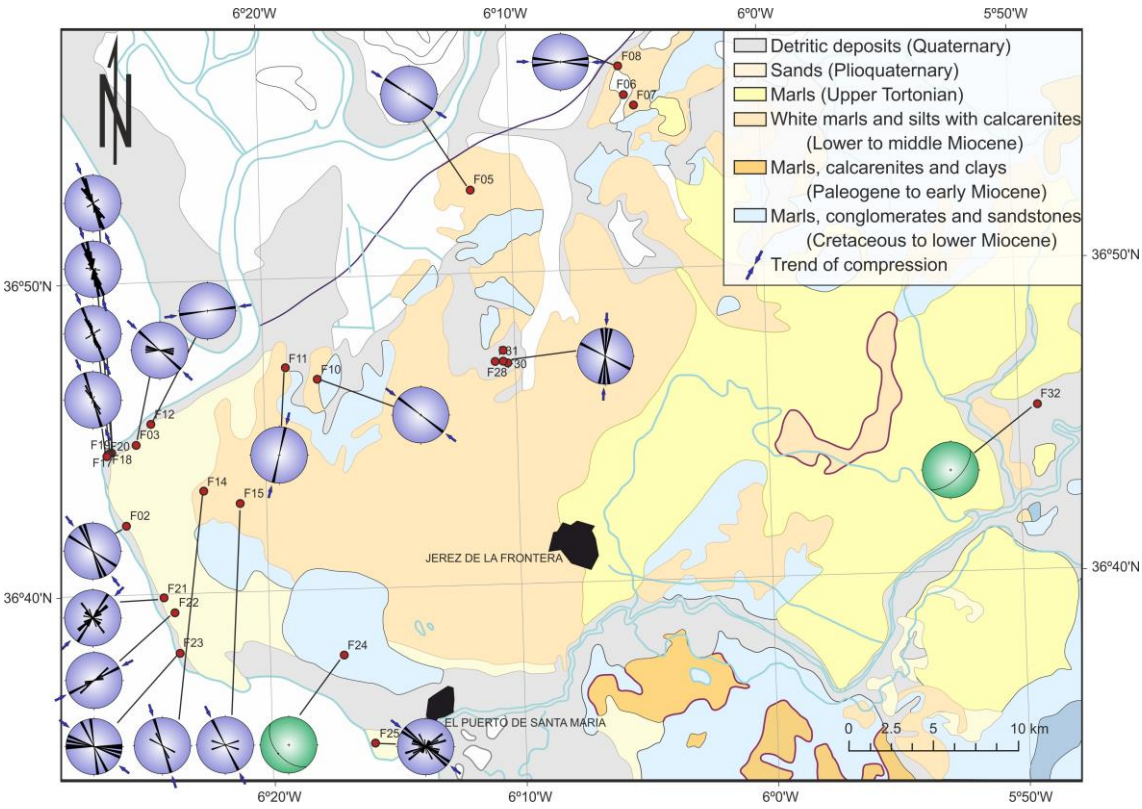

Figure 8.6: Fracture orientation and paleostresses. Rose diagrams of main outcrops (purple plot); maximum horizontal stress corresponds to the orientation of the main extensional joint set or to the acute angle between the conjugate or hybrid joint sets according to Hancock (1985). Faults in stereographic projection (green plot), lower hemisphere.

8.6 Discussion

Although the major tectonic structures that accommodated the accretion of the external Betics appear to have been inactive since the late Miocene, the rectilinear character of the westernmost Betic Cordillera mountain front suggests that it is still affected by active deformation. Although no large faults are recognized, active folds affect the marine Tortonian rocks up to the Holocene deposits (Fig. 8.7). Normal faults along antiformal culminations reveal local shallow NW–SE to NNW–SSE extensional trends (Figs. 8.5-8.7), which could be a consequence of the uplifted relief that developed as a result of deep compressional deformation.

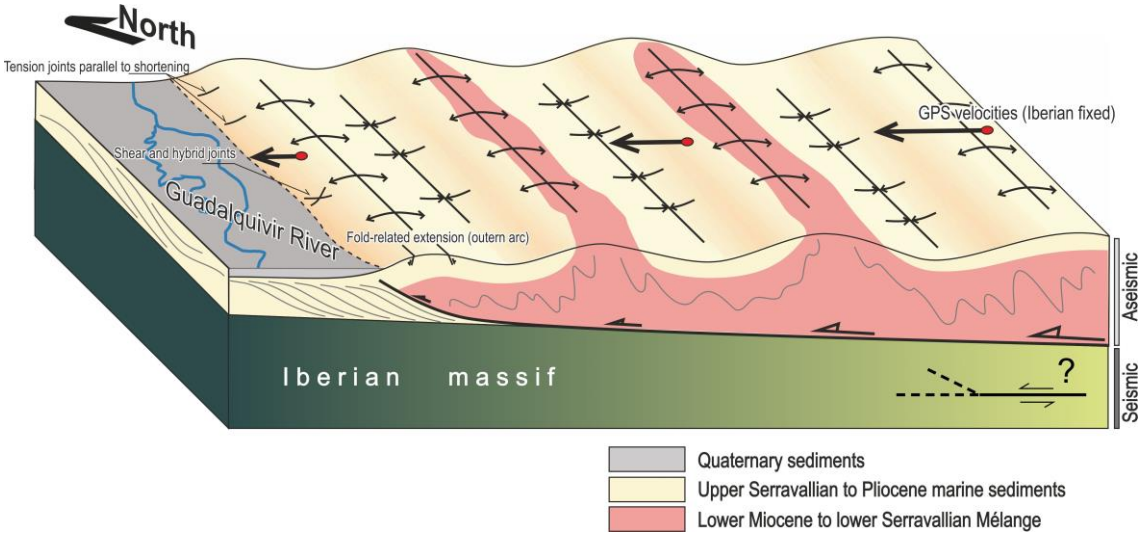

Figure 8.7: 3D model of the structures across the folded deformation front.

The decreasing magnitude of the WNW GPS velocities (from 3.4 mm/yr) toward the western mountain front with respect to the roughly stable foreland basin agrees with active folding along a broad band. The progressive crustal thickening of the Betic Cordillera produces a load and flexure of the Guadalquivir Basin Variscan basement (García-Castellanos *et al.*, 2002); the thickness of sedimentary infill increases toward the mountain front (Salvany *et al.*, 2011; Rodríguez-Ramírez *et al.*, 2014).

In spite of the wide ellipse errors of the GPS measurements (Fig. 8.1), WNW motion of the western Betic Cordillera with respect to the Eurasian plate is consistent with the NW-SE compression, underlining the relevance of present-day collision tectonics related to ongoing continental subduction, aided by the pull of the already subducted oceanic crust (Ruiz-Constán *et al.*, 2011; Fig. 8.8).

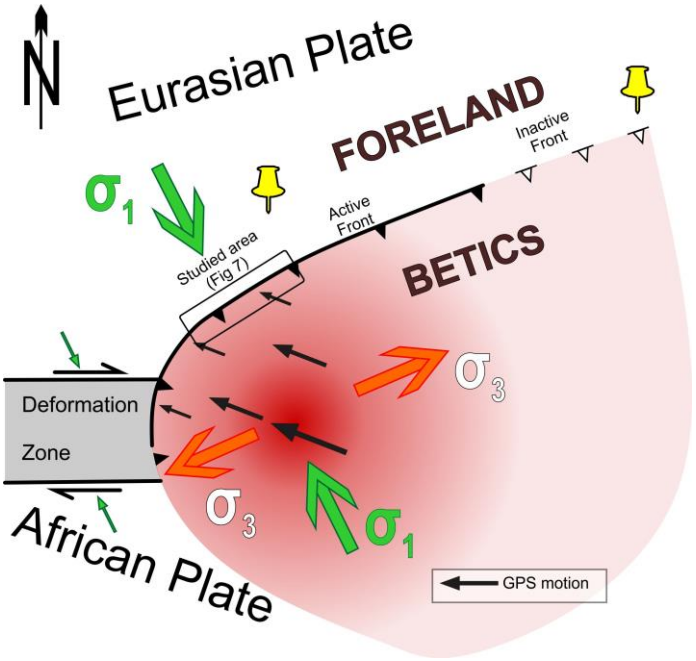

Figure 8.8: Tectonic model showing the GPS motion and compression trend. The regional NW-SE compression between Eurasian and African plates together with the NE-SW extension in the Betic Cordillera determines the relatively wesward-northwestard motion of the Alborán domain.

The active structures vary along the mountain front. The folds and soft rocks in the study area prevent the occurrence of shallow earthquakes. Coupling between the Alborán Domain and the Iberian massif promotes the occurrence of seismicity within the foreland. Westward, this area connects offshore in the Gulf of Cadiz, where Gutscher *et al.* (2002, 2012) documented present-day thrusting. Eastward, shallow earthquakes affect the Iberian crust in the Morón (Ruiz-Constán *et al.*, 2009) and Torreperogil areas (Pedrera *et al.*, 2013). In the central Betic Cordillera the front is essentially inactive, and deformation occurs toward the interior of the mountain belt (Ruano *et al.*, 2004).

8.7 Conclusions

The compilation of geomorphic, field geological, geophysical and available GPS data provides evidence that the westernmost Betic Cordillera mountain front is active, and that it produced the south-eastward increase in the thickness of the sedimentary infill of the Guadalquivir Basin, which affects up to Holocene deposits. The mountain front has a variable character due to the different lithologies. Shallow seismicity related to reverse and strike-slip faults occurs in the Morón area; to the west, active folds accommodate the deformation along the westernmost mountain front in the Trebujena-Chipiona area (Fig. 8.7); finally, thrusts affect the Gulf of Cadiz.

The obliquity between the WNW-ward motion of the Cordillera with respect to the foreland, and the NW–SE trend of compression related to the Eurasian-African plate motion, may result from oblique collision (Fig. 8.8) related at depth to active continental subduction. These newly integrated results confirm that Alpine compressional deformation continues in this sector of the western Mediterranean.

Acknowledgements

Professor C. Doglioni, Dr. R. Reilinger and an anonymous reviewer have improved the significance of this contribution. Financed by the projects CGL2010-21048, P09-RNM-5388 and RNM148.

Chapter 9

Active rollback in the Gibraltar Arc: evidences from CGPS data in the Western Betic Cordillera

González-Castillo, L.[1], Galindo-Zaldívar, J.[1, 2], Junge, A.[3], de Lacy, M.C. [3,4], Borque, M.J. [3,4], Martínez-Moreno, F.J.[1], García-Armenteros, J.A.[3,4], Gil, A.J.[3,4]

Published on:

Tectonophysics, 2015

DOI: 10.1016/j.tecto.2015.03.010

(Received 21 October 2014; Accepted 20 March 2015)

[1] Departamento de Geodinámica, Universidad de Granada, Spain.

[2] Instituto Andaluz de Ciencias de la Tierra. CSIC-UGR. Spain.

[3] Dpto. Ing. Cartográfica, Geodesia y Fotogrametría, Universidad de Jaen. Spain.

[4] Centro de Estudios Avanzados en Ciencias de la Tierra (CEACTierra), Universidad de Jaén, Spain.

ABSTRACT

The Gibraltar Arc, located in the western Mediterranean Sea, is an arcuate Alpine orogen formed by the Betic and Rif Cordilleras, separated by the Alborán Sea. New continuous GPS data (2008-2013) obtained in the Topo-Iberia stations of the western Betic Cordillera allow us to improve the present-day deformation pattern related to active tectonics in this collision area between the Eurasian and African plates. These data indicate a very consistent westward motion of the Betic Cordillera with respect to the relatively stable Iberian Massif foreland. The displacement in the Betics increases toward the south and west, reaching maximum values in the Gibraltar Strait area (4.27 mm/yr in Ceuta, CEU1, and 4.06 mm/yr in San Fernando, SFER), then progressively decreasing toward the northwestern mountain front. The recent geological structures and seismicity evidence moderate deformation in a roughly NW-SE to WNW-ESE compressional stress setting in the mountain frontal areas, and moderate extension toward the internal part of the cordillera. The mountain front undergoes progressive development of folds affecting at least up to Pliocene deposits, with similar recent geological and geodetical rates. This folded strip helps to accommodate the active deformation with scarce associated seismicity. The displacement pattern is in agreement with the present-day clockwise rotation of the tectonic units in the northern branch of the Gibraltar Arc. Our data support that the westward emplacement of the Betic Cordillera continues to be active in a rollback tectonic scenario.

Keywords: CGPS stations; Western Mediterranean; active deformations; present-day rollback; tectonic rotation.

Highlights

- New CGPS stations support fast westward displacements of the Western Betics.
- Active dextral rotations are in agreement with the tectonic arc development.
- A folded strip of several tens of km accommodates the frontal deformations.
- Integration of CGPS and geological data supports active rollback in the Betics.

9.1 Introduction

The geodetical networks based on GPS observations provide new insights to constrain the pattern of active motion and rotation in oroclinals, as the Bolivian oroclinal (Allmendinger *et al.*, 2005), St. Elias orogen in Alaska (Elliot *et al.*, 2013) and central Anatolia (Aktug *et al.*, 2013). The Betic-Rif Cordillera, connected through the Gibraltar Arc (Fig. 9.1), is a strongly curved oroclinal. New accurate GPS geodetical data are essential to constrain the active tectonic deformations.

In the western Mediterranean, NW-SE convergence of 4 to 5 mm/yr, depending on different geodynamic models, occurs in-between the major Eurasian and African plates (DeMets *et al.*, 1994, Nocquet, 2012). Geodetic networks provide deformation patterns that show the activity of geological structures and eventually reveal the general deformation pattern. Up to now, GPS data from continuously recording GPS stations (CGPS) and survey-mode GPS sites show a roughly NW-WNW displacement in the western part of the Betic Cordillera (Serpelloni *et al.*, 2007; Vernant *et al.*, 2010; Koulali *et al.*, 2011) with respect to the Iberian Massif. These data demonstrate that the building up of this Alpine cordillera continues at present, in agreement with the regional seismicity related to the plate boundary. However, models based on these studies generally aim to trace sharp rectilinear Eurasian-African plate boundaries, without integrating the widespread active tectonic structures observed in these Cordilleras.

Different models have been proposed for the development of the Gibraltar Arc, based on the presence of subduction structures (Araña and Vegas, 1974; Torres-Roldán *et al.*, 1986; De Jong, 1991 and 1993; Wortel and Spakman, 1992; Zeck *et al.*, 1992 and Zeck,1996, Pedrera *et al.*, 2011; Ruiz-Constán *et al.*, 2011), lithospheric delamination (Houseman *et al.*, 1981; Platt and Vissers, 1989; García-Dueñas *et al.*, 1992; Seber *et al.*, 1996; Calvert *et al.*, 2000; de Lis Mancilla *et al.*, 2013) or slab rollback (Blanco and Spakman, 1993; Morley, 1993;

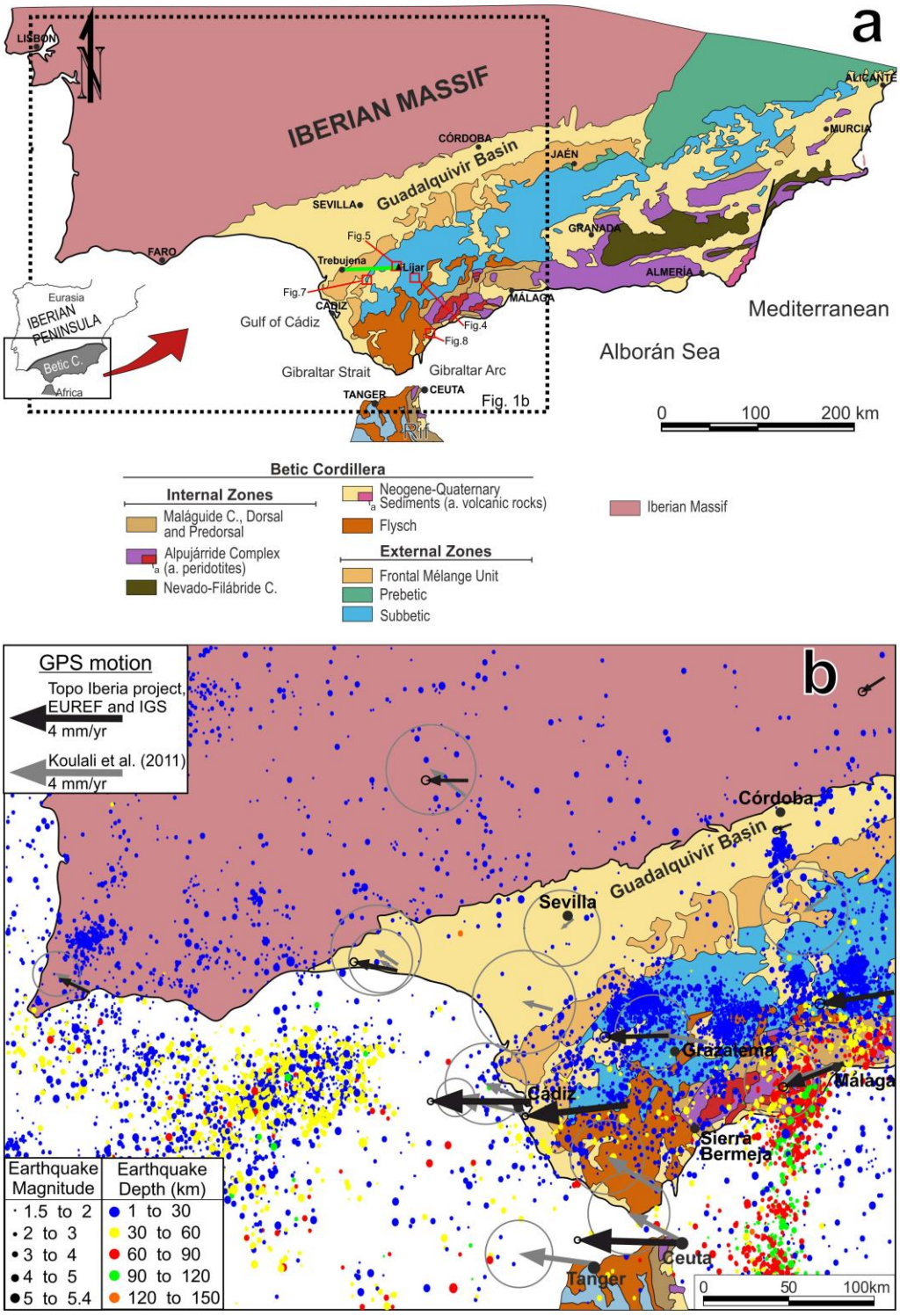

Figure 9.1: The western Betic Cordillera and its foreland. (a) Geological setting of the western Betic Cordillera and its foreland. Dashed rectangle highlights the studied area. Small squares locate Figs. 9.4, 9.5, 9.7 and 9.8. Green line indicates the Trebujena-Líjar cross-section. (b) Tectonic sketch of the area studied including seismicity (database of Instituto Geográfico Nacional, www.ign.es) and CGPS data. Residual velocity field is referred to Eurasia and 95% confidence ellipses.

Royden, 1993; Lonergan and White, 1997; Hoernle *et al.*, 1999; Wortel and Spakman, 2000; Gill *et al.* 2004; Thiebot and Gutscher, 2006; Brun and Faccena, 2008). Although most of them focus on the Miocene evolution, Gutscher *et al.* (2002), Thiebot and Gutscher (2006), Pedrera *et al.* (2011) and Ruiz-Constán *et al.* (2012) suggest that the subduction is still active at present. In addition, slab rollback models have been proposed based on GPS data from the Rif (Fadil *et al.*, 2006; Pérouse *et al.*, 2010). Its origin and recent evolution are still controversial due to a lack of accurate data on its structure at depth, as well as the superposition of deformations and the variable features of the recent tectonic movements.

The aim of this paper is to present the results of new CGPS data from some stations (Fig. 9.1) that belonged to the Topo-Iberia research. As part of this project, a network of 26 CGPS stations covering the Spanish part of the Iberian Peninsula and Northern Morocco were set (Lacy *et al.*, 2012; Gárate *et al.*, 2014). These new data for the period between March 2008 and December 2013 attest a westward displacement of the Betic-Rif Cordillera, reaching maximum values toward the south, near Gibraltar Strait area. Given their high quality and novelty, the data presented here shed light on the active tectonic structures of the western Betic Cordillera.

9.2 Geological Setting

The Betic-Rif Cordillera constitutes an arcuate Alpine orogeny, connected through the Gibraltar Arc, formed by the interaction of the Eurasian-African plates in the Western Mediterranean (Fig. 9.1). The Betic Cordillera is divided into the Internal Zones (Alborán Domain), Flysch Units and External Zones (South Iberian Domain) located over the Iberian Massif foreland. The Internal Zones are formed by metamorphic complexes that include Paleozoic rocks. They comprise three main complexes: from bottom to top, the Nevado-Filábride,

Alpujárride and Maláguide, in addition to the Dorsal and Predorsal. The most complete Alpujárride units have a sequence of metamorphic rocks with peridotites at the base. The Flysch Units correspond to an accretionary wedge constituted by Early Cretaceous to Lower Miocene siliciclastic deposits, located between the External and Internal Zones (Luján *et al.*, 2006). The External zones represent a thin-skinned fold and thrust belt formed by Mesozoic and Cenozoic carbonate and detritic deposits (Crespo-Blanc *et al.*, 2012). Furthermore, there is widespread development of intramontane basins which, together with the Guadalquivir foreland basin, are filled by sedimentary rocks from Miocene to Quaternary ages (Roldán, 1995; Riaza and Martínez del Olmo, 1996; Salvany *et al.*, 2011, Rodríguez-Ramírez *et al.*, 2014). The frontal area of the Betic Cordillera, located along the mountain front that bounds to the south the Guadalquivir basin, features a synorogenic early Miocene to early Serravallian Olisthostromic unit of the Guadalquivir (Perconig, 1960-1962) also called Mélange Unit (Bourgois, 1978; Pérez-López and Sanz de Galdeano, 1994; Pedrera *et al.*, 2012; Roldán *et al.*, 2012). The activity of this arcuate orogen (Balanyá *et al.*, 2007, 2012; Expósito *et al.*, 2012) has determined a clockwise rotation of tectonic units in the Betics and counter-clockwise in the Rif, as evidenced by paleomagnetic data (Platzman, 1990; Platzman and Lowrie, 1992; Platt *et al.*, 2003). In the western Betics, rotation varies in every unit probably reaching as much as 60ºsince Cretaceous time. The present-day relief has developed during the last 10 Ma (Braga *et al.*, 2003) in a roughly NW-SE to WNW-ESE compressional setting (Pedrera *et al.*, 2011; Palano *et al.*, 2013).

The widespread seismicity in the region (Buforn *et al.*, 1995 and database of the Instituto Geográfico Nacional, www.ign.es) is associated with the tectonic activity (Ruiz-Constán *et al.*, 2012) and related to the Eurasian-Africa oblique collision. Most of the western Betic Cordillera is affected by compressional deformations related to the overthrusting of its tectonic units onto the Iberian Massif foreland (Ruiz-Constán *et al.*, 2012). However, the eastern part of the Betics has mainly undergone extensional tectonics since Middle Miocene

(Galindo-Zaldívar *et al.*, 2003), although the transition from extensional to compressional deformations related to top-to-the west displacements and its timing are under discussion (Galindo-Zaldívar *et al.*, 2000). Although most of the earthquakes are shallow nearby the Betic Cordillera mountain front, they are deeper toward the western Alborán Sea, reaching 120 km deep along an arcuate band related to active subduction processes (Buforn *et al.*, 1995; Morales *et al.*, 1999; Pedrera *et al.*, 2011; Ruiz-Constán *et al.*, 2011).

GPS research in the Betic-Rif Cordillera is based on the installation of survey-mode GPS networks to study local structures such as the Zafarraya fault (Galindo-Zaldívar *et al.*, 2003), Balanegra Fault (Marín-Lechado *et al.*, 2010), CuaTeNeo GPS network in the eastern Betic Cordillera (Echeverría *et al.*, 2013) and Granada Basin (Gil *et al.*, 2002; Ruiz *et al.*, 2003). CGPS data —often combined with GPS campaign observations— have allowed researchers to determine the general deformation pattern of the Betic-Rif Cordillera with respect to the Iberian foreland, which represents the stable Eurasian plate. Most GPS contributions are aimed to distinguish different crustal blocks along the plate boundary (Fadil *et al.*, 2006; Serpelloni *et al.*, 2007; Vernant *et al.*, 2010; Koulali *et al.*, 2011), generally lacking interpretation of particular active structures. Serpelloni *et al.* (2007) derived a relative westward motion of the Betic-Rif Cordillera based on very scarce data. Fadil *et al.* (2006) focus on the Rif, proposing rollback of a delaminated subcontinental lithospheric slab, while Tahayt (2008) evidenced westward motion in the Gibraltar Strait area with respect to Eurasia. Pérez-Peña *et al.* (2010) study the Betics and northern Rif, supporting roughly NW motion (ranging from N to W) and relating the displacement to several major faults and seismicity. Pérouse *et al.* (2010) use a GPS displacement model to propose a local detached slab in the Rif. Vernant *et al.* (2010) and De Lis Mancilla *et al.* (2013) also present scarce data in the Betics, with motions ranging from WSW in the eastern Betics to WNW in the western Betics. Koulali *et al.* (2011) present campaign GPS data between 1999

and 2009, showing the arcuate displacement pattern in greater detail (Fig. 9.1b). These results contrast with the current and innovative results presented in this paper, based on recent data (2008-2013) from the Topo-Iberia stations, which show a roughly westward motion of the western Betics.

9.3 Methodology

This study presents the current GPS velocity field in the western Betic Cordillera derived from CGPS observations from March 2008 up to December 2013. The sub-network used in this paper consists of 10 sites (Figs. 9.1 and 9.2) which are operated by different Institutions: ALJI, LOJA, CAST, LIJA (Topo-Iberia research project), COBA, HUEL, MALA, CEU1, LAGO (EUREF Permanent Network, a science-driven network of continuously operating GPS reference stations of the International Association of Geodesy) and SFER (International GNSS Service, IGS). It is very important to emphasize that the locations of the Topo-Iberia sites are in the field (not on buildings) and founded

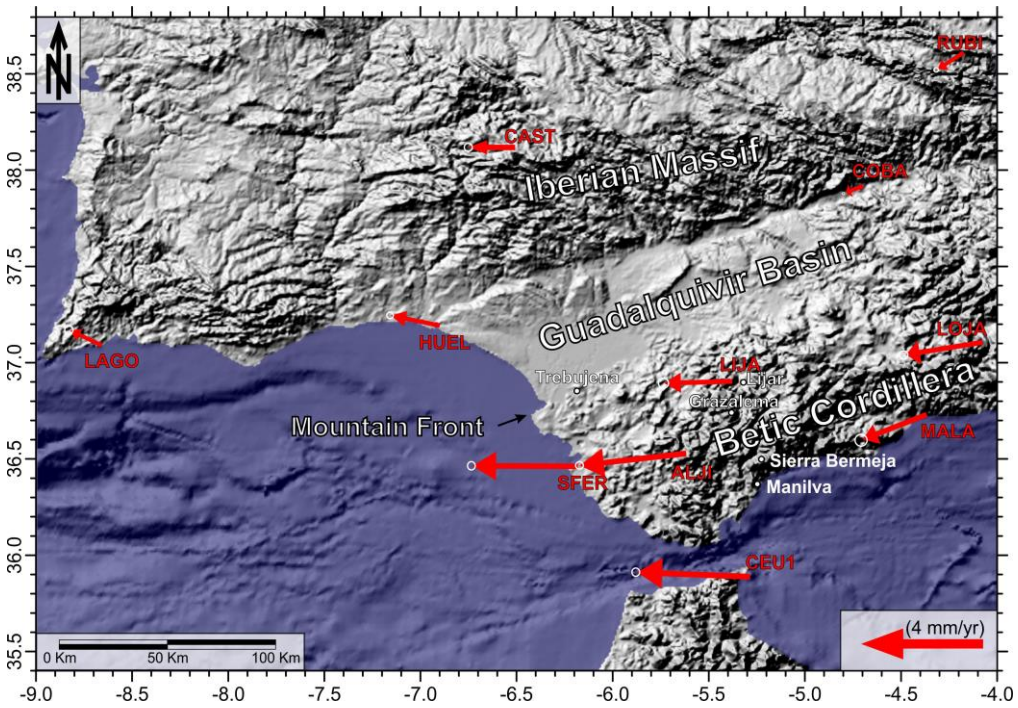

Figure 9.2: Topography and CGPS data of the area studied. Residual velocity field is referred to Eurasia and 95% confidence ellipses.

on bedrock, implying a high stability of the concrete pillars and a high quality of the observations. Firstly, a previous quality check of CGPS data was carried out using the TEQC software developed by UNAVCO (Estey and Meertens 1999). Secondly, data processing was performed using the Bernesse software (Dach *et al.* 2007). A daily GPS network solution in a loosely constrained reference frame was estimated. The GPS observable is formed by double-differencing the L1 and L2 phase observations. GPS orbits and Earth's orientation parameters were held fixed to the combined IGS products and a priori error of 10 m is assigned to all site coordinates in order to get the loosely constrained coordinates. These solutions could be combined regardless of the datum definition of each contributing solution. The solution reference frame is defined stochastically by the input data and is basically unknown, though the estimation of relative rigid transformations (rotation-translation scale) between reference frames becomes necessary; this naturally leads to a combined solution not distorted by any constraint or transformation. Then, the daily network solutions were minimally constrained and transformed into EPN_A_IGb08 (EUREF Permanent Network station Positions in IGb08 reference frame) estimating translations and scale parameters. Finally, the velocity field was estimated by means of the NEVE software, which manages the complete stochastic model (Devoti *et al.* 2008). Velocities were estimated simultaneously, together with annual signals and sporadic offsets at epochs of instrumental changes. Velocity errors were derived from the direct propagation of the daily covariance matrix.

Geological field observations involved recent and active structures that could accommodate the present-day deformation field of the western Betic Cordillera. Field research included observation of recent faults (fault surfaces and regime) and folds (orientation, dip of the limbs), as well as reviewing and improving the previous geological maps in areas of poor outcropping.

9.4 Displacements from GPS data in the western Betic Cordillera and its foreland

The CGPS-derived absolute velocities and associated errors in the IGb08 reference frame are given in Table 9.1 and Figure 9.3. A more effective representation of the estimated velocity field can be attained by presenting the residual velocities with respect to stable Eurasia, whose kinematics is defined through the rotation pole and rate. Figures 9.1 and 9.2 show the residual velocities at 95% of confidence with respect to the Eurasia fixed reference frame. These new GPS results provide a highly consistent displacement pattern of the western Betic Cordillera with respect to its foreland.

	Coordinates		Absolute velocities (mm/yr)				Residual velocities (mm/yr)			
Site	Lat. (°N)	Long. (°E)	VE	σE	VN	σN	VE	σE	VN	σN
CAST	38.1227	-6.5321	17.55	±0.03	17.17	±0.04	-1.60	±0.05	-0.01	±0.05
ALJI	36.5299	-5.6494	15.67	±0.05	16.72	±0.06	-4.00	±0.07	-0.44	±0.07
LIJA	36.9062	-5.4038	17.07	±0.04	17.06	±0.05	-2.56	±0.06	-0.09	±0.06
LOJA	37.1073	-4.1064	17.01	±0.04	16.67	±0.04	-2.81	±0.05	-0.44	±0.05
LAGO	37.0989	-8.6684	17.89	±0.03	17.71	±0.03	-1.11	±0.05	0.50	±0.05
COBA	37.9156	-4.7211	19.08	±0.03	16.99	±0.03	-0.45	±0.05	-0.14	±0.05
HUEL	37.2000	-6.9203	17.54	±0.03	17.49	±0.04	-1.75	±0.05	0.31	±0.05
MALA	36.7261	-4.3935	17.52	±0.04	16.14	±0.05	-2.33	±0.06	-0.99	±0.06
CEU1	35.8920	-5.3064	15.60	±0.04	17.36	±0.04	-4.26	±0.06	0.21	±0.05
SFER	36.4643	-6.2056	15.57	±0.01	17.16	±0.01	-4.01	±0.04	-0.01	±0.04

Table 9.1: CGPS-derived absolute velocities and associated errors in IGb08 reference frame and residual velocities with respect to Eurasia fixed.

Most of the sites located in the Iberian Massif have very low relative displacement with respect to stable Eurasia, and all of them have a roughly westward component. HUEL and CAST, are faster than COBA and RUBI (Fig. 9.2). Moreover, the stations in the western Gibraltar Arc (CEU1, LIJA, SFER) show a westward motion relative to its foreland (HUEL) (Figs. 9.1 and 9.2), the values reaching a maximum in the Gibraltar Strait (CEU1, 4.26 mm/yr) and its northern nearby region (ALJI 4.00 mm/yr), as well as in the area to the northwest (SFER site, 4.01 mm/yr). This displacement (Figs. 9.1 and 9.2)

slightly decreases toward the north (LIJA, 2.56 mm/yr) and east (MALA, 2.33 mm/yr and LOJA, 2.81 mm/yr). Further eastward, the relative displacement has a minor WSW component (LOJA and MALA) in contrast to the purely westward motion of the LIJA, SFER and CEU1 stations.

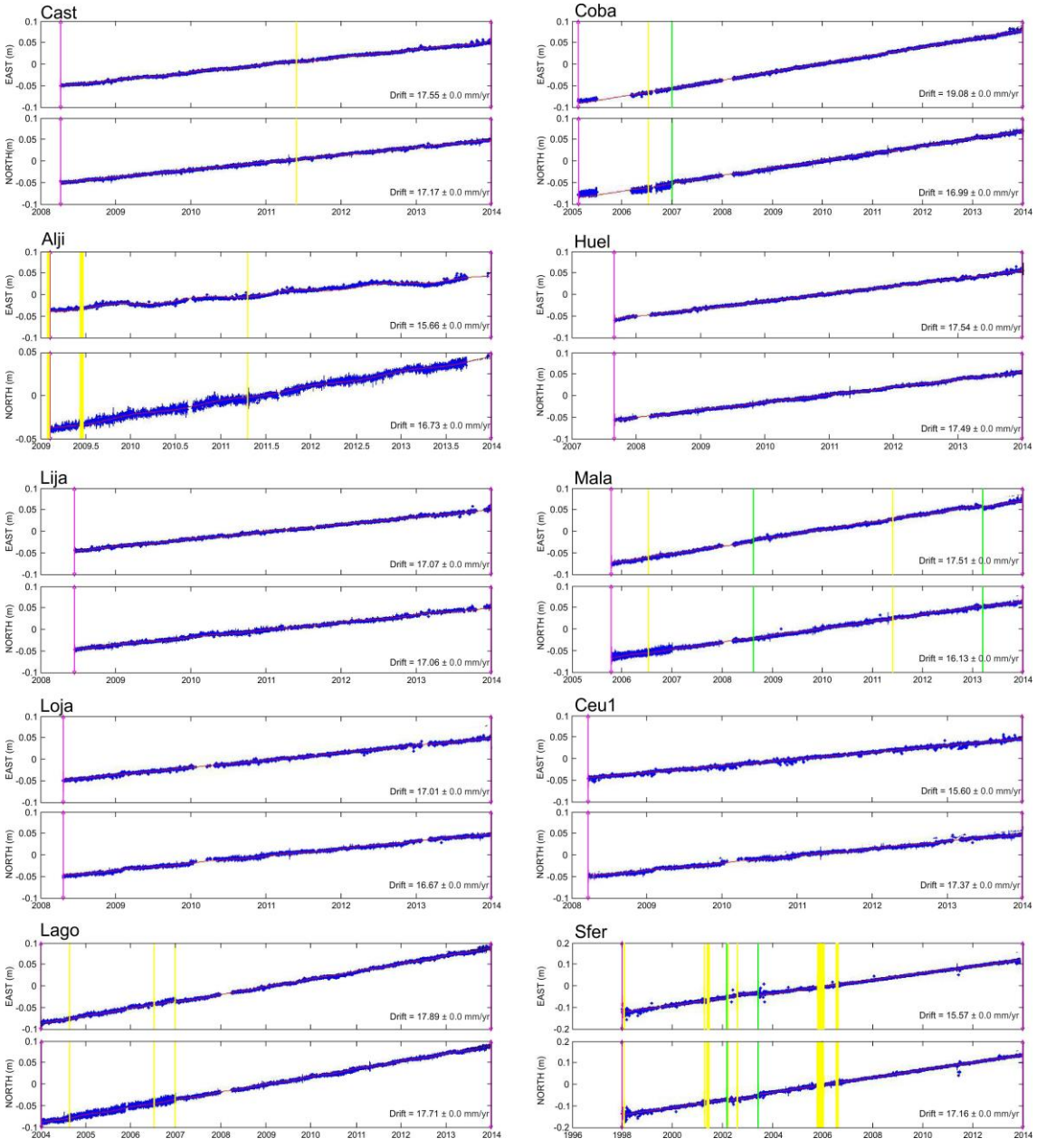

Figure 9.3: Position time series of the network stations (North and East components in metres. Yellow lines are considered outliers according to the software applied. Absolute velocities are included in Table 1.

In the northwestern front of the Betic Cordillera there is a high gradient of progressively decreasing displacement, up to the foreland located toward the NW, evidencing oblique contraction. Moreover, the moderate difference of the displacements between LOJA and MALA with respect to ALJI (Figs. 9.1 and 9.2) supports the occurrence of a low intensity widespread extension in the southeastern part of the study area.

9.5 Recent, active and other relevant structures

Field observations reveal the main features of the geological structures that may accommodate the present-day westward displacement of the western Betics with respect to its foreland. Most of the frontal area is formed by soft rocks of Miocene to Quaternary ages (Fig. 9.1), with scarce reference horizons. They unconformably lies over Cretaceous to Jurassic carbonate series. There are also olisthostromic masses mainly formed by Triassic sediments (Figs. 9.4, 9.5, and 9.6).

The westernmost front of the Cordillera (Figs. 9.1 and 9.2) constitutes a thin-skinned fold and thrust belt and huge olisthostromic masses derived from the External Zones. Folds affecting Jurassic and Cretaceous rocks (Sierra de Líjar, Fig. 9.4), as well as Upper Miocene sediments (Montellano area, Figs. 9.5 and 9.6), generally have NE-SW orientations ranging from N45ºE to N50ºE. More recent folds affect Pliocene sediments in the Montellano area (Fig. 9.5) and have axes N20ºE to N40ºE. The geometry of these folds varies from NW vergent moderately inclined (Sierra de Líjar, Fig. 9.4) to upright (Espera, Fig. 9.7). Southward along the Gibraltar Arc, folds also affect the inner sector of the Cordillera, as evidenced by the N-S oriented Manilva antiform (Figs. 9.6 and 9.8) formed in early-middle Miocene, but also affecting upper Miocene rocks (Balanyá *et al.*, 2012) and Pliocene sediments (Durand-Delga, 2006). Although the main observed structures are recent folds, scarce recent reverse faults can also be identified, for instance near Espera (Figs. 9.6 and 9.7). These

structures are responsible for accommodating recent shortening in the western Betics.

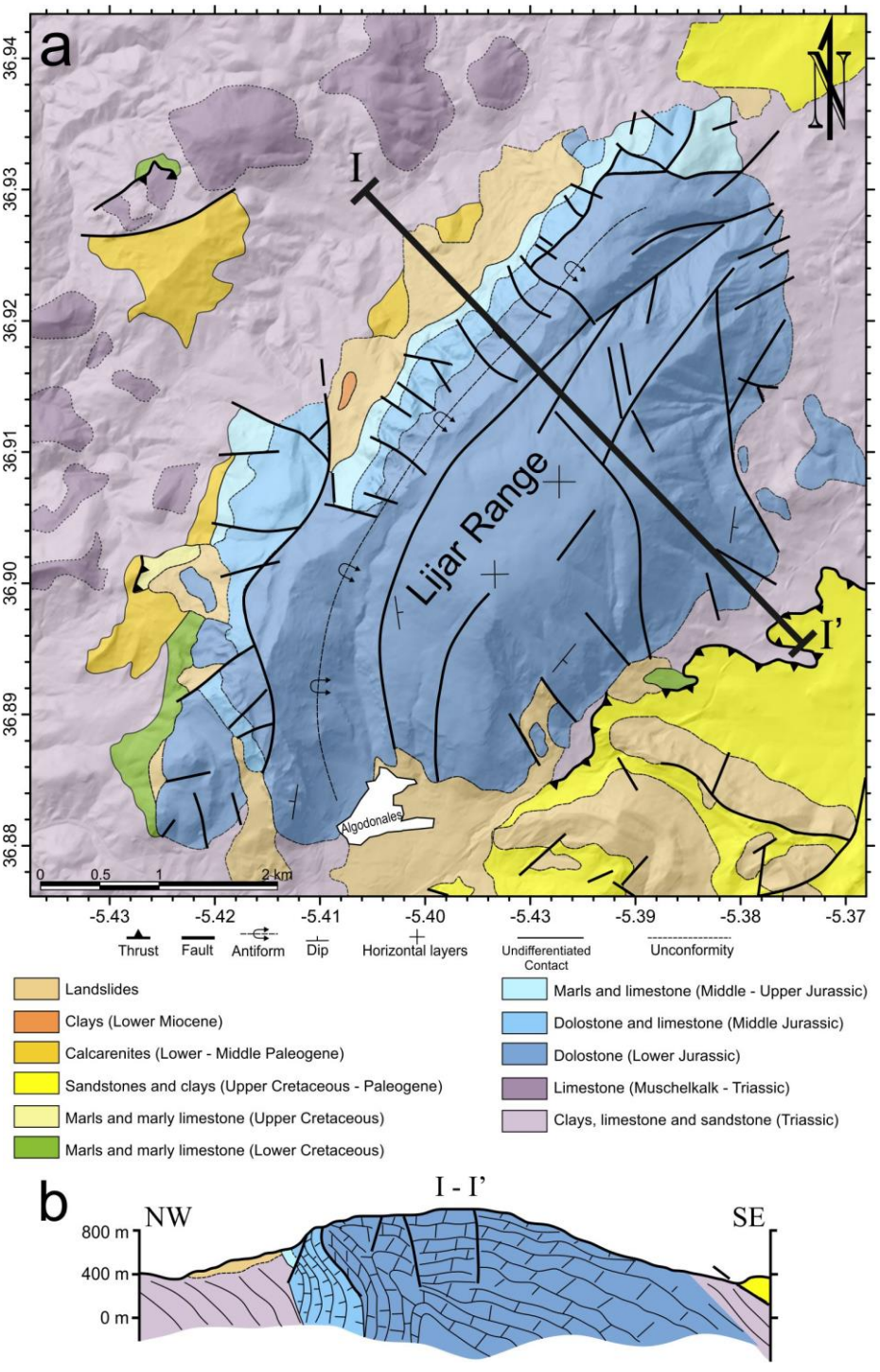

Figure 9.4: Structure of the Líjar range. (a) Geological map. (b) Cross-section. Modified from Cano-Medina (1981). See regional location in Fig. 9.1a.

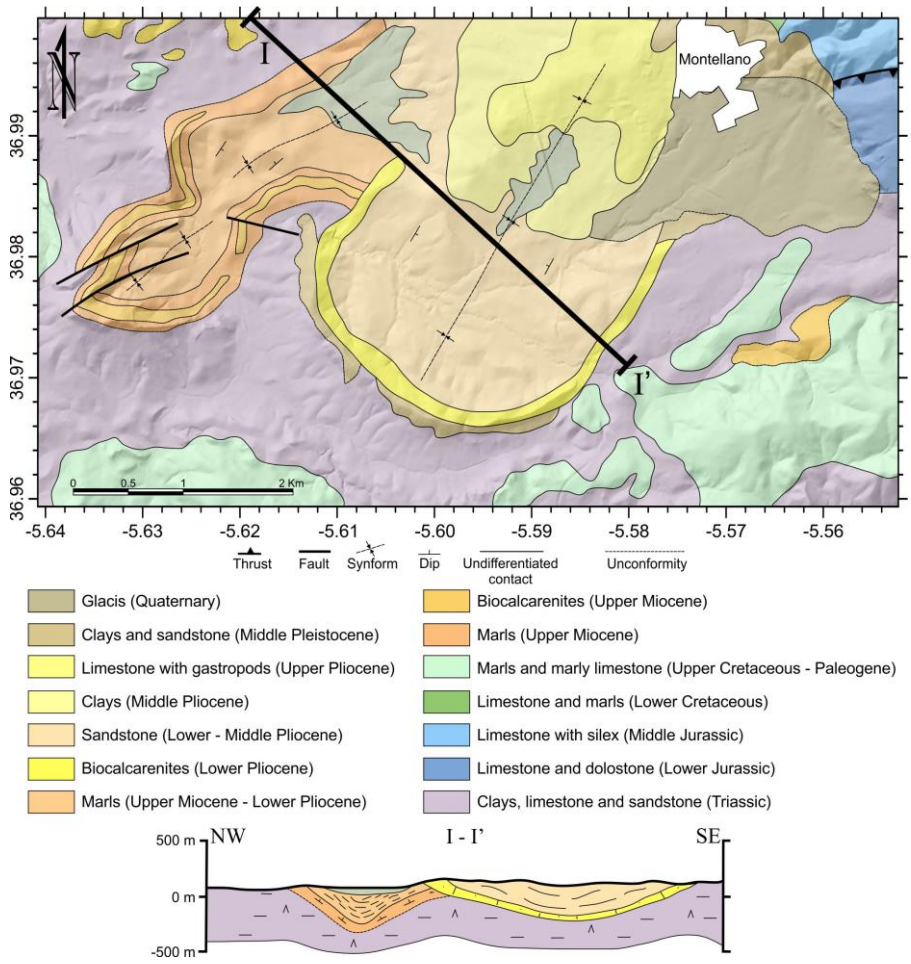

Figure 9.5: Structure of the Montellano area. (a) Geological map. (b) Cross-section. Modified from García de Domingo *et al.* (1985). See regional location in Fig. 9.1a.

Several E-W oriented faults occur in the Grazalema area (Figs. 9.1 and 9.6), separating sectors with different westward displacements. Despite the expected dextral kinematics, a detailed analysis of striae and S-C structures reveals that these faults have reverse kinematics and are inactive at present. Thus, we have not identified any remarkable tectonic structure that would justify the different displacement observed between LIJA and ALJI sites (Figs. 9.1 and 9.2). Therefore, the strong N-S gradient inferred might be due to the poor velocity estimation at ALJI station, which, in turn, could be related to a site effect (see time series; Fig. 9.3). Alternatively, these data may evidence a fast present-day block rotation. In addition, the N-S oriented faults between ALJI and MALA sites should have a normal regime, though they do not show typical features of active faults.

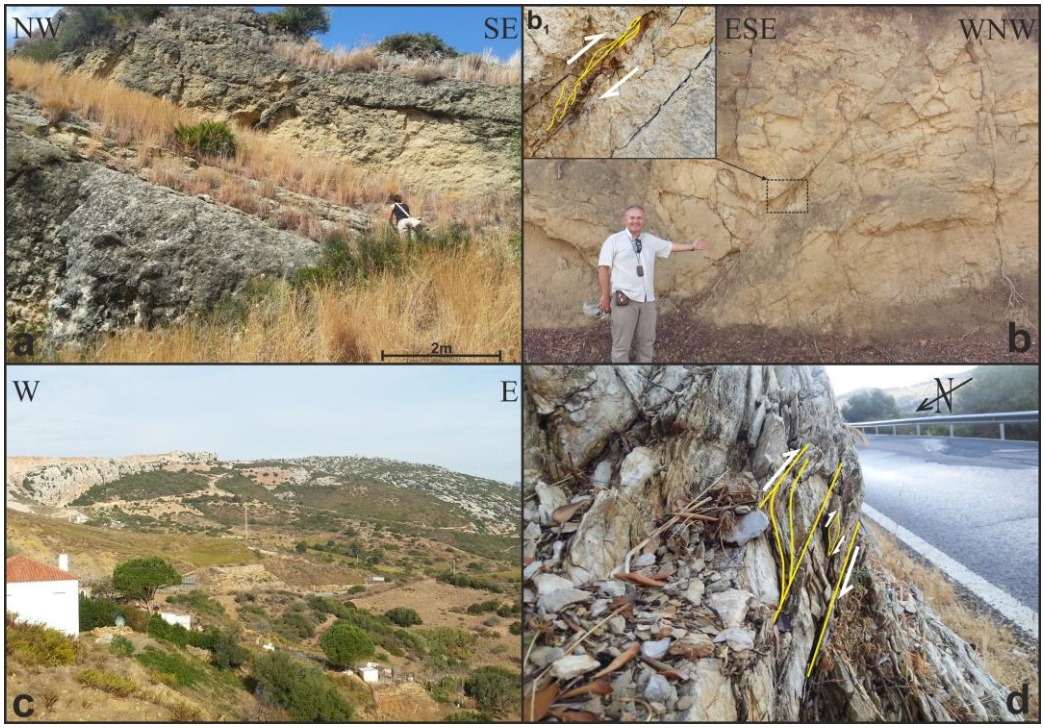

Figure 9.6: Field structures. (a) Dipping Upper Miocene biocalcarenite layer in the western limb of the Montellano synform. (b) Reverse fault in the Espera area. (b_1) Detailed view of fault gauge fabric. (c) Manilva N-S oriented antiform. (d) E-W oriented fault in Grazalema area with expected strike-slip but which only shows S-C structures of reverse fault.

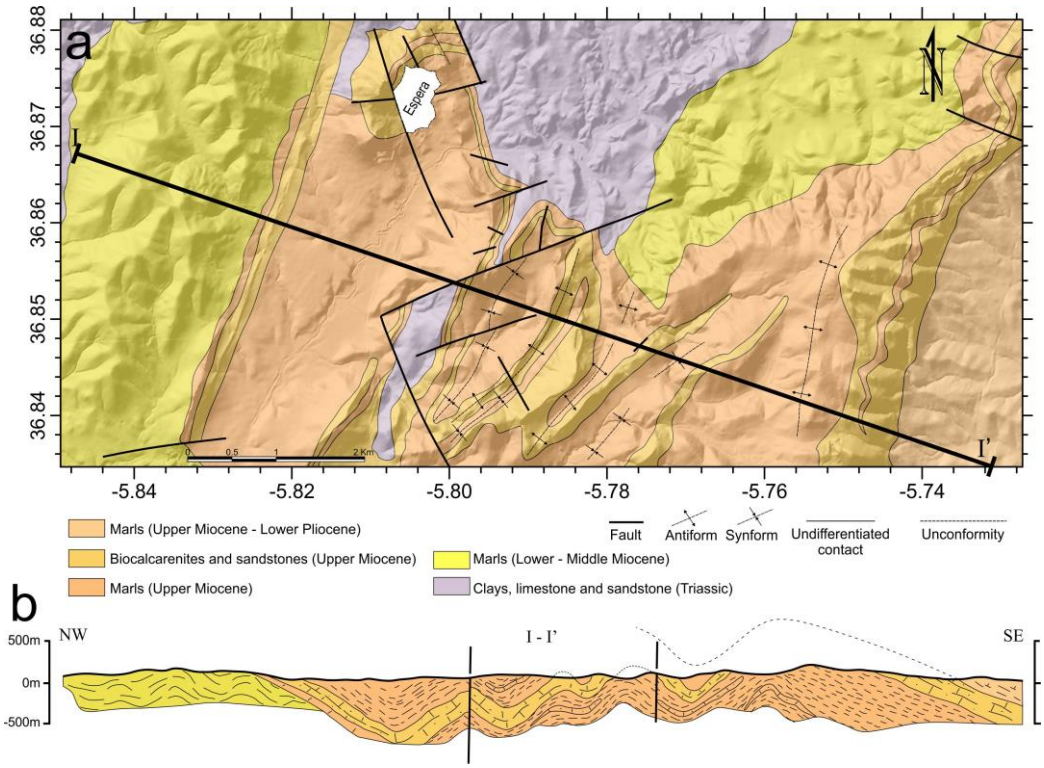

Figure 9.7: Folds affecting up to Pliocene sediments in the Espera area. (a) Geological map. (b) Cross-section. Modified from García de Domingo et al. (1985). See regional location in Fig. 1a.

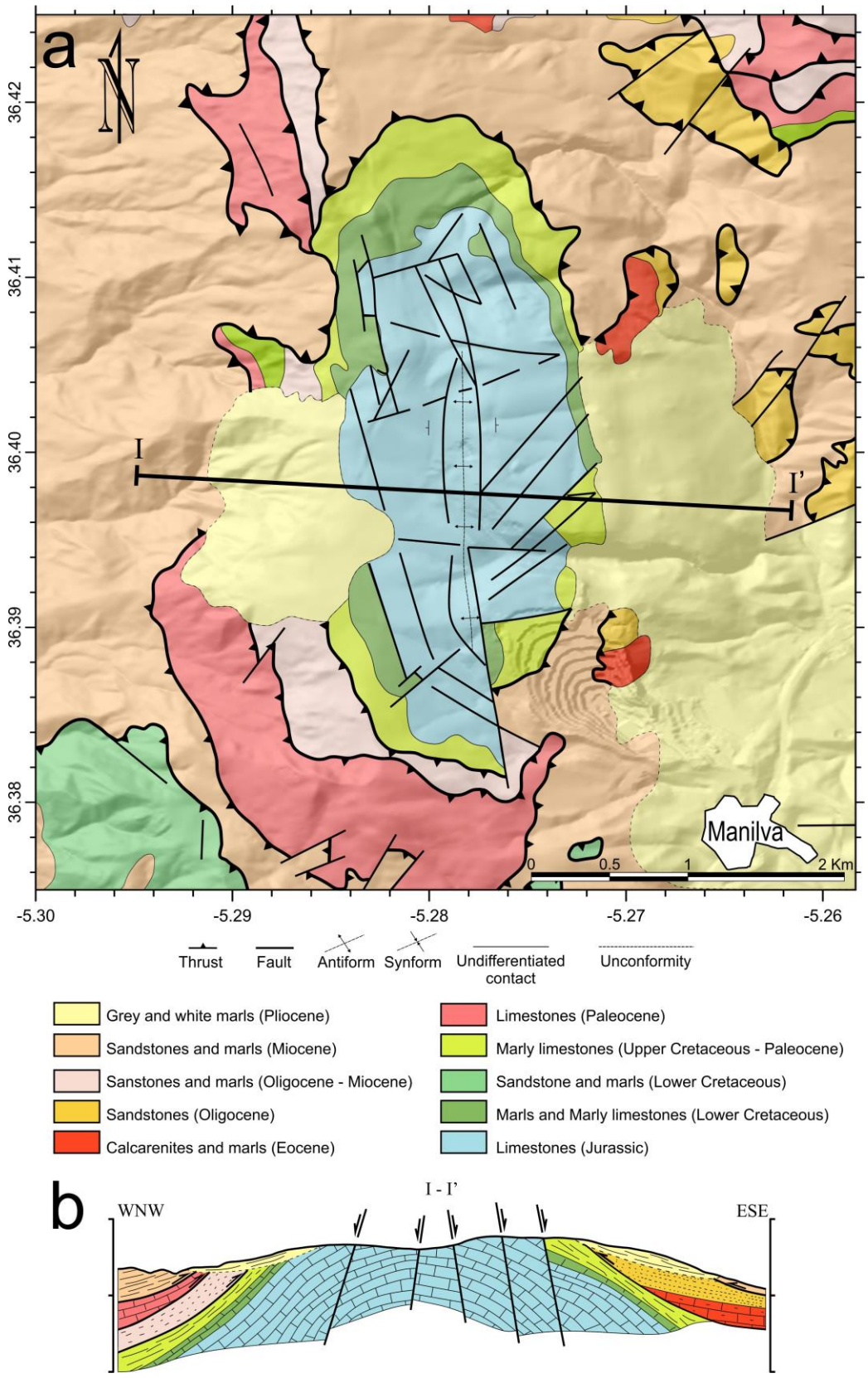

Figure 9.8: N-S oriented antiform in the Manilva area. This fold mainly developed during Miocene, though also affects Pliocene deposits. (a) Geological map. (b) Cross-section. Modified from Cano Medina and Torres Roldán (1980). See regional location in Fig. 1a.

9.6 Shortening in the western Betic mountain front and clockwise rotation

The cross-section of the Espera region (Fig. 9.7) allows us to derive a mean value of WNW-ESE to W-E shortening that may be taken into account for the whole frontal area. Considering the Messinian calcarenites as a reference level affected by Early Pliocene (5.3 to 3.6 Ma) folds, an average shortening of 16.1 % is estimated to have occurred. LIJA site and the westward Betic Cordillera mountain front in the direction of Trebujena are 61 km apart. Bearing in mind a roughly homogeneous shortening, folding has accommodated 11.70 km of deformation at a geological rate between 2.2 and 3.25 mm/yr, while the CGPS observations determine a present-day rate of 2.6 mm/yr.

The clockwise rotation of the western Betic units is of 60º (Platzman, 1990; Platzman and Lowrie, 1992; Platt *et al.*, 2003) since Cretaceous times (145.5 to 65.5 Ma). Considering that rotation started at 65.5 Ma, on average a rate of 0.916º/Ma can be inferred. If we take into account the different displacement rates at LIJA and ALJI stations, as well as the distance and angle between them, a clockwise block rotation of 2.06º/Ma would have been occurring at present, i.e. approximately twice the long-term geological rates but in agreement with the sense of rotation.

9.7 Discussion

We have analyzed data and used velocities from 10 CGPS Topo-Iberia and EUREF stations acquired in the period 2008-2013 to investigate present-day deformation in the Western Betic Cordillera. These new data provide very detailed information on deformation in the area. The new data depict a more consistent pattern of roughly parallel westward displacements that reach maximum values in the central part of the Gibraltar Arc (ALJI, CEU1) and decrease toward the NW Betic mountain front. This pattern contrasts with the previous marked arcuated patterns proposed by Vernant *et al.* (2010), Koulali *et*

al. (2011), Palano *et al.* (2013) and De Lis Mancilla *et al.* (2013), being however in agreement with the simpler patterns of Serpelloni *et al.* (2007).

The above deformation pattern agrees with an active westward displacement of the western Betics in the northern branch of the Gibraltar Arc. Toward the NW mountain front, a fold belt with scarce reverse faults accommodates the deformation over a basal detachment. The folds in the Montellano area (Fig. 9.5) evidence active deformation at least since the late Miocene. While the oldest folds have NE-SW trends, the most recent folds have a NNE-SSW orientation, closer to N-S. Although this setting may have been a consequence of changing stresses or convergence trends, it is more likely due to progressive clockwise rotation during oblique convergence in agreement with regional clockwise block rotations (Fig. 9.9). The N-S oriented antiform mainly developed during Miocene (Balanyá *et al.*, 2012) and affecting Pliocene sediments nearby Manilva (Durand-Delga, 2006) is compatible with the westward present-day displacement recorded in the westernmost part of the Gibraltar Arc.

The estimated values of geological shortening for the Líjar-Trebujena cross-section (2.2-3.25 mm/yr) are in line with the geodetic rates (2.6 mm/yr), thus supporting a continuous deformation in the western Betics since the Pliocene. Frontal folds accommodate most of the deformation and are responsible for the rectilinear character of the northwestern mountain front. The present-day clockwise rotation sense is also in agreement with paleomagnetic studies (Platzman, 1990; Platzman and Lowrie, 1992; Platt *et al.*, 2003).

The displacement pattern points to an active westward motion of the mountain belt along the Gibraltar Arc (Figs. 9.1, 9.2 and 9.10). Geodynamic models that involve only delamination would imply active extension in the whole orogeny. Therefore, our results do not give credit to delamination models. On

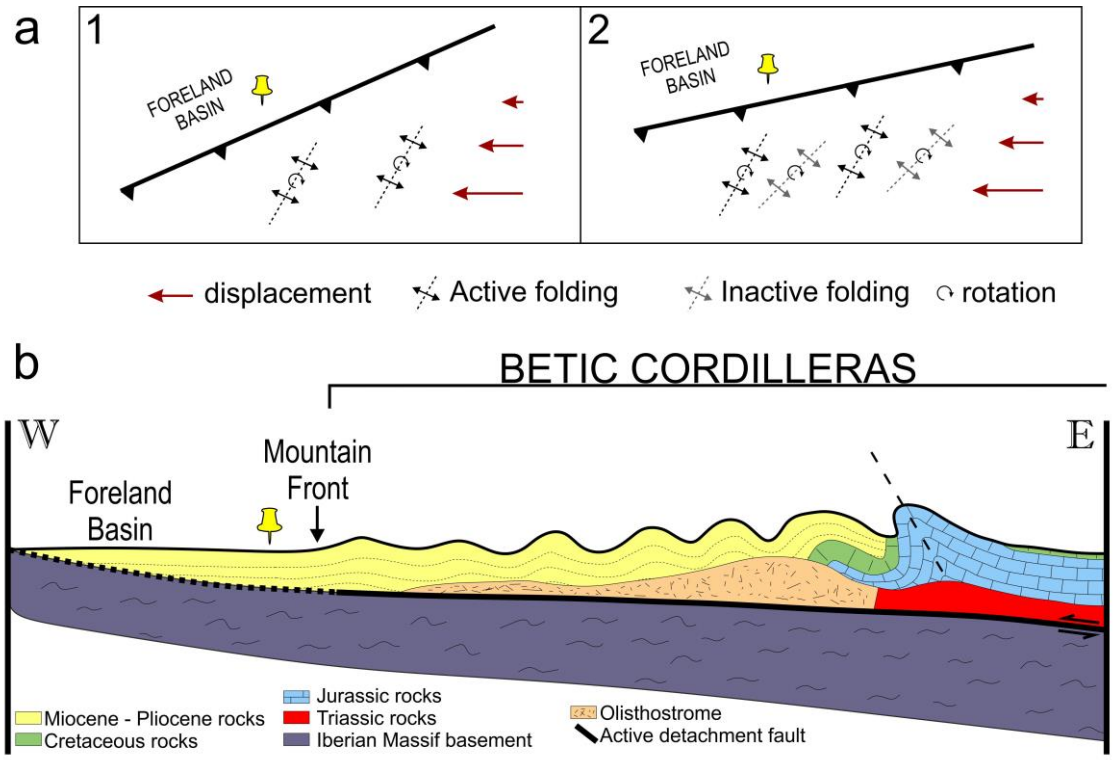

Figure 9.9: 3D model of the folded belt in the NW frontal zone of the Betics. (a) Progressive dextral rotation of folds due to oblique convergence, which probably determines the end of their activity and the development of a new fold generation with orientation more close to N-S. (b) The asymmetrical vergent folds toward the inner zones become symmetrical and more open toward the NW mountain front in a thin skinned tectonic scenario.

the contrary, models that consider a simple orogenic wedge with a subduction zone, are compatible with a continuous compressive westward motion. However, these simple models do not agree with the moderately present-day extension evidenced by the larger westward motion of LIJA and CEU1 sites with respect to MALA and LOJA. Finally, if subduction with related active slab rollback is considered (Fig. 9.10), the expected deformation pattern may fit quite well the obtained GPS results. This tectonic model determines, at surface, that the frontal compressive deformation area is related to an oblique dextral convergence mainly accommodated by folds. At a broader scale, this setting produces the progressive clockwise rotation of the more rigid tectonic blocks. The fact that subduction is active in the Betic Cordillera is evidenced by the

intermediate deep seismicity along the arcuate band parallel to the western boundary of the Alborán Sea (Fig. 9.1). This model for the Betic Cordillera is also compatible with models proposed for the Rif Cordillera (Fadil *et al.*, 2006; Pérouse *et al.*, 2010) that envisage slab rollback.

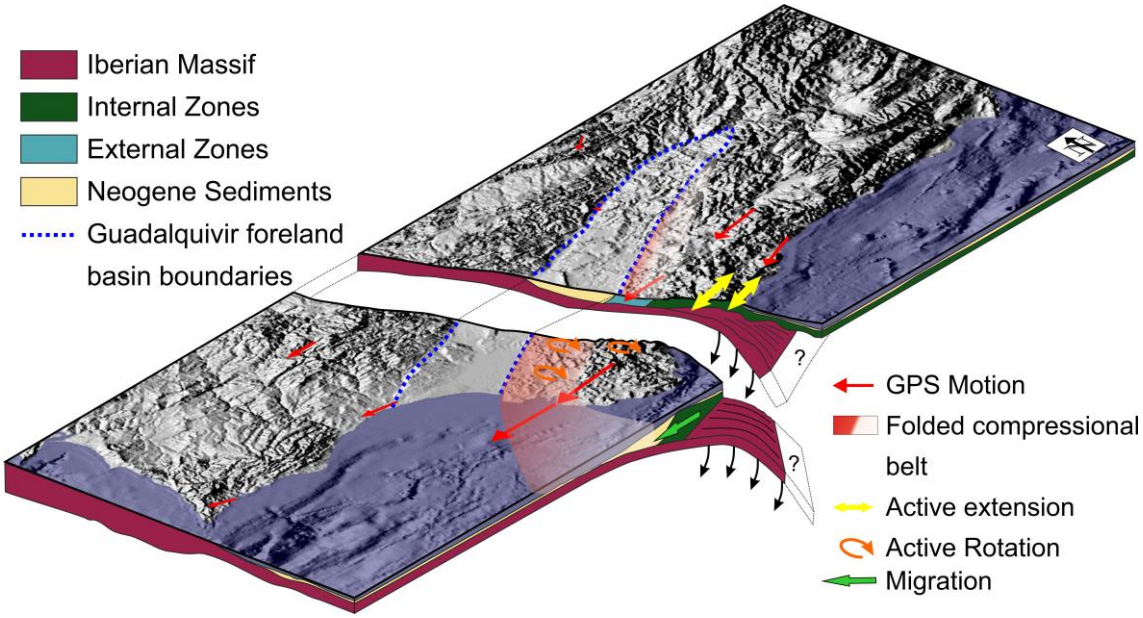

Figure 9.10: Tectonic model for the westernmost Betic Cordillera integrating CGPS data. The slab rollback tectonics determines the faster westward displacement of the westernmost portion of the orogen and the development of dextral rotations. At the same time, moderate E-W oriented extension occurs toward the southeastern sector of the studied region.

9.8 Conclusions

A CGPS monitoring by means of the Topo-Iberia stations has allowed us to determine the present-day deformation of the Western Betic Cordillera from recent data (2008-2013) affording higher detail and precision than previous assessments. Accordingly, the development of the Gibraltar Arc continues at present. Maximum relative westward displacements with respect to the foreland reach up to 4.27 mm/yr in the Gibraltar Strait. The rate of displacement decreases along a narrow band toward the northwest mountain front and toward

the eastward internal zones of the arcuate orogen. Furthermore, present-day clockwise rotation of geological units in the western Betics is shown to be faster (2.06º/Ma) than long-term geological rotations (0.916º/Ma). Such displacement values are compatible with the presence of a region undergoing contraction in the frontal part of the Cordillera, while moderate extension takes place eastward.

The oblique shortening of the Cordillera with respect to its foreland is accommodated by a deformation band affected mainly by folds, active at least since the Late Miocene. Local reverse faults have also been identified. While long-term WNW-ESE to W-E shortening rates from the LIJA station to the NW mountain front are of the order 2.2-3.25 mm/yr, present-day rates lie within this range, reaching 2.6 mm/yr. The presence of soft rocks and the thin-skinned tectonics characterizing most of the mountain front, would have concentrated the deformation along folds at shallow crustal levels, thus explaining the scarce seismicity in this region.

The new CGPS-derived velocity field for the Western Betic Cordillera, together with the intermediate-depth seismicity, is in agreement with active subduction and slab rollback.

Acknowledgements

We acknowledge the comments from Prof. Carlos Sanz de Galdeano, Prof. Antonio Azor and other two anonymous reviewers which highly improved this contribution. This research was funded by the Spanish Government through projects AYA2010-15501, CGL2010-21048, P09-RNM-5388 and CSD2006-0041 (European Regional Development Fund-ERDF) and the RNM148 and RNM282 research groups of the Junta de Andalucía. We thank all those persons involved in maintenance of the Topo-Iberia GPS network.

Part III

Chapter 10

General discussion

The new data presented in this Ph.D. Thesis further our knowledge of the crustal structure of the westernmost Betic Cordillera and its foreland beside the recent tectonic evolution of this area. Their relevance points to shed light on the discussion about the geodynamic models suggested for the Neogene to Present evolution of the Gibraltar Arc. This chapter initially includes discourse regarding the suitability of applied methodologies and their contribution to the body of knowledge regarding new crustal structures in the region, unknown to date. Right after, the recent evolution and present-day tectonic activity of the area are discussed in the framework of the new supporting data. Finally, the findings are integrated in order to highlight their significance with respect to geodynamic models proposed for the Betic-Rif-Alborán region. In order to avoid the repetition of discussions included in Part II of the volume, this chapter is meant to summarize and integrate the main subjects constituting the present Ph.D. Thesis. Even so, some concepts are repeated for the sake of consistency in expounding the discussion.

Crustal structure of the Westernmost Betic Cordillera and its foreland based on geophysical data supported by additional geological observations

Until now, only scarce detailed research efforts have been concerned with the crustal structure of the westernmost Betic Cordillera and its foreland, probably due to the poor quality of the outcrops highly conditioned by a flat topography, the covering vegetation and soils, and the low intensity of recent deformation. Geophysical studies, meanwhile, have been chiefly developed in the framework of seismic and seismology. Yet by combining geophysical

methods and geological observations we were able to analyse the main deep features in covered regions of this complex geological setting.

Regional magnetic data (Socias and Mezcua, 2002) may trace a general pattern of the distribution of the main magnetic bodies and hence improve the rough determination of crustal structures at depth. Even so, field magnetic measurements are essential to constrain the regional anomalies in detail and to elucidate local structures that are not identified by the regional data. Field measurements should be performed along profiles crossing the anomaly dipoles or the maxima in order to locate anomalous structures. In dipole anomalies, the magnetic anomalous bodies are positioned between the maxima and minima in a normal environment of middle latitudes, while in isolated maxima, the bodies are close to the anomalies. The Curie Point restricts the applicability of this method to a maximum of 30 Km depth in a normal geothermal gradient area, due to the fact that below this depth the higher rock temperature would make most of the ferromagnetic minerals lose their magnetic properties. The simultaneous modelling of aeromagnetic and field magnetic data in this region stand as a novel contribution of this Ph.D. thesis and the vantage point from which to accurately assess the location of the magnetic anomalous bodies in depth. From a qualitative standpoint, the difference between the magnetic anomaly intensity determined from aeromagnetic and field magnetic data increases as shallower the body is. While modelling, it is possible to fit both the calculated and the observed magnetic anomalies by changing the shape, depth and susceptibility of the polygons. The simultaneous aeromagnetic and field magnetic data modelling thus serves to constrain the results and reduce uncertainty. In view of the above, the magnetic studies related to this research have identified some geological features unknown to date. In this sense, the magnetic dipole related to the Monchique Alkaline Complex, which constitutes the most intense dipole in the Southwestern Iberian Peninsula, was analysed in detail in order to establish its eastward extension (Fig. 5.8). This study entailed magnetic observations along

the Portimão-Odemira and Olhão-Castro Verde profiles. In addition, an E-W magnetic profile crossing the Guadiana River besides two N-S aeromagnetic profiles located in both the East and West, sides of the river came to reveal the Guadiana fault (Fig. 5.8) as a major blind crustal structure probably of late variscan age. Magnetic data are traditionally related to gravity data, as both constitute potential fields and can support each other. In this way, the presence of the Guadiana fault is further founded on gravity data along the same E-W profile. The rectilinear character of the Guadiana River channel near its mouth and a set of joints following the trend of the proposed blind fault shed light on the presence of this major structure evidenced by weak surface deformations. Eastward, a magnetic maximum located above the Guadalquivir foreland basin could be in contact to the former dipole. Due to the location of this area, in a recently active tectonic zone, the anticipated geothermal gradient is higher than normal, meaning that the maximum depth of the magnetic method results is shallower. The fact that the magnetic anomaly intensity, amplitude and trend are similar for aeromagnetic and field magnetic data in the area points to a body whose top lies at great depth. Considering the geothermal gradient in the region, magnetic data lead us to discuss the nature and location of the top of this body, but do not provide insight as to the bottom depth. Still, this method highlights the presence of an anomalous body unknown to date.

The 3D character of the regional structures in the western Betic Cordillera, the substantial sea influence and the proximity of the Gibraltar Strait have restricted the magnetotelluric research in the region, thus far exclusively developed with low accuracy to the east and northeast (Rosell *et al.*, 2011; Ruiz-Constán *et al.*, 2010; Pous *et al.*, 2011). Given the location of the studied area, it is essential to constrain the effect of the sea and the narrow Gibraltar Strait on LMT data in order to precisely isolate the response of the geological structures. The bathymetry and the irregular coast line broadly define the LMT response in the region. As longer the period is, induction arrows show that the Atlantic Ocean prevails over the influence of the Mediterranean Sea. The phase tensor

pattern is quite homogeneous for this period due to the fact it is a large scale effect. The Gibraltar Strait condition the real part of the tipper vectors mainly for shorter periods and nearby areas. Meanwhile, the current channel through the Strait strongly affects the vertical component of the magnetic field. This effect, together with the Atlantic and Mediterranean Sea influence, has to be taken into account in any interpretation of LMT data in the region.

Long period magnetovariational observations were acquired at a grid of 26 sites in the westernmost Betic Cordillera in order to derive the induction arrows pattern in the area. Once the bathymetry as well as the known major geological structures was taken into account for 3D forward modelling, the different induction arrows patterns between the data and the 3D model for long periods underlined the presence of a deep conductive body. This high conductor structure is located within the southern part of the of the Guadalquivir foreland basin basement, just coinciding with the position of the magnetic anomaly maximum previously identified. Long period magnetovariational research enhances magnetic studies and helps to determine the depth extent and conductivity of the anomalous structure, which we call Villafranca body (Fig. 7.7). The extremely low resistivity of Villafranca body together with its magnetic properties constrains the lithological interpretation to an intermediate or basic body with a high sulphide content.

Recent evolution and active tectonic in the Westernmost Betic Cordillera from geological research, GPS data and shallow geophysical observations

The westernmost Betic Cordillera front has traditionally been considered to be an inactive thrust. The scarce outcrops and the absence of detailed geophysical and GPS data hampered proposals regarding the activity and structures in the area. Westward, the offshore Gulf of Cadiz is held to represent present-day thrusting (Gutscher *et al.*, 2002, 2012). Eastward, its activity has been delineated by shallow earthquakes related to reverse and strike slip faults

affecting the Iberian crust in the Morón and Torreperogil areas (Ruiz-Constán *et al.*, 2009; Pedrera *et al.*, 2013). In the central Betics the front is inactive and the deformation is highlighted toward the interior of the Cordillera (Ruano *et al.*, 2004). New geomorphological and field geological observations, together with GPS data for this region come to shed light on the present day tectonic activity of the westernmost mountain front. These results are supported by shallow geophysical data.

The Gulf of Cadiz coastline is underlined by a rectilinear step between the Chipiona and Sanlúcar de Barrameda towns; it extends at least 7 Km along the southern boundary of the Guadalquivir Basin. The sinuosity mountain index of 1.13 confirms the active tectonic character of the westernmost mountain front. A detailed audiomagnetotelluric profile orthogonal to the mountain front reveals the Guadalquivir Basin sedimentary infill at depth besides a sharp mountain front related to antiformal structures in the area. In addition, seismic reflection profiles orthogonal to the westernmost mountain front and at the Guadalquivir basin, support the development of folds along the western Betic front as well as a southeastward progradation and thickening of the Guadalquivir Basin infill affecting up to Holocene deposits (Salvany *et al.*, 2011; Rodríguez-Ramírez *et al.*, 2014).

Main deformation in the westernmost Betic Cordillera front entails recent and active folds affecting Tortonian up to Holocene deposits that evolve over a basal detachment (Fig. 8.7 and 9.9). The presence of soft rocks and deformation accommodated along folds at shallow crustal levels would explain the scarce seismicity of this region. Deformation along the oblique foreland boundary determines a progressive rotation. Indeed, while the oldest folds have NE-SW trends, the most recent folds are NNE-SSW to N-S oriented. Brittle deformation in the westernmost front is limited to tensional joint or hybrid joint sets forming an acute angle suggesting NW-SE compression and NE-SW tension. Scarce normal faults develop along an antiformal culmination, revealing a local shallow

NW-SE to NNW-SSE extensional trend as consequence of the relief uplift. The former area is mainly deformed by folding with N-S structures (Manilva antiform) affecting up to upper Miocene rocks and Pliocene sediments (Balanyá *et al.*, 2012; Durand-Delga, 2006).

Up to now, GPS data showed an arcuate displacement pattern (NW-WNW) for the western Betic Cordillera with respect to the stable Iberian Massif (Serpelloni *et al.*, 2007; Vernant *et al.*, 2010; Koulali *et al.*, 2011). These data were in line with the present day building up of the Betics, but their interpretations did not take into account the active tectonic structures in the area. The newest GPS data (2008-2013) indicate a very consistent homogeneous westward motion (Fig. 9.2) increasing toward the south and west, reaching maximum values in the Gibraltar Strait area (CEU, LIJA, SFER). The displacement progressively decreases toward the northwestern mountain front (LIJA), being minimal in the relatively stable foreland (LAGO, HUEL, CAST, COBA, RUBI). The southeasternmost stations (MALA, LOJA) show a lower displacement with respect to the Gibraltar Strait area.

This research proposes, for the first time, that the westernmost mountain front is still active and accommodates the deformation by folding, the ENE-WSW oblique foreland boundary acting as a barrier to the westward motion of the westernmost Betic Cordillera (Fig. 10.1). The folds would moreover be responsible of the rectilinear character of the westernmost Betic Cordillera front, and together with the southeastward thickening of the Guadalquivir Basin sedimentary infill, they suggest its present day activity. Southward along the Gibraltar Arc, in the inner parts on the Betic Cordillera (Espera and Grazalema areas), E-W scarce reverse and inactive faults cannot be related with the recent or present westward displacement of the Internal Zones. The absence of any tectonic structure justifying the different displacement between LIJA and ALJI areas, together with the NNE-SSE orientation of the more recent folds with respect to the NE-SW oldest trends, points to a progressive clockwise rotation

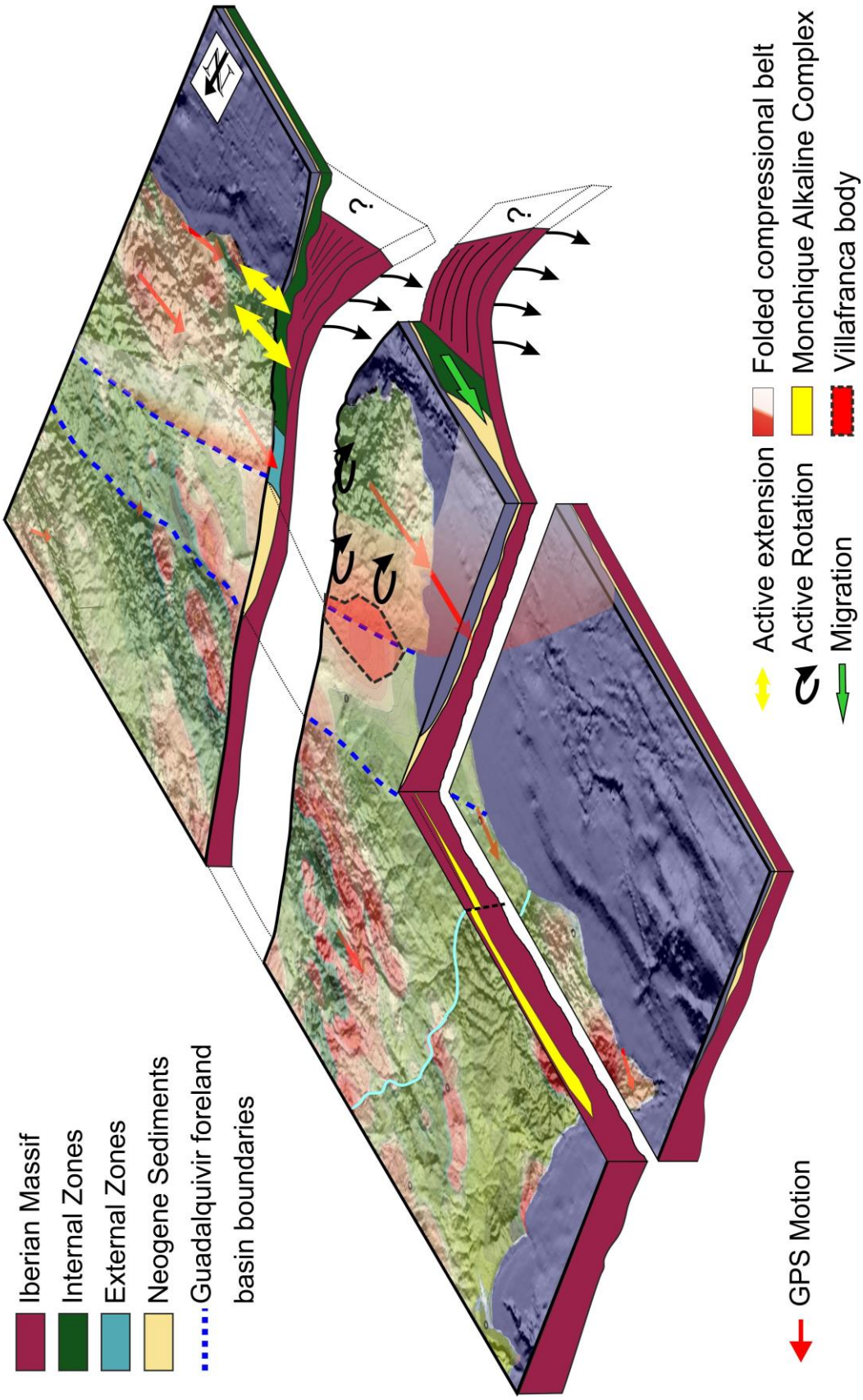

Figure 10.1: Final model of the crustal structure and recent tectonic of the westernmost Betic Cordillera and its foreland.

during oblique convergence in agreement with regional clockwise block rotations. The above interpretation also agrees with paleomagnetic studies that support a 60º clockwise rotation of the western Betic units since Cretaceous times (Platzman, 1990; Platzman and Lowrie, 1992; Platt *et al.*, 2003). From the region of maximum westward displacements in the Gibraltar Arc, there is an eastward decrease of the GPS rates that should generate extension in the eastern regions, as is corroborated far to the East in the Padul and Nigüelas faults nearby the city of Granada (Galindo-Zaldívar *et al.*, 2003).

Finally, the derived values of WNW-ESE to E-W geological shortening for the Líjar-Trebujena cross-section (2.2-3.25 mm/yr) compared to the geodetic present day rates (2.6 mm/yr) are similar and support continuous deformation in the western Betics since the Pliocene.

New insight into the tectonic evolution models of the Gibraltar Arc

The geological, geophysical and geodetical research carried out for this Ph.D. Thesis point to active westward motion of the Betic Cordillera along the Gibraltar Arc. As noted above, this motion is related to an oblique dextral convergence between the Eurasian and African plates in the western Mediterranean, mainly accommodated in the westernmost Betic Cordillera by folds over a main detachment and producing regional clockwise block rotations with relative extension to the eastward areas. In this setting, geodynamic models considering lithospheric delamination (García-Dueñas *et al.*, 1992; Seber *et al.*, 1996; Calvert *et al.*, 2000; de Lis Mancilla, 2013) would imply active extension in the whole area and do not fit the presented results. On the other hand, models based only on subduction processes (Araña and Vegas, 1974; De Jong, 1991 and 1993; Wortel and Spakman, 1992; Zeck *et al.*, 1992) would infer a compressive westward motion but do not explain the moderate extension highlighted by the gradient between the Western and Eastern GPS stations (CEU, SFER, ALJI, LIJA with respect to LOJA and MALA).

To conclude, this research supports a lithospheric subduction with related active slab rollback (Blanco and Spakman, 1993; Morley, 1993; Royden, 1993; Lonergan and White, 1997; Hoernle *et al.*, 1999; Wortel and Spakman, 2000; Gutscher *et al.*, 2002; Gil *et al.* 2004; Spakman and Wortel, 2004; Thiebot and Gutscher, 2006; Brun and Faccena, 2008; Pedrera *et al.*, 2011; Ruiz-Constán *et al.*, 2011, 2012a) to explain the tectonic activity of the westernmost Betic Cordillera and the proposed deformation pattern (Fig. 10.1). It is not possible to ensure the suitability of the slab detachment. Deep seismicity along the arcuate band parallel to the western boundary of the Alborán Sea suggests active subduction. The geodynamic model proposed for the Betic Cordillera is in agreement with the slab rollback suggested for the Rif (Pérouse *et al.*, 2010), in a different orientation, and may represent the normal behaviour during the development of the Gibraltar Arc.

Chapter 11

Conclusions

This chapter summarizes the findings compiled in the previous chapters for the purpose to underline the main contribution of this Ph.D. Thesis to the knowledge of the crustal structure and recent tectonic evolution of the westernmost Betic Cordillera and its foreland. Furthermore, the geodynamic model of the Gibraltar Arc supported by this research is highlighted. Integration of geological and geophysical methods is essential to determine the shallow and deep crustal structure mainly in areas with scarce outcrops and complex geological setting as the westernmost Betic Cordillera.

The simultaneous modelling of aeromagnetic and field magnetic data allow accurately constrain the features of the bodies responsible of the magnetic anomalies. The understanding of the magnetic anomalies in the southwestern Iberian Massif made possible to constrain the extension in depth of the Monchique Alkaline Complex with lenticular shape, 50 km wide and its eastward prolongation of more than 150 km. The intrusive body should have a weak remnant magnetization parallel to the induced one. Moreover, combining these data with gravity measurements as well as geomorphological and structural geology observations has been useful to identify the Guadiana fault, interpreted as major N-S oriented blind crustal fault of probable late Variscan age.

Long Period Magnetotelluric data constitute the most suitable tool to determine the conductivity of the deep crustal structure. In that way, MT response functions onshore are strongly influenced by the bathymetry and the coast line geometry in areas surrounded by sea water depending on the distance

and the period. In addition, a narrow strait connecting two seas concentrates the electric currents provoking large tipper vectors at sites close to the strait onshore but with negligible effect on phase tensor. Hence, it is essential to take into account the detailed bathymetry and coast line geometry in any MT research performed in areas nearby the Gibraltar Strait.

Long period magnetovariational observations in the westernmost Betic Cordillera supported by magnetic anomaly studies have elucidated the presence of a highly conductive (0.05 Ω·m) and magnetic anomalous body, the Villafranca Body. This up to date unknown structure should have sulphide nature and is located at 10 to 30 km depth, probably in an igneous host rock. Villafranca determines also the major magnetic anomaly located in the Variscan basement of the Guadalquivir foreland basin. It may represent a structure related to the Iberian Pyrite Belt, or else a body emplaced along the South Iberian Margin during the Mesozoic Tethys evolution.

The compilation of geological, geophysical and available GPS data supplies consistent arguments to support the present day tectonic activity of the westernmost frontal area of the Betic Cordillera. This fact produces the progressively southeastward increase of the Guadalquivir Basin infill reaching up to Holocene deposits. Recent and active folds accommodate the deformation along the westernmost mountain front and are responsible of its rectilinear character. The presence of soft rocks and the thin-skinned tectonics would have concentrated the deformation along folds at shallow levels over a basal detachment, thus explaining the scarce seismicity in this region. A WNW-ESE to E-W tectonic shortening occurs in the western Betics since the Pliocene, evidenced by a roughly constant rate (2.2-3.25 mm/yr) for Líjar-Trebujena cross-section.

New continuous GPS data evidence the maximum relative westward displacements of western Betic Cordillera with respect to the foreland reaching

up to 4.27 mm/yr in the Gibraltar Strait. The rate of displacement decreases along a narrow band toward the northwest mountain front and eastward, to the internal zones of the arcuate orogen. This behaviour supports the variscan foreland as a barrier to the westward motion of the Betic Cordillera. Such displacement values are compatible with the presence of a region undergoing contraction in the frontal part of the Cordillera, while moderate extension takes place eastward. In addition, a progressive clockwise rotation during oblique convergence is in agreement with regional GPS results (2.06° /Ma) faster than long-term geological rotations deduced from previous paleomagnetic data (0.916°/Ma). This fact is compatible with progressive rotation of fold axes pattern.

The new geological, geophysical and geodetical data in the Westernmost Betic Cordillera presented in this Ph.D. Thesis support the active subduction and slab rollback as the more confidence model for the recent evolution of the Gibraltar Arc.

Conclusiones

Este capítulo resume los resultados presentados, con el propósito de subrayar la principal contribución de esta Tesis al conocimiento de la estructura cortical y evolución tectónica reciente del extremo occidental de la Cordillera Bética y su antepaís. Asimismo, se destaca el modelo geodinámico de evolución del Arco de Gibraltar respaldado por este trabajo. La integración de métodos geológicos y geofísicos es fundamental para determinar la estructura superficial y profunda de la corteza, especialmente en áreas con pocos afloramientos y contexto geológico complejo, como la zona occidental de la Cordillera Bética.

La modelización simultánea de anomalías aeromagnéticas y magnéticas de campo nos permite constreñir de manera precisa las características de los cuerpos responsables de dichas anomalías. El análisis de las anomalías magnéticas en el Suroeste del Macizo Ibérico, ha hecho posible determinar la extensión en profundidad del Complejo Alcalino de Monchique, con forma lenticular y 50 km de anchura, así como su prolongación de más de 150 km hacia el Este. Este cuerpo intrusivo debe tener una magnetización remanente débil paralela a la inducida. Además, la combinación de estos datos con medidas gravimétricas junto con observaciones geomorfológicas y estructurales, ha permitido identificar la Falla del Guadiana, interpretada como una falla ciega de orientación N-S posiblemente de edad tardivarisca.

Los datos magnetotelúricos (MT) de largo periodo constituyen el mejor método de prospección geofísica para determinar la estructura conductora de la corteza en profundidad. La respuesta de los parámetros de MT en tierra está fuertemente influenciada por la batimetría y la geometría de la línea de costa en áreas rodeadas por agua de mar, en función de la distancia y el periodo. Además, un estrecho pequeño que conecte dos mares, concentra las corrientes eléctricas y

provoca *tippers vectors* de gran magnitud en estaciones en tierra cercanas a dicho estrecho, pero tiene efecto inapreciable en el *phase tensor*. Por tanto, es esencial tener en cuenta la batimetría y geometría de la línea de costa precisas en el desarrollo de cualquier investigación magnetotelúrica en zonas cercanas al Estrecho de Gibraltar.

El análisis de datos magnetotelúricos de largo periodo en el extremo occidental de la Cordillera Bética apoyados por el estudio de anomalías magnéticas, revelan la presencia de un cuerpo anómalo magnético y altamente conductor (0.05 Ω·m), Villafranca. Este cuerpo, desconocido hasta ahora, debe contener sulfuros probablemente en una roca de caja ígnea y se sitúa entre 10 y 30 km de profundidad. Villafranca determina además la mayor anomalía magnética localizada en el basamento de la cuenca de antepaís del Guadalquivir. Podría representar una estructura relacionada con la Faja Pirítica de la Zona Sudportuguesa o también un cuerpo emplazado en el margen Sudibérico durante la evolución Mesozoica del Tethys.

La compilación de datos geológicos, geofísicos y de GPS, aportan argumentos consistentes para afirmar la actividad tectónica actual del extremo Oeste de la Cordillera Bética. Dicha actividad produce el progresivo aumento del relleno de la cuenca del Guadalquivir hacia el Sureste que afecta hasta materiales Holocenos. La deformación es acomodada por pliegues activos y recientes que son los responsables del carácter rectilíneo del extremo occidental del frente montañoso. La presencia de rocas blandas y una tectónica de *thin-skinned* concentrarían la deformación a lo largo de pliegues superficiales sobre un despegue basal, lo que explicaría la escasa sismicidad en la zona. En el Oeste de la Cordillera Bética se ha producido un acortamiento tectónico desde el Plioceno en dirección ONO-ESE a E-O con una velocidad constante aproximada de 2.2-3.25 mm/a calculada para la sección Líjar-Trebujena.

Nuevos datos de GPS de registro continuo ponen de manifiesto el máximo desplazamiento relativo de la parte occidental de la Cordillera Bética hacia el Oeste respecto al antepaís, que alcanza valores hasta 4.27 mm/a en el Estrecho de Gibraltar. La velocidad de desplazamiento disminuye a lo largo de una banda ancha hacia el Noroeste en el frente montañoso y hacia el Este, en las partes internas del orógeno. Este contexto supone que el antepaís Varisco actúa como una barrera frente al movimiento hacia el Oeste de la Cordillera Bética. Los valores de desplazamiento son compatibles con la existencia de contracción en la parte frontal de la Cordillera y extensión moderada hacia el Este. Asimismo, la rotación calculada a partir de los datos regionales de GPS (2.06º/Ma) concuerda con un modelo de rotación horaria progresiva durante la convergencia oblicua, más rápida que las rotaciones geológicas obtenidas a partir de datos previos de paleomagnetismo (0.916º/Ma). Estos resultados son compatibles con el patrón general de rotación progresiva de los ejes de los pliegues.

Los nuevos datos geológicos, geofísicos y geodésicos en el extremo occidental de la Cordillera Bética presentados en esta Tesis favorecen la subducción activa y *slab rollback* como principal modelo de evolución reciente del Arco de Gibraltar.

References

Abad, I., Mata, M.P., Nieto, F., Velilla, N., 2001. The phyllosilicates in diagenetic-metamorphic rocks of the South Portuguese Zone, southwestern Portugal. The Canadian Mineralogist 39, 1571-1589.

Abad, I., Nieto, F., Velilla, N., 2002. Chemical and textural characterisation of diagenetic to low-grade metamorphic phyllosilicates in turbidite sandstones of the South Portuguese Zone: A comparison between metapelites and sandstones. Schweizerische Mineralogische und Petrographische Mitteilungen 82, 303-324.

Agarwal, A., Dosso, H., 1990. On the behaviour of the induction arrows over a buried conductive plate-a numerical model study. Physics of the Earth and Planetary Interiors 60, 265-277.

Aktuğ, B., Parmaksız, E., Kurt, M., Lenk, O., Kılıçoğlu, A., Gürdal, M.A., Özdemir, S., 2013. Deformation of Central Anatolia: GPS implications. Journal of Geodynamics 67, 78-96.

Aldaya, F., Campos, J., García-Dueñas, V., González-Lodeiro, F., Orozco, M., 1984. El contacto Alpujárrides/Nevado-Filábrides en la vertiente meridional de Sierra Nevada. Implicaciones tectónicas. Depart. Invest. Geol. CSIC Granada, 18-20.

Allmendinger, R.W., Smalley, R., Bevis, M., Caprio, H., Brooks, B., 2005. Bending the Bolivian orocline in real time. Geology, 33, 905-908.

Almeida, E., Pous, J., Santos, F.M., Fonseca, P., Marcuello, A., Queralt, P., Nolasco, R., Mendes-Victor, L., 2001. Electromagnetic imaging of a transpressional tectonics in SW Iberia. Geophysical Research Letters 28, 439-442.

Almeida, E., Monteiro-Santos, F., Mateus, A., Heise, W., Pous, J., 2005. Magnetotelluric measurements in SW Iberia: New data for the Variscan crustal structures. Geophysical Research Letters 32, L08312.

Alpert, L.A., Miller, M.S., Becker, T.W., Allam, A.A., 2013. Structure beneath the Alboran from geodynamic flow models and seismic anisotropy. Journal of Geophysical Research: Solid Earth 118, 4265-4277.

Anahnah, F., Galindo-Zaldívar, J., Chalouan, A., Pedrera, A., Ruano, P., Pous, J., Heise, W., Ruiz-Constan, A., Benmakhlouf, M., López-Garrido, A.C., Ahmamou, M.F., Sanz de Galdeano, C., Arzate, J., Ibarra, P., González-Castillo, L., Bouregba, N., Corbo, F., Asensio, E., 2011a. Deep resistivity cross section of the intraplate Atlas Mountains (NW Africa): New evidence of anomalous mantle and related Quaternary volcanism. Tectonics 30, TC5014.

Anahnah, F., Galindo-Zaldívar, J., Chalouan, A., Pous, J., Ruano, P., Pedrera, A., Ruiz-Constán, A., Ahmamou, M.F., Benmakhlouf, M., Ibarra, P., Asensio, E., 2011b. Crustal resistivity

structure of the southwestern transect of the Rif Cordillera (Morocco). Geochemistry, Geophysics, Geosystems 12, Q12016.

Andrieux, J., Fontbote, J.M., Mattauer, M., 1971. Sur un modèle explicatif de l'Arc de Gibraltar. Earth and Planetary Science Letters 12, 191-198.

Andrieux, J., Mattauer, M., 1973. Précisions sur un modèle explicatif de l'Arc de Gibraltar. Bulletin de la Societé Géologique de France 12, 115-118.

Araña, V., Vegas, R., 1974. Plate tectonics and volcanism in the Gibraltar arc. Tectonophysics 24, 197-212.

Ardizone, J., Mezcua, J., Socías, I., 1989. Mapa aeromagnético de España peninsular. Escala 1:1000000. Instituto Geográfico Nacional, Madrid.

Argus, D. F., Gordon, R. G., DeMets, C., Stein, S., 1989. Closure of the Africa - Eurasia - North America plate motion circuit and tectonics of the Gloria fault. Journal of Geophysical Research: Solid Earth 94, 5585-5602.

Azor, A., Rubatto, D., Simancas, J., González-Lodeiro, F., Martínez-Poyatos, D., Martín-Parra, L., Matas, J., 2008. Rheic Ocean ophiolitic remnants in southern Iberia questioned by SHRIMP U - Pb zircon ages on the Beja - Acebuches amphibolites. Tectonics 27, TC5006.

Bahr, K., 1988. Interpretation of the magnetotelluric impedance tensor: Regional induction and local telluric distortion. J. Geophys. 62, 119-127.

Bahr, K., 1991. Geological noise in magnetotelluric data: a classification of distortion types. Physics of the Earth and Planetary interiors 66, 24-38.

Bakker, H., Jong, K., Helmers, H., Biermann, C., 1989. The geodynamic evolution of the Internal Zone of the Betic Cordilleras (south - east Spain): a model based on structural analysis and geothermobarometry. Journal of Metamorphic Geology 7, 359-381.

Balanyá, J., García-Dueñas, V., 1987. Les directions structurales dans le Domaine d'Alborán de part et d'autre du Détroit de Gibraltar. Comptes Rendus de l'Académie des Sciences. Série 2, Mécanique, Physique, Chimie, Sciences de l'univers, Sciences de la Terre 304, 929-932.

Balanya, J. C., Crespo-Blanc, A., Diaz-Azpiroz, M., Expósito, I., Luján, M., 2007. Structural trend line pattern and strain partitioning around the Gibraltar Arc accretionary wedge: Insights as to the mode of orogenic arc building. Tectonics 26 (2), TC2005.

Balanyá, J. C., Crespo-Blanc, A., Diaz-Azpiroz, M., Expósito, I., Torcal, F., Pérez-Peña, V., Booth-Rea, G., 2012. Arc-parallel vs back-arc extension in the Western Gibraltar arc: Is the Gibraltar forearc still active? Geologica Acta 10 (3), 249-263.

Banda, E., Ansorge, J., 1980. Crustal structure under the central and eastern part of the Betic Cordillera. Geophysical Journal International 63, 515-532.

Bard, J., 1977. Signification tectonique des metatholeites d'affinité abyssale de la ceinture métamorphique de basse pression d'Aracena (Huelva, Espagne). Bulletin de la Societé geologique de France 19, 385-393.

Bedrosian, P.A., Unsworth, M.J., Egbert, G., 2002. Magnetotelluric imaging of the creeping segment of the San Andreas Fault near Hollister. Geophysical Research Letters 29, 1-1, 1-4.

Bernard-Griffiths, J., Gruau, G., Cornen, G., Azambre, B., Mace, J., 1997. Continental lithospheric contribution to alkaline magmatism: isotopic (Nd, Sr, Pb) and geochemical (REE) evidence from Serra de Monchique and Mount Ormonde complexes. Journal of Petrology 38, 115–132.

Bezada, M.J., Humphreys, E.D., Toomey, D.R., Harnafi, M., Dávila, J.M., Gallart, J., 2013. Evidence for slab rollback in westernmost Mediterranean from improved upper mantle imaging. Earth and Planetary Science Letters 368, 51-60.

Bianco, G., Devoti, R., Luceri, V., 2003. Combination of loosely constrained solutions, Proceedings of the IERS Workshop on Combination Research and Global Geophysical Fluids (Munich, 18-21 Nov 2002), IERS Technical Note, pp. 107-109.

Bilim, F., 2007. Investigations into the tectonic lineaments and thermal structure of Kutahya-Denizli region, western Anatolia, from using aeromagnetic, gravity and seismological data. Physics of the Earth and Planetary Interiors 165, 135-146.

Billi, A., Faccenna, C., Bellier, O., Minelli, L., Neri, G., Piromallo, C., Presti, D., Scrocca, D., Serpelloni, E., 2011. Recent tectonic reorganization of the Nubia-Eurasia convergent boundary heading for the closure of the western Mediterranean. Bulletin de la Société Géologique de France 182, 279-303.

Blakely, R.J., Simpson, R.W., 1986. Locating edges of source bodies from magnetic and gravity anomalies. Geophysics 51, 1494-1498.

Blakely, R.J., Wells, R.E., Tolan, T.L., Beeson, M.H., Trehu, A.M., Liberty, L.M., 2000. New aeromagnetic data reveal large strike-slip (?) faults in the northern Willamette Valley, Oregon: Geological Society of America Bulletin 112, 1225-1233.

Blakely, R.J., Wells, R.E., Weaver, C.S., Johnson, S.Y., 2002. Location, structure, and seismicity of the Seattle fault zone, Washington: Evidence from aeromagnetic anomalies, geologic mapping, and seismic-reflection data. Geological Society of America Bulletin 114, 169-177.

Blanco, M.J., Spakman, W., 1993. The P-wave velocity structure of the mantle below the Iberian Peninsula: evidence for subducted lithosphere below southern Spain. Tectonophysics 221, 13-34.

Blumenthal, M., 1927. Versuch einer tektonischen Gliederung der Betischen Kordilleren von central und Südwest Andalusien. Eclogae Geol. Helv. 20, 487–532.

Bohoyo, F., Galindo-Zaldívar, J., Serrano, I., 2000. Main features of the basic rock bodies of the Archidona Region derived from geophysical data (External Zones, Betic Cordillera). Comptes Rendus de l'Académie des Sciences-Series IIA-Earth and Planetary Science 330, 667-674.

Bokelmann, G., Maufroy, E., Buontempo, L., Morales, J., Barruol, G., 2011. Testing oceanic subduction and convective removal models for the Gibraltar arc: seismological constraints from dispersion and anisotropy. Tectonophysics 502, 28-37.

Bonini, W.E., Loomis, T.P., Robertson, J.D., 1973. Gravity anomalies, ultramafic intrusions, and the tectonics of the region around the Strait of Gibraltar. Journal of Geophysical Research 78, 1372-1382.

Booker, J.R., 2014. The Magnetotelluric Phase Tensor: A Critical Review. Surveys in Geophysics 35, 7-40.

Bouillin, J.P., Durand-Delga, M., Oliver, P., 1986. Betic- Rifian and Tyrrhenian arcs: distinctive features, genesis and development stages. The origin of arcs. Conference papers, Urbino, 1986, 281-304.

Bourgois, J., 1973. Présence et définition dans la région de Cañete la Real et de Grazalema d'une formation d'argiles à blocs (Province de Séville, Cadix et Malaga, Espagne). C.R. Acad. Sci. Paris, 276, 2939–2942.

Bourgois, J., 1978. La transversale de Ronda (Cordillères bétiques, Espagne): données géologiques pour un modèle d'évolution de l'arc de Gibraltar. Ph. D. Thesis. Annales Scientifiques de l'Université de Besançon, Géologie, 3e série, 30, 445 p.

Braga, J.C., Martı´n, J.M., Quesada, C., 2003. Patterns and average rates of late Neogene–Recent uplift of the Betic Cordillera, SE Spain. Geomorphology 50, 3-26.

Brun, J.P., Faccenna, C., 2008. Exhumation of high-pressure rocks driven by slab rollback. Earth and Planetary Science Letters 272, 1-7.

Buforn, E., Udias, A., Madariaga, R., 1991. Intermediate and deep earthquakes in Spain. Pure and Applied Geophysics 136, 375-393.

Buforn, E., Sanz de Galdeano, C., Udías, A., 1995. Seismotectonics of the Ibero-Maghrebian region. Tectonophysics 248, 247-261.

Buforn, E., Bezzeghoud, M., Udias, A., Pro, C., 2004. Seismic sources on the Iberia-African plate boundary and their tectonic implications. Pure and Applied Geophysics 161, 623-646.

Bull, W., McFadden L., 1977. Tectonic geomorphology north and south of the Garlock Fault, California. Doehring, D.O. Ed., Geomorphology in Arid regions, Publications in Geomorphology, State University of New York at Bingamton, 115 – 138.

Cagniard, L., 1953. Basic theory of the magneto-telluric method of geophysical prospecting. Geophysics 18, 605-635.

Caldwell, T.G., Bibby, H.M., Brown, C., 2004. The magnetotelluric phase tensor. Geophysical Journal International 158, 457-469.

Calvert, A., Sandvol, E., Seber, D., Barazangi, M., Roecker, S., Mourabit, T., Vidal, F., Alguacil, G., Jabour, N., 2000. Geodynamic evolution of the lithosphere and upper mantle beneath the Alboran region of the western Mediterranean: constraints from travel time tomography. Journal of Geophysical Research: Solid Earth 105, 10871-10898.

Cano-Medina, F., 1981. Mapa Geológico de España, Escala 1:50.000, hoja 1036 Olvera. IGME, Madrid.

Cano-Medina, F., Torres-Roldán, R., 1980. Mapa Geológico de España, Escala 1:50.000, hoja 1071 Jimena de la Frontera. IGME, Madrid.

Carbonell, R., Sallarés, V., Pous, J., Dañobeitia, J., Queralt, P., Ledo, J., García-Dueñas, V., 1998. A multidisciplinary geophysical study in the Betic chain (southern Iberia Peninsula). Tectonophysics 288, 137-152.

Carminati, E., Lustrino M., Doglioni, C., 2012. Geodynamic evolution of the central and western Mediterranean: Tectonics vs. igneous petrology constraints. Tectonophysics 579, 173–192.

Casas, A., Carbo, A., 1990. Deep structure of the Betic Cordillera derived from the interpretation of a complete Bouguer anomaly map. Journal of Geodynamics 12, 137-147.

Chalouan, A., Michard, A., 1990. The Ghomarides nappes, Rif coastal range, Morocco: a variscan chip in the Alpine belt. Tectonics 9, 1565-1583.

Chalouan, A., Michard, A., 2004. The Alpine Rif Belt (Morocco): a case of mountain building in a subduction-subduction-transform fault triple junction. Pure and Applied Geophysics 161, 489-519.

Chave, A.D., Jones, A.G., 2012. The magnetotelluric method: Theory and practice. Cambridge University Press.

Chemenda, A.I., Yang, R.K., Stephan, J.F., Konstantinovskaya, E.A., Ivanov, G.M., 2001. New results from physical modelling of arc–continent collision in Taiwan: evolutionary model. Tectonophysics 333, 159-178.

Cloetingh, S., Nieuwland, F., 1984. On the mechanics of lithospheric stretching and doming: a finite element analysis. Geologie en Mijnbouw 63, 315-322.

Comas, M., García-Dueñas, V., Jurado, M., 1992. Neogene tectonic evolution of the Alboran Sea from MCS data. Geo-Marine Letters 12, 157-164.

Crespo-Blanc, A., Balanyá, J. C., Exposito, I., Luján, M., Suades, E., 2012. Crescent-like large-scale structures in the external zones of the western Gibraltar Arc (Betic-Rif orogenic wedge). Journal of the Geological Society 169 (6), 667-679.

Dach, R., Hugentobler, U., Fridez, P., Meindl, M., 2007. Bernese GPS software version 5.0. Astronomical Institute, University of Bern 640.

Dañobeitia, J., Sallares, V., Gallart, J., 1998. Local earthquakes seismic tomography in the Betic Cordillera (southern Spain). Earth and Planetary Science Letters 160, 225-239.

Dañobeitia, J.J., Bartolomé, R., Checa, A., Maldonado, A., Slootweg, A.P., 1999. An interpretation of a prominent magnetic anomaly near the boundary between the Eurasian and African plates (Gulf of Cadiz, SW margin of Iberia). Marine geology 155, 45-62.

De Jong, K., 1991. Tectono-metamorphic studies and radiometric dating in the Betic Cordilleras (SE Spain): With implications for the dynamics of extension and compression in the western Mediterranean area. Ph. D. Thesis, Vrije Universiteit, 204 p.

De Jong, K., 1993. The tectono-metamorphic and chronologic development of the Betic Zone (SE Spain) with implications for the geodynamic evolution of the western Mediterranean area. Proceedings of the Koninklijke Nederlandse Akademie van Wetenschappen 96, 295-333.

de Lacy, M.C., Gil, A.J., Armenteros, J.A.G., Ruiz, A.M., Crespi, M., Mazzoni, A., 2012. A New Continuous GPS Network to Monitor Deformations in the Iberian Peninsula (Topo-Iberia Project). First Study of the Situation of the Betic System Area, in: Sneeuw, N., Novák, P., Crespi, M., Sansò, F. (Eds.), VII Hotine-Marussi Symposium on Mathematical Geodesy. Springer Berlin Heidelberg, pp. 387-392.

de Lis Mancilla, F., Stich, D., Berrocoso, M., Martín, R., Morales, J., Fernandez-Ros, A., Páez, R., Pérez-Peña, A., 2013. Delamination in the Betic Range: Deep structure, seismicity, and GPS motion. Geology 41, 307-310.

De Vicente, G., Cloetingh, S., Muñoz - Martín, A., Olaiz, A., Stich, D., Vegas, R., Galindo-Zaldivar, J., Fernández - Lozano, J., 2008. Inversion of moment tensor focal mechanisms for active stresses around the microcontinent Iberia: Tectonic implications. Tectonics, 27, TC1009.

DeMets, C., Gordon, R.G., Argus, D.F., Stein, S., 1990. Current plate motions. Geophysical Journal International 101, 425-478.

DeMets, C., Gordon, R.G., Argus, D.F., Stein, S., 1994. Effect of recent revisions to the geomagnetic reversal time scale on estimates of current plate motions. Geophysical Research Letters 21, 2191-2194.

Devoti, R., Riguzzi, F., Cuffaro, M., Doglioni, C., 2008. New GPS constraints on the kinematics of the Apennines subduction. Earth and Planetary Science Letters 273, 163-174.

Devoti, R., Esposito, A., Pietrantonio, G., Pisani, A.R., Riguzzi, F., 2011. Evidence of large scale deformation patterns from GPS data in the Italian subduction boundary. Earth and Planetary Science Letters 311, 230-241.

Dewey, J., Helman, M., Knott, S., Turco, E., Hutton, D., 1989. Kinematics of the western Mediterranean. Geological Society, London, Special Publications 45, 265-283.

Díaz, J., Gallart, J., 2009. Crustal structure beneath the Iberian Peninsula and surrounding waters: a new compilation of deep seismic sounding results. Physics of the Earth and Planetary Interiors 173, 181-190.

Diaz, J., Gallart, J., Villaseñor, A., Mancilla, F., Pazos, A., Córdoba, D., Pulgar, J.A., Ibarra, P., Harnafi, M., 2010. Mantle dynamics beneath the Gibraltar Arc (western Mediterranean) from shear-wave splitting measurements on a dense seismic array. Geophysical Research Letters 37, L18304.

Didon, J., Durand-Delga, M., Kornprobst, J., 1973. Homologies géologiques entre les deux rives du détroit de Gibraltar. Bulletin de la Societé Géologique de France, 77-105.

Docherty, C., Banda, E., 1995. Evidence for the eastward migration of the Alboran Sea based on regional subsidence analysis: A case for basin formation by delamination of the subcrustal lithosphere?. Tectonics 14, 804-818.

Doglioni C., Gueguen E., Sabat F., Fernandez M., 1997. The western Mediterranean extensional basins and the Alpine orogen. Terra Nova 9, 109-112.

Doglioni C., Fernandez M., Gueguen E., Sabat F., 1999. On the interference between the early Apennines-Maghrebides backarc extension and the Alps-Betics orogen in the Neogene Geodynamics of the Western Mediterranean. Boll. Soc. Geol. It. 118, 75-89.

Doglioni C., Gueguen E., Harabaglia P., Mongelli F., 1999. On the origin of W-directed subduction zones and applications to the western Mediterranean. Geol. Soc. Sp. Publ. 156, 541-561.

Dosso, H., Meng, Z., 1992. The coast effect response in geomagnetic field measurements. Physics of the Earth and Planetary interiors 70, 39-56.

Ducea, M.N., Park, S.K., 2000. Enhanced mantle conductivity from sulfide minerals, southern Sierra Nevada, California. Geophysical Research Letters 27, 2405-2408.

Duggen, S., Hoernle, K., van den Bogaard, P., Rupke, L., Phipps Morgan, J., 2003. Deep roots of the Messinian salinity crisis. Nature 422, 602-606.

Duggen, S., Hoernle, K., Klügel, A., Geldmacher, J., Thirlwall, M., Hauff, F., Lowry, D., Oates, N., 2008. Geochemical zonation of the Miocene Alborán Basin volcanism (westernmost Mediterranean): geodynamic implications. Contrib. Mineral. Petrol. 156, 577-593.

Durand-Delga, M., 2006. Geological adventures and misadventures of the Gibraltar Arc. Zeitschrift der Deutschen Gesellschaft für Geowissenschaften 157, 687-716.

Durand-Delga, M., Olivier, P., 1988. Evolution of the Alboran block margin from Early Mesozoic to Early Miocene time, The Atlas System of Morocco. Springer, pp. 463-480.

Durand-Delga, M., Rossi, P., Olivier, P., Puglisi, D., 2000. Situation structurale et nature ophiolitique de roches basiques jurassiques associées aux flyschs maghrébins du Rif (Maroc) et de Sicile (Italie). Comptes Rendus de l'Académie des Sciences-Series IIA-Earth and Planetary Science 331, 29-38.

Echeverría, A., Khazaradze, G., Asensio, E., Gárate, J., Martín-Dávila, J., Suriñach, E., 2013. Crustal deformation in eastern Betics from CuaTeNeo GPS network. Tectonophysics 608, 600-612.

Eden, C., Andrews, J., 1990. Middle to Upper Devonian melanges in SW Spain and their relationship to the Meneage formation in south Cornwall, Proc. Ussher Soc, pp. 217-222.

Egeler, C.G., Simon, O.J., 1969. Sur la Tectonique de la Zone Bétique: (Cordillères Bétiques, Espagne). Verh. K. Ned. Akad. Wet. 25, 1-90.

Elliott, J., Freymueller, J.T., Larsen, C.F., 2013. Active tectonics of the St. Elias orogen, Alaska, observed with GPS measurements. Journal of Geophysical Research: Solid Earth 118, 5625-5642.

Epov, M., Pospeeva, E., Vitte, L., 2012. Crust structure and composition in the southern Siberian craton (influence zone of Baikal rifting), from magnetotelluric data. Russian Geology and Geophysics 53, 293-306.

Estey, L.H., Meertens, C.M., 1999. TEQC: the multi-purpose toolkit for GPS/GLONASS data. GPS Solutions 3, 42-49.

Expósito, I., Balanya, J. C., Crespo-Blanc, A., Diaz-Azpiroz, M., Luján, M., 2012. Overthrust shear folding and contrasting deformation styles in a multiple decollement setting, Gibraltar Arc external wedge. Tectonophysics 576, 96-98.

Fadil, A., Vernant, P., McClusky, S., Reilinger, R., Gomez, F., Sari, D.B., Mourabit, T., Feigl, K., Barazangi, M., 2006. Active tectonics of the western Mediterranean: Geodetic evidence for rollback of a delaminated subcontinental lithospheric slab beneath the Rif Mountains, Morocco. Geology 34, 529-532.

Fallot, P., 1948. Les cordilléres betiques. Estud. Geol. 4, 83–172.

Féraud, G., Gastaud, J., Auzende, J.M., Olivet, J.L., Cornen, G., 1982. 40Ar/39Ar ages for the alkaline volcanism and basement of the Gorringe Bank, North Atlantic Ocean. Earth and Planetary Science Letters 57, 211–226.

Fernàndez, M., Berástegui, X., Puig, C., García-Castellanos, D., Jurado, M. J., Torné, M. and Banks, C., 1998. Geophysical and geological constraints on the evolution of the Guadalquivir foreland basin, Spain. In: Cenozoic Foreland Basins of Western Europe (A. Mascle et al., eds.). Spec. Publ. Geol. Soc. London 134, 29-48.

Fernàndez, M., Marzán, I., Torne, M., 2004. Lithospheric transition from the Variscan Iberian Massif to the Jurassic oceanic crust of the Central Atlantic. Tectonophysics 386, 97-115.

Finlay, C., Maus, S., Beggan, C., Hamoudi, M., Lowes, F., Olsen, N., Thébault, E., 2010. Evaluation of candidate geomagnetic field models for IGRF-11. Earth Planets and Space 62, 787.

Fullea, J., Fernàndez, M., Zeyen, H., Vergés, J., 2007. A rapid method to map the crustal and lithospheric thickness using elevation, geoid anomaly and thermal analysis. Application to the Gibraltar Arc System, Atlas Mountains and adjacent zones. Tectonophysics 430, 97-117.

Fullea, J., Fernàndez, M., Afonso, J.C., Vergés, J., Zeyen, H., 2010. The structure and evolution of the lithosphere–asthenosphere boundary beneath the Atlantic–Mediterranean Transition Region. Lithos 120, 74-95.

Galindo Zaldívar, J., 1986. Etapas de fallamiento neógenas en la mitad occidental de la depresión de Ugijar (Cordilleras Béticas). Estudios Geológicos 42, 1-10.

Galindo-Zaldivar, J., Gonzalez-Lodeiro, F., Jabaloy, A., 1989. Progressive extensional shear structures in a detachment contact in the western Sierra Nevada, (Betic Cordilleras, Spain). Geodinamica Acta 3, 73-85.

Galindo-Zaldívar, J., González-Lodeiro, F., Jabaloy, A., 1993. Stress and palaeostress in the Betic-Rif cordilleras (Miocene to the present). Tectonophysics 227, 105-126.

Galindo - Zaldívar, J., Jabaloy, A., González - Lodeiro, F., Aldaya, F., 1997. Crustal structure of the central sector of the Betic Cordillera (SE Spain). Tectonics 16, 18-37.

Galindo-Zaldivar, J., Gonzalez-Lodeiro, F., Jabaloy, A., Maldonado, A., Schreider, A. A. 1998. Models of magnetic and Bouguer gravity anomalies for the deep structure of the central Alboran Sea basin. Geo-Marine Letters 18, 10-18.

Galindo-Zaldívar, J., Ruano, P., Jabaloy, A., López-Chicano, M., 2000. Kinematics of faults between Subbetic Units during the Miocene (central sector of the Betic Cordillera). Comptes Rendus de l'Académie des Sciences-Series IIA-Earth and Planetary Science 331, 811-816.

Galindo-Zaldívar, J., Gil, A.J., Borque, M.J., González-Lodeiro, F., Jabaloy, A., Marín-Lechado, C., Ruano, P., Sanz de Galdeano, C., 2003. Active faulting in the internal zones of the central Betic Cordilleras (SE, Spain). Journal of Geodynamics 36, 239-250.

Galindo-Zaldívar, J., Ruiz-Constán, A., Pedrera, A., Ghidella, M., Montes, M., Nozal, F., Rodríguez-Fernández, L.R., 2013. Magnetic anomalies in Bahia Esperanza: A window of magmatic arc intrusions and glacier erosion over the northeastern Antarctic Peninsula. Tectonophysics 585, 68–76.

Gárate, J., Martín-Dávila, J., Khazaradze, G., Echeverria, A., Asensio, E., Gil, A.J., de Lacy, M.C., Armenteros, J.A., Ruiz, A.M., Gallastegui, J., Alvarez-Lobato, F., Ayala, C., Rodríguez-Caderot, G., Galindo-Zaldívar, J., Rimi, A., Harnafi, M., 2015. Topo-Iberia project: CGPS crustal velocity field in the Iberian Peninsula and Morocco. GPS Solutions, 19, 287-295.

García de Domingo, A., Hernaiz-Huerta, P.P., Cabra Gil, P., Pérez-González, A., 1985. Mapa Geológico de España, Escala 1:50.000, hoja 1035 Montellano. IGME, Madrid.

García-Casco, A., Torres-Roldan, R.L., 1996. Disequilibrium Induced by Fast Decompression in St－Bt－Grt－Ky－Sil－And Metapelites from the Betic Belt (Southern Spain). Journal of Petrology 37, 1207-1239.

Garcia - Castellanos, D., Fernandez, M., Torné, M., 2002. Modeling the evolution of the Guadalquivir foreland basin (southern Spain). Tectonics 21, 9-1.

Garcia-Castellanos, D., Estrada, F., Jiménez-Munt, I., Gorini, C., Fernández, M., Vergés, J., De Vicente, R., 2009. Catastrophic flood of the Mediterranean after the Messinian salinity crisis. Nature 462, 778-781.

Garcia-Castellanos, D., Villaseñor, A., 2011. Messinian salinity crisis regulated by competing tectonics and erosion at the Gibraltar arc. Nature 480, 359-363.

García-Dueñas, V., Balanyá, J., 1986. Estructura y naturaleza del Arco de Gibraltar. Maleo-Bol. Inf. Soc. Geol. Portugal 2, 23.

García-Dueñas, V., Balanyá, J., Martínez-Martínez, J., 1992. Miocene extensional detachments in the outcropping basement of the Northern Alboran Basin (Betics) and their tectonic implications. Geo-Marine Letters 12, 88-95.

García-Dueñas, V., Banda, E., Torné, M., Córdoba, D., 1994. A deep seismic reflection survey across the Betic Chain (southern Spain): first results. Tectonophysics 232, 77-89.

Garrett, S.W., 1990: Interpretation of reconnaisance gravity and aeromagnetic surveys of the Antarctic Peninsula. Jour. Geophys. Res. 95, 6759-6777.

Gerya, T.V., Yuen, D.A., Maresch, W.V., 2004.Thermomechanical modelling of slab detachment. Earth Planet. Sci. Lett. 226, 101–116.

Gil, A.J., Rodríguez-Caderot, G., Lacy, M.C., Ruiz, A.M., Sanz de Galdeano, C., Alfaro, P., 2002. Establishement of a non-permanent GPS network to monitor the recent NE-SW deformation in the Granada Basin (Betic Cordillera, Southern Spain). Studia Geophysica et Geodaetica 46, 395-410.

Gill, R., Aparicio, A., El Azzouzi, M., Hernandez, J., Thirlwall, M., Bourgois, J., Marriner, G., 2004. Depleted arc volcanism in the Alboran Sea and shoshonitic volcanism in Morocco: geochemical and isotopic constraints on Neogene tectonic processes. Lithos 78, 363-388.

Gómez-Pugnaire, M., Fernández-Soler, J., 1987. High-pressure metamorphism in metabasites from the Betic Cordilleras (SE Spain) and its evolution during the Alpine orogeny. Contrib Mineral Petrol 95, 231-244.

Gómez-Pugnaire, M.T., Galindo-Zaldívar, J., Rubatto, D., González-Lodeiro, F., López Sánchez-Vizcaíno, V., Jabaloy, A., 2004. A reinterpretation of the Nevado-Filábride and Alpujárride Complexes (Betic Cordillera): Field, petrography and U-Pb ages from

orthogneisses (western Sierra Nevada, S Spain). Schweizerische Mineralogische und Petrographische Mitteilungen 84, 303-322.

Gómez-Pugnaire, M.T., Rubatto, D., Fernández-Soler, J.M., Jabaloy, A., López-Sánchez-Vizcaíno, V., González-Lodeiro, F., Galindo-Zaldívar, J., Padrón-Navarta, J.A., 2012. Late Variscan magmatism in the Nevado-Filábride Complex: U-Pb geochronologic evidence for the pre-Mesozoic nature of the deepest Betic complex (SE Spain). Lithos 146–147, 93-111.

González-Castillo, L., Galindo-Zaldívar, J., Ruiz-Constán, A., Pedrera, A., 2014. Magnetic evidence of a crustal fault affecting a linear laccolith: The Guadiana Fault and the Monchique Alkaline Complex (SW Iberian Peninsula). Journal of Geodynamics 77, 149-157.

Grauch, V.J.S., Hudson, M.R., Minor, S.A., 2001. Aeromagnetic expression of faults that offset basin fill, Albuquerque basin, New Mexico. Geophysics 66, 707-720.

Gueguen E., Doglioni C., Fernandez M., 1997. Lithospheric boudinage in the Western Mediterranean back-arc basins. Terra Nova 9, 184-187.

Gueguen, E., Doglioni, C., Fernandez, M., 1998. On the post-25 Ma geodynamic evolution of the western Mediterranean. Tectonophysics 298, 259-269.

Gurria, E., Mezcua, J., 2000. Seismic tomography of the crust and lithospheric mantle in the Betic Cordillera and Alboran Sea. Tectonophysics 329, 99-119.

Gutscher, M.A., Malod, J., Rehault, J.P., Contrucci, I., Klingelhoefer, F., Mendes-Victor, L., Spakman, W., 2002. Evidence for active subduction beneath Gibraltar. Geology 30, 1071-1074.

Gutscher, M.A., Dominguez, S., Westbrook, G.K., Le Roy, P., Rosas, F., Duarte, J.C., Terrinha, P., Miranda, J.M., Graindorge, D., Gailler, A., Sallares, V., Bartolome, R., 2012. The Gibraltar subduction: A decade of new geophysical data. Tectonophysics 574, 72-91.

Hammer, S., 1939. Terrain corrections for Gravimeters Stations. Geophysics 4, 184-194.

Hammer, S., 1982. Critique of Terrain Corrections for Gravity Stations, Geophysics 47, 839-840.

Hancock, P.L., 1985. Brittle microtectonics: principles and practice. Journal of Structural Geology 7, 437-457.

Hatzfeld, D., 1976. Etude sismologique et gravimétrique de la structure profonde de la mer d'Alboran: Mise en évidence d'un manteau anormal. C.R. Acad. Sc. Paris 283, 1021-1024.

Häuserer, M., Junge, A., 2011. Electrical mantle anisotropy and crustal conductor: a 3-D conductivity model of the Rwenzori Region in western Uganda. Geophysical Journal International 185, 1235-1242.

Heimhofer, U., Adatte, T., Hochuli, P., Burla, S., Weissert, H., 2008. Coastal sediments from the Algarve: low-latitude climate archive for the Aptian-Albian. Int. J. Earth Sci. 97, 785–797

Heise, W., Bibby, H.M., Caldwell, T.G., Bannister, S.C., Ogawa, Y., Takakura, S., Uchida, T., 2007. Melt distribution beneath a young continental rift: the Taupo Volcanic Zone, New Zealand. Geophysical Research Letters 34.

Hinsbergen, D. J., Vissers, R. L., Spakman, W., 2014.Origin and consequences of western Mediterranean subduction, rollback, and slab segmentation. Tectonics 33, 393-419.

Hinsbergen, D.J., Vissers, R.L., Spakman, W., 2014. Origin and consequences of western Mediterranean subduction, rollback, and slab segmentation. Tectonics 33, 393-419.

Hoernle, K., van den Bogaard, P., Duggen, S., Mocek, B., Garbe-Schönberg, D., 1999. Evidence for Miocene subduction beneath the Alboran Sea (Western Mediterranean) from 40Ar/39Ar age dating and the geochemistry of volcanic rocks from holes 977A and 978A. In: Proceedings of the Ocean Drilling Project, Scientific Results 161., ed. by Zahn, R., Comas, M. C., KIaus, A. Ocean Drilling Project, College Station, TX, pp. 357-373.

Houseman, G.A., McKenzie, D.P., Molnar, P., 1981. Convective instability of a thickened boundary layer and its relevance for the thermal evolution of continental convergent belts. Journal of Geophysical Research: Solid Earth (1978–2012) 86, 6115-6132.

Hudson, M.R., Grauch, V.J.S., Minor, S.A., Caine, J.S., Hudson, A.M., 2001. Rock magnetic properties, magnetic anomalies, and intrabasin faulting: Santa Fe Group basin fill, Rio Grande rift, New Mexico: EOS, Transactions. American Geophysical Union 82, 338–339.

I.G.N., 1976. Mapa de anomalías de Bouguer. Escala 1:1,000,000. I.G.N., Madrid.

IAGA, 2010. International geomagnetic reference field: the eleventh generation. Geophysical Journal International 183, 1216–1230.

Jabaloy, A., Galindo-Zaldívar, J., González-Lodeiro, F., 1992. The Mecina Extensional System: its relation with the post-Aquitanian piggy-back basins and the paleostresses evolution (Betic Cordilleras, Spain). Geo-Marine Letters 12, 96-103.

Jones, A.G., 1993. Electromagnetic images of modern and ancient subduction zones. Tectonophysics 219, 29-45.

Jones, A.G., 1987. MT and reflection: an essential combination. Geophysical Journal International 89, 7-18.

Jones, A.G., Kurtz, R.D., Boerner, D.E., Craven, J.A., McNeice, G.W., Gough, D.I., DeLaurier, J.M., Ellis, R.G., 1992. Electromagnetic constraints on strike-slip fault geometry-The Fraser River fault system. Geology 20, 561-564.

Jones, A.G., Ferguson, I.J., Chave, A.D., Evans, R.L., McNeice, G.W., 2001. Electric lithosphere of the Slave craton. Geology 29, 423-426.

Kato, Y., Kikuchi, T., 1950. On the Phase Difference of Earth Current Induced by the Changes of the Earth's Magnetic Field.(Part II). Sci. Rep. Tohoku. Univ. Ser. V. Geophysics 2, 139–145.

Keller, E.A., Pinter, N., 1996. Active tectonics: Earthquakes, uplift and landscape. Upper Saddle River, New Jersey, Prentice-Hall, Englewood Cliffs, NJ.

Key, K., Constable, S., 2011. Coast effect distortion of marine magnetotelluric data: insights from a pilot study offshore northeastern Japan. Physics of the Earth and Planetary interiors 184, 194-207.

Korja, T., 2007. How is the European lithosphere imaged by magnetotellurics? Surveys in Geophysics 28, 239-272.

Koulali, A., Ouazar, D., Tahayt, A., King, R., Vernant, P., Reilinger, R., McClusky, S., Mourabit, T., Davila, J., Amraoui, N., 2011. New GPS constraints on active deformation along the Africa–Iberia plate boundary. Earth and Planetary Science Letters 308, 211-217.

Kurtz, R., De Laurier, J., Gupta, J., 1986. A magnetotelluric sounding across Vancouver Island detects the subducting Juan de Fuca plate. Nature 321, 596-599.

Kütter, S., 2009. Three-dimensional finite element simulation of magnetotelluric fields incorporating digital elevation models. Diploma thesis, TU Bergakademie Freiberg.

Leblanc, D., Olivier, P., 1984. Role of strike-slip faults in the Betic-Rifian orogeny. Tectonophysics 101, 345-355.

Lilley, F., Arora, B., 1982. The sign convention for quadrature Parkinson arrows in geomagnetic induction studies. Reviews of Geophysics 20, 513-518.

Lonergan, L., White, N., 1997. Origin of the Betic - Rif mountain belt. Tectonics 16, 504-522.

Loomis, T.P., 1975. Tertiary mantle diapirism, orogeny, and plate tectonics east of the Strait of Gibraltar. American Journal of Science 275, 1-30.

Lopes, F.C., Cunha, P.P., Le Gall, B., 2006. Cenozoic seismic stratigraphy and tectonic evolution of the Algarve margin (offshore Portugal, southwestern Iberian Peninsula). Marine Geology 231, 1-36.

Löwer, A., 2014. Magnetotellurische Erkundung geologischer Großstrukturen des südwestlichen Vogelsberges mit anisotroper, dreidimensionaler Modellierung der Leitfähigkeitsstrukturen. PhD-thesis, Goethe-Universität Frankfurt, Germany.

Luján, M., Crespo - Blanc, A., Balanyá, J.C., 2006. The Flysch Trough thrust imbricate (Betic Cordillera): a key element of the Gibraltar Arc orogenic wedge. Tectonics 25, TC6001.

Mackie, R., Bennett, B., Madden, T., 1988. Long-period magnetotelluric measurements near the central California coast: a land-locked view of the conductivity structure under the Pacific Ocean. Geophysical Journal International 95, 181-194.

Malleswari, D., Veeraswamy, K., 2014. Numerical simulation of coast effect on magnetotelluric measurements. Acta Geod. Geophys. 49, 17-35.

Mantero, E.M., Alonso-Chaves, F.M., García-Navarro, E., Azor, A., 2011. Tectonic style and structural analysis of the Puebla de Guzmán Antiform (Iberian Pyrite Belt, South

Portuguese Zone, SW Spain). Geological Society London, Special Publications 349, 203-222.

Manuppella, G., Marques, B., Rocha, R., 1988. Evolution tectono-sedimentaire du Bassin de 1'Algarve pendant le Jurassique. Int. Symp. Jur. Stratigr., 2nd, 1031-1046.

Marín-Lechado, C., Galindo-Zaldívar, J., Gil, A.J., Borque, M.J., de Lacy, M.C., Pedrera, A., López-Garrido, A.C., Alfaro, P., García-Tortosa, F., Ramos, M.I., Rodríguez-Caderot, G., Rodríguez-Fernández, J., Ruiz-Constán, A., Sanz de Galdeano, C., 2010. Levelling profiles and a GPS network to monitor the active folding and faulting deformation in the campo de Dalias (Betic Cordillera, Southeastern Spain). Sensors 10, 3504-3518.

Martí, A., Queralt, P., Roca, E., 2004. Geoelectric dimensionality in complex geological areas: application to the Spanish Betic Chain. Geophysical Journal International 157, 961-974.

Martí, A., Queralt, P., Roca, E., Ledo, J., Galindo - Zaldívar, J., 2009. Geodynamic implications for the formation of the Betic - Rif orogen from magnetotelluric studies. Journal of Geophysical Research: Solid Earth (1978–2012) 114 (B1).

Martín-Algarra, A., 1987.Evolución geológica alpina del contacto entre las Zonas Internas y las Zonas Externas de la Cordillera Bética. Ph. D. thesis, University of Granada, 1171 pp.

Martín - Algarra, A., Mazzoli, S., Perrone, V., Rodríguez - Cañero, R., Navas - Parejo, P., 2009. Variscan tectonics in the Malaguide Complex (Betic Cordillera, southern Spain): stratigraphic and structural Alpine versus pre - Alpine constraints from the Ardales area (Province of Malaga). I. Stratigraphy. The Journal of Geology 117, 241-262.

Martínez del Olmo, W., Garcia-Mallo, J., Leret-Verdu, G., Serrano-Oñate, A., Suarez Alba, J., 1984. Modelo tectonosedimentario del Bajo Guadalquivir. I Congreso Español de Geología 1, 199-213.

Martínez-Martínez, J.M., Booth-Rea, G., Azañón, J.M., Torcal, F., 2006. Active transfer fault zone linking a segmented extensional system (Betics, southern Spain): Insight into heterogeneous extension driven by edge delamination. Tectonophysics 422, 159-173.

Martínez-Poyatos, D., Carbonell, R., Palomeras, I., Simancas, J.F., Ayarza, P., Martí, D., Azor, A., Jabaloy, A., González-Cuadra, P., Tejero, R., 2012. Imaging the crustal structure of the Central Iberian Zone (Variscan Belt): The ALCUDIA deep seismic reflection transect. Tectonics 31, TC3017.

Maus, S., Gordon, D., Fairhead, D., 1997. Curie-temperature depth estimation using a self-similar magnetization model. Geophysical Journal International 129, 163-168.

McClusky, S., Balassanian, S., Barka, A., Demir, C., Ergintav, S., Georgiev, I., Veis, G., 2000. Global Positioning System constraints on plate kinematics and dynamics in the eastern Mediterranean and Caucasus. Journal of Geophysical Research 105, 5695-5719.

Medialdea, T., Suriñach, E., Vegas, R., Banda, E., Ansorge, J., 1986. Crustal structure under the western end of the Betic Cordillera (Spain), Annales geophysicae B4, 457-464.

Merle, R., Jourdan, F., Marzoli, A., Renne, P. R., Grange, M., Girardeau, J., 2009. Evidence of multi-phase Cretaceous to Quaternary alkaline magmatism onTore-Madeira Rise and neighbouring seamounts from 40Ar/ 39Ar ages. Journal of the Geological Society London 166, 879-894.

Miranda, J.M., Galdeano, A., Rossignol, J.C., Mendes-Victor, L.A., 1989. Aeromagnetic anomalies in mainland Portugal and their tectonic implications. Earth and Planetary Science Letters 95, 161-172.

Miranda, R., Valadares, V., Terrinha, P., Mata, J., do Rosario Azevedo, M., Gaspara, M., Kullberg, J. C., Ribeiro, C., 2009. Age constraints on the Late Cretaceous alkaline magmatism on the West Iberian Margin. Cretaceous Research 30, 575-586.

Monié, P., Galindo-Zaldívar, J., González-Lodeiro, F., Goffé, B., Jabaloy, A., 1991. 40Ar/39Ar geochronology of Alpine tectonism in the Betic Cordilleras (southern Spain). Journal of the Geological Society 148, 289-297.

Moniz C., González-Clavijo E., Matias L., Cabral, J., 2003. Estudo de lineamentos fotointerpretados na região do Algarve ocidental. Ciências da Terra (UNL), Lisboa, nº esp. V, CD-ROM, C53-C56.

Monteiro-Santos, F.A., Pous, J., Almeida, E.P., Queralt, P., Marcuello, A., Matias, H., Mendes-Victor, L.S.A., 1999. Magnetotelluric survey of the electrical conductivity of the crust across the Ossa Morena Zone and South Portuguese Zone suture. Tectonophysics 313, 449-462.

Monteiro-Santos, F.A., Mateus, A., Almeida, E.P., Pous, J., Mendes-Victor, L.S.A., 2002. Are some of the deep crustal conductive features found in SW Iberia caused by graphite? Earth and Planetary Science Letters 201, 353-367.

Morales, J., Serrano, I., Vidal, F., Torcal, F., 1997. The depth of the earthquake activity in the Central Betics (Southern Spain). Geophysical Research Letters 24, 3289-3292.

Morales, J., Serrano, I., Jabaloy, A., Galindo-Zaldivar, J., Zhao, D., Torcal, F., Vidal, F., González-Lodeiro, F., 1999. Active continental subduction beneath the Betic Cordillera and the Alboran Sea. Geology 27, 735-738.

Morley, C.K., 1993. Discussion of origins of hinterland basins to the Rif-Betic Cordillera and Carpathians. Tectonophysics 226, 359-376.

Muñoz, G., Heise, W., Paz, C., Almeida, E., Monteiro-Santos, F., Pous, J., 2005. New magnetotelluric data trough the boundary between the Ossa Morena and Centroiberian Zones. Geologica Acta 3, 215-223.

Muñoz, G., Mateus, A., Pous, J., Heise, W., Monteiro-Santos, F., Almeida, E., 2008. Unraveling middle‐crust conductive layers in Paleozoic Orogens through 3D modeling of magnetotelluric data: The Ossa-Morena Zone case study (SW Iberian Variscides). Journal of Geophysical Research: Solid Earth (1978–2012) 113, B06106.

Nocquet, J.M., 2012. Present-day kinematics of the Mediterranean: A comprehensive overview of GPS results. Tectonophysics 579, 220-242.

Oliveira, J.T., 1990. Stratigraphy and syn-sedimentary tectonism in the South Portuguese Zone. In: Pre-Mesozoic Geology of Iberia. Dallmeyer, D., Martinez, E. (Eds.). Springer Verlag, Berlín, Heidelberg, 334–347.

Olsen, N., 1998. The electrical conductivity of the mantle beneath Europe derived from C-responses from 3 to 720 hr. Geophysical Journal International 133, 298-308.

Onézime, J., Charvet, J., Faure, M., Bourdier, J.L., Chauvet, A., 2003. A new geodynamic interpretation for the South Portuguese Zone (SW Iberia) and the Iberian Pyrite Belt genesis. Tectonics 22, 1027.

Palano, M., González, P.J., Fernández, J., 2013. Strain and stress fields along the Gibraltar Orogenic Arc: constraints on active geodynamics. Gondwana Research, 23, 1071-1088.

Palomeras, I., Thurner, S., Levander, A., Liu, K., Villasenor, A., Carbonell, R., and Harnafi, M., 2014. Finite‐frequency Rayleigh wave tomography of the western Mediterranean: Mapping its lithospheric structure. Geochemistry, Geophysics, Geosystems, 15, 140-160.

Parker, R.L., Booker, J.R., 1996. Optimal one-dimensional inversion and bounding of magnetotelluric apparent resistivity and phase measurements. Physics of the Earth and Planetary Interiors, 98, 269-282.

Pedley, R.C., Busby, J.P., Dabeck, Z.K., 1993. GRAVMAG User Manual- Interactive 2.5D gravity and magnetic modelling. British Geological Survey, Technical Report WK/93/26/R.

Pedrera, A., Galindo-Zaldívar, J., Ruíz-Constán, A., Duque, C., Marín-Lechado, C., Serrano, I., 2009. Recent large fold nucleation in the upper crust: Insight from gravity, magnetic, magnetotelluric and seismicity data (Sierra de Los Filabres–Sierra de Las Estancias, Internal Zones, Betic Cordillera). Tectonophysics 463, 145-160.

Pedrera, A., de Lis Mancilla, F., Ruiz-Constán, A., Galindo-Zaldívar, J., Morales, J., Arzate, J., Marín-Lechado, C., Ruano, P., Buontempo, L., Anahnah, F., Stich, D., 2010. Crustal-scale transcurrent fault development in a weak-layered crust from an integrated geophysical research: Carboneras Fault Zone, eastern Betic Cordillera, Spain. Geochemistry, Geophysics, Geosystems 11, Q12005.

Pedrera, A., Ruiz-Constán, A., Galindo-Zaldívar, J., Chalouan, A., Sanz de Galdeano, C., Marín-Lechado, C., Ruano, P., Benmakhlouf, M., Akil, M., López-Garrido, A.C., Chabli, A., Ahmamou, M., González-Castillo, L., 2011. Is there an active subduction beneath the Gibraltar orogenic arc? Constraints from Pliocene to present-day stress field. Journal of Geodynamics 52, 83-96.

Pedrera, A., Marín-Lechado, C., Martos-Rosillo, S., Roldán, F.J., 2012. Curved fold-and-thrust accretion during the extrusion of a synorogenic viscous allochthonous sheet: The Estepa Range (External Zones, Western Betic Cordillera, Spain). Tectonics 31, TC4013.

Pedrera, A., Ruiz-Constán, A. Marín-Lechado, C. Galindo-Zaldívar, J. González, A., Peláez J.A. 2013, Seismic transpressive basement faults and monocline development in a foreland basin (Eastern Guadalquivir, SE Spain), Tectonics 32, 1571–1586.

Perconig, E. 1960-62. Sur la constitution géologique de l'Andalousie occidentale, en particulier du bassin du Guadalquivir (Espagne méridionale). Livre Mém. Paul Fallot, Mém. Hors Sér. S.G.F., 231-256.

Pérez-López, A., Sanz de Galdeano, C., 1994. Tectónica de los materiales triásicos en el sector central de la Zona Subbética (Cordillera Bética). Rev. Soc. Geol. España 7 (1-2), 141-153.

Pérez-Peña, A., Martín-Davila, J., Gárate, J., Berrocoso, M., Buforn, E., 2010. Velocity field and tectonic strain in Southern Spain and surrounding areas derived from GPS episodic measurements. Journal of Geodynamics 49, 232-240.

Pérouse, E., Vernant, P., Chéry, J., Reilinger, R., McClusky, S., 2010. Active surface deformation and sub-lithospheric processes in the western Mediterranean constrained by numerical models. Geology 38, 823-826.

Pilkington, M., 2007. Locating geologic contacts with magnitude transforms of magnetic data. Journal of Applied Geophysics 63, 80-89.

Piña-Varas, P., Ledo, J., Queralt, P., Marcuello, A., Bellmunt, F., Hidalgo, R., Messeiller, M., 2014. 3-D Magnetotelluric Exploration of Tenerife Geothermal System (Canary Islands, Spain). Surveys in Geophysics 35, 1045-1064.

Pinheiro L.M., Wilson R.C.L., Pena dos Reis R., Whitmarsh R.B., Ribeiro A., 1996. The Western Iberia Margin: A geophysical and geological overview. Whitmarsh, R.B., Sawyer, D.S., Klaus, A., Masson, D.G. (Eds.). Proceedings of the Ocean Drilling Program, Scientific Results, 149.

Piromallo, C., Morelli, A., 2003. P wave tomography of the mantle under the Alpine - Mediterranean area. Journal of Geophysical Research 108, 2065, B2.

Platt, J., Vissers, R., 1989. Extensional collapse of thickened continental lithosphere: A working hypothesis for the Alboran Sea and Gibraltar arc. Geology 17, 540-543.

Platt, J., Allerton, S., Kirker, A., Mandeville, C., Mayfield, A., Platzman, E., Rimi, A., 2003. The ultimate arc: Differential displacement, oroclinal bending, and vertical axis rotation in the External Betic-Rif arc. Tectonics 22.

Platzman, E., 1990. Paleomagnetism and tectonics in the Gibraltar arc. Diss. Naturwiss. ETH Zürich, Nr. 9161, 1990.

Platzman, E., Lowrie, W., 1992. Paleomagnetic evidence for rotation of the Iberian Peninsula and the external Betic Cordillera, Southern Spain. Earth and Planetary Science Letters 108, 45-60.

Pous, J., Queralt, P., Ledo, J., Roca, E., 1999. A high electrical conductive zone at lower crustal depth beneath the Betic Chain (Spain). Earth and Planetary Science Letters 167, 35-45.

Pous, J., Heise, W., Schnegg, P.A., Muñoz, G., Martı´, J., Soriano, C., 2002. Magnetotelluric study of the Las Cañadas caldera (Tenerife, Canary Islands): structural and hydrogeological implications. Earth and Planetary Science Letters 204, 249-263.

Pous, J., Muñoz, G., Heise, W., Melgarejo, J.C., Quesada, C., 2004. Electromagnetic imaging of Variscan crustal structures in SW Iberia: the role of interconnected graphite. Earth and Planetary Science Letters 217, 435-450.

Pous, J., Martínez-Poyatos, D., Heise, W., Santos, F.M., Galindo - Zaldívar, J., Ibarra, P., Pedrera, A., Ruiz - Constán, A., Anahnah, F., Gonçalves, R., 2011. Constraints on the crustal structure of the internal Variscan Belt in SW Europe: A magnetotelluric transect along the eastern part of Central Iberian Zone, Iberian Massif. Journal of Geophysical Research: Solid Earth (1978–2012) 116 (B2).

Reid, A.B., 2003. Euler magnetic structural index of a thin-bed fault. Geophysics 68, 1255–1256.

Riaza, C., del Olmo, W.M., 1996. S3 Depositional model of the Guadalquivir-Gulf of Cadiz Tertiary basin. In: Friend, P.F., Dabrio, C.J. (Eds.). Tertiary Basins of Spain: The stratigraphic record of crustal kinematics, Cambridge University Press, Cambridge, pp. 330- 338.

Ribeiro, A., Antunes, M.T., Ferreira, M.P., Rocha, R.B., Soares, A.F., Zbyszewski, G., Moitinho de Almeida, F., Carvalho, D., Monteiro, J.H., 1979. Introduction à la Géologie generale du Portugal. Ed. Serv. Geol. Portugal, 114.

Ribeiro, A., Manuppella, G., Oliveira, J.T., 1984. Tectonica das orlas sedimentares. J.T. Oliveira (Ed.), Carta Geologica de Portugal. Escala l/200,000: Noticia Explicativa da Folba 7. Serv. Geol. Port. Lisbon, 65-66.

Ribeiro A., Kullberg M.C., J.C., Kullberg, G., Manuppella, Phipps, S., 1990. A review of Alpine tectonics in Portugal: Foreland detachment in basement and cover rocks. Tectonophysics 184, 357- 366.

Ribeiro, A., Quesada, C., Dallmeyer, R.D., 1990. Geodynamic Evolution of the Iberian Massif, in: Dallmeyer, R.D., Garcia, E. (Eds.), Pre-Mesozoic Geology of Iberia. Springer Berlin Heidelberg, pp. 399-409.

Ritter, O., Junge, A., Dawes, G.J., 1998. New equipment and processing for magnetotelluric remote reference observations. Geophysical Journal International 132, 535-548.

Rock, N. M. S., 1978. Petrology and petrogenesis of the Monchique alkaline complex, southern Portugal. Journal of Petrology 19, 171-214.

Rock, N.M.S., 1982. The Late Cretaceous alkaline igneous province in the Iberian Peninsule and its tectonic significance. Lithos 15, 111–131.

Rodi, W., Mackie, R.L., 2001. Nonlinear conjugate gradients algorithm for 2-D magnetotelluric inversion. Geophysics, 66, 174-187.

Rodríguez-Ramírez, A., Flores-Hurtado, E., Contreras, C., Villarías-Robles, J.J., Jiménez-Moreno, G., Pérez-Asensio, J.N., López-Sáez, J.A., Celestino-Pérez, S., Cerrillo-Cuenca, E., León, A., 2014. The role of neo-tectonics in the sedimentary infilling and geomorphological evolution of the Guadalquivir estuary (Gulf of Cadiz, SW Spain) during the Holocene. Geomorphology 219, 126-140.

Roest, W., Srivastava, S., 1991. Kinematics of the plate boundaries between Eurasia, Iberia, and Africa in the North Atlantic from the Late Cretaceous to the present. Geology 19, 613-616.

Roest, W.R., Verhoef, J., Macnab, R., 1996. Magnetic Anomaly Map of the Atlantic North of 30° . Scale 1:10.000.000

Roldán, F.J., 1995. Evolución Neógena de la Cuenca del Guadalquivir. PhD Thesis, Universidad de Granada, 259 pp.

Roldán, F.J., Rodríguez Fernández, J., Azañón, J.M., 2012. La Unidad Olistostrómica, una formación clave para entender la historia neógena de las Zonas Externas de la Cordillera Bética. Geogaceta 52, 103-106.

Rosell, O., Martí, A., Marcuello, À., Ledo, J., Queralt, P., Roca, E., Campanyà, J., 2011. Deep electrical resistivity structure of the northern Gibraltar Arc (western Mediterranean): evidence of lithospheric slab break-off. Terra Nova 23, 179-186.

Rosenbaum, G., Lister, G.S., Duboz, C., 2002. Relative motions of Africa, Iberia and Europe during Alpine orogeny. Tectonophysics 359, 117-129.

Rosenbaum, G., Lister, G.S., 2004. Formation of arcuate orogenic belts in the western Mediterranean region. Geological Society of America Special Papers 383, 41-56.

Royden, L.H., 1993. Evolution of retreating subduction boundaries formed during continental collision. Tectonics 12, 629-638.

Ruano, P., Galindo-Zaldívar, J., Jabaloy, A., 2004. Recent tectonic structures in a transect of the Central Betic Cordillera. Pure Appl. Geophys. 161, 541–563.

Ruiz, A.M., Ferhat, G., Alfaro, P., Sanz de Galdeano, C., Lacy, M.C., Rodríguez-Caderot, G., Gil, A.J., 2003. Geodetic measurements of crustal deformation on NW-SE faults of the Betic Cordillera, southern Spain, 1999-2001. Journal of Geodynamics 35, 259-272.

Ruiz-Constán, A., 2009. Lithospheric structure of the Western Betic Cordillera and its foreland: implications in the recent tectonic evolution. Ph.D. Thesis, University of Granada.

Ruiz - Constán, A., Stich, D., Galindo - Zaldívar, J., Morales, J., 2009. Is the northwestern Betic Cordillera mountain front active in the context of the convergent Eurasia–Africa plate boundary? Terra Nova 21, 352-359.

Ruiz-Constán, A., Galindo-Zaldivar, J., Pedrera, A., Arzate, J.A., Pous, J., Anahnah, F., Heise, W., Santos, F.A.M., Marín-Lechado, C., 2010. Deep deformation pattern from electrical anisotropy in an arched orogen (Betic Cordillera, western Mediterranean). Geology 38, 731-734.

Ruiz-Constán, A., Galindo-Zaldívar, J., Pedrera, A., Célérier, B., Marín-Lechado, C., 2011. Stress distribution at the transition from subduction to continental collision (northwestern and central Betic Cordillera). Geochemistry, Geophysics, Geosystems 12.

Ruiz-Constán, A., Pedrera, A., Galindo-Zaldívar, J., Pous, J., Arzate, J., Roldán-García, F.J., Marin-Lechado, C., Anahnah, F., 2012a. Constraints on the frontal crustal structure of a continental collision from an integrated geophysical research: the central-western Betic Cordillera (SW Spain). Geochemistry, Geophysics, Geosystems, 13.

Ruiz-Constán, A., Pedrera, A., Galindo-Zaldivar, J., Stich, D., Morales, J., 2012b. Recent and active tectonics in the western part of the Betic Cordillera. Journal of Iberian Geology 38, 161-174.

Saheel A.S, Samsudin A.R.B., Hamzah U.B., 2011. Mapping of Faults in the Libyan Sirte Basin by Magnetic Surveys. Sains Malaysiana 40, 853–864

Salvany, J.M., Larrasoaña, J.C., Mediavilla, C., Rebollo, A., 2011. Chronology and tectono-sedimentary evolution of the Upper Pliocene to Quaternary deposits of the lower Guadalquivir foreland basin, SW Spain. Sedimentary Geology 241, 22-39.

Sánchez-Jiménez, N., 2003. Estructura gravimétrica y magnética de la corteza del suroeste peninsular (zona surportuguesa y zona de Ossa-Morena). Ph. D. Thesis. Universidad Complutense de Madrid, Servicio de Publicaciones.

Sánchez-Jiménez, N., Bergamín, J.F., Fernández Rodríguez, C., Castro Dorado, A., 1996. Modelización gravimétrica en el SW de la Península Ibérica. Geogaceta 20-4, 951-954.

Santos, F.A.M., Nolasco, M., Almeida, E.P., Pous, J., 2001. Coast effects on magnetic and magnetotelluric transfer functions and their correction: application to MT soundings carried out in SW Iberia. Earth and Planetary Science Letters 186, 283-295.

Sanz de Galdeano, C., 1983. Los accidentes y fracturas principales de las Cordilleras Béticas. Estudios Geológicos 39, 157-165.

Sanz de Galdeano, C., 1990. Geologic evolution of the Betic Cordilleras in the Western Mediterranean, Miocene to the present. Tectonophysics 172, 107-119.

Sanz de Galdeano, C., Vera, J.A., 1992. Stratigraphic record and palaeogeographical context of the Neogene basins in the Betic Cordillera, Spain. Basin Research 4, 21-35.

Sanz de Galdeano, C., Alfaro, P., 2004. Tectonic significance of the present relief of the Betic Cordillera. Geomorphology 63, 175-190.

Sanz de Galdeano, C., Lozano, J., Puga, E., 2008. El «Trías de Antequera»: naturaleza, origen y estructura. Revista de la Sociedad Geológica de España 21, 111-124.

Schettino, A., Turco, E., 2011. Tectonic history of the western Tethys since the Late Triassic. Geological Society of America Bulletin 123, 89-105.

Schmucker, U., 1970. Anomalies of geomagnetic variations in the southwestern United States. Bull. Scripps Inst. Oceanogr. 13, 165p.

Schultz, A., Kurtz, R., Chave, A., Jones, A., 1993. Conductivity discontinuities in the upper mantle beneath a stable craton. Geophysical Research Letters 20, 2941-2944.

Seber, D., Barazangi, M., Ibenbrahim, A., Demnati, A., 1996. Geophysical evidence for lithospheric delamination beneath the Alboran Sea and Rif–Betic mountains. Nature 379, 785 - 790.

Serpelloni, E., Vannucci, G., Pondrelli, S., Argnani, A., Casula, G., Anzidei, M., Baldi, P., Gasperini, P., 2007. Kinematics of the Western Africa-Eurasia plate boundary from focal mechanisms and GPS data. Geophysical Journal International 169, 1180-1200.

Serrano, I., Morales, J., Zhao, D., Torcal, F., Vidal, F., 1998. P-wave tomographic images in the Central Betics-Alboran sea (South Spain) using local earthquakes: Contribution for a continental collision. Geophysical Research Letters 25, 4031-4034.

Serrano, I., Bohoyo, F., Galindo-Zaldívar, J., Morales, J., Zhao, D., 2002. Geophysical signatures of a basic body rock placed in the upper crust of the External Zones of the Betic Cordillera (Southern Spain). Geophysical Research Letters 29, 1-4.

Serrano, I., Hearn, T., Morales, J., Torcal, F., 2005. Seismic anisotropy and velocity structure beneath the southern half of the Iberian Peninsula. Physics of the Earth and Planetary interiors 150, 317-330.

Sierro, F.J., González-Delgado, J.A., Dabrio, C.J., Flores, J.A., Civis, J., 1990. The Neogene of the Guadalquivir Basin (SW Spain). Paleontol. Evol., Mem. Espec. 2, 209 – 250.

Silva, J.B., Oliveira, J.T., Ribeiro, A., 1990. South Portuguese Zone, Structural outline. In: Pre-Mesozoic Geology of Iberia. Dallmeyer, R.D., Martínez-García, E. (Eds.). Springer-Verlag, Berlín, Heidelberg, 348-362.

Simancas, J., Carbonell, R., González-Lodeiro, F., Pérez-Estaún, A., Juhlin, C., Ayarza, P., Kashubin, A., Azor, A., Martínez-Poyatos, D., Almodovar, G.R., 2003. Crustal structure of the transpressional Variscan orogen of SW Iberia: SW Iberia deep seismic reflection profile (IBERSEIS). Tectonics 22.

Simancas, F., Ramos, I.E., Pérez, A.A., Poyatos, D.J.M., González-Lodeiro, F., 2004. From the Cadomian orogenesis to the early Palaeozoic Variscan rifting in southwest Iberia. Journal of Iberian Geology 30, 53-72.

Socías, I., Mezcua, J., Lynam, J., Del Potro, R., 1991. Interpretation of an aeromagnetic survey of the Spanish mainland. Earth and Planetary Science Letters 105, 55-64.

Socias, I., Mezcua, J., 2002. Mapa de Anomalias Magneticas de la Peninsula Ibérica. Instituto Geográfico Nacional (IGN), Madrid.

Spakman, W., Wortel, R., 2004. A tomographic view on western Mediterranean geodynamics. In The TRANSMED atlas.The Mediterranean region from crust to mantle (pp. 31-52). Springer Berlin Heidelberg.

Stănică, D., Stănică, M., 1993. An electrical resistivity lithospheric model in the Carpathian Orogen from Romania. Physics of the Earth and Planetary Interiors 81, 99-105.

Stich, D., Martín, R., Morales, J., 2010.Moment tensor inversion for Iberia–Maghreb earthquakes 2005–2008. Tectonophysics 483, 390-398.

Suriñach, E., Udías, A., 1978. Determinación de la raíz de Sierra Nevada-Filabres a partir de medidas de refracción sísmica y gravimetría, Geodinámica de la Cordillera Bética y Mar de Alborán. University of Granada, pp. 25-34.

Suriñach, E., Vegas, R., 1993. Estructura general de la corteza en una transversal del Mar de Alborán a partir de datos de sísmica de refracción-reflexión de gran ángulo. Interpretación geodinámica. Geogaceta 14, 126-128.

Tahayt, A., Mourabit, T., Rigo, A., Feigl, K.L., Fadil, A., McClusky, S., Reilinger, R., Serroukh, M., Ouazzani-Touhami, A., Sari, D.B., 2008. Mouvements actuels des blocs tectoniques dans l'arc Bético-Rifain à partir des mesures GPS entre 1999 et 2005. Comptes Rendus Geoscience 340, 400-413.

Tapponnier, P., 1977. Evolution tectonique du systeme alpin en Mediterranee; poinconnement et ecrasement rigide-plastique. Bulletin de la Societé Géologique de France Series 7 Vol. XIX, 437-460.

Telford, W.M., Geldart, L.P., Sheriff, R.E., 1990. Applied Geophysics, Cambridge University press, 770 pp.

Terrinha, P. A. G., 1998. Structural geology and tectonic evolution of the Algarve Basin. - Unpublished PhD Thesis, Imperial College, University of London, U. K., 430 p., 134 Figs., London.

Terrinha, P. A. G., Ribeiro, C., Kullberg, J. C., Lopes, C., Rocha, R. B., Ribeiro, A., 2002. Compressive episodes and faunal isolation during rifting in the Algarve and Lusitanian Basins, Southwest Iberia. Journ. Geology 110, 101-113.

Thiebot, E., Gutscher, M.A., 2006. The Gibraltar Arc seismogenic zone (part 1): constraints on a shallow east dipping fault plane source for the 1755 Lisbon earthquake provided by seismic data, gravity and thermal modeling. Tectonophysics 426, 135-152.

Tikhonov, A., 1950. The determination of the electrical properties of deep layers of the Earth's crust. Dokl. Acad. Nauk. SSR 73, 295-297.

Torné, M., Banda, E., 1992. Crustal thinning from the Betic Cordillera to the Alboran Sea. Geo-Marine Letters 12, 76-81.

Torne, M., Fernandez, M., Comas, M., Soto, J., 2000. Lithospheric structure beneath the Alboran Basin: results from 3D gravity modeling and tectonic relevance. Journal of Geophysical Research: Solid Earth (1978–2012) 105, 3209-3228.

Tornos, F., 2006. Environment of formation and styles of volcanogenic massive sulfides: the Iberian Pyrite Belt. Ore Geology Reviews 28, 259-307.

Tornos, F., Chiaradia, M., Fontboté, L., 1998. Geoquímica isotópica del plomo en las mineralizaciones de la zona de Ossa Morena (ZOM): implicaciones metalogenéticas y geotectónicas. Boletín de la Sociedad Española de Mineralogía, 206-207.

Torres-Roldan, R., Poli, G., Peccerillo, A., 1986. An Early Miocene arc-tholeiitic magmatic dike event from the Alboran Sea - Evidence for precollisional subduction and back-arc crustal extension in the westernmost Mediterranean. Geologische Rundschau 75, 219-234.

Unsworth, M.J., Malin, P.E., Egbert, G.D., Booker, J.R., 1997. Internal structure of the San Andreas fault at Parkfield, California. Geology 25, 359-362.

Valadares, V., González-Clavijo, E.J., 2004. New data on the geology of the Monchique Intrusive Alkaline Complex (SW Portugal). Geogaceta 36, 39-42.

Van Bemmelen, R.W., 1927. Bijdrage tot de bouw der betische ketens in de Provincie Granada, Spanje. Thesis Tech. Univ. Delft p. 176.

Vauchez, A., Tommasi, A., 2003. Wrench faults down to the asthenosphere: geological and geophysical evidence and thermomechanical effects. Geological Society, London, Special Publications 210, 15-34.

Vernant, P., Fadil, A., Mourabit, T., Ouazar, D., Koulali, A., Davila, J.M., Garate, J., McClusky, S., Reilinger, R., 2010. Geodetic constraints on active tectonics of the Western Mediterranean: Implications for the kinematics and dynamics of the Nubia-Eurasia plate boundary zone. Journal of Geodynamics 49, 123-129.

Vieira da Silva, N., Mateus, A., Monteiro-Santos, F., Almeida, E., Pous, J., 2007. 3-D electromagnetic imaging of a Palaeozoic plate-tectonic boundary segment in SW Iberian Variscides (S Alentejo, Portugal). Tectonophysics 445, 98-115.

Vissers, R.L.M., 1981. A structural study of the Central Sierra de los Filabres (Betic Zone, SE Spain), with emphasis on deformational process and their relation to the Alpine Metamorphism. GUA Papers on Geology 1, 15, 154 pp.

Vozoff, K., 1980. Electromagnetic methods in applied geophysics. Geophysical surveys 4, 9-29.

Vozoff, K., 1991. The magnetotelluric method. In: Nabighian, M.N. (Ed.), Electromagnetic Methods in Applied Geophysics, 2, pp. 641–711

Wannamaker, P.E., Booker, J.R., Jones, A.G., Chave, A.D., Filloux, J.H., Waff, H.S., Law, L.K., 1989. Resistivity cross section through the Juan de Fuca subduction system and its tectonic implications. Journal of Geophysical Research: Solid Earth (1978–2012) 94, 14127-14144.

Watts, A., Piatt, J., Buhl, P., 1993. Tectonic evolution of the Alboran Sea basin. Basin Research 5, 153-177.

Weijermars, R., 1985. Uplift and subsidence history of the Alboran Basin and a profile of the Alboran Diapir (W-Mediterranean). Geologie en Mijnbouw 64, 349-356.

Wiese, H., 1962. Geomagnetische Tiefentellurik Teil II: die Streichrichtung der Untergrundstrukturen des elektrischen Widerstandes, erschlossen aus geomagnetischen Variationen. Geofisica pura e applicata 52, 83-103.

Wortel, M., Spakman, W., 1992. Structure and dynamics of subducted lithosphere in the Mediterranean region. Proceedings of the Koninklijke Nederlandse Akademie van Wetenschappen 95, 325-347.

Wortel, M., Spakman, W., 2000. Subduction and slab detachment in the Mediterranean-Carpathian region. Science 290, 1910-1917.

Worzewski, T., Jegen, M., Kopp, H., Brasse, H., Castillo, W.T., 2011. Magnetotelluric image of the fluid cycle in the Costa Rican subduction zone. Nature Geoscience 4, 108-111.

Yang, J., Min, D.J., Yoo, H.S., 2010. Sea effect correction in magnetotelluric (MT) data and its application to MT soundings carried out in Jeju Island, Korea. Geophysical Journal International 182, 727-740.

Zeck, H.P., 1996. Betic-Rif orogeny: subduction of Mesozoic Tethys lithosphere under eastward drifting Iberia, slab detachment shortly before 22 Ma, and subsequent uplift and extensional tectonics. Tectonophysics 254, 1-16.

Zeck, H.P., Monié, P., Villa, I., Hansen, B., 1992. Very high rates of cooling and uplift in the Alpine belt of the Betic Cordilleras, southern Spain. Geology 20, 79-82.